

AD-A041 004

HARRIS CORP MELBOURNE FLA ELECTRONIC SYSTEMS DIV

F/G 17/2

STUDY OF ALTERNATIVE TECHNIQUES FOR COMMUNICATION NETWORK TIMIN--ETC(U)

MAR 77

DCA100-76-R-0028

NL

UNCLASSIFIED

1 OF 4

AD
A041 004





AD A 041004

FINAL REPORT

**STUDY OF ALTERNATIVE TECHNIQUES
FOR
COMMUNICATION NETWORK
TIMING/SYNCHRONIZATION**



AD No. _____
DDC FILE COPY

DISTRIBUTION STATEMENT A
Approved for public release;
Distribution Unlimited



HARRIS
COMMUNICATIONS AND
INFORMATION HANDLING

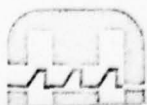
HARRIS CORPORATION Electronic Systems Division
P.O. Box 37, Melbourne, Florida 32901 305/727-4000

FINAL REPORT

**STUDY OF ALTERNATIVE TECHNIQUES
FOR
COMMUNICATION NETWORK
TIMING/SYNCHRONIZATION**

23 March 1977
Final Report
Approved for Public Release;
Distribution Unlimited

Prepared for:
Defense Communications Agency
Defense Communications Engineering Center
1860 Wiehle Avenue
Reston, Virginia 22090



HARRIS

HARRIS CORPORATION Electronic Systems Division

Unclassified R220 20 June 1977


SECURITY CLASSIFICATION OF THIS PAGE (When Data Entered)

REPORT DOCUMENTATION PAGE		READ INSTRUCTIONS BEFORE COMPLETING FORM
1. REPORT NUMBER DCA 100-76-R-0028	2. GOVT ACCESSION NO.	3. RECIPIENT'S CATALOG NUMBER
4. TITLE (and Subtitle) Study of Alternative Techniques for Communication Network Timing/Synchronization		5. TYPE OF REPORT & PERIOD COVERED Final Jan 76 - Mar 77
		6. PERFORMING ORG. REPORT NUMBER
7. AUTHOR(s) None Recorded		8. CONTRACT OR GRANT NUMBER(s) DCA 100-76-R-0028
9. PERFORMING ORGANIZATION NAME AND ADDRESS Harris Corporation, Electronic Systems Division P.O. Box 37 Melbourne, Florida 32901		10. PROGRAM ELEMENT, PROJECT, TASK AREA & WORK UNIT NUMBERS Program Element 33126K Project No. 14100 Task No. 14102-D-01
11. CONTROLLING OFFICE NAME AND ADDRESS Defense Communications Engineering Center 1860 Wiehle Avenue ATTN: Code R220 Reston, Virginia 22090		12. REPORT DATE March 23, 1977
		13. NUMBER OF PAGES 301
14. MONITORING AGENCY NAME & ADDRESS (If different from Controlling Office)		15. SECURITY CLASS. (of this report) Unclassified
		15a. DECLASSIFICATION/DOWNGRADING SCHEDULE
16. DISTRIBUTION STATEMENT (of this Report) Approved for public release; distribution unlimited		
17. DISTRIBUTION STATEMENT (of the abstract entered in Block 20, if different from Report) Same as above		
18. SUPPLEMENTARY NOTES Review Relevance Five Years from Submission Date		
19. KEY WORDS (Continue on reverse side if necessary; identify by block number) Timing, Synchronization, Communication Networks, Digital Communications, Time Division Multiplexing		
20. ABSTRACT (Continue on reverse side if necessary and identify by block number) In digital point-to-point communications, it is only necessary that the receiver be correctly synchronized to the received bit stream and it is not necessary to synchronize the transmitters. However, in a large digital communications network where the signals remain in digital form through time division multiplexers and/or switches, each bit must be available at the correct time to fill its assigned time slot. This is a report on the study of this problem. It evaluates the requirements for a timing subsystem for the future DCS, gives rationale for those characteristics of a DCS timing		

Unclassified R200 20 June 1977

SECURITY CLASSIFICATION OF THIS PAGE(When Data Entered)

subsystem which will best meet the needs of the DoD and the U.S. Government. The conclusions of the study state, "The results of both the analysis and simulation efforts have led to the recommendation of time reference distribution as the technique to employ at the major nodes of the switched digital Defense Communications System." The study also recommends that the master-slave technique be used at lower level nodes.



SECURITY CLASSIFICATION OF THIS PAGE(When Data Entered)

FINAL REPORT

**STUDY OF ALTERNATIVE TECHNIQUES
FOR
COMMUNICATION NETWORK
TIMING/SYNCHRONIZATION**



MARCH 23, 1977

ACCESSION for	
NTIS	Wallo Section <input checked="" type="checkbox"/>
DDC	Buff Section <input type="checkbox"/>
UNANNOUNCED	<input type="checkbox"/>
JUSTIFICATION	
BY	
DISTRIBUTION/AVAILABILITY CODES	
Dist.	AVAIL. and/or SPECIAL
A	

TABLE OF CONTENTS

<u>Paragraph</u>	<u>Title</u>	<u>Page</u>
1.0	INTRODUCTION	1-2
2.0	OVERVIEW OF CANDIDATE TECHNIQUES	2-2
3.0	BASELINE DESIGNS FOR DISCIPLINED TECHNIQUES	3-2
3.1	Master-Slave Tradeoffs	3-2
3.1.1	Master-Slave Block Diagram	3-2
3.1.2	Design Tradeoffs	3-4
3.1.3	Survivability	3-17
3.2	Mutual Synchronization Trade-Offs	3-19
3.2.1	Mutual Synchronization Block Diagram	3-19
3.2.2	System Stability	3-21
3.2.3	Design Considerations	3-24
3.2.4	Simulation Results	3-27
3.3	Time Reference Distribution Trade-Offs	3-31
3.3.1	Time Reference Distribution Block Diagram	3-32
3.3.2	Time Reference Distribution Tradeoffs	3-34
3.3.3	Effect of Link Asymmetries	3-40
4.0	DESIRABLE CHARACTERISTICS	4-2
4.1	Survivability	4-2
4.2	Error Propagation	4-3
4.3	Compatibility With Other Global Timing Systems	4-3
4.4	Precise Time Availability	4-3
4.5	Stability	4-4
4.6	Monitorability	4-4
4.7	Susceptibility	4-5
4.8	Flexibility	4-5
4.9	Interoperability	4-6
4.10	Availability	4-6
5.0	NETWORK CONFIGURATIONS	5-2
5.1	Network Connectivities	5-2
5.2	Other Network Configuration Parameters	5-8
6.0	OPERATING AND STRESS SCENARIOS	6-2
6.1	Introduction	6-2
6.2	Types of Perturbations	6-3
6.3	Scenarios	6-4

TABLE OF CONTENTS (Continued)

<u>Paragraph</u>	<u>Title</u>	<u>Page</u>
7.0	SIMULATION	7-2
7.1	Goals	7-2
7.2	Models	7-3
7.2.1	Timing Techniques	7-3
7.2.2	Normal Link Variations	7-16
7.2.3	Statistical Clock Model	7-26
7.3	Simulation Results	7-29
7.3.1	The Simulation Plan	7-29
7.3.2	Network Configurations	7-30
7.3.3	Loop Parameters	7-30
7.3.4	Input Signals	7-30
7.3.5	Stress Events	7-36
7.3.6	Simulation Run Results	7-46
8.0	EVALUATION OF TIMING TECHNIQUES	8-2
8.1	Survivability	8-2
8.2	Error Propagation	8-9
8.3	Compatibility With Other Global Timing Sources	8-20
8.4	Precise Time Availability	8-22
8.5	Stability	8-23
8.6	Monitorability	8-26
8.6.1	Comparison of Techniques	8-26
8.6.2	Time Reference Distribution	8-27
8.6.3	Inferences	8-28
8.6.4	Example Fault Scenario	8-30
8.6.5	Availability Impact	8-30
8.6.6	Benefits	8-32
8.6.7	Conclusions	8-32
8.7	Susceptibility	8-33
8.8	Flexibility	8-36
8.9	Interoperability	8-37
8.10	Availability	8-38
8.10.1	Comparison of Techniques	8-38
8.10.2	Subjective Evaluation	8-40
9.0	RANKING OF THE DESIRABLE CHARACTERISTICS	9-2
10.0	COST EVALUATION	10-2
10.1	Relative Costs	10-2

TABLE OF CONTENTS (Continued)

<u>Paragraph</u>	<u>Title</u>	<u>Page</u>
11.0	ALTERNATIVE TIMING SUBSYSTEMS	11-2
11.1	Introduction	11-2
11.2	Network Considerations	11-2
11.3	Major Network Synchronization Components	11-5
11.4	Timing Subsystems	11-5
12.0	CONCLUSIONS	12-2
13.0	TESTING PROGRAM	13-2
13.1	Parameters To Be Tested	13-2
13.2	Summary and Test Example	13-5
14.0	ADDITIONAL EFFORT	14-2
APPENDICES		
A	Frequency Acquisition	A-1
B	Survivability Analysis	B-1
C	Impact of Future Technology	C-1
D	References and Bibliography	D-1

SECTION 1.0
INTRODUCTION

The principal goals of this study were to select a preferred timing subsystem for the future integrated switched digital Defense Communications System (DCS) and to quantitatively justify the selected subsystem. In this introductory section, the outline of the report is discussed with the primary objective of elaborating on the solution methodology that was undertaken to provide the required outputs.

Several techniques for timing and synchronization exist on which to base either selected portions or the entire timing subsystem for the DCS. These techniques are master-slave, pulse stuffing, mutual synchronization, independent clocks and time reference distribution. The initial step in the solution methodology was to thoroughly analyze these techniques. Section 2.0 presents an overview of the techniques stressing similarities and differences between approaches. In addition, this section provides the rationale for addressing some techniques in greater detail than others. Section 3.0 deals with the baseline designs of the synchronous techniques, the purpose being that there is great design flexibility within each of the three broad generic terms. A comparative analysis of techniques would not be meaningful if each technique was not itself specifically defined.

As will be noted in Section 2.0, perhaps the most basic function of a timing subsystem is to ensure that each nodal clock runs at or extremely close to the same average frequency. As a result of an initial examination, it was concluded that a common average frequency could be achieved by any of the candidate techniques. It thus became necessary to select a more detailed set of criteria on which to base a comparative analysis of the candidate techniques. The discussions presented in Sections 4.0, 5.0 and 6.0 constitute the set of criteria or test bed in which each of the candidate techniques was evaluated. Section 4.0 defines and justifies a set of desirable characteristics that if provided by the candidate techniques would increase the overall utility of the subsystem. Section 5.0 outlines different network configurations in which the various techniques were evaluated to determine their relative performance. Several configurations rather than one were selected since the actual network configuration in which the selected timing subsystem will operate is not firmly defined. Each network configuration was selected to be realistic and to highlight potential weaknesses or strengths in the techniques.

Section 6.0 discusses a number of scenarios and the resultant stresses on the timing subsystem. It was concluded that the degree to which the candidates provided the desirable characteristics when confronted with the defined set of scenarios was the best available barometer of subsystem effectiveness.

Sections 7.0 and 8.0 detail the techniques used and the results achieved in determining the effectiveness of each technique. Specifically, Section 7.0 deals with the simulation that was generated to provide performance data on each of the synchronous techniques within the framework of specific networks. The models used in the simulation are discussed as well as the results. Section 8.0 utilizes the results of the simulation exercise as well as an extensive analysis effort to evaluate the degree that each candidate technique provides the desirable characteristics. Section 9.0 ranks these desirable characteristics according to their importance or criticality. An appropriate combination of the importance of the characteristics and the degree of the characteristics are provided by each technique can then be used to rate the techniques.

Section 10.0 provides relative cost estimates for the techniques to serve as an input along with the performance evaluations in selecting the preferred timing subsystem.

Section 11.0 presents a discussion of alternate timing subsystems which in general are hybrid combinations of techniques.

Section 12.0 presents conclusions in terms of both techniques and subsystems.

Section 13.0 outlines a suggested test program that could provide valuable additional data.

Section 14.0, the concluding section, outlines an additional effort that appears as the appropriate next step in the development of a future DCS timing subsystem.

SECTION 2.0
OVERVIEW OF CANDIDATE TECHNIQUES

The basic functions to be provided by a network timing and synchronization subsystem are first to ensure that each nodal clock runs at the same average frequency, and second, to ensure a high probability of the maintenance of bit count integrity. It is worthwhile to point out that the first function is necessary but not sufficient for the provision of the second. The second function can only be provided if sufficient buffering exists to compensate both for differences in instantaneous frequency between clocks and for the variations in delay that exist on the links connecting the nodal clocks. That is to say, with enough buffering, any technique that maintains the nodal clocks at the same average frequency will also provide a high probability of maintaining bit count integrity. However, those techniques that require less buffering for a given bit slip rate are preferable to those that require more buffering. Although not completely defensible from a cost point of view (because of the relatively low-cost of buffers), this statement is supportable since it is certainly true that as buffer size tends to increase, especially on a series of tandem links, delay, which is undesirable, also increases. In examining the techniques, it is apparent that those that maintain closer instantaneous frequencies between nodal clocks, especially in the face of different stresses, and those that can cope with variable delays on the links will require less buffering; and therefore, be more desirable.

Several timing techniques exist on which a timing subsystem can be based. Five techniques were initially considered for examination. These were master-slave, mutual synchronization, time reference distribution, pulse stuffing and independent clocks. As mentioned in Section 1.0 the most promising techniques have been scrutinized in order to determine the degree to which each provides the desirable characteristics listed in Section 4.0. This task was undertaken because it was felt that each of the techniques could ensure that the nodal clocks would run at the same average frequency under normal operating conditions. However, what had to be explored was first, how each system would react under stress; second, what ancillary benefits would be provided by the techniques and third, the closeness of instantaneous clock frequencies for each technique. The remainder of this section will provide an overview of each of the techniques, stressing the similarities and differences between techniques. Furthermore, the rationale for pursuing some alternatives in greater depth than others will be provided.

The techniques that have been considered can be divided into two general categories, those that are unlocked or undisciplined clock approaches and those that depend on locked or disciplined clocks. Pulse stuffing and independent clocks belong in the first category; mutual synchronization, master-slave and time reference distribution belong in the second category. After an initial examination, it was decided that as a category, the disciplined clock techniques held much greater promise than the undisciplined clock techniques. This decision, which was based in the case of pulse stuffing from a cost point of view and in the case of independent clocks on both a cost point of view and on the necessity of accepting periodic bit slips. This is explained in the paragraphs below which summarize these two techniques.

Pulse Stuffing

Pulse stuffing has been widely applied as an approach for time-division multiplexing of asynchronous bit streams. In this technique, the nominal data rate of the output of the multiplexer is chosen to be higher than the sum of the nominal data rates of the inputs to the multiplexer. The data on each of the input data channels is written into an elastic buffer and withdrawn as required by the multiplexer. Occasionally, a buffer will be low, and thus no data will be read out. Instead, a stuff bit is transmitted. These stuff bits are identified by sync signals which are transmitted with the data. These sync signals are used by the demultiplexer in removal of the stuff bits. The insertion and removal of stuff bits results in timing jitter which must be reduced by using a narrowband phase-locked loop to generate the READ clock for the elastic buffer.

There are four basic steps one must take in designing a pulse stuffed multiplexer.

1. Select the multiplexer data rate sufficiently high to accommodate the expected frequency uncertainty of the data channels and the multiplexer clock.
2. Allocate adequate overhead to have a very reliable indicator of framing and stuff bit locations.

3. Determine buffer sizes so that buffer overflow will not occur with worst-case frequency offsets and worst-case waiting times.
4. Make the loop bandwidth of the PLL generating the read clock for the destuff buffer small enough to remove timing jitter caused by the stuff-destuff process.

The disadvantages of the technique are, first, that it is inconvenient to use to synchronize a large number of lower capacity channels for time division switching. This is due to the significant amount of processing per channel that is required (such as buffering, stuffing, destuffing and filtering to remove timing jitter). Second, a stuff-destuff device would be required at every digital channel terminal, at every channel termination on a digital switch and at every channel input to a multiplexer. Based on these shortcomings, pulse stuffing was not considered further as a network synchronization technique.

Independent Clocks

Another approach for using unlocked clocks involves using a very stable independent clock at each node. All subscribers at a node are then slaved to this nodal clock. Thus, all data arriving at a node from subscribers will be synchronized. Data arriving via trunks from other nodes having independent clocks must be buffered. This buffer must be sized to accommodate the possible frequency offsets between the independent clocks and variations in frequency due to transmission phenomena.

If the nodal clocks are set to run at a nominal data rate of f_o and the data rate of any two nodal clocks is within Δf_o of f_o , then the maximum difference in data rate between any two nodal clocks is $2\Delta f_o$. Assuming that a buffer size of m bits is chosen (set initially at half full) the time required for a buffer overflow is at least

$$T = \frac{m/2}{2\Delta f_o} \quad (1)$$

letting

$$S = \frac{\Delta f_o}{f_o} \quad (2)$$

denote the long term clock stability factor (1) becomes

$$T = \frac{m}{4Sf_o} \quad (3)$$

Then using Equation (3) the buffer size which guarantees that the time between overflows or underflows is at least T seconds can be computed. If one had an atomic frequency standard with $S = 10^{-11}$, then using Equation (3) we find that a buffer size of 1040 bits is required (at $f_o = 10$ Mb/s) to guarantee a period of 30 days between buffer overflows. Thus, one can see that buffer sizes may be significant with this approach even using atomic clocks.

There are two disadvantages that the independent clock technique has vis a vis any of the disciplined clock approaches. First, because clocks are not disciplined, ultimate inherent accuracy must be demanded from individual clocks. Thus, the number of cesium clocks required in the network will be significantly larger than any of the locked clock approaches. This results in a significant cost impact. Second, despite the highly accurate clocks, periodic bit slips must be accepted since clocks are not disciplined.

Despite these basic disadvantages, the independent clocks approach was not eliminated as a viable candidate partly because of certain other inherent advantages and partly because the effort necessary to analyze the network performance of this basically uncomplicated technique was small as compared to the locked clock approaches which required an extensive simulation effort.

Synchronous Techniques

Three techniques based on disciplined clocks have been explored. In this section, a brief overview of each technique is presented with the detailed in-depth analysis deferred to Section 3.0.

The inherent characteristic common to any synchronous clock technique is that the nodal clock at each node within the network is disciplined so that its frequency, phase or both is maintained within some small tolerance of the like parameters of some reference timing signal. The fundamental differences between the three techniques, master-slave, mutual synchronization and time reference distribution is the choice of the reference timing signal.

Master-slave is a very straightforward approach. Timing is distributed through a master-slave tree. The nodal clock is derived by locking a very narrowband phase-locked loop to the received bit timing from one of the incoming trunks. This approach has been used in many of the commercial systems that have been built (Western Union, Datran, and AT&T). Generally, a hierarchical approach with a number of diverse routes for timing distribution has been used. This gives an added measure of survivability, since it minimizes the probability that a given node will be forced to operate asynchronously due to a failure in the particular link from which it derives timing. An added degree of sophistication that is feasible with respect to alternate routing is adaptive reorganization. This feature is compatible with either master-slave or time reference distribution since both are based on hierarchical tree structures. However, since it requires a duplex control link and such a link is already part of the time reference distribution system and not a part of master-slave system, this feature has been incorporated in the time reference distribution approach.

Mutual synchronization is a synchronous technique where the reference for the local nodal clock is an average of the timing signals derived from each of the incoming trunks. Obviously, the loss of a single link will not necessitate a network reorganization as it might in a master-slave system. However, unlike a master-slave system, a link perturbation on any of the incoming trunks can have an effect on the nodal clock. In general, it can be said that a common average frequency for all nodes in the network is achieved in the mutual synchronization system at the expense of significant variations in instantaneous frequencies between nodes.

Time reference distribution is more closely related to a master-slave system than any other technique. In fact, it can be described as a double-ended master-slave system that is referenced to some standard of precise time and includes both an adaptive reorganization capability and a separation of error measurement and error correction. This point is worthy of elaboration. In order to elaborate on this statement, four points must be discussed. These are:

- Double-ended versus single-ended
- Adaptive reorganization
- Reference to precise time
- Separation of error measurement and error correction

As the techniques have been defined, master-slave is a single-ended system and TRD is a double-ended system. The single-ended approach uses a reference timing signal local to the clock being disciplined. That is, the reference signal is the timing signal derived from one of the received trunks. This signal is essentially the timing signal generated at some distant node, corrupted by the link variations inherent in the media and corrected by the appropriate filtering in the receive node. Such a system does not require an overhead link for timing information. The double-ended system attempts to lock the local nodal clock directly to the timing signal generated at the distant disciplining node. This is accomplished in TRD by measuring the phase offset between clocks via a time transfer technique* and correcting the disciplined clock so that the measured phase difference between clocks is driven to zero. The time transfer technique requires an overhead link from the disciplining node to the disciplined node. The reader is directed to Section 3.0 for a detailed discussion of the implementation of the technique.

The adaptive reorganization capability included in the time reference distribution approach addresses the problem of how nodes within the network attain a timing reference after the primary reference has gone down. The adaptive reorganization approach essentially results in a *real-time rating of all the potential timing reference sources available for a node*. This rating is based on link qualities, clock types and timing distribution paths to the ultimate master. The technique guarantees that the best available reference for each node is selected in case of failure. The requirement placed on the network for this service is an overhead channel required for the distribution of link and nodal rankings. The alternative to the adaptive reorganization scheme is a fixed reorganization scheme that can result in deleterious timing results in the face of certain combinations of failures.

A valuable by-product of the TRD approach results if the network master is referenced to a source of precise time such as UTC at the Naval Observatory. If this is done, the network will now have available at each node a source of precise time. A double-ended system such as TRD is the only type that can provide this characteristic. The resulting benefits are discussed elsewhere in this report.

The overhead link required in the TRD approach for time transfer and adaptive reorganization can also be used for the transmission of measured but uncorrected clock errors from

* See Paragraph 3.3

node to node. As is shown in Section 3.0, the TRD approach provides a natural division between error measurement and error correction. If the time interval for error correction is long, the measured, but uncorrected, error on a series of tandem links may be provided via overhead to nodes lower in the hierarchy. This permits the simultaneous correction of all clocks in the network directly to the master clock.

This section presented brief overviews of the candidate techniques. Perhaps the major point being conveyed in this section dealt with the similarities and differences between the three synchronous techniques. In summary, any synchronous network technique must deal with two specific problems: The loss of the reference timing signal which if not replaced results in asynchronous operation and media link variations which result in a frequency difference between the transmitted timing signal at the disciplining node and the received timing signal at the disciplined node. The first problem is addressed similarly by master-slave and TRD (although in different levels of sophistication) by the substitution of another reference. Mutual synchronization addresses the problem by at no time having a single nodal input constitute the reference timing signal for a node. In case of link variations, master-slave and mutual synchronization have similar approaches and TRD takes a completely different approach. The goal with respect to link variations is to not have such variations affect the frequency of the disciplined nodal clock. If this goal is achieved, the buffer requirement on any link in the network is minimized since the accumulation of frequency errors on a series of tandem links is avoided. The approach taken by mutual synchronization and master-slave is essentially to filter out all but very long term variations. The approach taken by TRD is to remove all such media effects via the double-ended time transfer approach.

SECTION 3.0
BASELINE DESIGNS FOR DISCIPLINED TECHNIQUES

3.0 BASELINE DESIGNS FOR DISCIPLINED TECHNIQUES

The three disciplined techniques being considered are master-slave, mutual synchronization, and time reference distribution. In this section we perform tradeoffs leading to the selection of a good approach for implementing each of these techniques. We do not make the claim that the design parameters are optimum, only that they are "good" considering the environment in which the timing subsystem must operate.

This was done to provide a concrete baseline by which to compare the disciplined techniques.

3.1 Master-Slave Tradeoffs

The tradeoffs for a master-slave system involve loop type, loop parameters, phase detector type, clock stabilities, buffer sizes, and method of providing alternate references considering the expected stress environment in which the network must operate.

3.1.1 Master-Slave Block Diagram

A typical block diagram of the nodal timing subsystem for the master-slave technique is shown in Figure 3.1.1. The selector on the left selects the source to which the nodal clock is to be slaved. The inputs to this selector consist of clocks generated from incoming data links or from external reference sources such as USNO or Loran C. The selector on the right is used to select one of the redundant nodal clocks as input to the frequency synthesizer. The frequency synthesizer generates all the frequencies needed for switching and multiplexing equipment at the node. Two redundant phase-lock loops are shown, however, more frequency sources may be added for increased redundancy. The actual number of frequency sources is determined by the required nodal availability and reliability of the basic frequency sources. Redundancy of other nodal timing subsystem hardware is not shown in order to avoid cluttering the diagram. All of the frequency sources are phase-locked to the selected input frequency source. This is done so that in the event of a local clock failure a smooth transition can be made from one local source to the next. Each of the VCO's can be allowed to coast through link outages through a command from the control section to force holding the VCO's control voltage at the same value as immediately before the dropout for the duration of the dropout.

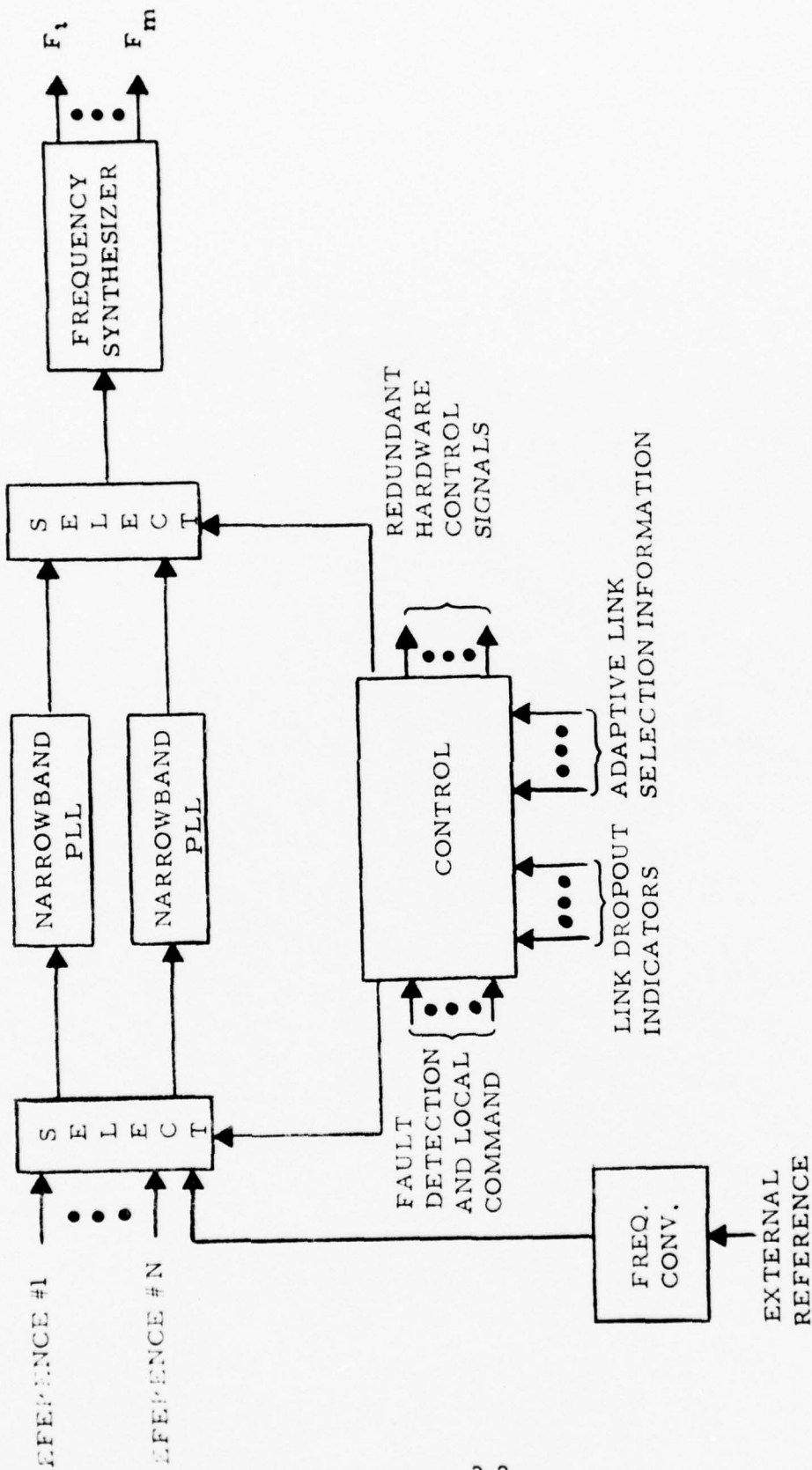


Figure 3.1.1.1. Master Slave Nodal Timing Subsystem Block Diagram (Dual Redundant)

The control section provides operational control of the timing subsystem, reconfigures the redundant hardware in case of failures and controls selection of different links or references to phase lock the local clock to in case of changes in link status. Its inputs consist of nodal fault detection signals, local command signals, link dropout signals, and remote node status signals via orderwire channels. The input orderwire information can be used to implement an adaptive timing distribution network reorganization scheme for slaving the nodal clock to the best available source. This type of adaptive scheme should be used in large-scale military networks to achieve survivability in stress situations. A discussion of this problem is given in Paragraph 8.1. Typically, a network master frequency source uses a primary standard. Thus, three cesium frequency standards might be used in a triply redundant configuration to achieve reliability. To achieve greater survivability of network synchronization, one might also provide several slave nodes with atomic frequency standards to act as masters if the network master is lost. It is probably desirable to slave the network master to a common reference frequency source such as U.S. Naval Observatory (USNO). This will allow better interoperability with other networks referenced to USNO.

3.1.2 Design Tradeoffs

Consider the baseband phase-locked loop model shown in Figure 3.1.2. The closed-loop transfer function of the phase-locked loop may be written as

$$\frac{\theta_o(s)}{\theta_i(s)} = \frac{K_v F(s)}{s + K_v F(s)} \quad (3.1.2-1)$$

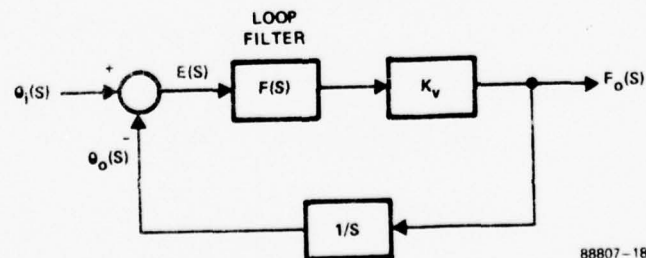


Figure 3.1.2

The output of the phase detector may be written as

$$E(s) = \theta_i(s) - \theta_o(s) = \frac{s \theta_i(s)}{s + K_v F(s)} \quad (3.1.2-2)$$

frequency may be written as

$$F_o(s) = \frac{s K_v F(s) \theta_i(s)}{s + K_v F(s)} \quad (3.1.2-3)$$

A type one loop is obtained with a simple low-pass loop filter, i.e., $F(s) = a/(s + a)$. In this case the closed-loop transfer function becomes

$$\frac{\theta_o(s)}{\theta_i(s)} = \frac{\omega_n^2}{s^2 + 2 \xi \omega_n s + \omega_n^2} \quad (3.1.2-4)$$

where $\omega_n = \sqrt{a K_v}$ and $\xi = \sqrt{a/4 K_v}$.

A type two loop is obtained by using an integral plus proportional loop filter, i.e., $F(s) = (s + a)/s$. Then the closed loop transfer function becomes

$$\frac{\theta_o(s)}{\theta_i(s)} = \frac{2 \xi \omega_n s + \omega_n^2}{s^2 + 2 \xi \omega_n s + \omega_n^2} \quad (3.1.2-5)$$

where $\omega_n = \sqrt{a K_v}$ and $\xi = \sqrt{K_v/4 a}$.

Phase-locked loops with these two loop types will be analyzed in this section for application to the network synchronization problem. They have considerably different properties in some respects, but one can also obtain a blend of the properties of both by using the loop filter $F(s) = \frac{a(s+b)}{b(s+a)}$.

3.1.2.1 Type One Loop

A linear analysis will be presented (no cycle slips occur in the loop). Since it turns out that this is a desirable implementation, the results are valid. Therefore, it is assumed that a

phase detector that is linear over several cycles is used (an extended-range phase detector). The parameter tradeoffs that will be examined are all closely interrelated.

The purpose of the nodal synchronizer is to provide a stable nodal clock that closely follows the network frequency. Variations in frequency due to path delay variations should be filtered out. It is assumed that a narrowband loop will be used for this purpose. Variations with a period of a few minutes will be filtered by such a loop. The most troublesome variations are those with a daily period ($\omega_d = 73 \times 10^{-6}$ rad/sec). For cable and microwave the equivalent frequency offsets due to daily path delay variations would be a few parts in 10^{10} . Satellite links present much worse path delay variations (a few parts in 10^8), but it is safe to assume that Doppler correction can be used to provide a reference with much greater stability (even if this correction was in error by 1 percent, the resulting stability would be a few parts in 10^{10}). This could be done by using the satellite orbital parameters, the ground terminal locations, and the time to calculate the impact of the satellite motion on the phase error and to use this result to correct the measured phase error. Since the network master would be no more accurate than $\pm 10^{-11}$, the effects of daily path delay variations need to be attenuated by about a factor of 10 to make them about the same magnitude as the master clock variations. We should point out that it is more important to maintain the nodal frequency very accurately when a reference is lost than to heavily filter these slow path delay variations when a reference is available. The problem associated with trying to filter these variations at all times is the long acquisition time and the large steady-state phase error that must be built up to hold the VCO in lock. This loop requires a nonzero phase error to track a frequency offset. From Equation (3.1.2-2) this phase error may be written as

$$E(s) = \frac{s(s + 2 \xi \omega_n) \theta_i(s)}{s^2 + 2 \xi \omega_n s + \omega_n^2} \quad (3.1.2-6)$$

For a step in frequency, $\theta_i(s) = \Delta \omega / s^2$. The final value theorem shows that the steady-state phase error is

$$\epsilon_{ss} = \lim_{s \rightarrow 0} sE(s) = \frac{2 \xi \Delta \omega}{\omega_n^2} \quad (3.1.2-7)$$

Thus, the peak phase error that must be accommodated by the phase detector is proportional to ξ and inversely proportional to the natural frequency of the loop.

Smaller values of ξ tend to speed acquisition time (down to $\xi = 0.707$) and to reduce steady-state phase error. However, the value of ω_n required to provide a given amount of filtering of the input frequency jitter decreases for smaller values of ξ which tends to increase steady-state phase error. Thus, one should also examine this effect.

Using a low-pass loop filter

$$F_o(s) = \frac{\omega_n^2 s \theta_i(s)}{s^2 + 2 \xi \omega_n s + \omega_n^2} \quad (3.1.2-9)$$

Then

$$\frac{F_o(s)}{F_i(s)} = \frac{\omega_n^2}{s^2 + 2 \xi \omega_n s + \omega_n^2} \quad (3.1.2-10)$$

This transfer function has magnitude

$$\left| \frac{F_o(j\omega)}{F_i(j\omega)} \right| = \frac{\omega_n^2}{\sqrt{\omega^4 + (4\xi^2 - 2)\omega^2\omega_n^2 + \omega_n^4}} \quad \left| \frac{F_o(j\omega_d)}{F_i(j\omega_d)} \right| = 0.1.$$

To filter daily jitter by a factor of 10 it is required that

The value of ω_n required to achieve this is a function of ξ . One can see from Figure 3.1.2.1 and from Equation (3.1.2-7) that as long as the ratio increases linearly with ξ as it does for $\xi > 2.5$ there will be no change in steady-state phase error. But for $\xi < 2.5$ the ratio ω_n/ω_d increases much more slowly with ξ which indicates that small values of ξ will result in small steady-state phase error.

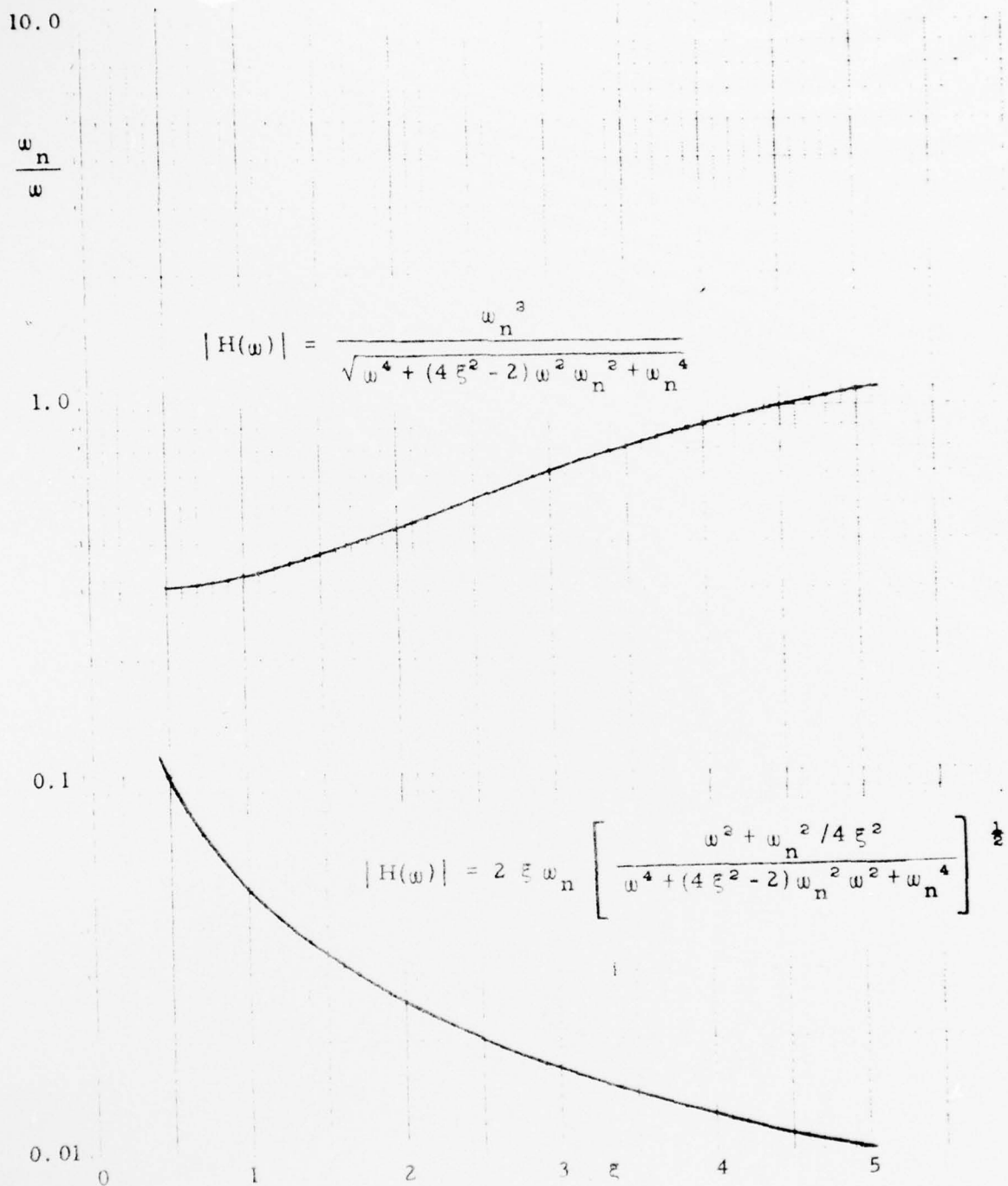


Figure 3.1.2.1. Value of ω_n/ω Required to Make $|H(\omega)| = 0.1$ as a Function of ξ

The value of $\xi = 0.707$ gives the shortest acquisition time for constant ω_n . This is not exactly the case here since the value of ω_n required to maintain $\left| F_o(j\omega_d)/F_i(j\omega_d) \right| = 0.1$ increases as ξ increases. However, the increase is not rapid enough to make higher values of ξ give better acquisition time. In addition, values of ξ less 0.707 greatly increase the oscillatory nature of the loop response, and these variations would be passed on to other nodes. Finally, the value $\xi = 0.707$ gives the smallest steady-state phase error for any value of $\xi \geq 0.707$. Thus, the value of $\xi = 0.707$ appears to be the best choice for this loop.

Assuming that the effects of daily path delay variations will be heavily filtered (requiring $\omega_n = 0.32 \omega_d$) and that $\xi = 0.707$ will be used, the requirements on phase detector range can be examined. There is a direct trade between oscillator stability and phase detector range. The maximum phase error is about $1.05 \epsilon_{ss}$ due to the slight overshoot with $\xi = 0.707$. The steady-state phase error is given by Equation (3.1.2-7). From this equation the long term clock stability required to keep the maximum phase error less than any amount can be calculated (at a specific reference frequency) from

$$S = \frac{\Delta \omega}{\omega} = \frac{R \omega_n}{3.1 \xi \omega} \quad (3.1.2-11)$$

where R is the phase detector range ($\pm R$ radians). At reference frequencies of several megabits and $\pm \pi$ radian range, this will result in a stability requirement of a few parts in 10^{11} (which cannot be achieved by quartz clocks). One could ease this requirement (to 10^{-8}) by extending the range of the phase detector the required amount. This approach would also require buffers of similar size, and these would add several milliseconds of additional delay at every node that would otherwise not be required. The other alternative is to increase ω_n and use a much smaller phase detector range. In this case the nodal frequency would be significantly affected by path delay variations and this would degrade performance when the loop must "coast" without a reference since it would "coast" at this perturbed frequency. In contrast, the type two loop filter has an integrator which can be designed to have a very long time constant. The integrator output provides the VCO with a control voltage which is a much more accurate measure of the true network frequency.

3.1.2.2 Type Two Loop

Two principal differences of this type of loop are that the integrators in the loop filter provides "frequency memory" for use when "coasting" without a reference and that the loop bandwidth can be changed as an acquisition aid to speed up acquisition from large frequency offsets. The loop parameters used in tracking do not impose a limit on the acquisition time as they do when using a type one loop. This will allow the use of very narrowband loops while still retaining good acquisition performance. Several approaches have been examined in Appendix C, and some of the results are used in this section. We will assume the two-bandwidth approach is used. It should be rather easy to implement in a digital loop.

An extended range phase detector improves the performance of the loop significantly in this application by allowing the use of narrower bandwidths, and it will be assumed that it is used. The phase detector must have a range larger than the peak phase error that will ever be seen. This will ensure that the loop operates in the linear region. The manner in which the performance is improved over the phase detector with a one-cycle range is in improved acquisition time and ability to acquire greater frequency offsets for identical ξ and ω_n . For any frequency offset outside the "lock range" of the one-cycle phase detector, this loop will slip cycles and require longer to acquire. The acquisition time of the one-cycle phase detector becomes poorer and poorer relative to the extended range phase detector as the offset is increased until the offset becomes larger than the loop capture range. At this point, the one-cycle phase detector cannot even achieve lock. To make this loop have acquisition times similar to those of the extended range phase detector would require a considerably larger loop bandwidth, and attaining a very narrow loop bandwidth is one of the principal goals for the network synchronization problem. There is one other useful feature of the extended range phase detector. Since the type two loop tracks a frequency offset with zero steady-state phase error, and it does not slip cycles with an extended range phase detector, then each nodal clock will stay close in phase to the clock to which it is referenced. This helps keep the probability of buffer overflows small.

The purpose of the using the narrowband loop is to heavily filter the jitter caused by perturbations in the network such as path delay variations so that each nodal clock is very stable. The type two loop has a peaked closed loop transfer function so there will be amplification of

some jitter frequencies. The amount of amplification is easy to estimate. From Equation (3.1.2-5) we can determine the magnitude of the frequency transfer function

$$\left| \frac{F_o(j\omega)}{F_i(j\omega)} \right| = 2 \xi \omega_n \left[\frac{\omega^2 + \omega_n^2 / 4 \xi^2}{\omega^4 + (4 \xi^2 - 2) \omega_n^2 \omega^2 + \omega_n^4} \right]^{1/2} . \quad (3.1.2-12)$$

The maximum value of this transfer function has been determined and is shown in Figure 3.1.2.2. There is considerable amplification of some jitter frequencies at the smaller values of ξ . For example, at $\xi = 0.707$ the peak occurs at $\omega = 0.78 \omega_n$, and that jitter is amplified by a factor of 1.27. For ten such nodes in tandem, this jitter would be amplified by a factor of $(1.27)^{10} = 10.9$. This is clearly unacceptable, but the problem can be alleviated by choosing larger values for damping coefficient ξ . For example, at $\xi = 4$ the peak occurs at $\omega = 0.4 \omega_n$, and that jitter is amplified by a factor of only 1.013. For ten of these nodes in tandem, the jitter would only be amplified by a factor of $(1.013)^{10} = 1.14$. Thus, with this loop the higher values of ξ will have to be used.

In selecting parameters for the narrowband loop, one can examine two different approaches. First, one could attempt to filter the effect of daily variations all the time. This would require extremely narrowband loops, and the loops would be extremely slow to respond to any variations in reference frequency. On the other hand, one could require only that the loop heavily filters the effects of daily variations on its frequency memory and thus on its frequency when in the "coasting" mode (operating without a reference). By this, we mean that effects of path delay variations on the integrator output are heavily filtered. To do this one must ensure that the time constant integrator is long enough for the integrator output to closely reflect the network frequency averaged over the past several days. This will allow a much larger ω_n to be used, and this approach accomplishes the critical task of providing a nodal clock with frequency extremely close to the network frequency during loss of reference.

If one desires to heavily filter the jitter at all times, the effect of the filter is given by the frequency transfer function Equation (3.1.2-12). Assuming that we wish to make $|H(\omega)| = 0.1$ the value of ω_n / ω required to achieve this as a function of ξ is shown in Figure 3.1.2.1. Note the rapidity with which the value of ω_n required to achieve the filtering decreases with increasing ξ . A large value of ξ must be used or other jitter frequencies will be

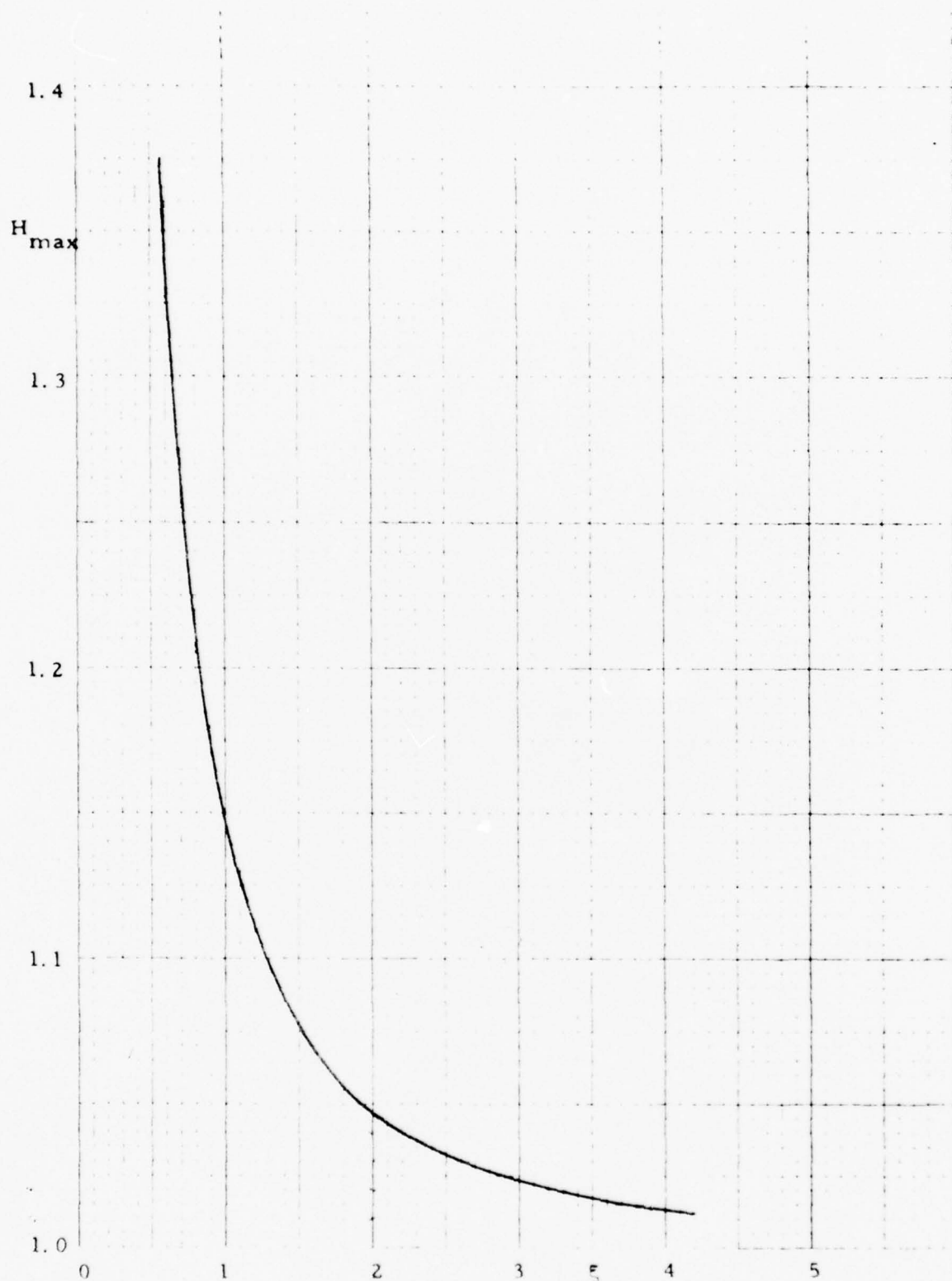


Figure 3.1.2.2. Maximum Value of $|H(\omega)|$ Given by (4.2-12) as a Function of ξ

greatly amplified. Even at a value of $\xi = 2.5$ the value of ω_n required to attenuate daily jitter by a factor of 10 is $\omega_n = 0.02 \omega_d$.

In contrast, assume that one only attempts to filter the effects of daily jitter on the integrator output. The output frequency is determined only by the voltage on the integrator which is the integrated past history of the phase error, $E(s)$. Then the output frequency is

$$\begin{aligned} F_o(s) &= \frac{aK_v}{s} E(s) \\ &= \frac{\omega_n^2 F_i(s)}{s^2 + 2\xi\omega_n s + \omega_n^2} \end{aligned} \quad (3.1.2-13)$$

The magnitude of the frequency transfer function is identical to Equation (3.1.2-10). The value of ω_n/ω required to make $|H(\omega)| = 0.1$ has been shown previously in Figure 3.1.1 as a function of ξ .

We note that in contrast to the previous example that as one increases ξ that ω_n can be increased. In fact, for large ξ one can make $|H(\omega)| = K$ by choosing $\omega_n \approx 2\xi K \omega_i$. If we assumed that operation with values of ξ in the range from 3 to 5 one can increase ω_n by a factor of 36 to 100 by only requiring that the effect of daily jitter on the integrator output be filtered.

Thus, we are recommending the use of a type two loop with ω_n and ξ chosen to heavily filter the effects of daily jitter only on the integrator output. As an example, if we pick $\xi = 4$, $\omega_n = 0.8 \omega_d$ is needed to attenuate the daily jitter by a factor of 10. From Figure 3.1.2.2 we find that the peak amplification of any jitter frequency is 1.013 and this occurs at frequency $\omega = 0.32 \omega_d$ (which corresponds to buffer fill for the extended range phase detector) from Figure 3.1.2.2. Since this loop is overdamped ($\xi > 1$), the phase error (in cycles) caused by a frequency offset is

$$\theta_e(t) = \frac{\lambda f}{2\omega_n \sqrt{\xi^2 - 1}} \begin{bmatrix} e^{-\alpha_2 t} & -e^{-\alpha_1 t} \end{bmatrix}, \quad (3.1.2-14)$$

where $\alpha_1 = \omega_n (\xi + \sqrt{\xi^2 - 1})$

and $\alpha_2 = \omega_n (\xi - \sqrt{\xi^2 - 1})$.

For large ξ , $\alpha_1 \approx 2 \xi \omega_n$ and $\alpha_2 \approx \omega_n / 2 \xi$. The time at which peak phase error occurs is found to be

$$t_m = \frac{\ln \alpha_1 - \ln \alpha_2}{\alpha_1 - \alpha_2} , \quad (3.1.2-15)$$

and the value of $\theta_e(t_m)$ is

$$\theta_e(t_m) = \frac{\Delta f}{\sigma} \left[\alpha_1^{-\alpha_2/\sigma} \alpha_2^{+\alpha_2/\sigma} - \alpha_1^{-\alpha_1/\sigma} \alpha_2^{+\alpha_1/\sigma} + \alpha_1/\sigma \right] , \quad (3.1.2-16)$$

where $\sigma = \alpha_1 - \alpha_2$. For these loop parameters the phase error gradually rises to a peak with time constant $\tau_1 = 1/\alpha_1$. This peak occurs after a little over four time constants or about 2.5 hours. The loop then slowly reduces this phase error to zero with a time constant of $\tau_2 = 1/\alpha_2$ or about 37.5 hours. The second time constant is the time constant associated with the integrator output. The peak phase error caused by a step in frequency decreases with increasing ξ (for constant ω_n) . The reason for this is that the two time constants get further apart with τ_1 decreasing and τ_2 increasing. This decrease in τ_1 allows the loop to more rapidly respond to changes in reference frequency, thereby preventing the accumulation of large phase errors. For these loop parameters perturbations caused by fractional frequency steps of 10^{-9} or less and the typical path delay variations mentioned previously will cause maximum phase errors of no more than about 1 μ s. Acquisition from large frequency offsets of several parts in 10^8 will cause much larger peak phase errors and will be handled by switching to a special acquisition mode with a much wider bandwidth loop.

The tradeoffs leading to the choice of parameters for the acquisition mode are given in Appendix C, but a summary of the parameters is given here. Switchover to the acquisition mode will occur when the phase error gets larger than about 2 μ s. The acquisition loop will then have to respond to a frequency step and a 2 μ s phase step. The loop bandwidth should be chosen

wide enough to allow a rapid pull-in, but it should not be too wide or the frequency transient due to the $2 \mu\text{s}$ phase step will be very large. The peak frequency change due to a phase step for the type two loop is

$$\Delta f_p = 2 \xi \omega_n \Delta \theta \quad (3.1.2-17)$$

The acquisition mode parameters selected were $\xi = 0.707$ and $\omega_n = 0.007 \text{ rad/sec}$. With these parameters and a $2 \mu\text{s}$ initial phase offset then the observed Δf_p corresponds to a fractional instability of 6.4×10^{-9} . This is about the same order of magnitude but in the opposite direction as the initial frequency offsets that could cause the loop to go into the acquisition mode. Of course, if one desired to have a smaller frequency change due to the phase step, it could be obtained by using a narrower loop bandwidth for the acquisition mode. One must remain in the acquisition mode long enough to ensure that the voltage built up on the integrator in the loop filter will hold the VCO sufficiently close to the reference frequency to avoid another buildup of a $2 \mu\text{s}$ phase error after switchover to the tracking parameters. To be conservative we have estimated that remaining in the acquisition mode for a total of $9 / \xi \omega_n$ seconds is more than adequate. For these parameters this corresponds to about 30 minutes in the acquisition mode.

One other question that needs to be examined is the behavior of the loop when the VCO is subject to a linear frequency drift. From Equation (3.1.2-2) the phase error of the type two loop can be written as

$$E(s) = \frac{s^2 \theta_i(s)}{s^2 + 2 \xi \omega_n s + \omega_n^2} \quad (3.1.2-18)$$

Assume that the frequency drift can be described by

$$\omega_i^{(t)} = \beta t \quad (3.1.2-19)$$

which gives

$$\theta_i(t) = \beta / s^3 \quad (3.1.2-20)$$

The type 2 loop responds to this input with a constant steady-state phase error. This error is obtained from the final value theorem as

$$\begin{aligned}\epsilon_{ss} &= \lim_{s \rightarrow 0} sE(s) \\ &= \frac{\beta}{\omega_n^2} .\end{aligned}\tag{3.1.2-21}$$

If one uses a very good crystal VCO as is used in the Bell System with a drift of 10^{-10} parts/day (or 1.16×10^{-15} parts/second) with the tracking parameters we have selected, the steady-state phase error is found to be $0.37 \mu\text{s}$. This is small enough so that it does not impact our choice of the $2 \mu\text{s}$ threshold for the switchover from the tracking to the acquisition mode.

The type two loop is much more suitable for this application than the type one loop. Its most useful feature is "frequency memory." The integrator time constant can be selected long enough to provide heavy filtering of daily jitter. Thus, the frequency memory provides a very accurate indication of average network frequency over a period of several days. The type two loop can also be used with a wider acquisition bandwidth which will allow much faster acquisition than the type one loop in the presence of large frequency offsets. This will allow much better performance in a military environment where there may be frequency losses of the reference and significant perturbations in network frequency under stress conditions.

A summary of loop parameters for the master-slave approach is given in Table 3.1.2.2.

Table 3.1.2.2. Loop Parameters for the Master-Slave Approach.

<u>Tracking</u>	$\xi = 4$,	$\omega_n = 5.6 \times 10^{-5}$ rad/sec
For a drift rate of $1 \times 10^{-10} \times f_o$ per day, these parameters give a steady-state phase error of $0.37 \mu\text{s}$.		
<u>Fast Acquisition</u>	$\xi = 0.707$,	$\omega_n = 0.007$ rad/sec
The loop will acquire from a combined fractional frequency offset of 2×10^{-8} and a phase offset of $2 \mu\text{s}$ in 1800 s .		

It was mentioned previously that a loop filter of the type $F(s) = \frac{a(s+b)}{b(s+a)}$ will give a loop many of the properties of both types of filters mentioned previously. By proper choice of parameters the steady-state error can be made considerably smaller than that obtained with the filter $F(s) = \frac{a}{s+a}$. In addition, one can also use a two bandwidth filter approach to provide both good acquisition and good filtering performance. However, in order to obtain the type of behavior which we consider desirable, one will have to select parameters so that the performance very nearly approximates that of the type two loop and this will be nearly identical to the behavior just discussed. The parameters for this loop can be chosen such that the closed loop transfer function, $|H(\omega)| < 1, \omega > 0$. Thus, no jitter frequencies will be amplified. This is significant for mutual synchronization systems, so this type of filter will be discussed in that section.

3.1.3 Survivability

Survivability indicates the degree to which the timing subsystem continues to perform its function (to provide network timing) during periods of stress. To achieve this, fall-back modes of operation must be provided so that the timing subsystem itself will not cause significant degradation in capability of the network to provide dependable digital communications during these periods. Network synchronization is necessary because the slip rate that two nodes will experience in communicating is directly proportional to the frequency offset between their nodal clocks. If this offset increases in a stressed environment, then slip rate increases which leads to misaligned frames in multiplexers and switches and a need to resynchronize cryptos. Since timing subsystem performance is directly tied to slip rate, slip rate as a function of the level of stress indicates the survivability of the timing approach.

There are two parts to the problem of minimizing the slip rate in a digital network:

1. Keep the nodal clocks of all communicating node pairs synchronous as much as possible.
2. Minimize the frequency offset between the nodal clocks of asynchronous communicating nodes and minimize the amount of time they must communicate with asynchronous nodal clocks.

To put these comments in perspective, note that if one uses the independent clock technique, there are asynchronous clocks at every node. The slip rate due to buffer overflows is strictly a function of the clock accuracy and the buffer size and will not change as a function of stress level. On the other hand, the analysis in Paragraph 8.1 indicates that one could reduce the slip rate by slaving these clocks to a common master through some master-slave timing distribution hierarchy. This would make all nodal clocks synchronous and slips due to buffer overflows could be avoided entirely providing there were no link or node failures. If link or node failures occur, some nodes may lose their reference to the master. Then some nodes with asynchronous nodal clocks may be communicating and could experience slips. Such nodes will be called "asynchronous communicating nodes." These nodes will remain asynchronous until they once again become locked to a common reference.

The results of the analysis in Paragraph 8.1 indicate that some performance improvements over an independent clock approach may be obtained by using one or more fixed references in a master-slave manner, but these improvements are not that great when the link outage probability is high because the timing distribution network is disrupted so frequently. This is the reason that master-slave systems have been frequently criticized as not having survivability. However, one can make an additional improvement in a master-slave system by giving it the capability of adaptively reconfiguring the timing distribution network as link outages occur. This technique has been implemented in the Dataroute network⁹² and has been proposed for use with Time Reference Distribution.^{169, 170} This approach has the properties that:

1. All communicating nodes are synchronous in the steady state (after a sufficiently long period following the last failure).
2. The only time a nodal clock will act as a self-reference is while the timing distribution network is being reconfigured.

The use of an adaptive timing distribution network gives the master-slave approach a very high degree of survivability. The system can be designed so that no slips occur in the steady state. The only time slips can occur is during the transients associated with reconfiguring the network. Obviously, one of these transients occurs every time an outage occurs, and any single outage can cause the network to be reconfigured in such a manner that several nodes may have to act as a self-reference during this process. Performance in a stress environment is influenced by both the

time required to reconfigure the timing distribution network and the length of time a node can act as a self-reference without experiencing slips (which is a function of the buffer size and frequency offset). There is a trade-off here between time required for reconfiguration, buffer size, and the fractional frequency offset between the nodal clock and the network frequency. For example, a cesium clock could operate without a reference for 24 hours while accumulating only about 1 μ s of phase error relative to the network master. In actual practice, though it should be no problem to accomplish network reconfiguration in 10 minutes. In this case, even the phase errors accumulated with quartz clocks will be rather small. The analysis of Paragraph 8.1 indicates the impact of these parameters and for practical values of them that this technique will have an extremely high degree of survivability.

3.2 Mutual Synchronization Trade-Offs

In this section we address the implementation of a mutual synchronization approach for network synchronization. Many of the trade-offs are similar to those discussed in the previous section with respect to the master-slave approach. These include the decisions one must make regarding loop type, loop parameters, phase detector type, clock stabilities, and buffer sizes. Additional considerations encountered only with mutual synchronization include the individual phase detector weightings and the system stability.

3.2.1 Mutual Synchronization Block Diagram

A block diagram of the nodal timing subsystem for the mutual synchronization technique is shown in Figure 3.2.1. A dual redundant clock system is shown but more than two clocks can be utilized to increase reliability if required. The blocks labeled "Phase Detectors" contain a phase detector for each input frequency source. The sources are obtained from incoming data links or from external references such as USNO or Loran C. The phases between each of the incoming frequency sources and each local clock are then weighted according to some relative quality measure of path and ultimate source. Those weighted phase differences associated with a particular VCO are then summed in order to obtain a composite phase difference. This composite phase difference is then smoothed, filtered and amplified by the loop filter circuit having frequency domain transfer function $F(s)$ is selected to filter out path delay variations of the incoming links

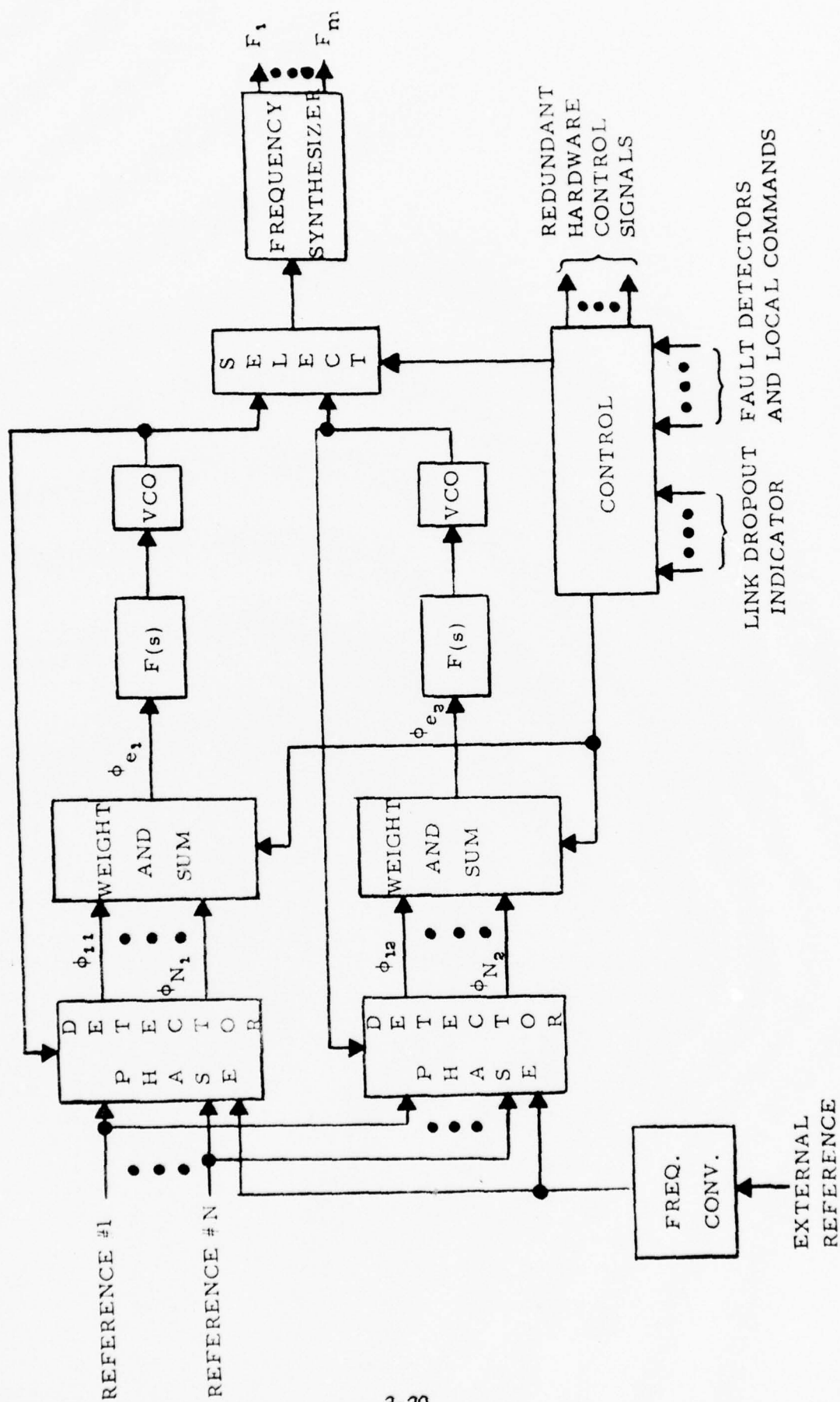


Figure 3.2.1. Mutual Sync Nodal Timing Subsystem Block Diagram (Dual Redundant)

and thereby provide a stable local source that is phase locked to the long term average of the network frequency. The outputs of the voltage controlled oscillator are fed back to the phase detectors and also applied to the input of a selector switch which serves to select one VCO as input to a frequency synthesizer (which generates all the frequencies needed to operate the nodal switching and multiplexing equipment). The control section provides a means for controlling the operation of the nodal timing subsystem, for reconfiguring in case of nodal hardware failures and for controlling the weightings of the various link clock/local clock phase differences. The inputs to the control section include local command signals, nodal fault detector signal, and link drop-out indicators from link receivers. The mutual sync timing subsystem is quite similar to that of the master-slave technique. In a manner similar to the master-slave technique, the redundant local clocks are all phase locked to the network frequency so that smooth transitions can be made from one local clock to the next. In case of long term loss of links the control section will determine a new set of phase error weightings.

3.2.2 System Stability

Constraints on system parameters required to produce a stable mutual synchronization between have taken two forms. First, one must ensure that the relationship between path delays and loop gain is proper. This results in upper bounds on gain-delay products (loop gains and link delays) that have been derived by many investigators.^{107, 40, 115, 45, 46} These stability bounds are dependent on the specific network configuration. However, the maximum value of gain-delay product that can typically be tolerated is on the order of 1. Since very narrowband loops (implying very small loop gain) will be used, link delays of many seconds would be required before there would be a stability problem. Thus, in a real network one would not have to be concerned about the gain-delay products being large enough to cause network instability.

The other constraint needed to ensure stability is on the loop filter parameters. Stability analyses for single-ended mutual synchronization systems have shown that in order for a mutual synchronization system to be stable requires a closed loop phase response that satisfies

$$\left| \frac{\theta_o(j\omega)}{\theta_i(j\omega)} \right| = |H(\omega)| < 1, \omega > 0 \quad (3.2.2-1)$$

It can be shown that type two loops with filters of the form $F(s) = (s + a) / s$ never satisfy this condition (we note that $|H(\omega_n)| > 1$). This means that phase jitter at the natural frequency ω_n will be amplified each time it passes through the timing regeneration circuitry at a node. Since this is a closed-loop system of many interconnected PLL's, one can see that the amplification of phase jitter is the source of the instability. Thus, the designer is restricted to type one loops.

One could examine several type one loops for use in this system. If no loop filter is used, a first-order loop results. It is obvious from the transfer function that such a loop satisfies condition Equation (3.2.2-1). If the loop has a single low-pass filter of the form $F(s) = a / (s + a)$, then one can show that the closed-loop transfer function Equation (3.1.2-4) satisfies condition Equation (3.2.2-1) providing that the damping coefficient, ξ , is greater than $1/\sqrt{2}$. This is the loop analyzed in Paragraph 3.1.2 for the master-slave system, and many of the same conclusions apply here, but to use this loop we must simply ensure that the damping coefficient is always large enough to give a stable system.

Another loop filter that one could use is of the form $F(s) = a(s + b) / b(s + a)$. This filter gives a type one loop, but its performance can be made to approximate that of a type two loop by making the pole be very close to the origin relative to the zero. However, the requirements for stability in a mutual sync system are more severe than those for the simple low-pass filter. The closed-loop transfer function can be found from Equation (3.1.2-1) as

$$\frac{\theta_o(s)}{\theta_i(s)} = \frac{(2\xi - c)\sigma_n s + \omega_n^2}{s^2 + 2\xi\omega_n s + \omega_n^2}, \quad (3.2.2-2)$$

where $\omega_n = \sqrt{a K_v}$, $c = \sqrt{a / K_v}$, and $\xi = c(K_v + b) / 2$. The magnitude of the transfer function is then found to be

$$|H(\omega)| = \left| \frac{\theta_o(j\omega)}{\theta_i(j\omega)} \right| = \left[\frac{(2\xi - c)^2 \omega_n^2 \omega^2 + \omega_n^4}{4 + (4\xi^2 - 2)\omega_n^2 \omega^2 + \omega_n^4} \right]^{1/2}. \quad (3.2.2-3)$$

To find the conditions under which a mutual sync system with this filter is stable we must determine the conditions under which $|H(\omega)| < 1$ for $\omega > 0$. Since both numerator and denominator of Equation (3.2.2-3) have an ω_n^4 term, the condition Equation (3.2.2-1) implies that the requirement for stability reduces to

$$(2\xi - c)^2 \omega_n^2 \omega^2 < \omega^4 + (4\xi^2 - 2) \omega_n^2 \omega^2; \omega > 0. \quad (3.2.2-4)$$

This in turn reduces to the requirement that

$$\xi > (c^2 + 2) / 4c. \quad (3.2.2-5)$$

Thus, the stability requirement leads to a lower bound on the acceptable values of the damping coefficient, ξ . Another consideration is that one must place the pole of the loop filter closer to the origin than the zero, i.e., this requires $b > a$. This condition leads to an upper bound on the acceptable values of ξ .

One can write the parameter b as

$$b = \frac{\omega_n}{2\xi - c}. \quad (3.2.2-6)$$

Then $b > a$ requires that

$$\xi < (c^2 + 1) / 2c. \quad (3.2.2-7)$$

The desired range of operation of this loop is for very small values of c . Unfortunately, one can see from the upper and lower bounds on the allowable values for ξ that asymptotically at very small values of c both the upper and lower bounds on ξ approach $1/2 c$. In fact, even for $c = 0.1$ the allowable range for ξ is found to be $5.03 < \xi < 5.05$. Of course, this range is much too small to allow practical implementation of the loop.

Thus, because of stability considerations we will consider only loop filters of the form $F(s) = a/(s + a)$ for use in mutual sync systems. Design considerations for this type of loop are discussed in the following subsection.

3.2.3 Design Considerations

Design considerations for a loop with a filter of the form $F(s) = a/(s + a)$ were treated in considerable detail for use in a master-slave system in Paragraph 3.1.2.1. Many of the same results apply to this problem.

In that analysis we found that one cannot use a fast acquisition strategy such as a two-bandwidth filter, but one can make good use of an extended range phase detector to aid the acquisition process and provide more tracking range. We also found that if one specified the amount of attenuation at a fixed jitter frequency then the steady-state phase error and acquisition time are best at low values of ξ . The value $\xi = 0.707$ was picked as the best for this loop. Since this value of ξ is at the lower bound for stable values of ξ in a mutual sync system, it is obvious that a larger value will have to be picked. One should increase ξ by enough to ensure that with the desired hardware implementation one cannot have changes in ξ that will allow the system to become unstable. In addition, larger values of ξ are desirable because the transient response of a mutual synchronization is more oscillatory than that of a single loop. We will tentatively pick $\xi = 1$ being a value that should be close to the proper value. One can show that the steady-state phase error for this value of ξ is only about 37 percent higher than that needed for $\xi = 0.707$ (to attenuate a specified jitter frequency by a factor of 10). From Equation (3.1.2-6) the transform of the phase error (at $\xi = 1$) may be written as

$$E(s) = \frac{s(s + 2\omega_n)}{(s + \omega_n)^2} \theta_i(s) \quad (3.2.3-1)$$

The phase error due to a step in frequency, $\Delta\omega$, is then found to be

$$e(t) = \frac{2\Delta\omega}{\omega_n} \left[1 - (1 + \omega_n t/2) e^{-\omega_n t} \right] \quad (3.2.3-2)$$

It is easily verified that the phase error settles to within 1 percent of the final steady-state error after six time constants (at $t = 6/\omega_n$). This will be defined as the acquisition time. If one tries to attenuate daily jitter by a factor of 10, then the value of ω_n needed at $\xi = 1$ is found from Figure 3.1.2.2 to be $\omega_n = 0.33 \omega_d = 2.41 \times 10^{-5}$ rad/s. Unfortunately, this gives an acquisition time of about 69 hours. This would be an undesirable feature in a military environment. While a particular node is attempting to acquire, other nodes are also locking to its frequency which is

different from the network frequency. Thus, during the acquisition period its frequency will tend to pull the network frequency to a different value which, of course, is undesirable. Speeding up the acquisition process may help this problem. This is rather important, and this is the type of behavior one must be concerned with in evaluating the performance in a stress environment where link and node outages may occur frequently. A better choice might be to reduce the acquisition time to 1 hour. The value of ω_n required is $\omega_n = 1.67 \times 10^{-3}$ rad/s. The steady-state phase errors for these two loop bandwidths are 830 and 12 μ s, respectively, for a fractional frequency offset of 10^{-8} .

The above discussion approached the design problem principally on an individual node basis, but this approach is not really adequate. There are some rather significant differences between the behavior of master-slave and mutual sync systems which lead to different design considerations. One such consideration is system stability discussed in the previous subsection. Another difference is that a mutual synchronization system does not settle down to a predetermined system frequency. The final system frequency is determined by factors such as the individual VCO center frequencies, changes in link delays, loop parameters, and the manner in which the network is brought into operation. Unlike the master-slave system, the system frequency of a mutual sync system can be permanently changed by a change in a link delay. One can see this from the following example. Suppose we have a mutual sync system where the error signal applied to the loop filter is the average of the phase errors measured on all links to other nodes. If a step decrease in link delay, $\Delta\tau$, occurred on each link simultaneously, then all phase errors measured will instantaneously increase by $f\Delta\tau$. This error signal will be filtered and then used to influence the VCO frequency, but the VCO's at all nodes will change identically. Since all VCO's are changing in the same direction, we can assume that the increase in error signal will be maintained at $f\Delta\tau$. Thus, one can determine the change in VCO frequency by

$$\Delta F(s) = \frac{aK_v}{s+a} E(s), \quad (3.2.3-3)$$

where the error signal $E(s) = f\Delta\tau/s$. Then the change in VCO frequency at all nodes are the same and is equal to

$$\Delta f(t) = K_v f \Delta\tau (1 - e^{-at}), \quad (3.2.3-4)$$

and the steady-state fractional change in system frequency due to the change in delay is

$$\frac{\Delta f}{f} = K_v \Delta \tau \quad . \quad (3.2.3-5)$$

If one knows the maximum amount by which any link delay may change, then Equation (3.2.3-5) can be used to determine the value of loop gain required to keep the fractional change in system frequency less than a predetermined amount. This estimate should be rather conservative, though, since Equation (3.2.3-5) was computed assuming that all delays change simultaneously by the maximum amount. Obviously, this will not happen in a large network. Some delays will be increasing and others decreasing resulting in a cancellation effect on system frequency. For the example just considered with the 1-hour acquisition time ($\omega_n = 1.67 \times 10^{-3}$ rad/s) we find that the fractional change in system frequency due to link delay variations computed from Equation (3.2.3-5) is equal to 8.3×10^{-10} for a maximum path delay variation of $\pm 1 \mu\text{s}$ (this is a good "ball park" estimate for the links on the DCS with the exception of satellite links). The calculated stability of the system frequency is adequate, and the actual stability should be much better than this bound. This trade-off and other similar trade-offs are discussed in a paper by Moreland.¹³³

Another difference with a master-slave system is that the error signal applied to the loop filter is an average of the phase errors measured with all of the links at that node. Thus, for the loop with $\omega_n = 1.67 \times 10^{-3}$ rad/s the maximum error signal was calculated to be $12 \mu\text{s}$. The worst-case would be if all links but one had significant phase error but opposite in sign from the other link which required a large phase error to generate the proper error signal. Thus, the required range on the phase detectors (and hence the buffer sizes) can be considerably different from the maximum error signal that must be applied to the loop filter. Unfortunately, there does not seem to be any way to calculate the maximum phase error on each link. Moreland¹³³ considered this problem from the viewpoint of how much the phases of nodal clocks will change relative to each other due strictly to changes in path delays. He presented the dumbbell configuration as the worst-case topology for this problem. The dumbbell topology has the nodes separated into two groups (each group being highly connected) with only one link connecting the two groups. He claims the worst-case occurs when all links connecting one of the groups of nodes experience an increase in delay while the links connecting the other group experience a decrease in delay. This can cause a much larger change in phase difference between the clocks

on either end of the single link connecting the two groups of nodes. However, once again this is a rather extreme case. In addition, what we are really interested in is the peak phase error that will be observed on any link relative to the maximum required error signal (which is $12 \mu s$ in our example). This peak phase error is probably influenced more by the relative offsets in VCO center frequencies at each node than by path delay variations.

Another important set of parameters are the phase detector weighting coefficients. Each node weights the phase errors measured by a set of relative weightings. Suppose node k has N references available. Then each of these references will be assigned a relative weight, the weight from node i being denoted by w_{ki} . At any given time, only some of these references may be available. Of course, the actual weighting of those references should reflect only the active references. Assuming a subset s of these references are active, then the active nodes should be weighted by a weight of the form $w_i = w_{ki}/w_s$, where

$$w_s = \sum_s w_{ki} \quad . \quad (3.2.3-6)$$

If the phase error measured on link i is denoted by θ_{ei} , then the error signal applied to the loop filter is

$$\theta_e = \frac{1}{w_s} \sum_s w_{ki} \theta_{ei} \quad . \quad (3.2.3-7)$$

For example, one possible weighting is to weight all references equally. In this case, if there are n active references, each will be weighted by the factor $1/n$. Equal weighting has one significant advantage in that it provides an added measure of survivability. The system frequency is not heavily influenced by a small fraction of all the nodes. One might try to obtain a more stable network frequency by more strongly weighting the most accurate clocks and the links least affected by path delay variations. This does work, but the network frequency will be more strongly perturbed by failures of these more strongly weighted nodes and links. Determining the best trade between these properties is somewhat subjective and thus difficult to do analytically.

3.2.4 Simulation Results

Some simulation results will be presented in this section to illustrate the behavior of a mutual synchronization network. These simulations were performed using the dumbbell

topology, and most used the topology shown in Figure 3.2.4. The initial simulations were done to determine acquisition behavior and to choose ξ . The parameters discussed in the previous

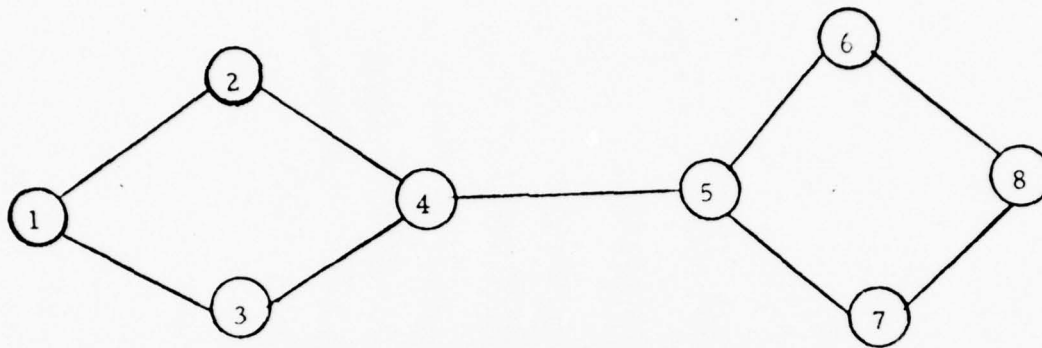


Figure 3.2.4. Eight-Node Dumbbell Network

section ($\xi = 1$, $\omega_n = 1.67 \times 10^{-3}$ rad/s) were chosen as a baseline. Damping varied about $\xi = 1$ while changing ω_n slightly to keep the -20 dB point on the closed loop response at the same jitter frequency with $\xi = 1$. The nominal frequency was chosen to be 1.544 MHz with the initial VCO fractional frequency offsets being -10^{-8} for Nodes 1-4 and $+10^{-8}$ Hz for Nodes 5-8. Phase error weightings were equal. It was found that increasing ξ increases acquisition time and the penalty by using $\xi = 1$ rather than ξ near 0.707 is about 30 percent (steady-state phase errors will also be higher by about the same amount). This seems like a good trade to obtain better stability. The very narrow loops prevent the network from exhibiting any tendency to oscillate. Thus, the values of $\xi = 1$ and $\omega_n = 1.67 \times 10^{-3}$ rad/s were chosen for the remainder of the simulations. It was found that for $\xi = 1$ the initial acquisition required 11.7 hours compared with the acquisition time for a single loop of only 1 hour. One would expect the acquisition time for any topology to be several times that of a single loop. However, this topology extends the time considerably due to the fact that the nodes on the right-hand and left-hand sides affect each other only through a single link 4 5. It is also for this reason that the steady-state phase errors build up in an unbalanced manner. The worst cases are at Nodes 4 and 5. At Node 5 the phase errors with respect to Nodes 4, 6, and 7 are -107, 36, and 36 μ s, respectively, giving an average phase error of 12 μ s. The difference between the magnitude of the individual phase errors and the average phase error indicates the difficulty of making a good estimate of the size of the individual phase errors (and thus buffers). They will be a function of both network topology which is always subject to change and the nominal center frequencies of the VCO's at

each node. Another simulation was performed to observe the change in behavior if the VCO nominal center frequencies were more randomly chosen. The VCO fractional frequency offsets were changed to $+10^{-8}$ at Nodes 1 and 2 and to -10^{-8} at Nodes 6 and 7. As a result, the acquisition time was improved by about a factor of two, and the peak with respect to other nodes is considerably reduced. Node 5 is connected to three other nodes (4, 6, and 7) each with the same nominal VCO frequency so the steady-state phase errors with respect to each of those nodes is virtually identical at about $-12.3 \mu\text{s}$. However, Node 4 is connected to nodes with differing nominal VCO frequencies. In this case the steady-state phase errors with respect to Nodes 2, 3, and 5 are $26.5-2.6$, and $12.3 \mu\text{s}$, respectively. We note that the peak phase error does not occur on the dumbbell link.

The response can be speeded up by having more coupling between the two halves of the network. This can be done through a change in the phase error weightings. A simulation was performed identical to the previous simulation, but with a different phase error weighting scheme. Nodes 2 and 3 weighted the phase error with respect to Node 4 twice that of Node 1. Likewise, Nodes 6 and 7 did the same in the other half of the network. In addition, Nodes 4 and 5 weight the phase errors measured relative to each other twice that of other nodes to which they are connected. This allows nodes at the center of the network to have more influence than those on the extremities. Thus, the system will tend to behave more like a master-slave system. In this case the acquisition time and the phase error between Nodes 4 and 5 were reduced by about a factor of 2 by changing the phase error weightings. Obviously, further improvements can be obtained by changing the weighting coefficients by a factor greater than 2. The penalty one pays in doing this is that the system will be strongly influenced by a small number of nodes and links, and thus outages on these nodes and links can cause severe perturbations in nodal frequencies.

Another simulation was done to illustrate the impact of a link dropout. Each node had the same loop parameters and VCO offset as in the previous simulations with equal phase error weightings. After acquisition was completed, Links 5-6 drop out. Before the dropout the system frequency had a very small fractional offset (2×10^{-10}) from the nominal system frequency. After the transients due to the dropout settle out (about 12 hours) the system frequency had a rather small negative offset (-10^{-9}) for a net fractional change of -1.2×10^{-9} in the steady-state system frequency. However, the transient frequency changes were an order of

magnitude higher. The reason is that when Links 5-6 drop out, Node 5 then obtains its average phase error from only Nodes 4 and 7 and Node 6 obtains its phase error only from Node 8. This causes a large step change in the average phase error driving the loop at each of these nodes. The frequencies at these nodes are most severely affected by this transient. At Node 5 the maximum value of the transient fractional change in frequency was -1.4×10^{-8} while at Node 6, the maximum value was $+1.4 \times 10^{-8}$. The magnitude of these transients are roughly the same as those encountered during initial acquisition except at the nodes far removed from the location of the outage.

Simulations were also performed using 6 and 10 node dumbbell networks to determine the effect of network size. As one might expect, we found that the acquisition time and individual phase errors increased with N , the number of nodes. For the frequency offsets we used, we found that the steady-state phase error between the two dumbbell nodes behaved as

$$\phi_e = 31 N^{0.9} \mu s \quad (3.2.4-1)$$

This could not be interpreted as a general rule since the phase error would depend on both topology and phase error weighting coefficients, but it indicates again the difficulty of estimating the individual phase errors.

The most severe problem observed thus far is that link and node outages can cause severe perturbations in nodal frequencies. If the nominal frequency of the VCO at a node is significantly offset from the network frequency, then any outage that causes removal of one of its references causes a step change in the phase error driving the loop filter. This, in turn, causes a significant change in the nodal frequency which eventually impacts the frequencies at all other nodes. However, one can probably reduce the magnitude of this transient by not allowing such a large step change in phase error be applied to the loop filter. This might be done by slowly forcing the phase error due to the lost link to approach zero. In addition, the weighting coefficients should not be abruptly changed but should be gradually changed over a period of time to the desired value. The time frame over which this should occur has not been determined at this point but should be a significant fraction of the network settling time which for this example was about 12 hours. A similar approach would be required when the link becomes operational and its reference is used again. Of course, implied in this approach is that the phase error stored due to the lost reference is accurate. One would have to provide measures

to ensure that the phase error did not drastically change just prior to the outage. However, even if this approach could virtually eliminate the severe transient, then one would still have the permanent change in system frequency caused by the dropout. The magnitude of this change was about an order of magnitude less than that of the transient. This technique above for reducing the magnitude of the transient will help to some extent, but it must be evaluated further before good estimate of its value can be obtained.

A summary of loop parameters for the mutual sync approach is given in Table 3.2.4.

Table 3.2.4. Loop Parameters for the Mutual Sync Approach

$$\xi = 1, \omega_n = 1.67 \times 10^{-3} \text{ rad/s}$$

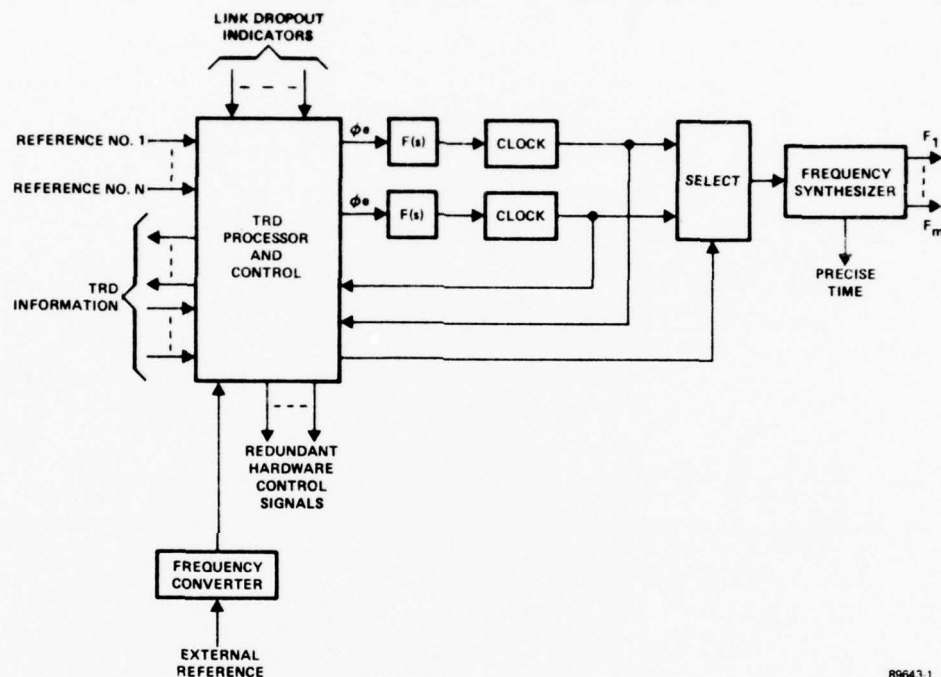
For a fractional frequency offset of 1×10^{-8} , these parameters give a steady state phase error of $2 \mu\text{s}$.

3.3 Time Reference Distribution Trade-Offs

In this section we address the implementation of a time reference distribution approach for network synchronization. Conceptually, the approach is quite similar to the master-slave approach, and some of the trade-offs are similar to those made for the master-slave system. A TRD-type system has been implemented in the Canadian Dataroute and is working quite well.

3.3.1 Time Reference Distribution Block Diagram

A block diagram of the nodal timing subsystem for time reference distribution is shown in Figure 3.3.1. Again, a dual redundant clock system is shown but more than two clocks can be utilized to increase reliability if required.



89643-1

Figure 3.3.1. Time Reference Distribution Timing Subsystem Block Diagram

An error measurement device is shown which performs the function of measuring the timing error (or difference in precise time) between the local clock and each of the N incoming references. This is done using the following double-ended technique. First, each reference carries periodic timing marks, e.g., the framing pulses on a multiplexed data stream. Assume that Node b is measuring its error with respect to Node a . The time of the clocks at these nodes are T_a and T_b , and the link delays from a to b and from b to a are D_{ab} and D_{ba} , respectively. Then the time differences measured at each of these nodes between the local clock and the received timing marks are

$$\Delta T_a = T_a - T_b + D_{ba} \quad (3.3.1-1)$$

and

$$\Delta T_b = T_b - T_a + D_{ab} \quad (3.3.1-2)$$

These measured timing errors contain an error term due to link delays, but they can be used to find the actual timing difference between Nodes a and b. Thus, these measured quantities are transferred to their respective TRD control elements which then exchange this data. This is done at all nodes for the measured timing errors on all incoming references.

The TRD control element is also shown accepting TRD orderwire information associated with each of these references. This information allows the processor to adaptively select the best one of the incoming references. Assume that Node b has selected to use Node a as a reference which, in turn, is referenced to the network master through another path. Then the control element at Node b can compute its actual timing error relative to Node a as $(\Delta T_a - \Delta T_b)/2$. A unique feature of TRD is that Node b can then calculate its timing error relative to the network master if it knows the error of Node a with respect to the master (the measured but uncorrected error at Node a). The negative of the timing error at Node b with respect to the network master is estimated by

$$\begin{aligned} \Delta T_{bm} &= \Delta T_{am} + (\Delta T_a - \Delta T_b)/2 \\ &= \Delta T_{am} + T_a - T_b + (D_{ba} - D_{ab})/2 \end{aligned} \quad (3.3.1-3)$$

This is equal to the desired clock correction term if all link delays are equal in both directions and time difference measurements are perfect. All that is required to implement this is that each and every pair of nodes exchange their clock correction term with respect to the master (ΔT_{bm}). The corrections (ΔT_{bm}) are processed by an error processor which determines how fast, clock correction should be made. Numerous approaches for implementing the error processor could work. We have taken the approach that since TRD provides closed loop control of the nodal frequency, one can design the error processor as one would design a loop filter in a phase-locked loop. It is chosen to behave like a very narrowband loop. The output of this filter provides the correction voltage for the clock. Any type of clock (either atomic or quartz) may be used in the configuration

shown. The only functions that would be different would be different filter parameters and a different technique for clock correction. With an atomic clock one could provide the clock correction by either frequency adjustment of the clock or by an outboard phase shifter. From a performance point-of-view it does not matter which approach is used; they accomplish the same result.

The rest of the system is very similar to the master-slave system except that precise time is provided. The control section provides operational control of the timing subsystem and reconfigures the redundant hardware in case of failures.

3.3.2 Time Reference Distribution Tradeoffs

The time reference distribution technique is basically a double-ended master-slave system with reference to the absolute phase of the master. There are several unique advantages to this approach. The double-ended feature eliminates the effect of path delay variations on nodal frequencies. In addition, by supplying neighbors with information about the measured but uncorrected error in the local clock each nodal clock is corrected based on an estimated error with respect to the network master. This can eliminate the effects of instabilities in clocks in the path between the local node and the master. Finally, clock correction based on ΔT_{bm} allows the difference between absolute phases of the local clock and the master to be kept small, and hence precise time can be distributed. Many of the tradeoffs one must make in selecting a design for such a system are similar to those discussed in Paragraph 3.1 for the master-slave technique while others are entirely different. Some of the more significant areas where implementation decisions must be made are the following:

- Adaptive timing distribution network organization approach
- Overhead data communication requirements
- Transmission of the periodic timing mark
- Measurement of timing error
- Processing of timing error measurements and clock correction
- Clock stabilities

We have not had time in this study to perform all of the tradeoffs associated with these areas to allow a detailed design to be made. We have only performed tradeoffs in those areas which would significantly impact the comparison between TRD and the other approaches.

The purpose of the adaptive timing distribution network organization technique is to allow each node to select its best reference and thus provide TRD with a high degree of survivability. The first approach for accomplishing this was proposed by Darwin and Prim. Modifications of this technique have been proposed by Stover,²⁰⁵ The Canadian Dataroute network uses a similar organization technique.⁹² Thus, this problem has been rather thoroughly investigated, and we did not see the need for additional work. We have selected the update counter approach recently presented by Perreault. Differing approaches to the problem may organize or reorganize with different degrees of rapidity. However, the effect of a change in the approach on performance of TRD would be minor.

Based on a rough examination of the overhead requirements associated with TRD they appear to be rather small. At the sampling rates envisioned, a few hundred bit per second will be required for transmission of timing error measurements and identification of timing marks. In addition, a few hundred bits per second will be required for data transfer associated with the adaptive reorganization technique (200 b/s were required for this in the Canadian Dataroute). Thus, the overhead requirements are in the neighborhood of 1 kb/s for each reference available at a node.

The periodic timing marks could be implemented most conveniently by utilizing a multiplexer framing pattern as the timing mark and identifying the precise time of each mark through data transmitted on an overhead channel. One good candidate is the framing pattern that will be most widely available, that of the T1 data stream. One bit of the frame sync pattern is transmitted every 193 bits (or every 125 ms) in the T1 data stream. If better resolution in estimating the timing error is desired, a framing pattern from a higher level multiplexer could easily be used.

3.3.2.1 Timing Error Processing and Clock Correction

Stover²⁰⁵ has suggested that the timing error samples (ΔT_{bm}) as given in Equation (3.3.1-3) measured with respect to the master clock be processed and used to correct the phase of the local clock. As mentioned previously, we have chosen to implement the error processor as one would implement a loop filter. Although we believe our approach to be a very good one, we are not arguing that it is optimum. One could use other approaches for error processing that would work very well. The filter we have chosen has characteristics very similar to that we have chosen for the master-slave approach. This approach allows a frequency offset to be tracked with zero steady-state timing error, and a linear frequency drift to be tracked with a constant error proportional to $1/\omega_n^2$. In establishing the parameters for this technique, we will use much of the analysis developed in Paragraph 3.1.

The following analysis assumes an analog implementation. Actually, the timing error samples will be taken at discrete intervals, but they will be taken so frequently relative to the loop time constant that the behavior will closely approximate that of an analog system. After establishing the desired parameters, we will determine how often phase error samples must be taken.

The error processing filter we have selected is shown in Figure 3.3.2.1. It is just an integral plus proportional filter. If timing errors ΔT_{bm} measured in NS are fed to the filter, a

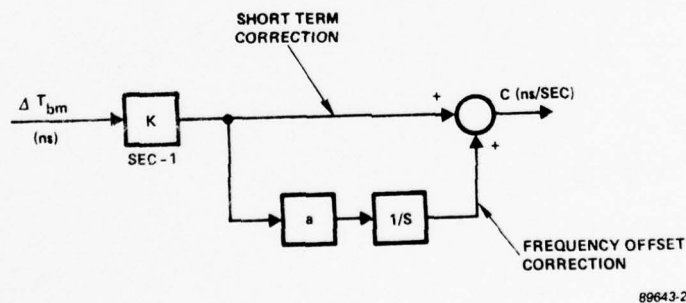


Figure 3.3.2.1. Error Processing Filter for TRD

correction term C in nS/s appears on the output. As indicated the proportional term performs the short term phase correction while the integral term performs the correction for a frequency offset between the local clock and the master. The time constants for these two correction terms can be made considerably different by choosing a $\ll k$ (i.e., selecting a large value of ξ).

We have determined two sets of filter parameters, one set for cesium clocks and another set for quartz clocks. The accuracy of cesium clocks is typically 1 part in 10^{11} . The network master will be cesium, and, therefore, the nominal frequency of any other cesium clock in the network will be offset from the frequency of the master by at most 2 parts in 10^{11} . Thus, the inherent high degree of accuracy of cesium clocks ensures that they will not have to acquire from large frequency offsets. Since these clocks are highly stable, the parameters will be chosen such that the nodal frequency will not deviate much from the frequency of the network master (by no more than a few parts in 10^{11}).

We are principally concerned with the behavior of this system acquisition from phase and frequency offsets. This behavior is identical to that of a type two phase-locked loop. The peak frequency change, Δf_p , due to a step change in phase is given by Equation (3.1.2-17). Step changes in phase can be introduced by a change to another reference link, but these should be much less than $1 \mu\text{s}$. Rapid changes in link asymmetries and measurement errors can also cause phase steps at the input to the loop, but the magnitude of these should be much less than that caused by a change in reference. Assume, for the moment, that the loop parameters used in the master-slave system are chosen ($\xi = 4$ and $\omega_n = 5.6 \times 10^{-5} \text{ rad/s}$). Then

$$K = 4.5 \times 10^{-4} \text{ s}^{-1} \text{ and } a = 7 \times 10^{-6} \text{ s}^{-1}$$

The peak frequency change due to a $1 \mu\text{s}$ phase step is a fractional frequency change of $K\Delta T_{\text{bm}}$ or 4.5×10^{-10} . It would be desirable to reduce this frequency swing by about an order of magnitude. This can be done by reducing the product K by an order of magnitude. The large value of ξ was chosen in the master-slave system to prevent a large accumulation of jitter due to path delay variations. Since these variations are removed by TRD we do not need to make ξ so large. From Figure 3.1.2.2 we see that if $\xi = 2$ is chosen, we can still keep the peak value of $|H(\omega)| < 1.05$. Thus, $\xi = 2$ can be chosen without causing much jitter accumulation. Assuming this value of ξ is chosen, then by reducing ω_n by a factor of 5 to $1.12 \times 10^{-5} \text{ rad/s}$ the fractional frequency

instability caused by a $1 \mu\text{s}$ phase step can be reduced by a factor of 10 to 4.5×10^{-11} . Of course, smaller phase steps will cause proportionately smaller swings in frequency.

To see if these parameters were entirely satisfactory, we also checked the peak phase error that occurs during acquisition from a frequency offset. The peak phase error for the overdamped loop is given by Equation (3.1.2-16). For a large value of damping, this is approximately

$$\Delta T_{\text{peak}} \approx \Delta f / K f_o \quad (3.3.2-1)$$

The loop should not have to acquire from any fractional frequency offset greater than 2×10^{-11} since the master will also be cesium. Then from Equation (3.3.2-1) the peak timing error during acquisition is

$$\Delta T_{\text{peak}} = 0.44 \mu\text{s} \quad .$$

This is well within the goal of keeping all nodal clocks within $\pm 2 \mu\text{s}$ of the network master.

TRD can also be used with quartz clocks, but the lower stability of the quartz clocks will force a change in filter parameters. The principal problem is frequency drift. Assume for the purposes of this discussion that the crystal VCO has a drift rate of 1 part in 10^{10} per day. For the loop parameters found above for the cesium clock, the steady-state phase error caused by the drift is found from Equation (3.1.2-21) to be $\epsilon_{ss} = 9.23 \mu\text{s}$ which is unsatisfactory. This steady-state error can be reduced by a factor of 100 by increasing ω_n by a factor of 10 to $\omega_n = 1.12 \times 10^{-4} \text{ rad/s}$. With this value of ω_n we find that the peak frequency swing due to a one cycle phase step has increased by a factor of 10 to a fractional instability of 2.9×10^{-10} over that obtained with the cesium clock. This is still good frequency stability. However, the crystal clocks may have to acquire from initial frequency offsets as high as a few parts in 10^8 . From Equation (3.1.2-16) we find that during acquisition from a fractional frequency offset of 2×10^{-8} the peak phase error with these loop parameters is $39 \mu\text{s}$ which is too high. A wider bandwidth fast acquisition mode for crystal clocks is desirable. The same strategy used with the master-slave approach should be adequate for TRD. If the phase error gets larger than $2 \mu\text{s}$ then the loop will switch to an acquisition bandwidth with loop parameters $\xi = 0.707$ and $\omega_n = 0.007 \text{ rad/s}$. The initial phase offset on the acquisition loop will cause a peak frequency swing of 6.4×10^{-9} . Close lock will be achieved in 30 minutes.

Table 3.3.2-1. TRD Error Processing Filter Parameters

Cesium Clocks

Only tracking parameters are used

$$\omega_n = 1.12 \times 10^{-5} \text{ rad/s}, \xi = 2$$

These give $K = 4.5 \times 10^{-5} \text{ s}^{-1}$ and $a = 2.8 \times 10^{-6} \text{ s}^{-1}$.

This gives a peak frequency error of 4.5×10^{-11} when a step of $1 \mu\text{s}$ of phase offset is applied. They give a peak phase error of $0.44 \mu\text{s}$ when a fractional frequency step of 2×10^{-11} is applied.

Quartz Crystal Clocks

Tracking $\omega_n = 1.12 \times 10^{-4} \text{ rad/s}, \xi = 2$. This results in $K = 4.5 \times 10^{-4} \text{ s}^{-1}$ and $a = 2.8 \times 10^{-5} \text{ s}^{-1}$. For drift rate of 1×10^{-10} per day, these parameters provide a steady-state phase error of $0.09 \mu\text{s}$.

Fast Acquisition $\omega_n = 0.007 \text{ rad/s}, \xi = 0.707$. This results in $K = 0.001 \text{ s}^{-1}$ and $a = 0.005 \text{ s}^{-1}$.

These parameters were used in the simulations for comparisons with the other techniques. It is possible that one could make several improvements on this approach. For example, Stover¹⁷⁰ has indicated that it will probably be desirable for a node initially entering the network to make a step phase correction to its clock. This can easily be done and will avoid the transient associated with acquisition from a phase offset. In addition, it may be desirable to use a much longer time constant on the integrator for cesium clocks (decrease a). This will have the effect of making frequency offset corrections as a result of a much longer averaging time. An averaging time of several weeks could be used. Then if the reference is lost, the clock corrections will continue to be made by the integrator output and they will be the result of estimating the frequency offset between the local clock and the network master over a several week period. Of course, this change in the value of a can be made without changing the value of K so the short-term phase corrections would not be changed much. All that has to be done is to increase ξ and decrease ω_n by the same factor.

These loops are digital loops and thus the sampling rate must be chosen high enough relative to the filter time constants. The shortest time constant in the system is that of the acquisition mode for crystal clocks. The time constant is $\frac{1}{\xi \omega_n} = 202$ s. Six to eight phase error samples per time constant is adequate to approximate analog performance. However, assume that we oversample and input a sample every 20 s to the loop filter. Each sample should be as accurate as possible, so to achieve greater accuracy it should be an average of many samples. It is well known that if one is trying to estimate a quantity from independent noisy measurements that the standard deviation of the average value of n measurements is $1/\sqrt{n}$ times the standard deviation of a single measurement. If we assume that each timing error measurement can be made to within 100 ns, then by making 10 measurements per second and averaging 200 such measurements every 20 s to obtain an average timing error, the measurement error can be reduced to 7 ns. While these numbers may not reflect the system one might design, they indicate the tradeoff between measurement error and sampling rate. If measurement error is greater, then one can increase the number of samples/second to obtain the same accuracy of phase error samples at the input of the loop filter. The penalty one would incur by increasing the sampling rate would be increased overhead data transmission.

3.3.3 Effect of Link Asymmetries

One of the significant advantages of TRD is that being a double-ended system, it removes the effect of path delay variations on nodal frequencies. However, in doing this, it does become sensitive to asymmetries in reciprocal path delays. The link asymmetries may be classified into three groups.

- Fixed asymmetries in equipment delays
- Variable asymmetries in equipment delays
- Variable asymmetries in path delays of transmission links

The phase error measured at any node with respect to the master is given by Equation (3.3.1-3). The effect of an asymmetry is the change the phase error estimates by the quantity $(D_{ba} - D_{ab})/2$. Thus, the effect on TRD of a change in link asymmetry by a certain amount is identical to the effect on a master-slave system (with the same loop parameters) of a change in path delay of the same magnitude.

Fixed asymmetries in equipment delays for the two directions of a link are due to slightly different signal transit time through hardware such as transmitters, receivers, multiplexers, and demultiplexers. One should consider these effects when deciding where to make the phase error measurement. Thus, making this measurement at the highest multiplexing level may be best.

Although they are typically rather small, fixed asymmetries in equipment delays will cause a one-time frequency transient during acquisition as a result of having to acquire a phase offset. This will cause a permanent error in the precise time kept at the node equal to half the magnitude of the asymmetry, but it will not affect the nodal frequency after the initial transient. However, if the node needs to acquire a reference on another link, then the different asymmetry will cause the loop to have acquired from another phase offset which again causes a one-time frequency transient. These effects can be eliminated by measurement of the asymmetries and allowing the phase error estimator to account for them in calculating the phase error.

To optimize performance variable asymmetries in equipment delays should be accounted for in estimating phase error. One case of significance is when a TRD node is referenced to another TRD node through an intermediate node which does MUX-DEMUX operations but does not have a TRD nodal timing subsystem. Assume, for the moment, that the framing bit on a T1 data stream is used as the timing mark. Then the delay through the node in the two directions may be unequal due to different buffer delays in the two directions. One can envision several approaches for handling this problem. These buffer delays should be measured periodically at the intermediate nodes and reported via an overhead channel to the other nodes concerned so that corrections to the phase error estimate can be made. Another approach, would be to provide elastic buffers in the transmit channel and provide the necessary control for ensuring that the buffer fill in each transmit channel is such that the delays in both directions of all TRD paths through the node are equal.

The magnitude of variable asymmetries in path delays of transmission links should be much less than the magnitude of one-way path delay variations. For a satellite link, there is considerable variation in total path delay, but since the link is LOS, there will be no asymmetry in path delay. A microwave link is also LOS, and there will be very little variation in total path delay as well as link asymmetry. Cable is subject to path delay variations due to temperature changes. However, the delay is affected in the same manner in both directions

and there are no changes in link asymmetry. For each of these types of links, the TRD system should perform much better than the master-slave system. In a link with scattered propagation such as a tropo asymmetries may occur, but no measurements of reciprocal link delays for tropo have been made. However, consider a link where the path delay of a link can vary by $\pm\Delta D$ about the nominal delay, D . The worst-case asymmetry occurs when the path delay in one direction is $D + \Delta D$ while the delay in the other direction is $D - \Delta D$. The total asymmetry is $2 \Delta D$. The total asymmetry is $2-D$ and contribution of this asymmetry to measurement error is ΔD . Note that this will affect the nodal frequency for TRD in the same manner as a change in path delay of ΔD would affect the master-slave system. However, to have this occur would require that the delay in one direction of the link change by $+\Delta D$ while the delay in the other direction of the link changes by $-\Delta D$. This situation is much less likely to occur than having a single link change by ΔD which would affect a master-slave system in the same manner.

In summary, fixed asymmetries which are not calibrated out cause a steady-state error in the precise time of nodal clocks. These errors can cause transients in nodal frequencies during acquisition but no perturbations thereafter. Variable asymmetries which are not calibrated out can cause perturbations in nodal frequencies in much the same way that path delay variations can cause perturbations in nodal frequencies in a master-slave or mutual sync systems. However, since the magnitude of the asymmetries is much less than the magnitude of path delay variations, the resulting perturbations are less.

SECTION 4.0
DESIRABLE CHARACTERISTICS

4.0 DESIRABLE CHARACTERISTICS

A number of characteristics have been identified that if possessed by a timing subsystem would be considered advantageous from a system viewpoint. These desirable characteristics, although not necessary for the provision of a minimal level of performance, do enhance the overall utility of the timing subsystem. The desirable characteristics are survivability, limited error propagation, compatibility with other global timing subsystems, precise time availability, stability, monitorability, minimum susceptibility, flexibility, interoperability and maximum availability. In the paragraphs below, each of these characteristics is defined and is justified as being important in the overall subsystem evaluation. In a subsequent section, each of the alternative techniques is evaluated with respect to the degree to which it provides these desirable characteristics.

4.1 Survivability

Survivability indicates the degree to which the timing subsystem continues to perform its function (to provide network timing) during periods of stress. Fallback modes of operation shall be provided so that the timing subsystem itself will not cause significant degradation in overall DCS network capability during these periods.

There are two main reasons why this characteristic is important:

1. One of the primary goals of the DCS is to provide dependable digital communications for its users during periods of network stress.
2. The network timing subsystem must be operational to provide acceptable digital communication during such periods.

Of course, the reason that network synchronization is necessary is that the slip rate that two nodes will experience in communicating is directly proportional to the frequency offset between their nodal clocks. If this offset increases in a stressed environment, then bit slips increase which lead to misaligned frames in multiplexers and switches and a need to resynchronize cryptos. If the slip rate becomes excessive, data traffic will experience an unacceptably high error rate and the quality of voice transmissions will degrade significantly.

4.2 Error Propagation

It is desirable to prevent disturbances (such as stresses or path delay variations) in one part of the network from propagating and influencing the phase of nodal clocks in other parts of the network.

This is an important characteristic because in preventing the propagation of perturbations in nodal frequencies from node to node throughout the network one maximizes the stability of each nodal clock and minimizes the buffer size required to achieve a desired slip rate. The parameter that will be used as a measure of error propagation is the offset in phase of each nodal clock from their steady state values as a result of certain network stresses.

4.3 Compatibility With Other Global Timing Subsystems

This characteristic refers to the degree with which the DCS network frequency and/or precise time agrees with that provided by other global Navigation/Timing Systems such as Loran-C, Omega and GPS.

There are two principle reasons why this characteristic is important:

1. The navigation system timing could be used as an external reference in a fallback mode thus increasing the survivability of the DCS timing system.
2. The precise time or frequency provided by the DCS timing subsystem would be available to the navigation system to increase its reliability or capability.

4.4 Precise Time Availability

Precise time can be defined as the correct absolute time as kept by a standards laboratory such as the USNO. The timing subsystem could be designed to acquire and disseminate precise time from the USNO within some margin of error. The availability of and accuracy of the precise time thus distributed throughout the network is a characteristic by which we shall evaluate the timing subsystems.

There are four main reasons why this characteristic is important:

1. The network is automatically referenced to UTC and has the advantages of better interoperability with other networks referenced to UTC and compatibility with other global timing systems.
2. Precise time is useful in assisting synchronization of spread spectrum equipment and in providing synchronization for TDMA networks.
3. Precise time would be more widely available to those users of precise time within the government. This will simplify their problems of updating their precise time standards.
4. Navigation systems could use the DCS timing to increase their reliability and capability.

4.5 Stability

The DCS timing subsystem must be a stable system (as a feedback control system).

This is important because if the system were not stable, then a number of bad things could happen such as nodal clocks being continually pulled off in one direction or simply being unable to maintain network synchronism. The result of such an occurrence would be buffer overflows and therefore, continual bit slips.

The mutual synchronization approach has closed feedback loops and stability is of concern here. However, stability can be nominally guaranteed by proper selection of the loop filter in the phase-locked loops. The question of whether stability is a problem under certain network stresses for this technique or whether it is a problem for the other approaches which transmit control information from node to node (for example, to modify the timing distribution chain) does need to be examined. We must prove the stability of each alternative. If there is any possibility of instability, we must determine what can be done to ensure that this does not happen.

4.6 Monitorability

Monitorability is the level to which the timing subsystem can provide data used in assessing its own performance. It is apparent that monitorability is valuable at least to the

extent that an option such as a redundant piece of equipment or an alternate link is available and can be utilized as a result of decisions made on the basis of monitored information.

Monitorability is a significant characteristic because it can lead to greater availability. If potential failures can be identified prior to failures actually occurring, these situations can be remedied on an off-line basis. The result is therefore both an increase in MTBF and a reduction in MTTR and therefore a greater availability.

4.7 Susceptibility

Susceptibility is the degree to which the timing subsystem may be spoofed, jammed or disrupted by an enemy via electronic means as well as disrupted due to natural phenomena.

Because of the critical nature of the DCS mission, it is apparent that it could be a focal point of enemy action during conflict. Therefore, susceptibility is a key characteristic. Any timing subsystem that by its nature increases the susceptibility of the DCS as a whole represents a significant handicap. Slip rate will again be the measurable quantity in evaluating susceptibility. The evaluation consists of measuring the rate of accumulation of phase error between the nodal clocks (slip rate is directly proportional to the rate of accumulation of phase error between the nodal clocks at two nodes and inversely proportional to the buffer size) under a variety of possible stress scenarios.

4.8 Flexibility

Flexibility is the degree to which the timing subsystem is compatible with the orderly implementation, growth and extension of the future synchronous switched digital DCS.

Flexibility is an extremely important characteristic as a result of both the time frame for eventual utilization and the transition period during which the system must operate effectively. The timing subsystem itself is aimed at a system to be operational in the 1980's and until then, daily traffic consisting of voice and data must be accommodated by the system.

4.9

Interoperability

Interoperability is the degree to which the timing subsystem influences the traffic interface between DCS and other military and commercial communications systems.

Interoperability is a significant characteristic since a portion of the DCS traffic will traverse both DCS as well as other systems (i.e., Tri-Tac) between origination point and destination point. Furthermore, the DCS consists of both leased facilities (CONUS) and owned facilities (OCONUS). The degree of design independence and control is far greater in the owned facilities than in the leased facilities. Thus, there will be a major interface within the DCS itself.

4.10

Availability

Availability is the quotient of mean-time-before-failure (MTBF) and the sum of mean-time-before-failure (MTBF) and the mean-time-to-repair (MTTR). Availability is a significant characteristic for all major systems and its importance is apparent for the timing subsystem by nature of the mission of the DCS.

SECTION 5.0
NETWORK CONFIGURATIONS

5.0 NETWORK CONFIGURATIONS

This section delineates the network configurations that will serve as the test beds in which the performance of the alternative timing techniques will be evaluated. Each network configuration has been chosen to combine realism with relevance. Realism meaning that the configuration represents an interconnection of nodes that is representative of a world wide communications network or portions thereof. Relevance being defined as aiding in the selection process between alternative timing techniques. That is, the network configurations have been chosen with the purpose of highlighting strengths and weaknesses of the various timing techniques.

To completely specify the network configuration for the simulation the following parameters have to be defined: the connectivity arrangement between the nodes, the distance between each pair of connected nodes, the bandwidth of each link, the type of transmission media used between each pair of connected nodes and an indication as to which nodes are external to the DCS (and therefore links to these nodes constitute interface links).

The method that has been selected to specify these configurations is to initially choose a set of connectivity patterns. These patterns are each appropriate combinations of the subpatterns (ring, fully connected, star) discussed in Section 11.0. The connectivity patterns that have been chosen are shown in Figures 5.1-1 through 5.1-5 and are described in following paragraphs.

5.1 Network Connectivities

a. Dumbbell Node Configurations

The Dumbbell Node Configuration (Figure 5.1-1) is so called because of its peculiar shape. It consists of two relatively congested communications areas interconnected by a relatively small number of links. In Figure 5.1-1, the left-hand grouping of nodes is primarily interconnected to the right hand group of nodes through Nodes 14 and 16. A secondary interconnection between the two groupings is made through Nodes 15 and 16. This particular type configuration is primarily found where large bodies of water or uninhabited land are crossed by communications systems. Across a body of water, for instance, the interconnecting

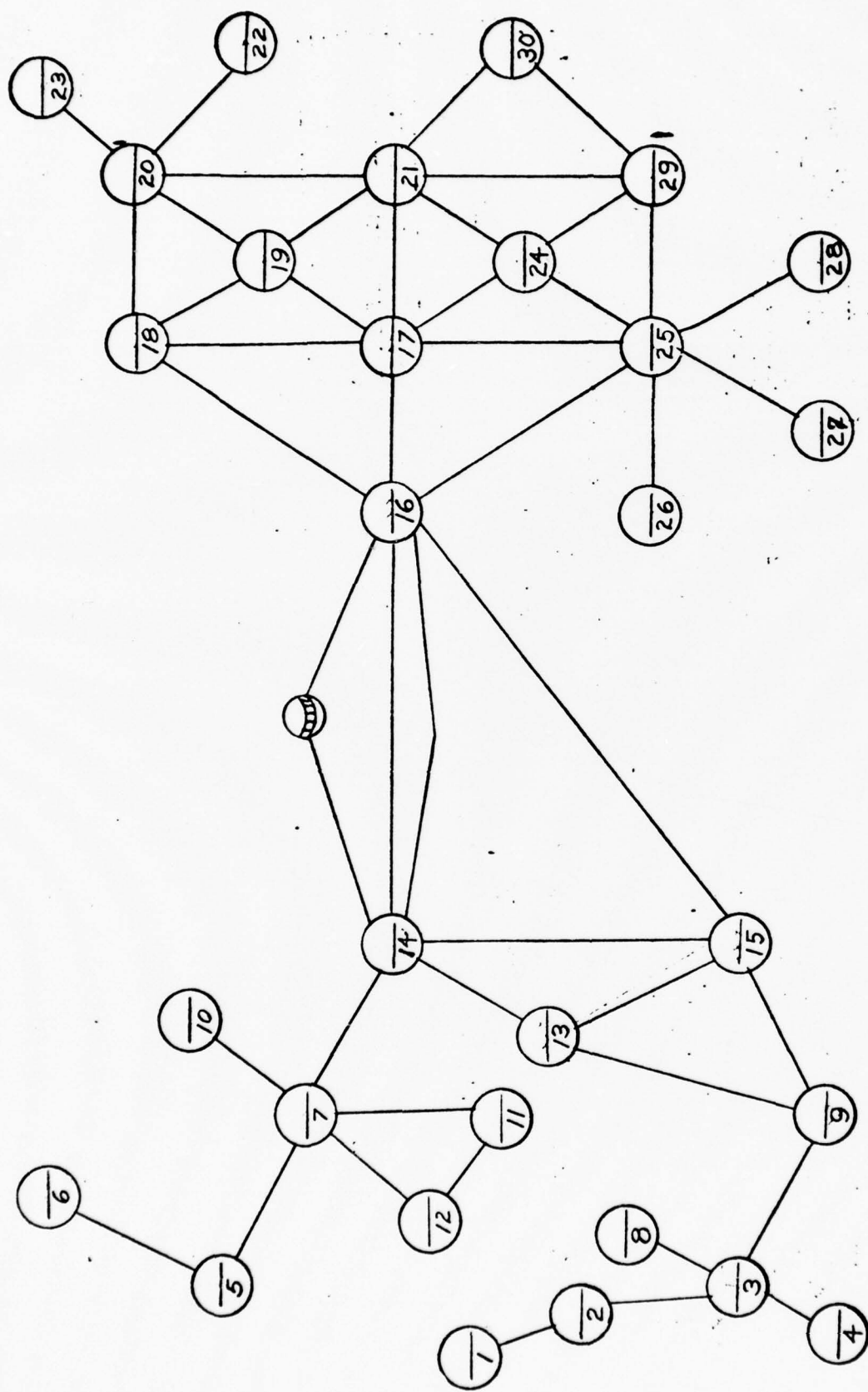


Figure 5.1-1. Dumbbell Node Configuration

links would be satellite or undersea cable. Across a body of land, it may be a microwave link or tropo or landline in place of submarine cable. The right-hand congested network is typical of a lattice-type network while the left-hand network is more random.

b. Meandering Node Configuration

The Meandering Node Configuration (Figure 5.1-2) is so named because of the backbone node path consisting of Nodes 5, 8, 14, 18, 20, 23, 24 and 29 are interconnected to a meandering path similar to a river. Each backbone node has clustered around it a number of concentrated nodes. The two extremes of the meandering configuration have little in the way of direct communications paths between them except the satellite. This configuration shows the availability of a satellite communications path connecting, for instance, Nodes 8, 18 and 29.

c. Lattice Node Configuration

The Lattice Node Configuration (Figure 5.1-3) is typical of a highly developed and congested node configuration such as would exist in CONUS or in some of the highly congested European area. It illustrates a great many interconnecting paths available between nodes. This configuration has a fluency of alternate routing paths that are beneficial in peak traffic periods and to circumvent equipment outage. In this particular figure, the large majority of nodes can easily be made to belong to the highest level in the nodal hierarchy. This results from the equivalent amount of connectivity for these nodes.

d. Ladder Node Configuration

The Ladder Node Configuration (Figure 5.1-4) gets its name from the fact that sublevel nodes are arranged in the form of a ladder. To illustrate this, look at Nodes 23, 27, 29, 24, 28 and 30. These form the sides of the ladder and the interconnections between the nodes such as 27 to 18 and 29 to 30, form the rungs of a ladder. There are two ladder configurations shown on this diagram; one on the left side consisting of Nodes 1, 2, 3, 4, 5, and 6 and the one previously discussed on the right. The remaining nodes have been added arbitrarily. This configuration can illustrate the problems encountered when two of the lowest-level nodes (i.e., 29 and 3 or 1 and 29) attempt to communicate through a number of ascending order nodes.

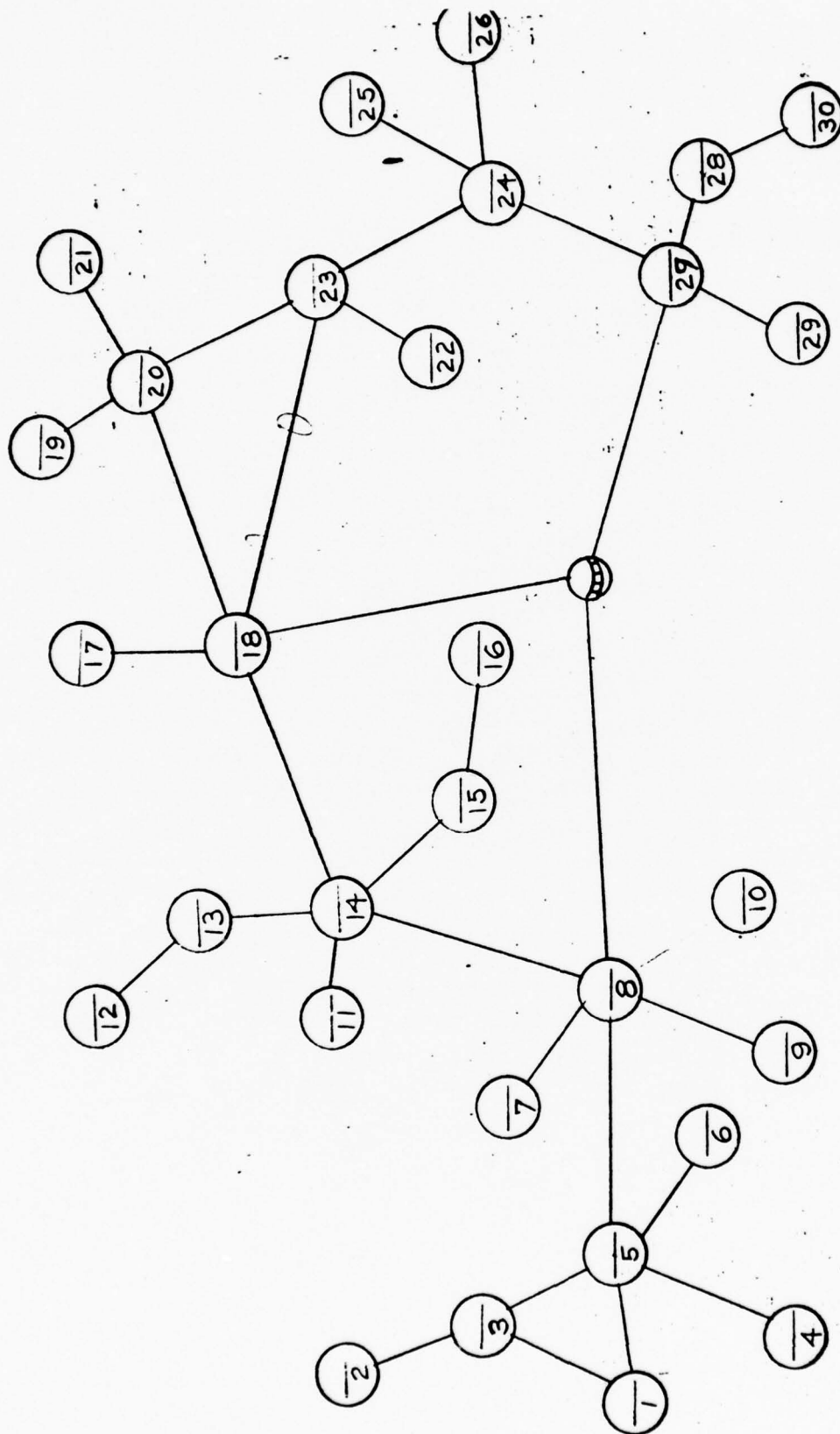


Figure 5.1-2. Meandering Node Configuration

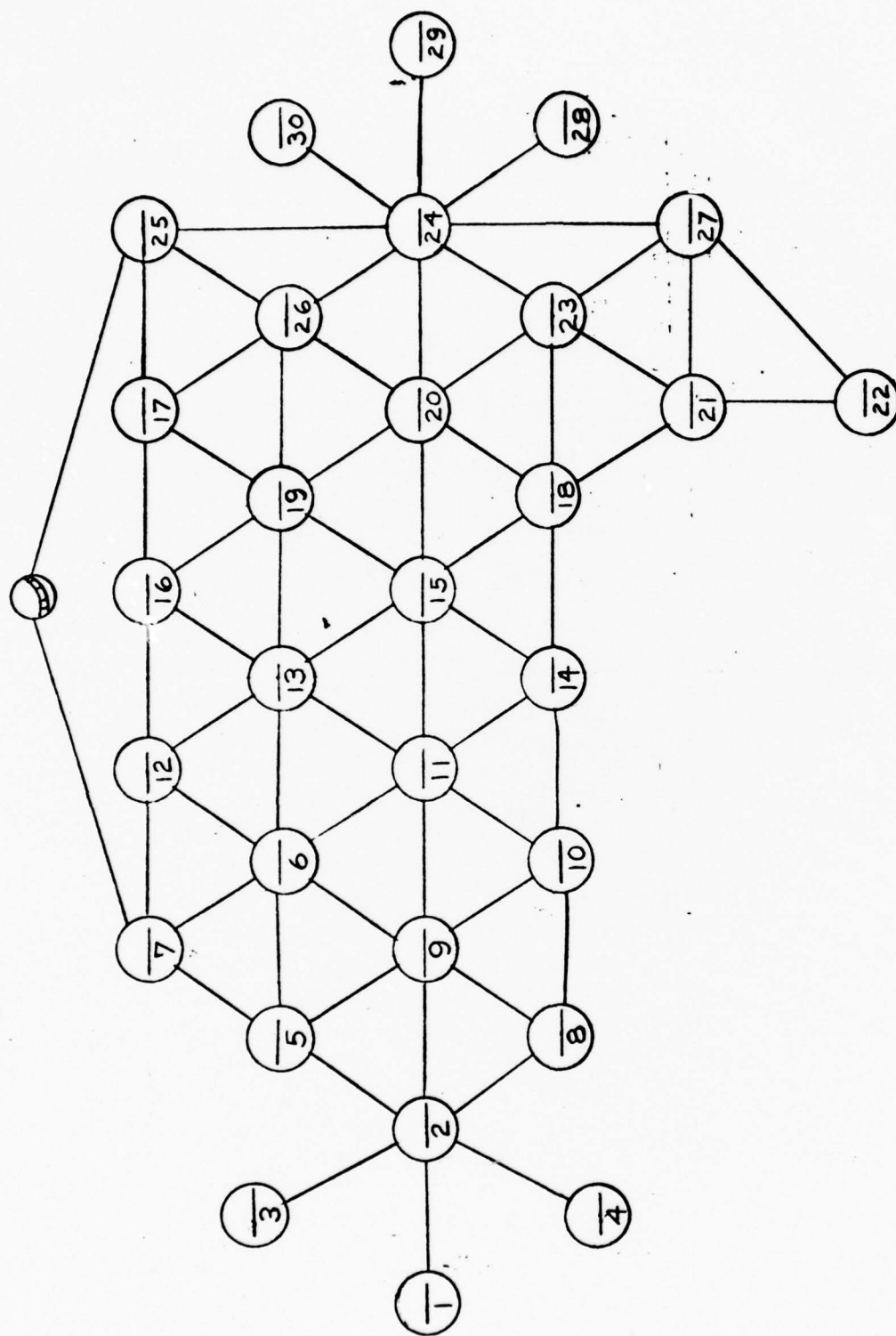


Figure 5.1-3. Lattice Node Configuration

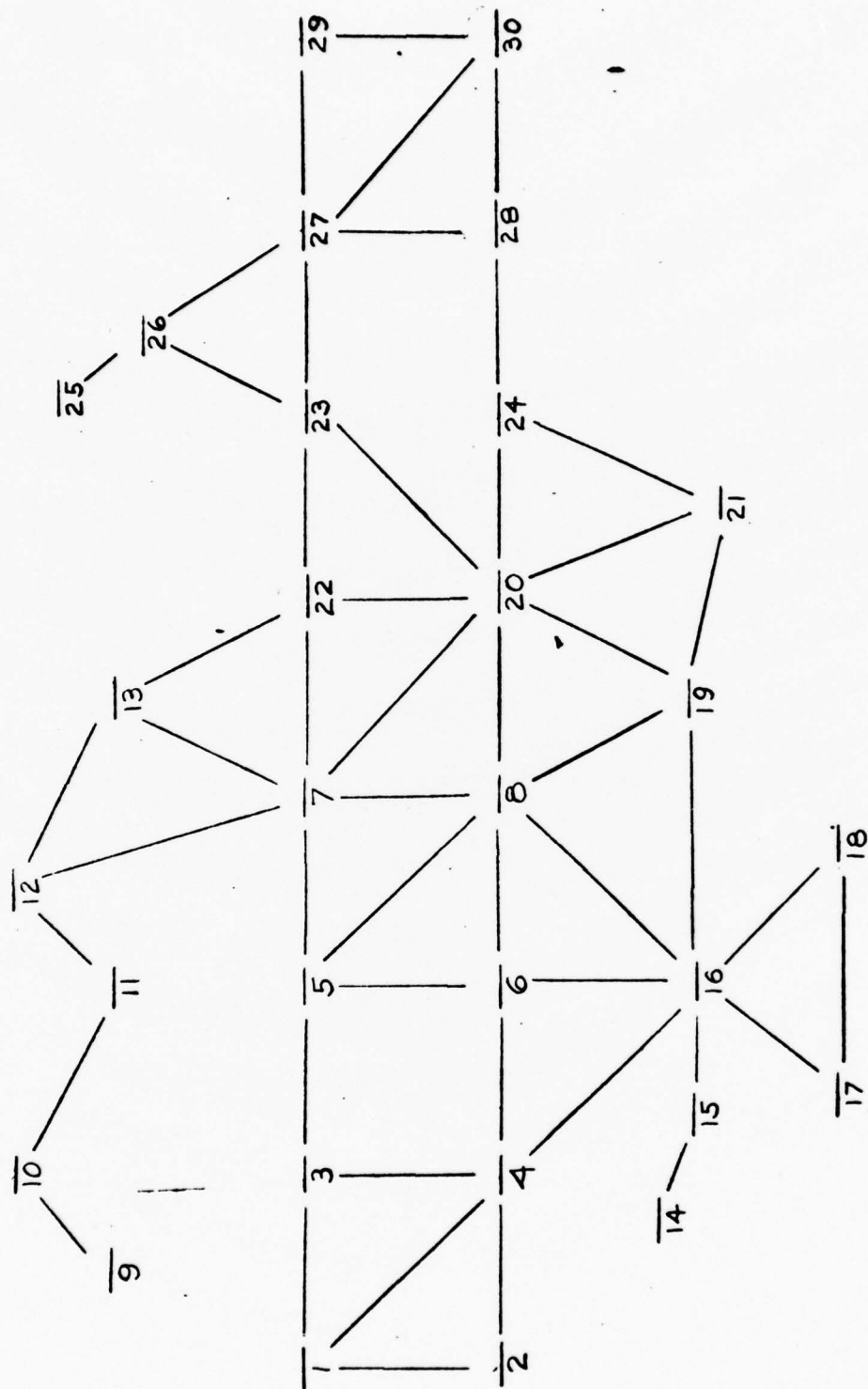


Figure 5.1-4. Ladder Node Configuration

e. Loop Node Configuration

The Loop Node Configuration (Figure 5.1-5) consists of a number of cross-connected loops. This particular configuration would be employed in a packet-switching type system where the links looping several nodes together would act as a bus to carry information around the loop. In this node configuration, the loops are cross-connected such that the loss of any one link will not isolate any node and the loss of two links will not isolate more than one node. In this particular configuration, Nodes 8, 10, 18, and 25 have more interconnecting links terminating at these nodes than the other nodes. This would indicate these nodes originated more traffic than the other nodes.

5.2 Other Network Configuration Parameters

Each of the network configurations consists of thirty nodes. The choice of 30 node networks was made as a realistic compromise between computational capability (in the simulation) and the achievement of relevant results.

The network connectivity patterns described above are key elements in specifying network configurations but they do not completely specify the configuration. In order to accomplish this, the type of link, link bandwidth and link distance must be specified for each pair of connected nodes. The types of links that will be included in the network configuration are LOS Microwave, cable and wire line, tropospheric and satellite.

Each is characterized by different propagation delay variations. The link distances will vary from approximately 44,000 miles for a satellite link to perhaps 10 miles for the wire or microwave link between a lower level node and the node to which it is slaved. The principal bit rate for the various links will be 1.544 Mb/s.

For each of the connectivity diagrams shown, appropriate combinations of link media, bit rates, and distances have been chosen. These are described in the section on simulation. Thus, a single connectivity diagram may define, by changing these parameters, one, two, three or more network configurations. Each network configuration so defined will serve as a test bed in the computer simulation to aid in the evaluation of the performance of the candidate timing techniques.

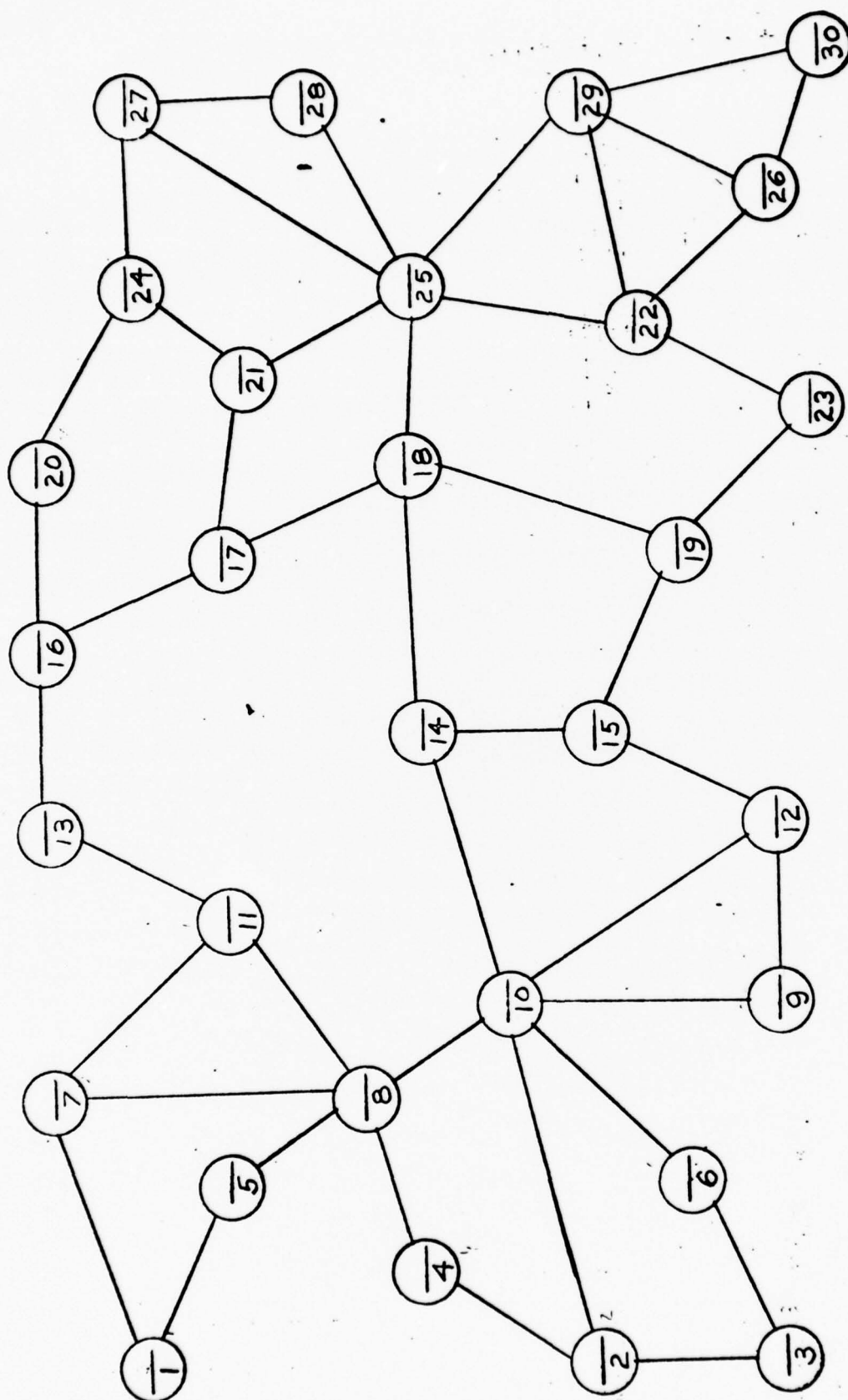


Figure 5.1-5. Loop Node Configuration

SECTION 6.0
OPERATING AND STRESS SCENARIOS

6.0 OPERATING AND STRESS SCENARIOS

6.1 Introduction

The ultimate objective of the scenario approach is to provide rigor to the process whereby a candidate technique or combination of techniques may be selected on the basis of performance, cost and other parameters for deployment as a prototype timing subsystem with reasonable assurance that the proper parameters have been addressed with appropriate emphasis. The ground rules for the general scenario development program include:

1. Scenarios will postulate an initial benign environment and progress through discrete changes in environment to maximum levels of anticipated stress.
2. Scenarios will be designed to address a limited number of parameters at any one time, holding all other parameters constant - thereby addressing a limited number of variables at any one time.
3. Scenarios must accommodate a dynamic environment where stresses cause transition (or no transition) from a prestress steady state to a poststress state, which may be stable or unstable.
4. Scenarios must pose stresses that are relevant and representative and approach the real world environment.

As indicated by the ground rules above, it is appropriate to evaluate the relative performance of the timing schemes initially in a peacetime environment and progress from the most minor perturbations on simple network configurations to more dramatic perturbations on a more complex network. In order to address a limited number of parameters at any one time, it is further proposed to place geographical constraints on the scenarios, with geographically-oriented groups of scenarios being exercised prior to attempting to assess interarea operability of the NTSS. The geographical constraint leads to the three main areas of the CONUS, Europe and the Pacific region.

One group of scenarios then, will consider operation within the CONUS in peacetime in what is considered a situation of normal stress. Equipment failure and natural phenomena cause node outages, weather causes microwave fading, lightning is an ever-present source of power outage or line surges, and maintenance problems, aging devices, etc., introduce degraded operation.

6.2 Types of Perturbations

Three types or categories of perturbations will be examined. These are the loss of a node, a change in clock frequency and link anomalies. For each category there are at least two and perhaps several specific perturbations within the category. With respect to the loss of a node either a major or an intermediate node may be considered. For changes in clock frequency, an impulsive change, a step change, or a change in drift rate may be considered. In the case of an impulsive change it may take place at a single node or simultaneously at a large number of nodes. The link anomalies category would include fading on a microwave link, path delay variations and jamming.

Perturbations that can impact the primary and/or secondary timing standard and associated circuitry in the peacetime "normal operation" mode include problems of routine operation and maintenance and the inherent stability (drift, aging) of the devices involved. In addition, the effects of direct nuclear radiation (X-rays, neutrons, and gamma-rays) as well as the electromagnetic effects of the electromagnetic pulse (EMP) must be considered.

Those perturbations that impact the communications node itself and which can cause a collateral effect on the timing device or NTSS technique include lightning, with associated power related and computer operation problems, and other natural phenomena (flood, fire, etc.) leading to more catastrophic impacts. Also, prime power supply maintenance can impact the operation of the node as well as poor technical control orderwire procedures.

With reference to perturbations occurring external to the node, the most dramatic impact is expected to result from links interconnecting the node under evaluation with the remainder of the system and at nodes directly linked to the node in question. In terms of the linking problem, loss of timing information can result from natural fading phenomena in the peacetime "normal operation" scenarios.

The loss of a node, in the majority of the NTSS techniques, will require the exercising of predetermined operations, possibly to choose an alternate route to derive timing, call upon the use of the local timing source for a temporary period of time, etc. The loss of an adjoining node may cause either a degraded mode of operation for a period of time or initial acceptable performance which degrades with time.

6.3 Scenarios

The subsections that follow list the scenarios that were considered. In each subsection the scenario is described by the event or series of events that take place; the resultant stress that is placed on the timing subsystem and the rationale for the inclusion of the particular scenario.

Scenario A

This scenario is node oriented and applicable to peacetime, CONUS, operation. Assume that improper maintenance procedures on a cesium beam tube primary standard at a major node result in the failure to degauss the electromagnetic shield.

Stress

The aging rate of the cesium standard changes over a period of 1 day to a figure of 5×10^{-10} per 24 hours, the aging rate of the associated quartz oscillator.

Rationale

In order to isolate the c-field from the earth's magnetic field and external electromagnetic environments (radar, communications, transmitters, etc.,) it is necessary to enclose the tube of the standard in electromagnetic shielding material and degauss the shield at periodic intervals to guard against saturation. Failure to do so will impact the c-field and cause a change in frequency of the primary standard. It is assumed that as soon as the threshold of electromagnetic isolation is reached, i.e., saturation, the c-field will be impacted by the surrounding electromagnetic environment with a resultant change in basic frequency. As the external environment changes, the frequency of the atomic standard will change and the crystal oscillator will track within its limits of control. If these limits are exceeded, the assumption is made that the aging rate of the device becomes the aging rate of the associated quartz oscillator.

Maintenance problems are realistic to assume and some will surely cause a change in the frequency of the primary standard. This scenario should exercise the effectiveness of all of the timing schemes anticipated for possible employment.

Scenario B

This scenario is node oriented and applicable to peacetime, CONUS operation.

Assume that a major node of the DCS employs a cesium standard in which component parameters in the dc supply change with age.

Stress

The inherent stability of the standard changes from $\pm 1 \times 10^{-11}$ for the life of the beam tube to $\pm 1 \times 10^{-11}$ per month.

Rational

The output of the primary atomic standard is derived from a highly stable 5 MHz voltage controlled crystal oscillator whose frequency is locked to the invariant resonance of the cesium atom undergoing a change in atomic state in the beam tube. The change in atomic state is highly dependent upon the application of a very precisely controlled magnetic field which, in turn, is set up by a precise dc supply. Any stress applied to the power supply which degrades its performance will impact the precise frequency of the cesium beam tube, thereby changing the error signal fed back to the voltage-controlled crystal oscillator and impacting the output frequency. For purposes of this discussion, we will assume aging of components in the dc supply as the perturbing source which results in an aging figure more appropriate to a rubidium secondary standard.

Aging of components can be expected even in very precise and well controlled equipments such as the cesium primary standard. Normally, an alarm would show this out of specification condition, however, poor maintenance procedures could subvert this safety feature.

Scenario C

This scenario is system oriented and is applicable primarily to wartime; however, it could occur in peacetime or as a precursor to war. In this case, there would be no wartime collateral effects.

Assume that a nuclear device is detonated exoatmospherically. All satellites within direct line-of-sight of the burst will be perturbed by the effects of direct radiation and all ground-based electronics will feel the effects of the classical electromagnetic pulse (EMP).

Stress

All unhardened satellites will be rendered inoperative and will not return to operation. The minimum impact to ground-based facilities is assumed to be random pulses of voltage and current on signal lines, power lines, computers and peripherals such that every node is rendered inoperative for a period of a few hundred milliseconds. All buffers are scrambled and all crypto synchronization is lost simultaneously over the entire system. No permanent damage results to nodal equipment.

Rationale

This scenario can exist either as a result of a nontreaty member testing a nuclear device exoatmospherically in peacetime or the U.S. or an adversary detonating such a device "for effect" as a precursor to warfare. The low level of stress assumed for the ground based system is a minimum stress scenario for high altitude EMP effects. Satellites will survive or be lost depending upon levels of hardness and specific satellite links will be designated as lost in the scenario. Reconstitution time of the ground based facility timing subsystem and the ease of resynchronization will be evaluated.

Scenario D

This scenario is node oriented and is applicable to wartime.

Assume that a backbone node is attacked by a team of saboteurs. The communication facility is completely and permanently disabled. Alternate routing capabilities exist for information transfer to all other major nodes of the system.

Stress

The loss of the node will require rerouting of traffic, traffic delays and may require alternate paths for the distribution of timing.

Rationale

This is a minimum stress scenario when taken in context with an entire communication system. Many nodes could be lost nearly simultaneously as a result of sabotage and direct attack.

Scenario E

This scenario is system oriented and is applicable to wartime - OCONUS.

Assume a determined jamming attack by the enemy which initially disables one backbone node, followed by a multiplicity of nodes as time progresses until 25 percent of the nodes of the system are inoperative. At a predetermined time all jamming ceases and all nodes return to normal operational capability simultaneously.

Stress

There is gradual increase in stress on a system with time until the system reaches the maximum degree of inoperability. The system is again stressed as relinking occurs at the end of the jamming attack.

Rationale

This is a routine wartime stress on any communication system located within range of ground based enemy jammers. The perturbations to the nodal timing at nodes not directly affected by the jamming will vary between timing subsystems. The magnitude, duration and recovery from this perturbation is of concern.

Scenario F

This scenario is link oriented and is applicable to peacetime.

Assume that as a result of atmospheric phenomena, a microwave communications link connecting two backbone nodes of the DCS experiences typical signal fading such that bit error rates vary as a function of time until such time as the errors become excessive.

Stress

The random variation and gradual increase in bit error rate will result in errors in timing subsystem control information and will ultimately result in loss of the link.

Rationale

This problem must be addressed routinely by any communications system using microwave links; however, its effect on the system would be much less pronounced than the loss of a physical communications node.

Scenario G

This scenario is link oriented and applicable specifically to time reference distribution. Assume that a major node of the DCS transfers time through a satellite link and the satellite fails. The node then shifts to a backup mode of access to UTC, i.e., LORAN-C.

Stress

The accuracy with which absolute time can be transferred from this node throughout the system changes from a figure of 100 nanoseconds for the satellite path to 50 microseconds for LORAN-C.

Rationale

This scenario is important to an assessment of the Time Reference Distribution Technique for peacetime evaluation. The tolerance figures would change since the access route to UTC would change from a satellite link to OMEGA, a future OCONUS LORAN-C, etc. It is realistic since many stresses will cause changes in the choice of paths through intervening nodes and links to a source of UTC. Each of the paths will offer a maximum optimum figure for absolute synchronization.

We anticipate showing that the inclusion of Precise Time Availability causes no added vulnerability to the system; on the contrary, it adds an important capability to the DCS, both CONUS and OCONUS. This scenario will help determine the applicability of an external time reference as a backup to a time reference distribution approach.

Scenario H

This scenario is node oriented and applicable to peacetime, CONUS operation.

Assume that within a specific level in a nodal hierarchy VCXO's are utilized as the clocks at each of the nodes. The short term stability of these clocks is 1×10^{-11} . Due to a local electrical power transient the short term stability of one clock degrades to 1×10^{-6} .

Rationale

Such changes in crystal oscillators are possible as a result of both electrical and mechanical transients. How this perturbation at this single node is manifested in the clocks at other nodes will vary according to timing technique. It is these variations that will be examined.

SECTION 7.0
SIMULATION

7.0 SIMULATION

7.1 Goals

The purpose of the simulation is to provide a means for studying the reaction of a complex interconnected network to various disturbances and stresses. It is mainly due to the numbers of nodes and links that must be used in a representative model that a computer simulation is deemed necessary. The two or three node case can be analyzed without such aids. Normal disturbances include clock jitter, clock drift, initial frequency and phase offsets and normal link delay variations. Abnormal stresses include clock failures, node failures, link failures and abnormal link delay variations. The simulator can also be used as a design tool by obtaining fine grained information for selection of phase-lock loop parameters, buffer sizes and clock stabilities. Further, the simulator can be used for comparing the performances of various timing techniques. The major parameters used in such comparisons include the following:

1. The speed with which the network disposes of a transient condition
2. The degree of closeness that the nodal clock frequencies are held together
3. The amount of phase error that can be found at the various nodes

During the period of recovery from a disturbance occurring somewhere in the network, the timing subsystem is more vulnerable to any other disturbances that might occur. During transient conditions, error detection equipment has a degraded frame of reference and reconfiguration apparatus is more susceptible to error in the worst-case and, at best, is subject to a delayed response. Thus, shorter transient time is a desirable feature. The ideal condition is that all clocks in the network remain exactly together. By providing receiving buffers on each link, some tolerance to temporary differences in clock frequencies may be obtained. However, any two communicating nodes must have an average difference frequency of zero if finite size buffers are used and loss of data is avoided. Thus, clocks held closely together is a desirable attribute. Small phase error at any instant of time is desirable because phase error represents a difference in clock time readings and is stored potential which may be converted to a kinetic change in clock frequencies as a result of some future disturbance.

7.2 Models

The simulator is designed to model master-slave, mutual sync, independent clocks, and time reference distribution techniques. Each model consists of a set of nodes connected together by a set of communications links. The major differences between the techniques are the manners in which reference information is obtained at each node from other nodes in the network. Secondary differences are concerned with the manner in which this information is filtered and compared with the local clock on an instantaneous basis. The characteristics of the nodal clocks and communications links are the same no matter which timing technique is utilized. Therefore, these will be discussed separately from the individual techniques.

7.2.1 Timing Techniques

7.2.1.1 Independent Clocks

The independent clocks technique uses no reference information, hence, the name. Since no two real clocks can remain together for more than a short period, occasional buffer overflow or underflow is assured with this technique. Thus, the major thing of interest under this scheme is the rate at which buffers overflow. This information can then be used to set up a convenient periodic interval within which data buffers may be reset at all nodes of the network. In the simple case in which each clock in the network is assumed to be a constant frequency offset from any other clock in the network, the amount of time to overflow a buffer of a given size between any two communicating nodes can be readily determined without the aid of a simulator. Actually, this might approximate the typical situation for this technique since high stability clocks would probably be used with this scheme, and hence would remain essentially constant over a period of time required to fill up a data buffer. Let f_1 and f_2 be the frequencies of two clocks whose nodes are assumed to be communicating and assume f_1 is the reference.

Then,

$$\phi = N \left(\frac{1}{f_1} - \frac{1}{f_2} \right) \quad (7.2.1.1-1)$$

or

$$N = \frac{f_1 f_2}{f_2 - f_1} \times \phi \Rightarrow \frac{N}{f_1} = \frac{f_2}{f_2 - f_1} \times \phi \quad (7.2.1.1-2)$$

where N is the number of cycles of f_1 . Letting $f_2 = (1 + \delta) f_1$ we obtain

$$T = \frac{N}{f_1} = \frac{(1 + \delta) f_1}{(1 + \delta) f_1 - f_1} \times \phi = \left(1 + \frac{1}{\delta} \right) \times \phi \quad (7.2.1.1-3)$$

But now for $|\delta| \ll 1$ this becomes approximately

$$T = \frac{N}{f_1} \cong \frac{\phi}{\delta} \quad (7.2.1.1-4)$$

7.2.1.2 Master-Slave

7.2.1.2.1 Dissemination of Reference Information

The master-slave technique has, superimposed on the communications network, a subset of links in the form of a tree structure over which *reference information for timing* purposes is disseminated. In the model being described, this reference timing information is assumed to be obtained from the bit transitions of the incoming data stream. However, this is not a necessary restriction on the timing technique since one data channel could be reserved to carry the timing information in some other form. Under this scheme, the amount of variation in the reference information received at each node from that of the master clock should increase as the tree level number increases due to intervening link delay variations. Some attenuation or amplification, depending on nodal filter characteristics, is applied to the variations in the reference information at each node as it progresses to succeeding levels in the timing tree. Thus, the aggregate variation seen at a particular node is that due to the immediately preceding link, plus that which leaked through the preceding node's filter plus high frequency variations from the previous node's clock.

7.2.1.2.2 Organization/Reorganization

Network organization refers to the structure of the tree over which the reference timing information is disseminated. For a given network, there may be a very large number of different trees which can be formed. The goal of network organization is to provide the best reference information to each node. Thus, the parameters of the organization scheme are link quality and nodal clock quality. Fortunately, the operations necessary for organization can be distributed over all the nodes of the network. This is true since each node and link can be assigned a normal quality factor and monitors can be provided to detect deviations from the norm. A given node may then either reference itself or obtain its reference information from one of its immediate neighbors via that neighbor's communicating link. The choice is for highest clock quality, link quality product. Reorganization refers to implementing a timing tree structure change after some change in status of a node or link of the network. In order to give the simulator user complete control of the organization/reorganization process and to simplify the simulation model, the tree structure is specified by the user via the input data stream. This is not a particularly burdensome requirement on the user since he must already specify the original structure and condition of all links and nodes and any changes thereto that are to take place during each simulation run via the input data stream.

7.2.1.2.3 Processing the Timing Information

A block diagram of the master-slave node is shown in Figure 3.1.1.

7.2.1.2.3.1 Loop Filters

For slave nodes, the model provides for either Type 1 or Type 2 filters. The Type 1 filter is a single pole filter with transfer function of the form $\frac{a}{s + a}$. The Type 2 filter is an integral plus proportional type with transfer function of the form $\frac{s + a}{s}$. Use of either of these filters in a phase-lock loop arrangement results in a second order loop. The major difference is that the Type 2 filter is able to track a constant offset between the reference signal frequency and the natural value of the local clock frequency with a zero average phase error, whereas the Type 1 filter requires an average phase error that is proportional to the amount of frequency offset.

7.2.1.2.3.2 Phase Detector

The model uses an extended range linear phase detector. Real implementations of this might utilize the receive data buffer or an up/down counter. Some performance comparisons are made between a 1 cycle nonlinear sinusoidal phase detector and the extended range linear phase detector in Appendix A.

7.2.1.2.3.3 Acquisition Mode Switching

In order to quickly acquire frequency lock from a large frequency offset as might be experienced when switching from one reference source to another and also provide some attenuation of daily path delay variations, two sets of loop parameters are provided for use with the Type 2 filter, one for tracking and one for fast acquisition. The method for switching from tracking parameters to acquisition and vice versa is as follows: each node is normally in its tracking mode until its phase error exceeds a threshold value ϕ_{th} whereupon it automatically switches to its acquisition parameters. It then remains in the acquisition mode for a period of time T_{acq} that is equal to several times the acquisition phase-lock loop's time constant. It then switches back to the tracking parameters. When the switch is made from tracking to acquisition, a step change in frequency of magnitude $2\xi\omega_n\phi_{th}$ in the direction opposite to that which originally produced ϕ_{th} is experienced. Normalized plots of the output frequency and phase error of the second order phase-lock loop using an extended range linear phase detector and the Type 2 filter for initial phase error and frequency offset are shown in Appendix A. Also, the scheme does not ensure zero phase error and zero frequency offset before switching from acquisition back to tracking parameters. However, this will be approximated to a sufficient degree provided no large disturbances to the reference information occurs during the acquisition interval. The major advantage of this mode switching scheme is its simplicity and hence, the ease with which it may be implemented.

7.2.1.3 Mutual Sync

7.2.1.3.1 Dissemination of Reference Information

The mutual sync technique was originally proposed to avoid the problems of network reorganization. The method used at each node is to obtain some weighted average of the

reference information from all of its immediate neighboring nodes. Thus, no reorganization is required except for removing any failed references from the composite error signal.

7.2.1.3.2 Processing the Reference Information

A block diagram of a mutual sync node is shown in Figure 3.2.1.

7.2.1.3.2.1 Phase Detector

The mutual sync node is quite similar to that of a master-slave node except for the method of obtaining the phase error voltage. In its simplest form, a separate phase detector is used for each of the incoming reference signals. The individual signals are then weighted in some fashion and the weighted signals are summed to produce the composite error signal. The simplest weighting scheme is to weight all signals equally, i.e., $\phi_e = \frac{1}{N} \sum_{i=1}^N \phi_{ei}$. The model utilizes extended range linear phase detectors for obtaining the phase error estimates.

7.2.1.3.2.2 Loop Filter

Since all the nodes of the network are connected together in a feedback arrangement, one must be careful in selecting the loop filters in order to avoid problems of instability. Basically, one must ensure that the closed loop gains of the individual nodes are less than 1 and that the gain-delay products are less than 1. The stability problem is discussed more fully in Section 3.0. The Type 2 filter does not meet the stability criteria but the Type 1 does for loop damping ratios greater than $1/\sqrt{2}$. Thus, the model utilizes Type 1 filters. Since the Type 1 filter requires a phase error proportional to the offset between the reference frequency and the local clock frequency, and individual error signal may be weighted by some factor considerably less than 1, phase error much larger than required for master-slave may exist in the mutual sync system. Should a reference source fail which has a large phase error, simple removal of this source from the composite error signal without careful reweighting of the remaining sources can result in a large change in local clock frequency. It should also be noted that because the entire network is interconnected in a feedback arrangement, it requires considerably longer for steady-state conditions to be reached following network disturbances than with the master-slave technique if the same filter time constants are used.

7.2.1.4 Time Reference Distribution (TRD)

7.2.1.4.1 Dissemination of Reference Information

The TRD technique utilizes the same kind of structure for disseminating reference information as is used for the master-slave technique. However, it is a double ended scheme, i.e., there is a two way exchange of information between adjacent nodes in a chain such that the effects of transmission delay variations are removed. In this manner the nodal clocks may be held as closely together as two way path delay asymmetries, and measurement errors allow. The model assumes that a special overhead channel is utilized for carrying the reference information. A further difference between the TRD and master-slave techniques is that reference information concerning an estimated error between the ultimate reference source and each node in the chain is added in and passed on to each succeeding node in the chain. This information is not filtered before being utilized.

7.2.1.4.2 Organization/Reorganization

The model utilizes an adaptive self-organizing scheme based on a system of clock quality factors and link demerits. The reference information is passed down each chain at discrete time intervals. Thus, the information becomes progressively older as it ascends to higher levels of the distribution tree. This is a source of a problem for the reorganization and clock correction schemes called the obsolete data problem. In order to avoid errors due to this phenomenon, the reorganization and correction schemes must examine enough information samples to be sure of its validity before utilizing it. The effects of this problem on clock correction can be mitigated somewhat if correction extends over many more samples than there are intervening nodes between the node in question and its ultimate reference.

7.2.1.4.3 Processing the Reference Information

A block diagram of the TRD node is shown in Figure 3.3.1.

7.2.1.4.3.1 Phase Detector

The TRD technique utilizes a discrete form of double ended linear phase detector. A special overhead channel is assumed to be available for periodically exchanging a set of reference information messages between adjacent nodes in each path of the tree. The exchange sequence is described as follows: let A and B be nodes in the same timing chain and let A be closer to the ultimate reference source than B. Node B sends a message to Node A containing the time T_{B1} on Node B's clock. After a delay of D_{BA} , the transmission delay from B to A, Node A receives this message. Upon receiving this message Node A notes his own time T_{A1} and forms the quantity $K_A = T_{A1} - (T_{B1} - D_{BA})$. Node A then transmits a message to Node B containing the reading on Node A's clock T_{A2} and the quantity K_A . After a delay D_{AB} , the transmission delay from A to B, Node B receives this message, notes his own clock reading T_{B2} and forms the quantity $K_B = T_{B2} - (T_{A2} - D_{AB})$. Node B then calculates the quantity

$$\begin{aligned} \frac{K_A - K_B}{2} &= \frac{T_{A1} - (T_{B1} - D_{BA}) - [T_{B2} - (T_{A2} - D_{AB})]}{2} \\ &= \frac{(T_{A1} - T_{B1}) + (T_{A2} - T_{B2}) + D_{BA} - D_{AB}}{2} \end{aligned}$$

Now, since the clocks are assumed to drift very little during the exchange interval, $(T_{A1} - T_{B1})$ and $(T_{A2} - T_{B2})$ are approximately equal to each other. Thus

$$\frac{K_A - K_B}{2} \cong T_A - T_B + \frac{D_{BA} - D_{AB}}{2}.$$

Therefore

$$T_A - T_B \cong \frac{K_A - K_B}{2} + \frac{D_{AB} - D_{BA}}{2}.$$

If the term $(D_{AB} - D_{BA})/2$ which represents the asymmetry in the two directions of the communications link is ignored, then the error of this process is that due to this asymmetry plus the error in recognizing the epochs at which messages are received plus any clock drifts during the exchange interval. Node B may use the estimated value $(T_A - T_B)$ in order to correct his own clock so that it corresponds to that of Node A. The model takes into account all three of the above error sources by allowing for specification of a single asymmetry term for each communicating link.

In addition to the error between Node B's clock and that of Node A, obtained from the above exchange of messages, each node in each chain, beginning from those closest to the ultimate network master, maintains an instantaneous estimate of error between its clock and the ultimate reference which it passes on to all nodes at higher branches of the tree. Thus, Node A also passes on to Node B an instantaneous estimate of Node A's error with respect to the ultimate master which Node B adds to the error just calculated between B and A. Node B is then able to track the ultimate reference without having to follow perturbations occurring at intervening nodes. The model takes this error with respect to the ultimate reference into consideration.

7.2.1.4.3.2 Clock Correction

There are a number of techniques for processing the phase error samples in order to obtain a correction signal to be applied to the local clock. The type of processing of the samples depends somewhat on the characteristics of the local clock. For example, cesium clocks may require a highly filtered correction signal in order to take advantage of their excellent long term frequency stability. Two cesium clocks operating with a constant frequency offset from each other of 2 parts in 10^{11} accumulate phase error at the rate

$$\phi_e = 2 \cdot 10^{-11} \cdot t$$

Thus, two such clocks will require 50,000 seconds to accumulate a phase error of $1 \mu s$. In light of the required response time it is conceivable that the phase error of such clocks could be maintained within acceptable bounds by a human operator. However, it is believed that an automated scheme is preferred. On the other hand, high quality quartz crystal clocks have a frequency drift of approximately 1 part in 10^{10} per day. If a node having a quartz clock with this drift rate were communicating with a node using a cesium clock and they were started at time $T = 0$ with zero frequency and phase error then phase difference would accumulate as

$$\phi_e = 1.157 \cdot 10^{15} \cdot t^2$$

One microsecond of phase difference would accumulate in 29,400 seconds. Thus, one difference in the requirements for correction signals for the cesium and quartz crystal clocks is that the quartz clock will require both phase and frequency correction while the cesium clock may require

only phase correction. It is believed, however, that frequency correction can improve the performance of the cesium clock.

The method of application of the correction signal to the local clock depends on whether a reference is presently available and whether or not one was available in the immediate past. The conditions of interest in regards to the reference are as follows:

1. Have one now and have had same for some time.
2. Do not have one now but have had one recently.
3. Have one now but have not had same for very long.

The correction procedure for 1. was covered above. In case 2. it is desirable that the nodal clock should have the ability to coast through certain reference outages without accumulating appreciable phase error. For the cesium clock this means that a long term average, A , of the previous samples should be applied. This same technique does not work as well with the quartz crystal clock because of its drift. What is needed with the quartz crystal clock is a long term average of the slope, S , of the previous samples as well as knowledge of the value B of the correction signal at some time T . During the coasting period the correction signal $B + S \cdot (t - T)$ can then be applied.

In case 3. the ability to quickly acquire from fairly large offsets is desired. This mode is used when switching references or when bringing a node into the network when the node has been off for some reason.

Except for case 2. with quartz crystal clocks, a phase-lock loop employing an integral plus proportional filter can be configured, by suitable choice of filter parameters, to satisfy most of the above requirements. The following discussion is intended to show how one might be led through a succession of refinements to such a scheme.

In order to make phase error corrections, particularly for cesium clocks, Stover²⁰⁵ initially suggested measuring phase error at each node with reference to the master clock and then providing a discrete step correction after the error had reached some threshold level. The correction could consist of either a step change in the local clock frequency for some period of time or a ramp phase change at the output of the clock for the same period of time. The latter method's advantage is that the clock is not disturbed. This scheme is similar in operation to a

AD-A041 004

HARRIS CORP MELBOURNE FLA ELECTRONIC SYSTEMS DIV
STUDY OF ALTERNATIVE TECHNIQUES FOR COMMUNICATION NETWORK TIMIN--ETC(U)
MAR 77

F/G 17/2
DCA100-76-R-0028
NL

UNCLASSIFIED

2 OF 4

AD
A041 004



discrete type of first order phase-lock loop since it will result in a steady state average phase error different from zero when a constant offset exists between the reference signal and the natural frequency of the local clock. A block diagram of this system is shown in Figure 7.2.1.4.3.2-1. It should be noted that this scheme has no provision for systematic frequency error.

Since systematic frequency error is one of the major contributors to the need for phase error corrections, it is believed that, as suggested by Stover²⁰⁵ particularly for quartz crystal clocks, the above simple scheme may be improved by making provisions for systematic frequency error correction. This may be accomplished by taking a discrete derivative of the phase error samples and applying this derivative signal permanently each time a phase correction is made. Figure 7.2.1.4.3.2-2 shows a block diagram of this technique.

Quantization errors in the scheme of Figure 7.2.1.4.3.2-2 can be reduced by making more frequent phase error measurements and lowering the phase error threshold above which corrections will be made. There appears to be no theoretical limit in the smallness of step size of the corrections. Thus, this scheme can be made to appear to the user of the local clock as a continuous process. However, the same result can be accomplished at reduced sampling and processing cost by removing the phase threshold detector and the frequency correction threshold enable gate and leaving phase error corrections applied permanently, i.e., pass the phase error corrections through an accumulator (discrete type of integrator). What was a frequency correction in Figure 7.2.1.4.3.2-2 now becomes a proportional term and the accumulated phase error becomes an integral term with these modifications, as shown in Figure 7.2.1.4.3.2-3. Scrutiny of Figure 7.2.1.4.3.2-3 reveals that it has the form of a discrete phase-lock loop employing an integral plus proportional loop filter. A more conventional drawing of this scheme is shown in Figure 7.2.1.4.3.2-4. Some advantages of this scheme over those from which it was evolved are the cost of its implementation and its recognizable potential for performance analysis by well known techniques. Three parameters completely describe the performance of this scheme. They are:

- a. Sampling rate of the phase error estimator
- b. Scale factor on the integral term (as in Figure 7.2.1.4.3.2-4)
- c. Scale factor on the sum of the integral and proportional terms (K in Figure 7.2.1.4.3.2-4)

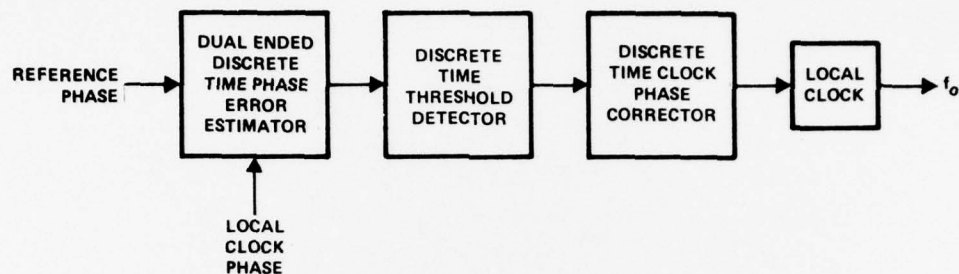
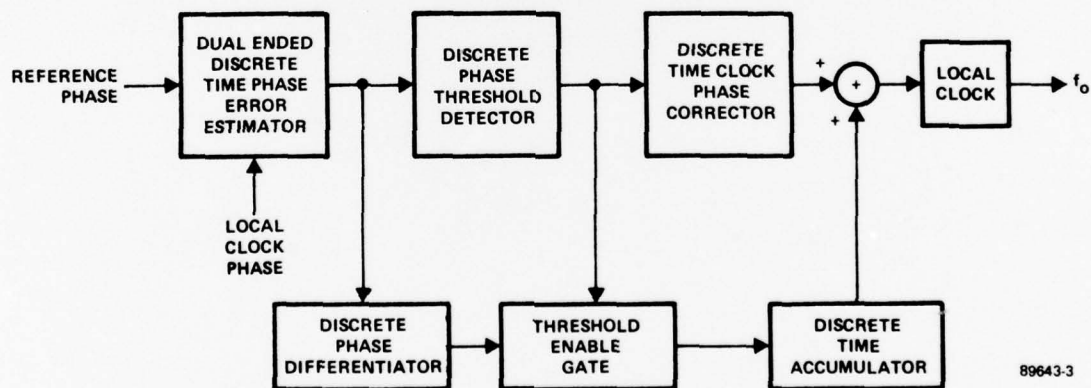


Figure 7.2.1.4.3.2-1. A Simple Scheme for TRD Clock Correction



89643-3

Figure 7.2.1.4.3.2-2. TRD Clock Corrector With Systematic Frequency Error Correction

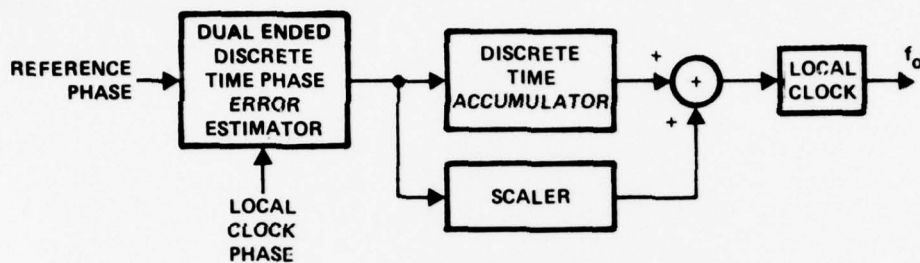


Figure 7.2.1.4.3.2-3. TRD Clock Corrector With Integral Plus Proportional Filtering of Phase Error Estimates

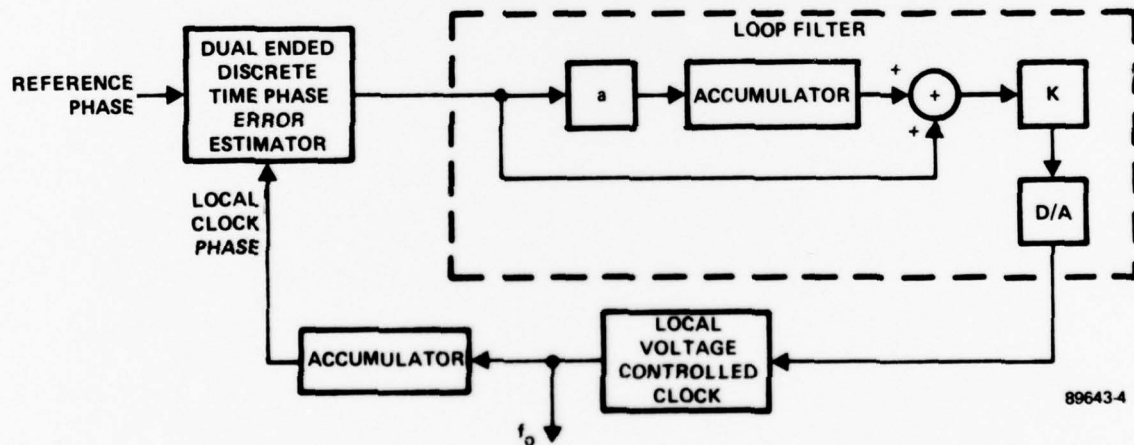


Figure 7.2.1.4.3.2-4. Phase-Lock Loop Version of Figure 7.2.1.4.3.2-3

Parameters a and K can be translated into familiar second-order closed loop damping (ζ) and undamped natural frequency (ω_n) parameters of feedback control theory. The sampling rate of the phase error estimator must be consistent with the loop filter characteristics, i.e., the values of a and K . A discussion of the required sampling rates was given in Paragraph 3.3.2.1 of this report. If quartz crystal clocks are used in the TRD network then a set of acquisition parameters are required in addition to tracking parameters due to the inherent instability of these devices. Cesium clocks need only be provided with a set of tracking parameters because their intrinsic stability is quite high. The wider bandwidth in the quartz clock acquisition mode sets a lower bound on the sampling rate of the phase error estimator. The drift rate of the crystal clock sets a lower bound on the loop bandwidth in the tracking mode. Normally, this bandwidth is made as narrow as possible in order to maintain a good estimate of average reference frequency so that the local clock never tracks very far from this long-term average. Thus, it is better able to coast through a reference outage with lower probability of bit slips. The bandwidth damping ratio product should also be kept small so that initial phase offsets experienced when entering the network or switching references do not cause large peak frequency transients of the local clock. Large peak frequency transients are particularly to be avoided in case the local clock is a cesium standard. On the other hand, extremely narrow bandwidth will cause the buildup of large peak phase errors as a result of step changes in reference frequency such as might be experienced when switching from one reference to the next. Thus, it appears that the quartz and cesium clocks require different sets of tracking loop parameters. The quartz crystal clock also requires a set of acquisition parameters in order to rapidly acquire from large offsets. Sets of parameters which take into account the factors discussed are shown in Table 3.3.2.1.

7.2.1.4.3.3 Acquisition Mode Switching

The TRD model utilizes the same scheme for switching from tracking parameters to fast acquisition as described for the master/slave technique in Paragraph 7.2.1.2.3.3.

7.2.2 Normal Link Variations

The discussion in this section is aimed at obtaining some reasonable descriptions of path length variations. However, very rough assumptions are made in order to keep the models as simple as possible. The fact that values chosen may not meet some particular situation does not necessarily invalidate the model since results can be scaled in accordance with the ratios of the correct values or parameters to those assumed in the model. The discussions are based primarily on referenced information.^{206,207,208,211}

7.2.2.1 Cable

Assume buried coaxial cable with polyethelene disk spacers occupying 10 percent the length space. The cable is assumed to be buried at least four feet deep. At this depth, it is believed that yearly variations in temperature will almost never exceed $\pm 30^\circ \text{F}$. However, the periods of interest for the timing subsystem are daily variations. We will assume a daily peak to peak temperature variation of 0.6°F . The two major contributors to propagation delay variations through the cable are those due to linear expansion and contraction of the length of the cable and changes in the dielectric constant both due to temperature. First, let us consider changes in the dielectric constant (permittivity) of the polyethelene spacing disks versus temperature.

Propagation velocity V is given by

$$V = \frac{c}{\sqrt{\epsilon_r}} \quad (7.2.2.1-1)$$

where c is the free space velocity of light and ϵ_r is the relative dielectric constant of the medium. Let δ be the magnitude of the per unit change in ϵ_r per unit change in temperature. Then

$$\begin{aligned} \Delta V &= \frac{C}{\sqrt{\epsilon_r}} - \frac{C}{\sqrt{(1+\delta)\epsilon_r}} \\ &= \frac{C}{\sqrt{\epsilon_r}} \left(1 - \frac{1}{\sqrt{1+\delta}} \right) \end{aligned} \quad (7.2.2.1-2)$$

Then

$$\frac{\Delta V}{V} = 1 - \frac{1}{\sqrt{1 + \delta}} \quad (7.2.2.1-3)$$

For polyethelene δ is approximately $1 \times 10^{-5}/^{\circ}\text{C}$. Using this value of δ we find

$$\frac{\Delta V}{V} \cong 5 \times 10^{-6}/^{\circ}\text{C}. \quad (7.2.2.1-4)$$

This is the proportional change in the spacer medium. Under the assumption that only 10 percent of the total length of the cable is occupied by polyethelene and the rest by air and that the velocity in air is approximately equal to c then the composite variation is

$$\frac{\Delta V}{V} = 0.9 \times 0 + 0.1 \times 5 \times 10^{-6} = 5 \times 10^{-7}/^{\circ}\text{C}. \quad (7.2.2.1-5)$$

The peak to peak daily proportional variation in velocity due to dielectric changes is then approximately 1.6×10^{-7} .

Copper has a linear expansion coefficient of approximately $10 \times 10^{-6}/^{\circ}\text{F}$.

Then with the assumed temperature variation the peak to peak cable length variation

$$\Delta L/L = 6 \times 10^{-6}.$$

Thus we see that the contribution to delay variation made by dielectric changes can be neglected in comparison to that made by the length change of the inner and outer conductors. In the remainder of the present derivation this will be done.

If the length is assumed to vary in a sinusoidal manner with a period of one day, then the variation in length ΔL is given as:

$$\Delta L = 3 \times 10^{-6} \times L_0 \times \sin(\omega_d t + \phi_r) \text{ units} \quad (7.2.2.1-6)$$

where L_0 is the nominal length of the cable, ω_d is the daily angular velocity $= 7.2685 \times 10^{-5}$,

and ϕ_r is some arbitrary phase angle. The time rate of change of this length variation (speed) is

$$\dot{\Delta L} = 3 \times 10^{-6} \times L_o \times \omega_d \cos (\omega_d t + \phi_r) \text{ units/sec} \quad (7.2.2.1-7)$$

Letting V_{nom} represent the nominal velocity through the cable, the Doppler frequency shift seen at the receiving end of the cable is

$$\Delta f \cong f_s \left(\frac{\dot{\Delta L}}{V_{\text{nom}}} \right) \quad (7.2.2.1-8)$$

where f_s is the frequency of the reference source. Substituting Equation (7.2.2.1-7) into Equation (7.2.2.1-8) we obtain

$$\frac{\Delta f}{f_s} = \frac{3 \times 10^{-6} \times L_o \times \omega_d \cos (\omega_d t + \phi_r)}{V_{\text{nom}}} \quad (7.2.2.1-9)$$

7.2.2.2 Satellite

Orbital variations in 24 hour synchronous artificial earth satellites caused by the earth's gravity field have been studied in some detail.^{210,209} Equations describing the motion of the satellite with respect to a point on the earth due to this cause are quite complicated. Inclusion of such expressions in the simple model being developed in this study would unduly complicate this portion of the model but would produce no discernable enhancement to the results of the simulation. On the other hand, a rough estimate of perturbations that the timing network may expect to see due to satellite motion can be obtained from geometrical considerations of eccentricity of orbit, maximum angle of inclination of plane of orbit with respect to equatorial plane, phasing of the periods of motion due to these two causes, and location of earth terminals. A computer program has been written at Harris ESD which takes these factors into consideration and calculates maximum and minimum ranges between satellite and earth terminal as well as maximum range rate. A selection of outputs from this program is

shown in Table 7.2.2.2 for a satellite assumed to have nominal position in the plane of the equator at 0° longitude and earth stations at 0° latitude, 0° longitude and 80° latitude, 0° longitude. Actually, instead of showing maximum and minimum ranges the table shows the difference between the daily maximum and minimum range. Military satellites are expected to have an orbital inclination of less than 3° .²¹² It is generally believed that eccentricity will be quite small but values are shown for 0.001, 0.003, and 0.010 in Table 7.2.2.2. The terminal at 80° latitude is at a very high latitude for the applications under consideration, but it appears to be close to worst-case. Thus, it appears that daily path variation may range from approximately zero at zero eccentricity and zero degrees elevation up to 4,919,000 feet at 0.01 eccentricity and 3.0 degrees elevation when the ground terminal is at 80° latitude. The maximum range rate may also vary from zero to approximately 180 feet per second. However, if it is assumed that the range difference varies in a sinusoidal manner with a daily period the model becomes extremely simple. This simplifying assumption will be made in this study. Using a nominal two way range, L_o , of 248×10^6 feet between the earth terminal and satellite, the path length variation equation then becomes

$$\Delta L = K L_o \sin(\omega_d t + \phi_r) \quad (7.2.2.2-1)$$

where $0 \leq K \leq 3.97 \times 10^{-2}$ and

$$\omega_d = 7.2685 \times 10^{-5}$$

Under these assumptions the daily fractional Doppler frequency change is

$$\frac{\Delta f}{f_s} = \frac{\dot{\Delta L}}{V_{\text{nom}}} \quad (7.2.2.2-2)$$

where f_s is frequency of incoming bit stream, $\dot{\Delta L}$ is the time derivative of ΔL and V_{nom} is the propagation velocity between satellite and earth terminal.

Due to the large changes in daily path length of satellite links in relation to that of other transmission facilities, it is anticipated that Doppler tracking and removal techniques

Table 7.2.2.2. Sample of Range and Range Rate Variations
Between Earth Terminals and Satellite

Arg. of Perigee	Eccentricity	Inclination	<u>Lat.</u> 0°	<u>Long.</u> 0°	<u>Lat.</u> 80°	<u>Long.</u> 0°
			Max-min range (feet)	Max range rate (feet/sec)	Max-min range (feet)	Max range rate (feet/sec)
90.0°	0.001	0.0	277000	10.09	273000	9.97
"	0.001	1.5	276000	10.09	1366000	49.80
"	0.001	3.0	277000	10.98	2457000	89.60
"	0.003	0.0	930000	30.26	821000	29.92
"	0.003	1.5	830000	30.26	1913000	69.75
"	0.003	3.0	830000	30.47	3005000	109.50
"	0.010	0.0	2767000	100.90	2735000	99.73
"	0.010	1.5	2766000	100.90	3828000	139.60
"	0.010	3.0	2767000	100.90	4919000	179.40
45°	0.001	0.0	277000	10.09	273000	9.97
"	0.001	1.5	276000	10.70	1292000	47.15
"	0.001	3.0	284000	12.55	2377000	86.8
"	0.003	0.0	830000	30.26	821000	29.92
"	0.003	1.5	830000	30.88	1865000	64.50
"	0.003	3.0	830000	32.73	2820000	103.10
"	0.010	0.0	1767000	100.90	2735000	99.73
"	0.010	1.5	2766000	101.50	3588000	131.00
"	0.010	3.0	2767000	103.30	4534000	165.70
0.0°	0.001	0.0	277000	10.09	273000	9.97
"	0.001	1.5	277000	10.09	1126000	41.13
"	0.001	3.0	277000	10.98	2184000	79.79
"	0.003	0.0	830000	30.26	821000	29.92
"	0.003	1.5	830000	30.26	1356000	49.64
"	0.003	3.0	830000	30.47	2322000	85.13
"	0.010	0.0	2767000	100.90	2735000	99.73
"	0.010	1.5	2767000	100.90	2924000	106.70
"	0.010	3.0	2767000	100.90	3478000	127.70

may be applied prior to obtaining reference signals via satellite links for the nodal timing sub-system. Actually, the length variation of a satellite path is quite predictable from knowledge of a particular satellite's orbit. It is anticipated that this knowledge can be used to advantage in such a Doppler removal device although this has not been investigated in this report.

7.2.2.3 Microwave

There are several factors which affect path delay variations of microwave links. These factors include temperature, humidity, atmospheric pressure, and rain or fog. The first three of these terms can be expressed in terms of "so called N units." The N unit is related to the index of refraction n (ratio of radio wave propagation velocity in vacuum to that in the medium) by

$$N = (n - 1) 10^6. \quad (7.2.2.3-1)$$

From this value of N we may obtain an equivalent change in path length ΔL ,

$$\Delta L = N \times 10^{-6} \times L_0 f(t) \quad (7.2.2.3-2)$$

where L_0 is nominal path length and $f(t)$ is a function of time which describes the manner in time in which the variation takes place. The time derivative of ΔL may be obtained in order to calculate the amount of frequency Doppler caused by the delay variation, i.e.,

$$\dot{\Delta L} = N \times 10^{-6} \times L_0 \times \dot{f}(t) \quad (7.2.2.3-3)$$

and

$$\Delta f \cong f_s \left(\frac{\dot{\Delta L}}{V_{\text{nom}}} \right) \quad (7.2.2.3-4)$$

Daily temperature changes may account for the most rapid fluctuation in the value of N . With constant pressure and humidity a daily temperature variation of 20°C peak to peak about a nominal 20°C results in a change in N of about 18 peak to peak. Largest monthly mean variation of N is about ± 25 units. Yearly temperature variations over the U.S. results in

variations in N from 230 to 400. Rain at approximately six inches per hour results in N changes of about 14 units. Thus, for simulation purposes, the following will be assumed:

Daily variations:

$$\Delta L = 10 \times 10^{-6} \times L_o \times \sin(\omega_d t + \phi_r) \quad (7.2.2.3-5)$$

where $\omega_d = 7.2685$ rad/sec

Stress due to rain or fog on selected links:

$$\Delta L = 14 \times R \times 10^{-6} \times [\mu(t - T) - \mu(t - (T + D))] \quad (7.2.2.3-6)$$

where ϕ_r is a random phase between 0 and 2π ,

R is a random number between 0 and 1,

D is a random number between 1,800 and 43,200 s,

T is the time in seconds at the start of the simulation at which the rain is to start, and

$$\mu(t - x) = \begin{cases} 0 & \text{for } t < x \\ 1 & \text{for } t \geq x \end{cases} .$$

7.2.2.4 Tropo

Tropospheric Refraction

The troposphere is that area of the atmosphere extending from the ground to a height of approximately six miles. On difference between the troposphere and the ionosphere is the fact that there is practically no ionization of the air molecules in the troposphere. The troposphere can act as a smooth refractive medium due to variation with altitude of the dielectric constant of the air. The water vapor content of the air will also change the dielectric constant. This smooth model gives rise to beyond the horizon reception due to tropospheric refraction.

Knife Edge Diffraction

According to Huygen's principle, electromagnetic energy is emitted by means of wavelets that start at every point along the beam and are transmitted in every direction. Thus,

points which lie in a region of geometric shadow may receive some of the energy. Obstructions which give rise to the knife edge effect are mountains, hills, trees and the earth's horizon. In the shadow region the beam is refracted by the change in dielectric constant of the troposphere. This principle is commonly observed at night when two cars meet each other on opposite sides of a hill.

Tropospheric Scattering

The major contributor to dependable long distance communication (approximately 300 miles) is caused by turbulence and is known as tropospheric scattering. According to one theory of scatter, the earth's atmosphere is in a constant state of motion. Because of this motion with respect to the earth, small turbulences or eddies are formed. These eddies are similar to the whirlpools in a rapidly moving stream of water. In the atmosphere, however, the eddies form spherical turbulences rather than the two-dimensional whirlpools in a stream. These spherical turbulences are called scattering blobs and are responsible for the scatter effect. The turbulent motion of air at each blob results in a variation in dielectric constant within the blob and a small amount of energy is scattered away from the incident beam. The effect is the same as if each blob received the signal and reradiated it. Figure 7.2.2.4-1 depicts this effect. The scattering blobs move through the common volume of space defined by transmitting and receiving antenna beams due mostly to the horizontal component of tropospheric winds. The geometry of this effect is shown in Figure 7.2.2.4-2. The energy reaching the receiving antenna is a composite of that gathered in from all the scattering blobs in the common volume of the transmitting and receiving beam space.

The problem at hand is to determine the maximum path length variation and the rate at which it may vary. The related problem of frequency of signal strength fades has been discussed by Crawford, et al.²⁰⁸ In the extreme case when only one scattering blob is in the common volume, we see from Figure 7.2.2.4-2B that the maximum path length variation is

$$\Delta L = L_0 \left(\frac{1}{\cos \frac{\beta}{2}} - 1 \right) . \quad (7.2.2.4-1)$$

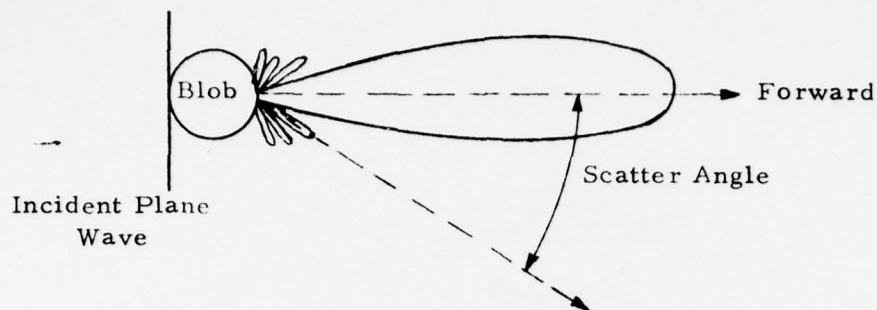
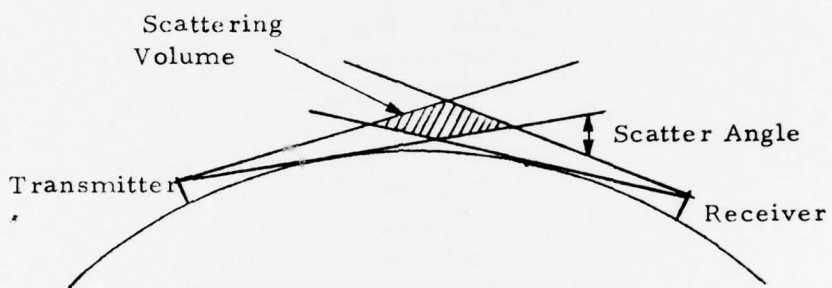
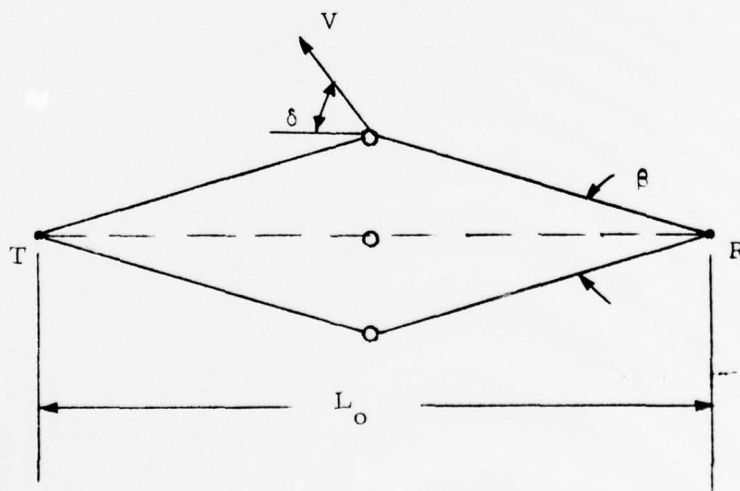


Figure 7.2.2.4-1. Directional Pattern of Scattering Blob



a - Vertical Cross Section



b - Horizontal Cross Section

Figure 7.2.2.4-2. Geometrical Model of Tropo Path

In this same case from (CW 59) the Doppler frequency is

$$\Delta f = \frac{1}{2\pi} \frac{d\phi}{dt} = \frac{\beta}{\lambda} V \sin \delta \quad (7.2.2.4-2)$$

Where λ = wave length of the carrier signal, V = horizontal component of tropospheric wind velocity, δ = angle between wind direction and line joining transmitter and receiver, and β = receiving and transmitting antenna beam widths (assumed to be equal). However, the model can be simplified if a suitable sinusoidal motion is assumed. If it is assumed that movement of the scattering blob from center beam to half power point of the beam represents one-fourth cycle of the length variation and a sinusoidal variation is assumed, then the period of this variation is

$$T = \frac{4 L_o \sin \beta/2}{V} \quad (7.2.2.4-3)$$

From Equation (7.2.2.4-1) and Equation (7.2.2.4-3) the maximum amount of path length variation and the minimum frequency with which the variations can occur may be obtained. However, it is believed that the path length is highly uncorrelated over much shorter intervals of time than the period obtained from Equation (7.2.2.4-3) with reasonable values of V . This is consistent with numerous scattering blobs being in the common volume at a given time. Nevertheless, this equation will be used to obtain an upper bound on the period of the path length variation. On the other hand, the frequency of the path length variation is not expected to be as great as that of the highest frequencies of signal strength fades. It is believed that the signal strength fades are caused by multipath signals arriving at the receiver with phases of such value as to subtract from each other. From²⁰⁸ signal strength fade frequencies varies from approximately .1 Hz to 10 Hz. This frequency depends on antenna beam widths. Narrower beamwidths will also reduce the peak amplitude of the length variation. The minimum period of signal strength fades will be taken as the minimum period of path length variations. Using $L_o = 300$ miles, $\beta = 1.8^\circ$, and $V = 50$ miles per hour, we obtain $|\Delta L| = 195$ feet and $\omega_x = 9.26 \times 10^{-3}$ rad/sec. Therefore, for purposes of simulation, let us assume that the tropospheric path length variation is given as follows:

$$\Delta L = K L_o \sin (\omega_x t + \phi_r) \quad (7.2.2.4-4)$$

where $0 \leq K \leq 1.23 \times 10^{-4}$

$$9.26 \times 10^{-3} \leq \omega_x \leq 2\pi \times 10 \cong 63$$

and ϕ_r is a random phase angle.

With $K = 1 \times 10^{-8}$ and $\omega_x = 3$, peak proportional frequency Doppler would be

$$\frac{|\Delta f|}{f_s L} = \frac{|\dot{\Delta L}|}{V_{nom}} = \frac{3 \times 10^{-8}}{186000} \approx 1.61 \times 10^{-13} \text{ parts/mile}.$$

7.2.3 Statistical Clock Model

Three types of timing clocks may be used in the DCS network. These include the cesium beam controlled oscillator, the rubidium gas cell resonator controlled oscillator and the quartz crystal oscillator. The cesium beam frequency reference is a primary standard. It has an intrinsic frequency which can be set up independent of any other source and has no systematic drift. The rubidium frequency standard is a secondary standard. It requires calibration against another oscillator and is then subject to a small amount of drift. The amount of drift is typically 10^{-1} to 10^{-2} times that of the best quartz crystal oscillator. The quartz crystal oscillator is also a secondary standard and is utilized in those applications which do not require the extreme accuracies and stabilities obtainable from the rubidium or cesium standards. No matter which of these types of clocks are utilized at any given time at any node, its essential properties may be described by a list of parameters which are controlled by random number generators. The parameter list should contain four parameters for each nodal clock. These parameters include frequency, short term stability, accuracy or long term stability, and drift rate. Frequency refers to nominal frequency. This parameter is generated for each node from a random generator at the beginning of each simulation run and is modified during the run by the accuracy random number generator or by the drift rate parameter. At each simulation step, a short-term stability offset is generated and added to the current value of nominal frequency to provide the mean

frequency for the simulation step. From H.P. literature, it appears that short term stability (up to approximately .4 second) is essentially the same for all three types of frequency standards if drift rates are not included for rubidium and quartz. H.P. literature shows measurements for square root of the sum of the squares of successive differences in average frequency measurements for measurement intervals from 10^{-3} to 10^{+4} seconds. Thus, the short term stability random number generator may sample from a normally distributed variable with zero mean and standard deviation equal to the $\frac{\delta \Delta f}{f}(2, \tau)$ given by H.P. where τ corresponds to the simulation step interval. These deviations are given as piecewise functions of τ for each clock type in Table 7.2.3.

Initial nominal frequencies may be selected from a normally distributed random variate with mean f and standard deviation equal to $1 \times 10^{-12} \times f$.

Systematic drift or aging for quartz crystal oscillators after an initial operating period of days appears to be in the range of $\pm 1.57 \times 10^{-15}$ /sec but is usually expressed in fractional parts per day, i.e., $\pm 1 \times 10^{-10}$ /day.

A similar systematic drift may be observed for rubidium, but it is 10 to 100 times less than that of quartz. Drift rates for rubidium are usually expressed in fractional parts per month, e.g., $\pm 1 \times 10^{-11}$ /month. These drifts for quartz and rubidium are normally taken to be the long term stability of these devices. Cesium beam standards do not exhibit systematic drift. Thus, a guaranteed long term stability or accuracy over a range of temperature and magnetic field intensity may be stated for this standard. The fractional long term stability for several of H.P. cesium beam standards is approximately 1×10^{-11} .

It should be noted that the information given in Table 7.2.3 includes the systematic drift in the short term stability data. Thus, if the short term stability and long term drift are to be applied separately, then the long term drift component should be subtracted from the data given for values of τ for which the drift component is an appreciable part of the values given.

Table 7.2.3. Short Term Stability Standard Deviations as a Function of Sample Time (From HP Data)

Quartz

$$-3 \leq \log_{10} \tau \leq -.55, \quad \log_{10} \sigma = -\log_{10} \tau - 11.7049$$

$$-.55 < \log_{10} \tau \leq 4, \quad \sigma = 7 \times 10^{-12} \text{ or } \log_{10} \sigma = -11.1549$$

$$\text{Systematic Drift } \pm 1 \times 10^{-10} / \text{day} \rightarrow 1.57 \times 10^{-15} / \text{sec}$$

Rubidium

$$-3 \leq \log_{10} \tau \leq -1, \quad \log_{10} \sigma = -\log_{10} \tau - 11.7049$$

$$-1 < \log_{10} \tau \leq 2, \quad \log_{10} \sigma = -.5 \log_{10} \tau - 11.1549$$

$$2 < \log_{10} \tau < 4, \quad \sigma = 7 \times 10^{-13} \text{ or } \log_{10} \sigma = -12.1549$$

$$\text{Systematic Drift } \pm 1 \times 10^{-11} / \text{month} \rightarrow 3.858 \times 10^{-18} / \text{sec}$$

Cesium

$$-3 \leq \log_{10} \tau \leq -.55, \quad \log_{10} \sigma = -\log_{10} \tau - 11.7049$$

$$-.55 \leq \log_{10} \tau \leq .6, \quad \sigma = 7 \times 10^{-12} \text{ or } \log_{10} \sigma = -11.1549$$

$$.6 \leq \log_{10} \tau < 4, \quad \sigma = -.5 \log_{10} \tau - 11.04$$

$$\text{Systematic Drift - None, Long Term Stability } \pm 1 \times 10^{-11}$$

7.3 Simulation Results

7.3.1 The Simulation Plan

A plan was drawn up at the midpoint of the study whereby the simulator could be used to test the sensitivity of the master-slave, mutual sync and TRD techniques to various disturbances and stresses. Since initial startup with a set of random phase errors and frequency offsets generates possibly as severe a transient as the network will ever see, it was decided that a set of runs for each of the network configurations should be made with only the initial conditions applied. Next the same set of runs were to be repeated but this time with the normal link delay variations applied. A third set of runs were then to be made with initial conditions, normal link delay variations and stress events applied. Finally, a set of runs were to be made with one of the network configurations for each of the timing techniques using identical initial conditions, link delay variations, stress events and duration of run in order to get a direct comparison of the different techniques under the same network configuration and inputs. The objective of the first three sets of runs was to test for sensitivity as a function of network topology, as a function of place of origin in the network at which a stress originates, i.e., near the connectivity center of the network as opposed to the fringe of the network and as a function of the type of disturbance, e.g., change in clock frequency or phase, change in link delay, loss of link and loss of node. In order to access these sensitivities, the plan called for observation of peak frequency offsets, phase errors, propagation distance of disturbance from place of origin measured in nodes, and how long it takes initial and transient conditions caused by the various stresses to die out.

Some of the above parameters were actually analyzed under more carefully controlled conditions with limited network structures in the discussion on error propagation in Section 8.0. However, the overall objective of the simulation plan was to see how the larger network behaves.

The plan proved to be overly ambitious in that all the simulations implied by the plan could not be obtained and completely analyzed in the limited time available, however some very useful information concerning the behavior of the timing techniques under what is believed to be real world conditions was obtained via the simulation effort. In working with the simulator, it was found that perhaps the true value of a simulation lies not so much in providing answers to

preconceived specific questions but rather more in causing the user to ponder his situation in sufficient detail that he, of necessity, discovers what the real questions are.

7.3.2 Network Configurations

The four network configurations used in the simulations are shown in Figures 7.3.2-1 through 7.3.2-4. When referring to these figures in the remainder of this section, they will be referred to simply by their alphabetical symbols, included on the figures. The overall characteristics of these network configurations are discussed in Section 5.0. The initial timing hierarchy for master-slave and TRD are indicated by arrowheads. The initial master node is denoted by the letter M above the node number. The links are marked according to type and distance. The nomenclature is M for line of sight microwave, C for coaxial cable, S for satellite and T for beyond the horizon tropospheric. The distances are in kilometers. Thus the Label C 660 indicates a cable link of distance 660 kilometers. Due to the limited storage availability on the Datacraft computer used in support of the simulation effort, all nodes and links could not be monitored. When monitoring a mutual sync node, all the incoming links to this node must be monitored. Thus, only a subset of the nodes were monitored. These are marked with a "*" for master slave and TRD and with a "+" for mutual sync. The monitored nodes were composed mostly of the backbone of the network with a few other nodes at Levels 2 and 3.

7.3.3 Loop Parameters

The values used in the simulations for nodal loop filter parameters were the same as those derived in Section 3.0.

7.3.4 Input Signals

7.3.4.1 Initial Conditions

Most of the nodal clock initial frequency offsets were set to zero, but a few nodes were chosen at random and assigned an offset from a normal distribution with zero mean and $\pm 3\sigma = \pm 1 \times 10^{-8} \times f_0$. The initial phase ϕ_i at the receiving end of links was computed as follows:

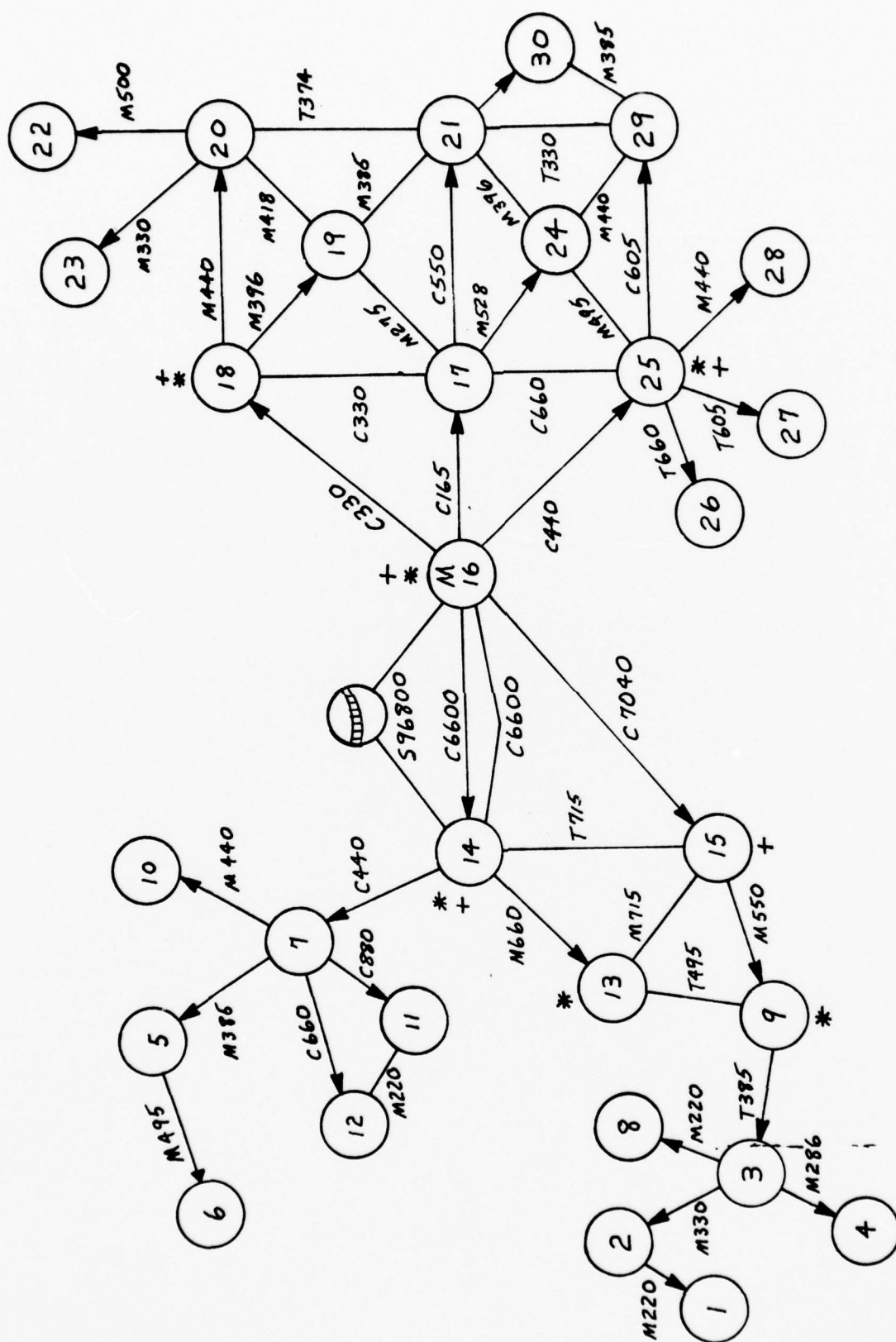


Figure 7.3.2-1. Dumbbell Node Configuration (Configuration A)

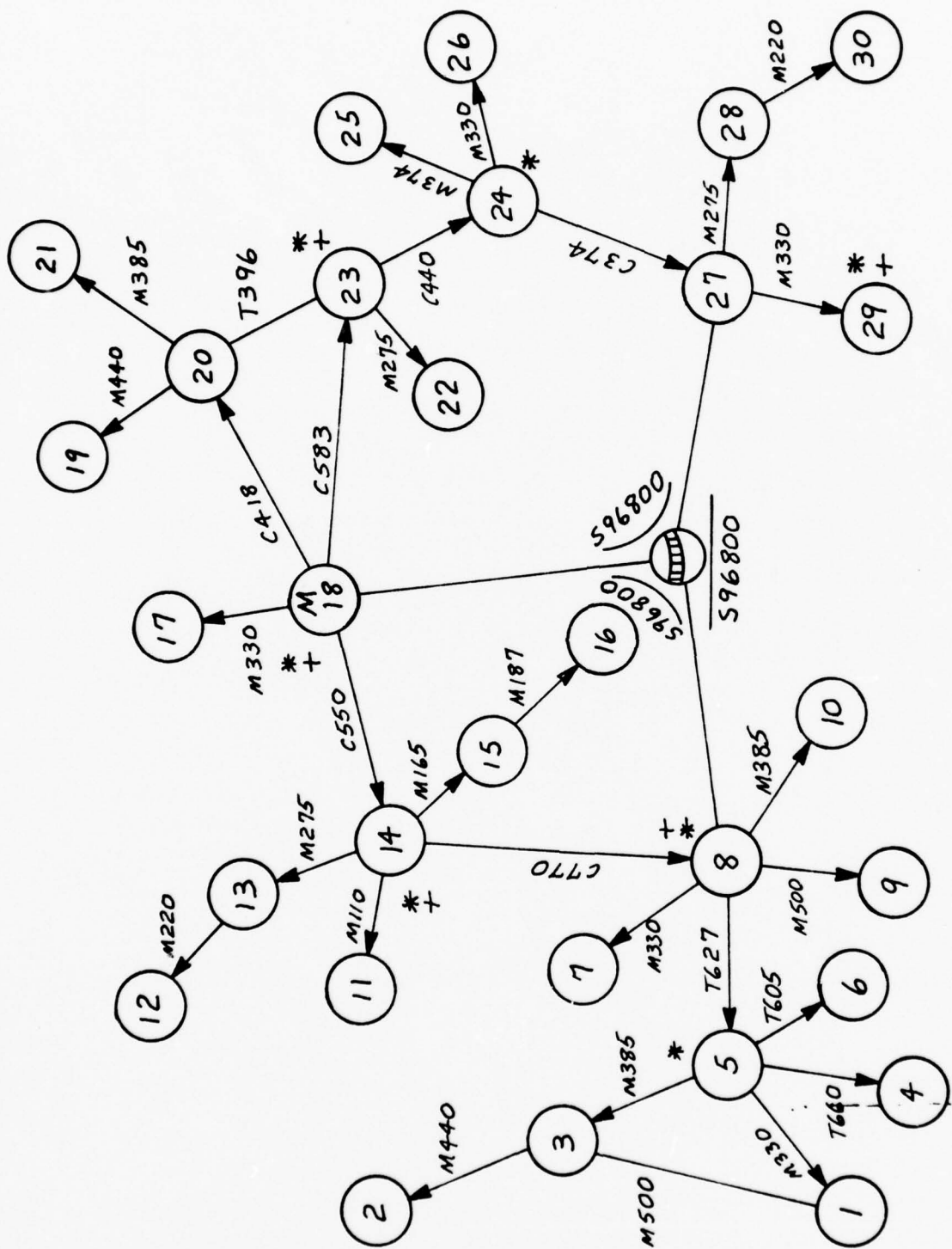


Figure 7.3.2-2. Meandering Node Configuration (Configuration B)

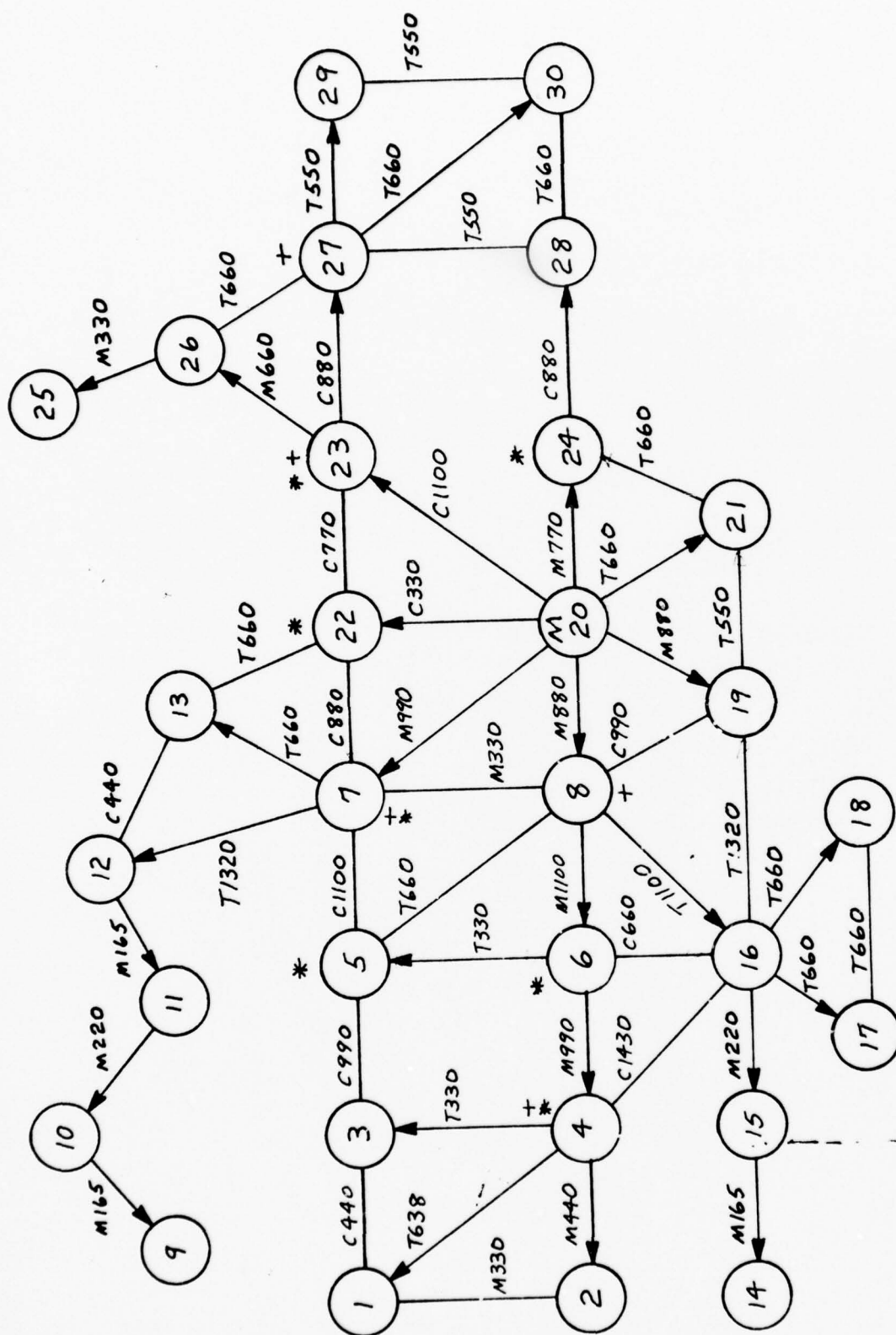


Figure 7.3.2-3. Ladder Node Configuration (Configuration D)

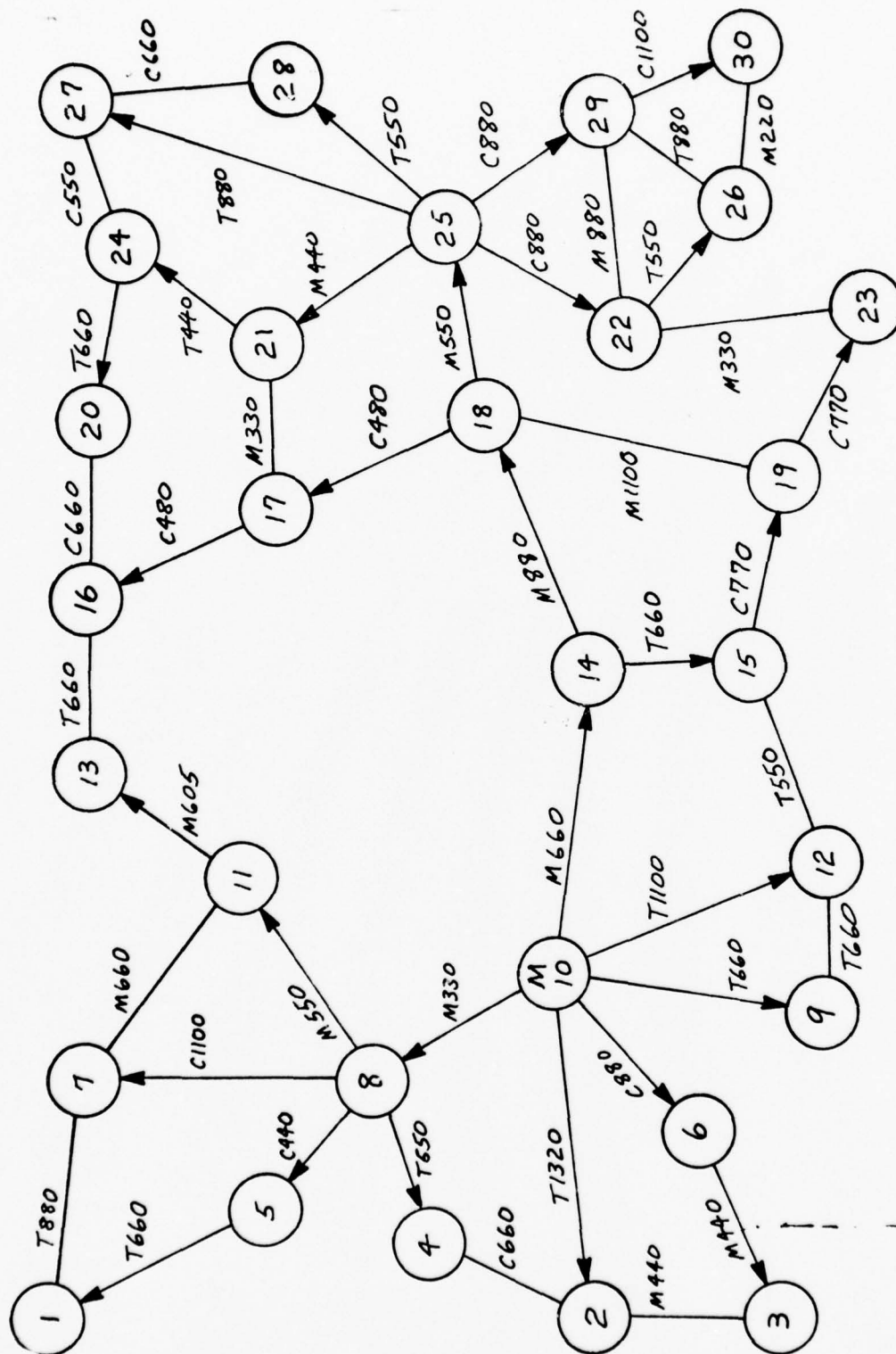


Figure 7.3.2-4. Loop Node Configuration (Configuration E)

$$\phi_1 = (ND + \pi) \bmod 2\pi - \pi$$

where ND is the nominal link delay in radians of the basic clock frequency, f_0 . The initial value of nominal link disturbance is then added to this value.

7.3.4.2 Normal Link Disturbances

Normal link disturbances of the maximum amplitude as discussed in Paragraph 7.2.2 were applied to all links except tropospheric variations were not applied. The tropospheric model indicates that the frequencies of the disturbances are sufficiently high that they would be attenuated enough by loop filters to be unnoticeable due to scale resolution of the output plots. Link asymmetries for TRD runs were adjusted to 1 percent of peak delay variation.

7.3.4.3 Clock Drift and Short Term Jitter

Clock drifts and jitter were not applied. With quartz clocks drifting in frequency at a rate of $\pm 1 \times 10^{-10} \times f_0$ per day, the total amount of drift would not be great enough to cause appreciable error if neglected. As indicated in Section 3.0 the Type 2 loop tracks a constant drift of β Hz/s with a phase error of β/ω_n^2 . The tracking loop parameters utilized with the master-slave configuration will produce a constant phase offset of $0.39 \mu\text{s}$ with $\beta = 10^{-10} \times f_0$ per day. For the Type 1 filter, constant drift will produce, in steady-state, a constantly increasing phase error of the form

$$\beta \left(\frac{1}{\omega_n^2} + \frac{2\xi}{\omega_n} t \right)$$

For the mutual sync nodes using $\xi = 1$, $\omega_n = 1.67 \times 10^{-3}$ and $\beta = 10^{-10} \times f_0$ per day this gives

$$\phi_e \cong 0.117 \mu\text{s accumulated per day.}$$

Since simulation runs were limited to approximately 3 days or less, drift terms were discarded. The clock models indicate that short term clock jitter will be filtered sufficiently by loop filters that it will be of no consequence in the simulation results.

7.3.5

Stress Events

The stress events for master-slave and TRD runs are shown in Figures 7.3.5-1 through 7.3.5-4. The events for mutual sync are shown in Figures 7.3.5-5 through 7.3.5-8. In addition, master-slave and TRD also utilize the stress event of Figure 7.3.5-9. In observing the results of the stress events, it should be kept in mind that the individual nodal frequency response to step changes in reference frequency or phase error will have shapes like that shown in Figure A6 and Figure A7 of Appendix A. The phase plots will show responses to step changes in reference frequency and phase error similar to those shown in Figure A8 and Figure A9 of Appendix A. However, the curves become more difficult to evaluate when multiple forcing functions combine to cause a composite time response from the connected network.

<u>EVENT TIME (s)</u>	<u>EVENT</u>
23000	Node 15 fails
23600	Node 9 slaves to Node 13
26000	Node 17 fails
26600	Node 21 slaves to Node 19
	Node 24 slaves to Node 25
30000	Node 18 fails
30500	Node 21 slaves to Node 24
	Node 19 slaves to Node 21
	Node 20 slaves to Node 21
31100	Node 25's clock frequency changes by $+1 \times 10^{-8} \times f_o$

Figure 7.3.5-1. Stress Events for Master-Slave and TRD; Configuration A

<u>EVENT TIME (s)</u>	<u>EVENT</u>
11000	Link (18-14) fails
12000	Node 8 slaves to Node 18
12400	Node 14 slaves to Node 8
15000	Node 18 clock frequency changes by $+1 \times 10^{-8} \times f_o$
16000	Node 14 free runs
18000	Node 8 slaves to Node 14
20000	Node 18 slaves to Node 8
22000	Link (18-23) fails
23000	Node 23 slaves to Node 20

Figure 7.3.5-2. Stress Events for Master-Slave and TRD; Configuration B

<u>EVENT TIME (s)</u>	<u>EVENT</u>
10000	Node 8 fails
11000	Node 20 fails
14000	Node 21 slaves to Node 19
	Node 24 slaves to Node 21
	Node 7 slaves to Node 22
	Node 23 slaves to Node 22
22000	Node 5 slaves to Node 7
	Node 6 slaves to Node 5
	Node 16 slaves to Node 6
	Node 19 slaves to Node 16

Figure 7.3.5-3. Stress Events for Master-Slave and TRD; Configuration D

<u>EVENT TIME (s)</u>	<u>EVENT</u>
11000	Link (10-14) fails
12000	Node 15 slaves to Node 12
	Node 14 slaves to Node 15
13000	Node 14 fails
16000	Node 18 slaves to Node 19
18000	Node 10 fails
20000	Node 19 slaves to Node 18
	Node 13 slaves to Node 16
	Node 11 slaves to Node 13
	Node 8 slaves to Node 11
	Node 2 slaves to Node 4
	Node 3 slaves to Node 2
	Node 6 slaves to Node 3
	Node 15 slaves to Node 19
	Node 12 slaves to Node 15
	Node 9 slaves to Node 12

Figure 7.3.5-4. Stress Events for Master-Slave and TRD; Configuration E

<u>EVENT TIME (s)</u>	<u>EVENT</u>
10000	Clocks at Nodes 18, 25, and 21 experience a step increase in natural frequency of $1 \times 10^{-8} \times f_o$
20000	Clocks at Nodes 15, 13, and 14 experience a step decrease in natural frequency of $1 \times 10^{-8} \times f_o$
40000	Link (16-18) fails
60000	Link (17-18) fails
100000	Delay on Link (14-16) increases by $1 \times 10^{-6} \times D_{nom}$
140000	Link (15-16) fails
180000	Node 17 fails
220000	Node 24 fails

Figure 7.3.5-5. Stress Events for Mutual Sync; Configuration A

<u>EVENT TIME (s)</u>	<u>EVENT</u>
10000	Link (8-18) delay decreases by $1 \times 10^{-6} \times D_{\text{nom}}$
20000	Node 20 fails
40000	Node 5 fails
80000	Link (23-24) fails
120000	Clock at Node 18 experiences a decrease in natural frequency of $1 \times 10^{-8} \times f_o$
180000	Link (8-18) fails

Figure 7.3.5-6. Stress Events for Mutual Sync; Configuration B

<u>EVENT TIME (s)</u>	<u>EVENT</u>
10000	Node 20 fails Nodes 7, 8, 19, 21, 22, 23, and 24 remove Node 20 from their reference
20000	Node 20 is restored and Nodes 7, 8, 19, 21, 22, 23, and 24 place Node 20 into their reference signal
30000	Node 4 fails and Nodes 1, 2, 3, 6, and 16 remove Node 4 from their weighting functions
40000	Node 4 is restored and Nodes 1, 2, 3, 6 and 16 replace Node 4 back into their reference signals
80000	Links (2-4), (4-5), (6-8), (8-20), (20-24), (24-28), (28-30) experience a ramp increase in delay of $1 \times 10^{-7} \times D_{nom}/\text{hour}$
100000	Delay in above links becomes stationary

Figure 7.3.5-7. Stress Events for Mutual Sync; Configuration D

<u>EVENT TIME (s)</u>	<u>EVENT</u>
10000	Node 22 fails and Nodes 23, 25, 26, and 27 remove Node 22 from their reference signals
20000	Node 22 is restored and Nodes 23, 25, 26, and 29 replace Node 22 back into their reference signals
40000	Node 10 fails and Nodes 2, 6, 8, 9, 12, and 14 remove Node 10 from their reference signals
50000	Node 10 is restored and Nodes 2, 6, 8, 9, 12, and 14 replace Node 10 back into their reference signals
80000	Node 14's clock experience a step increase of $1 \times 10^{-8} \times f_o$ in natural frequency
120000	Links (8-10), (10-14), (14-18), and (18-25) experience a ramp increase in delay of $1 \times 10^{-7} \times D_{nom}/\text{hour}$
160000	The delay of the above links become stationary

Figure 7.3.5-8. Stress Events for Mutual Sync; Configuration E

<u>EVENT TIME (s)</u>	<u>EVENT</u>
10000	Link (8-18) delay decreases by $1 \times 10^{-6} \times D_{nom}$
20000	Node 20 fails
40000	Node 5 fails
80000	Link (23-24) fails
	Node 27 slaves to Node 18
	Node 24 slaves to Node 27
120000	Clock at Node 18 experiences a decrease in natural frequency of $1 \times 10^{-8} \times f_o$
	Node 14 free runs
124000	Node 18 slaves to Node 14
180000	Link (8-18) fails

Figure 7.3.5-9. Comparison Stress Events for Master-Slave and TRD for Configuration B

7.3.6 Simulation Run Results

Although all the runs implied by the simulation plan were not obtained, considerable more result data was produced than could be included in this report in a comprehensible form. Therefore, runs that appear to be representative of the timing techniques, network configurations, disturbances and stress events were selected. From each of these selected runs link to node phase errors and nodal frequency errors for a few of the links and nodes experiencing perturbations most representative of the general network behavior, or which could serve to illustrate particular relationships between stimulus and response were plotted. Sets of runs were actually made consisting of initial transient only (IT), initial transient plus normal link disturbances (IT + ND), and initial transient plus normal link disturbances plus stress events (IT + ND + SE), but in order to reduce the volume of material only the IT + ND + SE runs from each set are shown in this report. The entire mutual sync networks were perturbed by normal satellite link disturbances but the effect was mostly swamped by the response to stress events as shown in the (IT + ND + SE) plots so the amplitudes of the phase and frequency errors due to normal link disturbance are shown in tabular form for mutual sync runs involving networks with satellite links.

7.3.6.1 Mutual Sync

Configuration A - Normal Link Variations

The loop time constants for the mutual sync nodes were chosen considerably shorter than those for the tracking mode of the master/slave or TRD techniques in order to provide a comparable response time on a node for node basis to transient conditions. The resulting magnitude of nodal gain for daily path delay variations turned out to be 1.0019. Thus, these variations passed through each node without attenuation. These variations can be observed on the initial transient plus normal link disturbance plots. There was only one satellite link, (14-16C), in this network configuration. This link was responsible for almost all of the daily variation in the network. The peak variation on the link was 1.2×10^{-10} s/km. The length of the link was set at 96,800 km. This gives a peak variation of 11.62×10^{-6} second. Since the variation was assumed to be sinusoidal with a period of 1 day, the resulting peak frequency doppler was $\frac{\Delta f_{\text{peak}}}{f_o} = 8.5 \times 10^{-10}$. Some of the nodes peak-to-peak frequency variations were as follows:

<u>Node</u>	<u>Daily peak-to-peak $\Delta f/f_0$ ($\times 10^{10}$)</u>
14	5.63
15	5.44
16	4.53
17	2.53
18	2.78
25	2.53
29	2.46

From this data, it is observed that the amount of frequency variation diminishes as the distance from the disturbance measured in nodes increases but this is not the only factor which must be taken into account. The number of connected neighbors and how far they are from the source of the disturbance also influences the amount of variation in the nodal frequency.

A few of the peak-to-peak phase errors between the receiving end of the indicated link and node were as follows:

<u>Link</u>	<u>to</u>	<u>Node</u>	<u>Daily peak-to-peak phase variation (microseconds)</u>
14-15		15	1.69
16-18		18	4.77
16-17		17	4.44
15-16		16	0.90
16-25		25	4.69
25-29		29	0.98
25-27		27	0.32
14-16C		16	13.68
14-16A		16	1.63

Composite Plots

Figures 7.3.6.1-1 and 7.3.6.1-2 show composite initial transient, normal link disturbance and stress event plots of link to node phase errors for Links 14-15, 16-17, and 16-25 and nodal frequency errors for Nodes 15, 17, and 25.

The step change in Nodes 18, 21 and 25's frequencies of $1 \times 10^{-8} \times f_0$ at time 10,000 seconds caused Node 17's clock to change by $32 \times 10^{-10} \times f_0$ but had little effect on the nodes in the left half of the network. The change of $1 \times 10^{-8} \times f_0$ in clocks 13, 14, and 15 at 20,000 seconds had little effect on the nodes of the right half of the network. Node 16 acted as a buffer during the period from 10,000 seconds to 20,000 seconds. The net result of these two changes was almost zero by 40,000 seconds. At 40,000 seconds when Link 16-18 failed Node 15's clock decreased in frequency by approximately $27.6 \times 10^{-10} \times f_0$. Loss of Link 17-18 at 60,000 seconds caused Node 17's clock frequency to decrease by about $17 \times 10^{-10} \times f_0$. The increase in delay on Link 14-16 at time 100,000 seconds caused almost no change in any of the three plotted nodes' frequencies. When Link 15-16 failed at time 140,000 seconds, Node 15 decreased in frequency by approximately $73 \times 10^{-10} \times f_0$. Failure of Node 17 at 180,000 seconds caused Node 15's clock frequency to decrease by approximately $17 \times 10^{-10} \times f_0$ and Node 25's by approximately $11 \times 10^{-10} \times f_0$. The smaller change in Node 25's frequency is attributed to the larger number of nodes connect to 25. Failure of Node 24 at 220,000 seconds caused 25's frequency to momentarily decrease by approximately $32 \times 10^{-10} \times f_0$.

Configuration B, Normal Link Variations

Although this configuration shows three satellite links, the simulator only utilized the two satellite Links 8-18 and 8-27. When the input was generated for this simulation run the satellite link between Nodes 18 and 27 was inadvertently replaced by a cable link of length 660 km. Nevertheless, the two satellite links were the source of most of the daily variation seen through the network. The daily peak-to-peak frequency and phase variations observed are as follows:

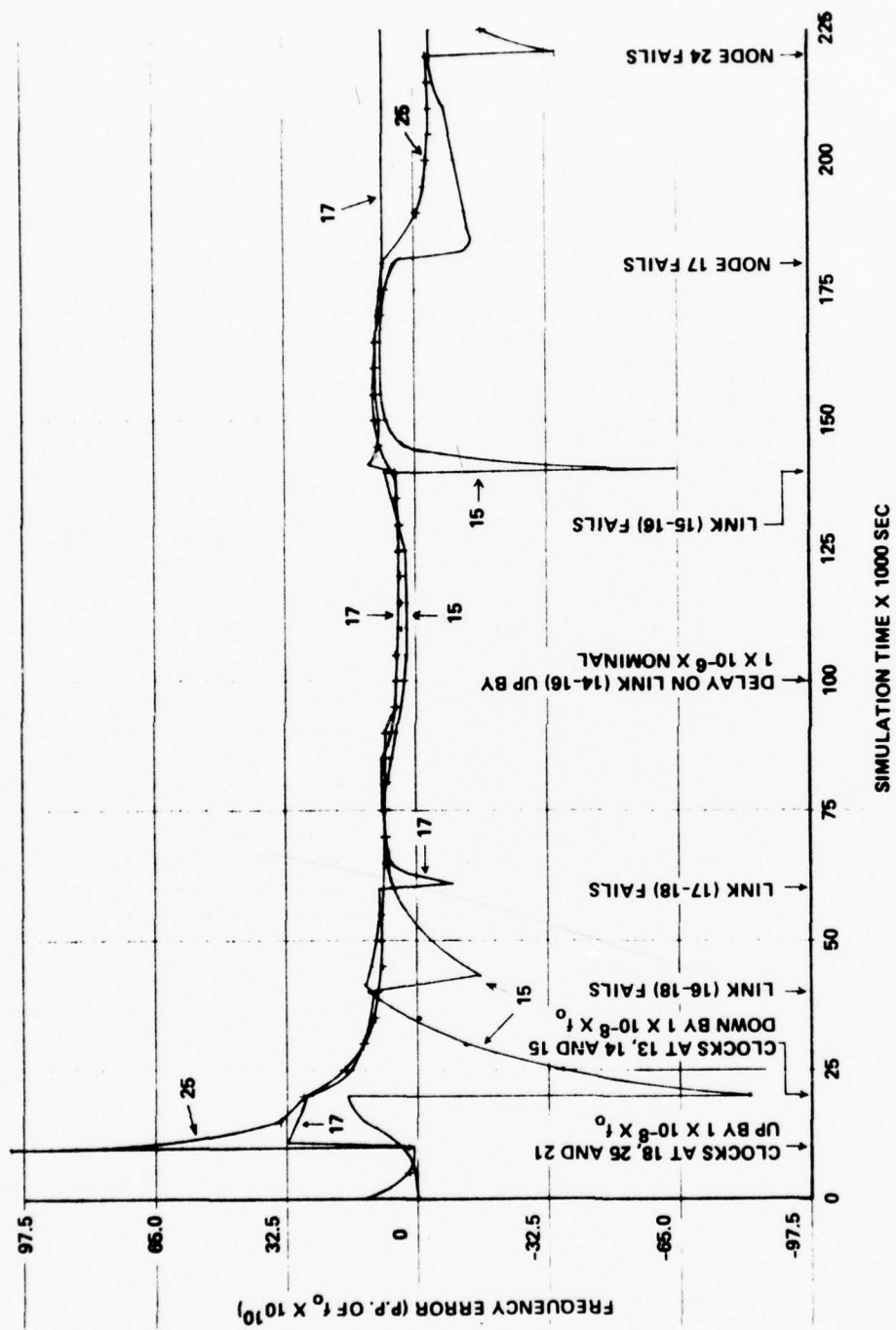
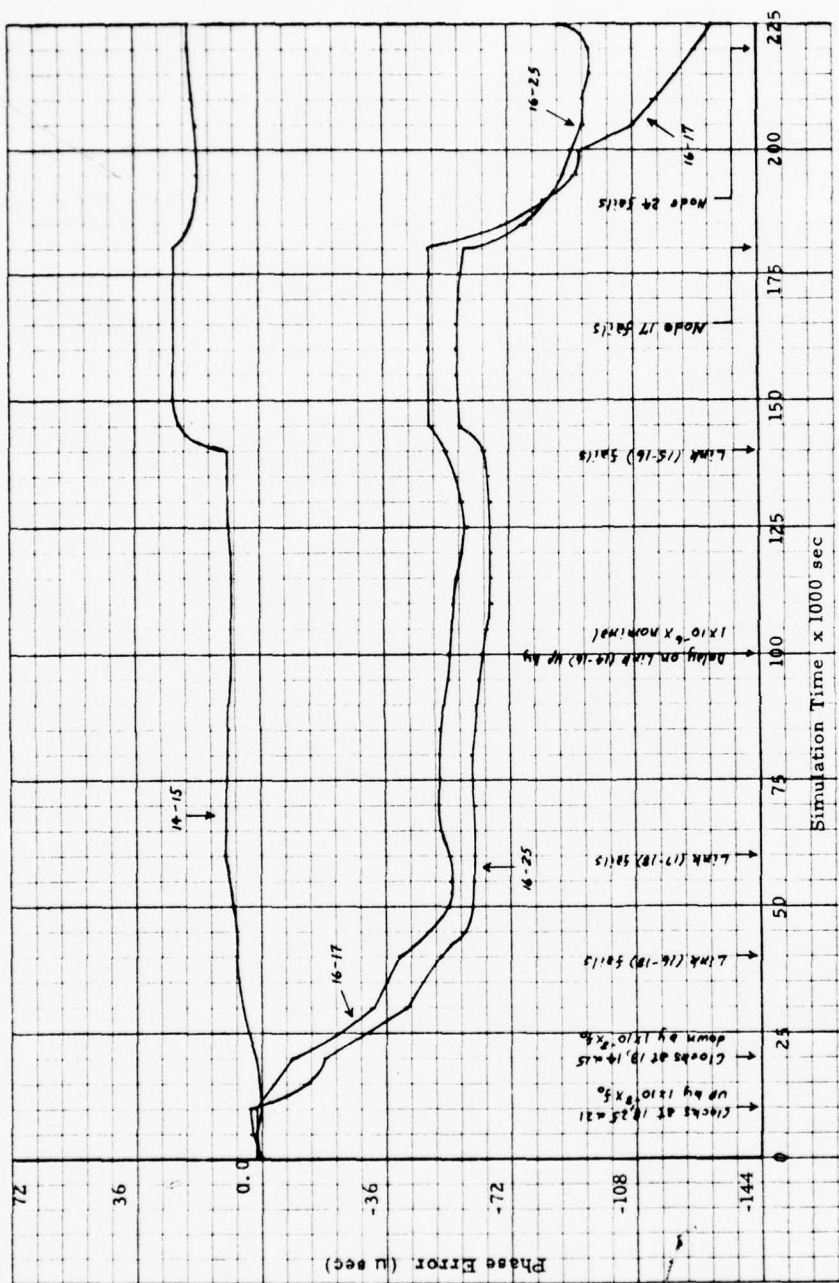


Figure 7.3.6.1-1. Mutual Sync, Configuration A, IT + ND + SE Frequency Plots



<u>Node</u>	<u>Daily peak-to-peak Frequency Variation $\left(\frac{\Delta f}{f_o} \times 10^{10}\right)$</u>
8	7.51
18	6.48
14	5.70
23	5.44
20	5.44
24	5.63
27	6.22
29	6.48
22	5.44
7	7.38
5	5.96
9	7.38
10	7.12
17	6.41

<u>Link</u>	<u>to</u>	<u>Node</u>	<u>Daily peak-to-peak Phase Variation (Cycles of f_o)</u>
27-29		29	1.18
18-14		14	4.21
18-20		20	5.73
18-23		23	5.46
18-27		27	0.86
23-24		24	0.08
8-14		14	8.23
8-18		18	22.20
27-8		8	15.00

Composite Plots

Figures 7.3.6.1-3 and 7.3.6.1-4 show composite initial transient, link disturbance and stress events plots of link to node phase errors for Links 8-14, 18-23, 27-8, and 27-29 and nodal frequency errors for Nodes 8, 14, 23, and 29.

The initial frequency transient at Node 8 is caused mostly by the combined initial frequency error at Node 10 of $26 \times 10^{-10} \times f_0$ and initial phase errors between Node 8 and the satellite links. Each of the nodes plotted experienced a daily frequency variation of approximately $9 \times 10^{-10} \times f_0$ due to satellite links between Nodes 8 and 18 and between Nodes 27 and 8. The link delay change on Link 8-18 at time 20,000 seconds was not noticeable except at Node 8 where it appears to have caused an increase in frequency of approximately $2 \times 10^{-10} \times f_0$. The failure of Node 5 at 40,000 seconds caused a change in Node 8's frequency of approximately $4.8 \times 10^{-10} \times f_0$. Failure of Link 23-24 at 80,000 seconds caused a change in Node 23's frequency of $16.25 \times 10^{-10} \times f_0$. The change of $1 \times 10^{-8} \times f_0$ in Node 18's nominal clock frequency at 120,000 seconds caused Node 23's frequency to change by approximately $26 \times 10^{-10} \times f_0$ and Nodes 8 and 29 by approximately $11 \times 10^{-10} \times f_0$. Failure of Link 8-18 at 18,000 seconds caused a change in Node 8's clock frequency of $15.6 \times 10^{-10} \times f_0$ and approximately $2.6 \times 10^{-10} \times f_0$ in those of Nodes 14 and 29. The change in Node 18's nominal clock frequency at 120,000 seconds appears to have changed the system frequency by $9 \times 10^{-10} \times f_0$. Although the link failures caused momentary transients in particular nodal frequencies whose amplitude were comparable to those caused by a change in nominal clock frequency of $1 \times 10^{-8} \times f_0$, the link failures do not appear to have caused a change in system frequency.

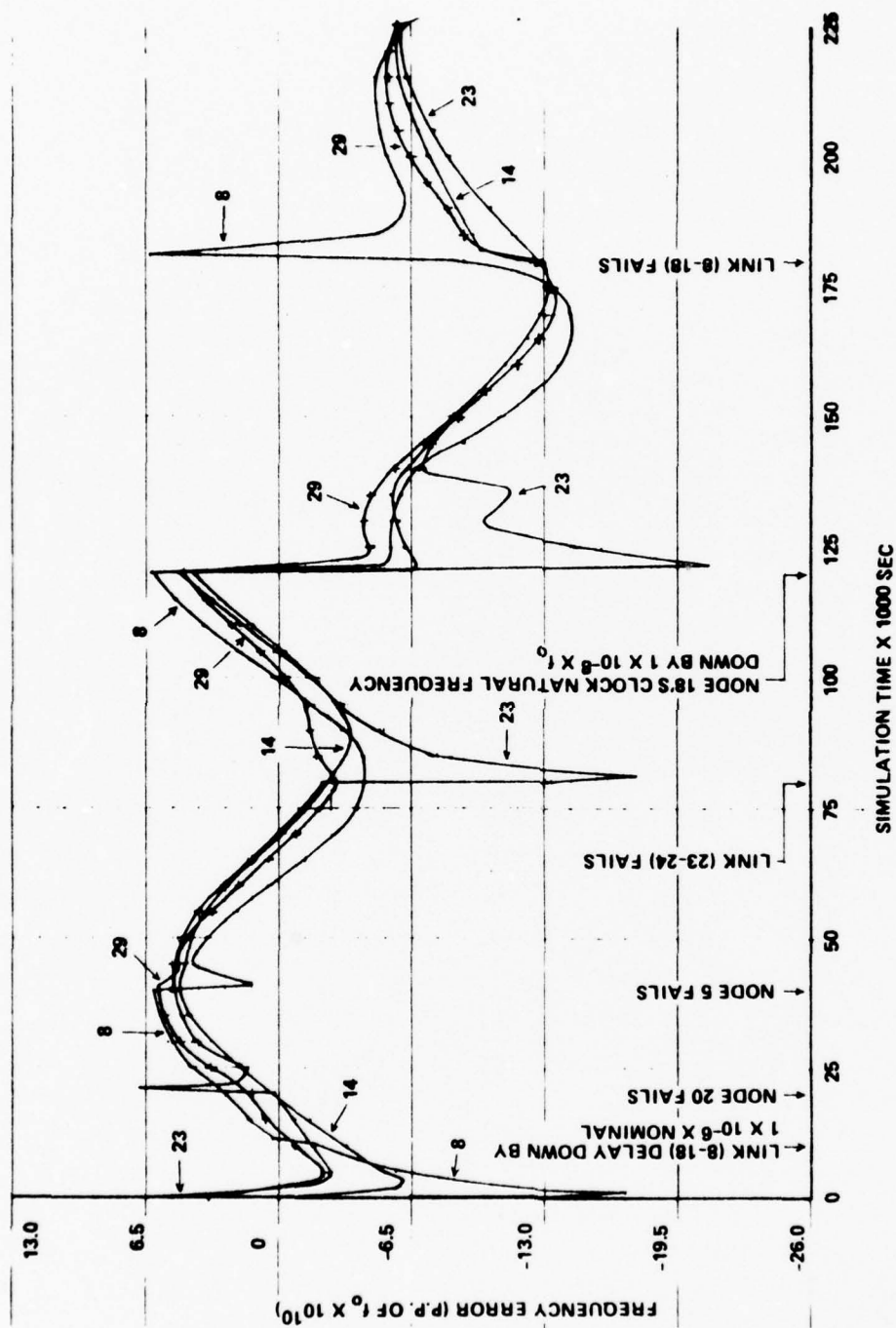


Figure 7.3.6.1-3. Mutual Sync, Configuration B, IT + ND + SE Frequency Plots

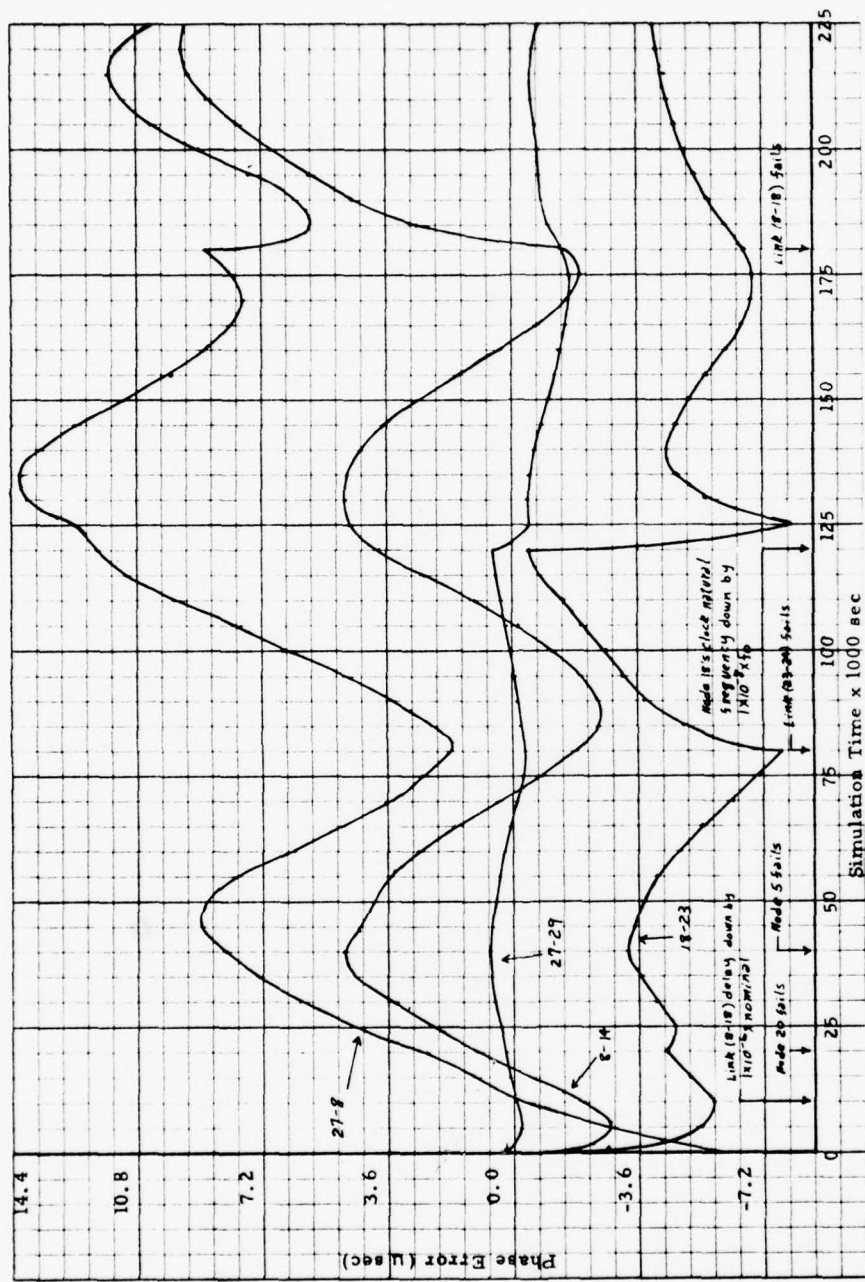


Figure 7.3.6.1-4. Mutual Sync, Configuration B, IT + ND + SE Frequency Plots

7.3.6.2 Master-Slave

Under the master-slave scheme, each node is slaved to the timing received via the communications link. Thus, it sees all link perturbations in this reference information. However, by making individual node's loop time constants long enough, these perturbations can be filtered sufficiently that only the long term average reaches the VCO control signal.

7.3.6.2.1 Configuration A

Figures 7.3.6.2.1-1 and 7.3.2.6.1-2 shows composite initial transient - normal link disturbance - stress events plots of link to node phase errors for Links 14-15, 16-17, 16-25, and 25-29 and nodal frequency errors for Nodes 15, 17, 25 and 29.

This run shows a transient and a step change in the natural frequency of a clock in the timing chain. Node 25 starts at time 0 with a frequency error of approximately $-2.7 \times 10^{-10} \times f_o$ and a phase error with respect to its reference via Link 16-25 of approximately $-0.47 \mu s$. These errors are cancelled by 6000 seconds. The other nodes experience similar initial transients. The time scale is broken at 6000 seconds and picks back up at 30,000 seconds. At 31,100 seconds Node 25's clock natural frequency makes a step increase of $1 \times 10^{-8} \times f_o$. At 31,300 seconds Node 25 has built up enough phase error with respect to its reference via Link 16-25 to trigger into its acquisition mode. This causes a frequency jump from approximately $f_o (1 + 91 \times 10^{-10})$ to $f_o (1 - 91 \times 10^{-10})$ at 31,300 seconds. The accumulated phase error and frequency error is then reduced to close to zero by 35,000 seconds. At 31,100 seconds Node 29 begins to follow Node 25 up in frequency but the phase error does not quite reach a high enough value at 31,300 seconds to trigger into acquisition mode. The errors at Node 29 are also reduced to zero between 31,300 and 35,000 seconds. The phase error of approximately $0.4 \mu s$ associated with Link 14-15 is between two communicating nodes in separate timing chains with each node one level from the master.

7.3.6.2.2 Configuration D

Figures 7.3.6.2.2-1 and 7.3.6.2.2-2 show composite initial transient - normal link disturbance - stress events plots for link to node phase errors for Links 5-7, 6-16, 22-23, and 24-28 and nodal frequency error for Nodes 7, 16, 23, and 28.

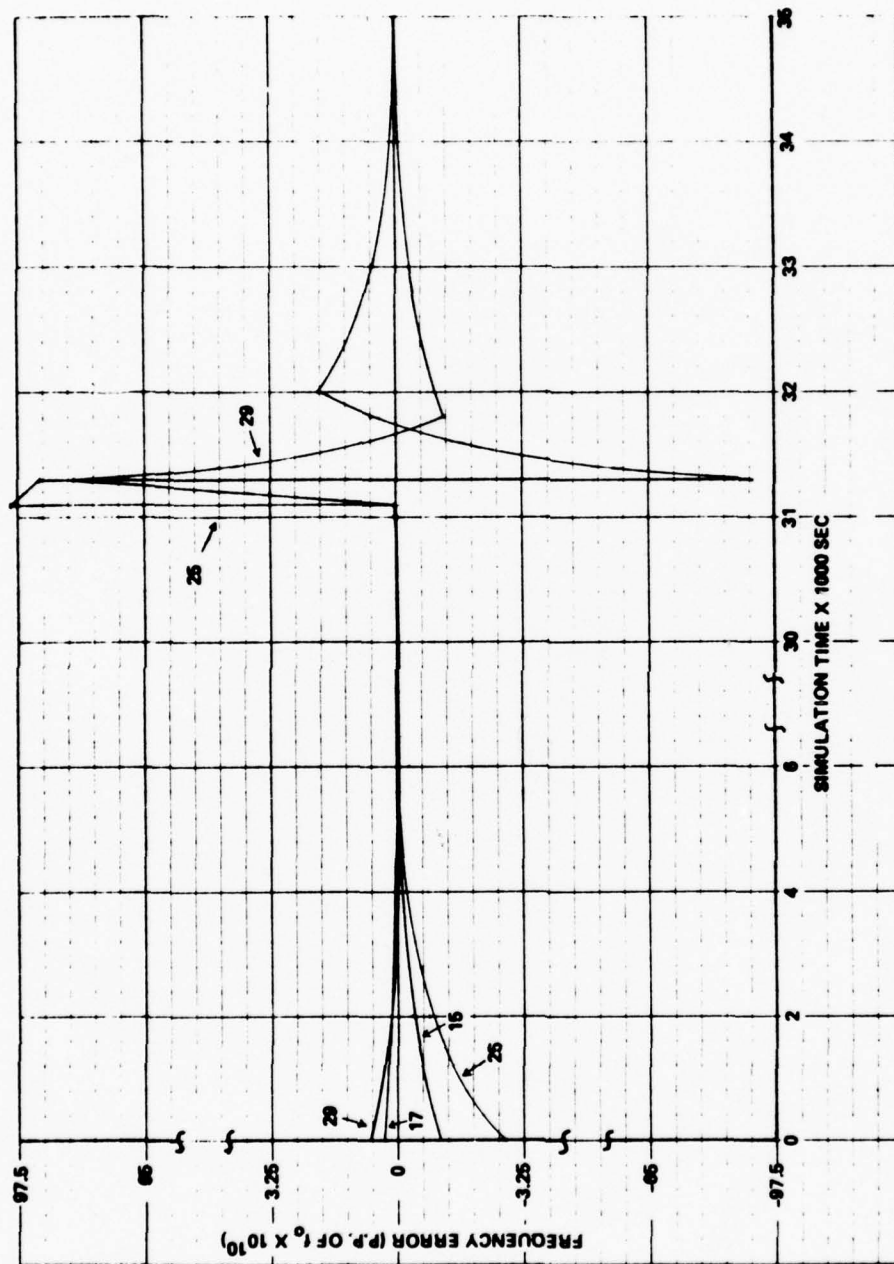


Figure 7.3.6.2.1-1. Master-Slave, Configuration A, IT + ND + SE Frequency Plots

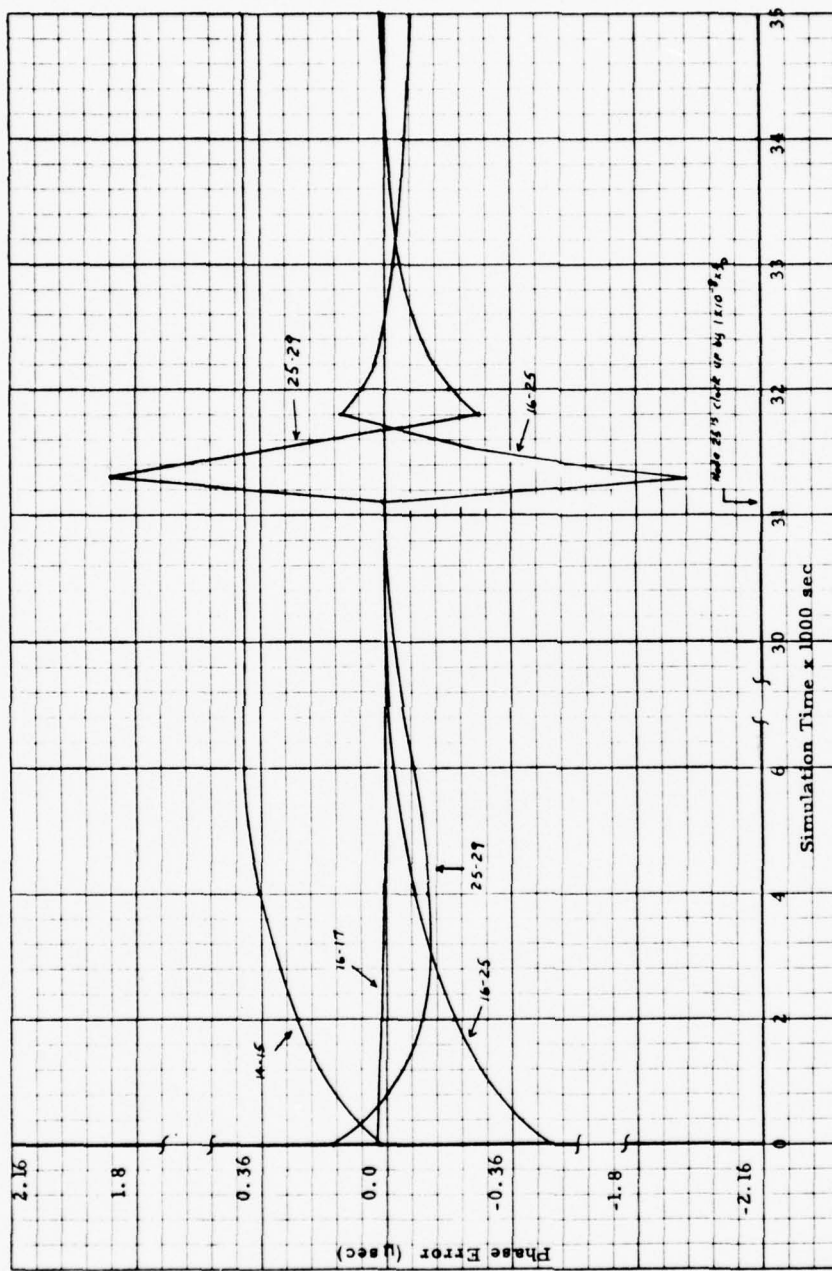


Figure 7.3.6.2.1-2. Master-Slave Configuration A, IT + ND + SE Phase Plots

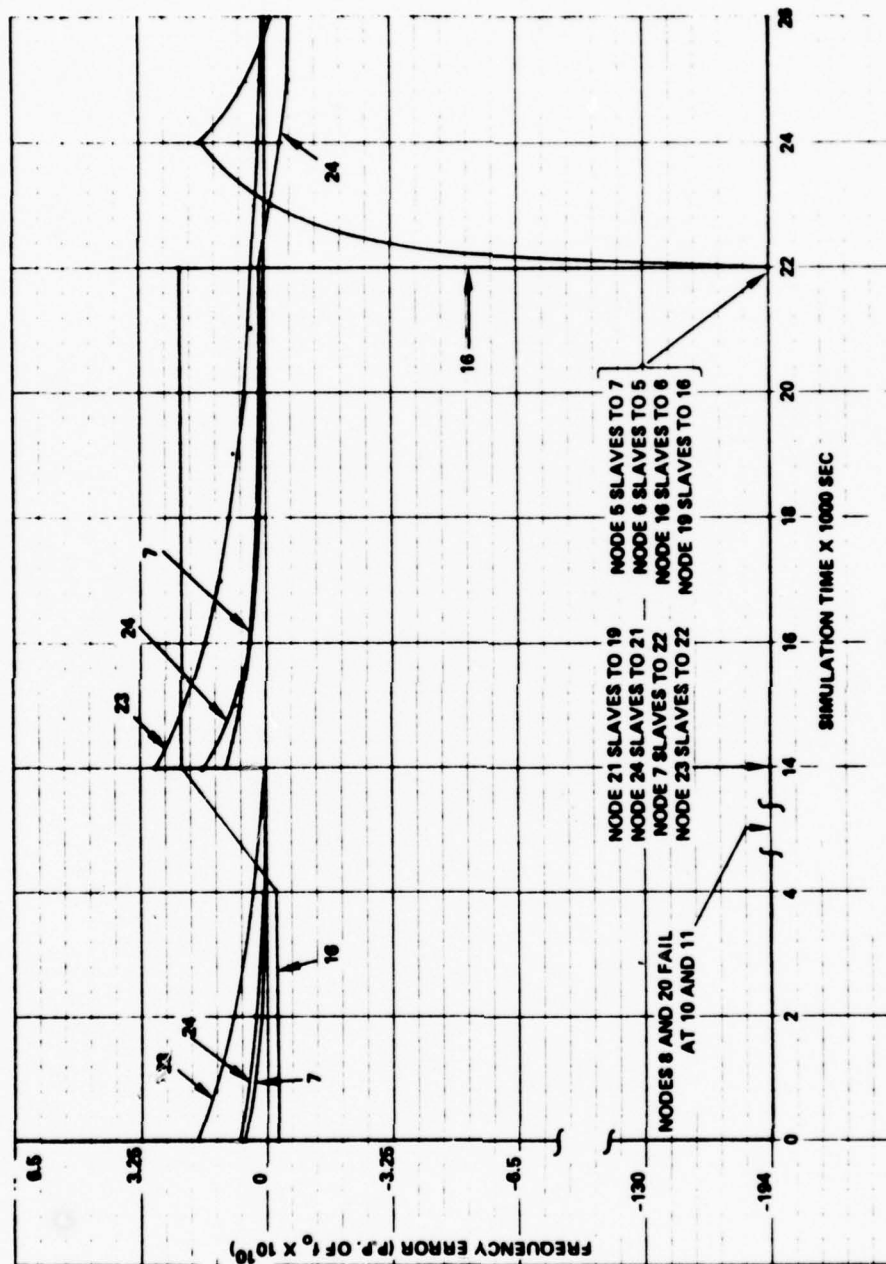


Figure 7.3.6.2.2-1. Master-Slave, Configuration D, Frequency Plots, IT + ND + SE

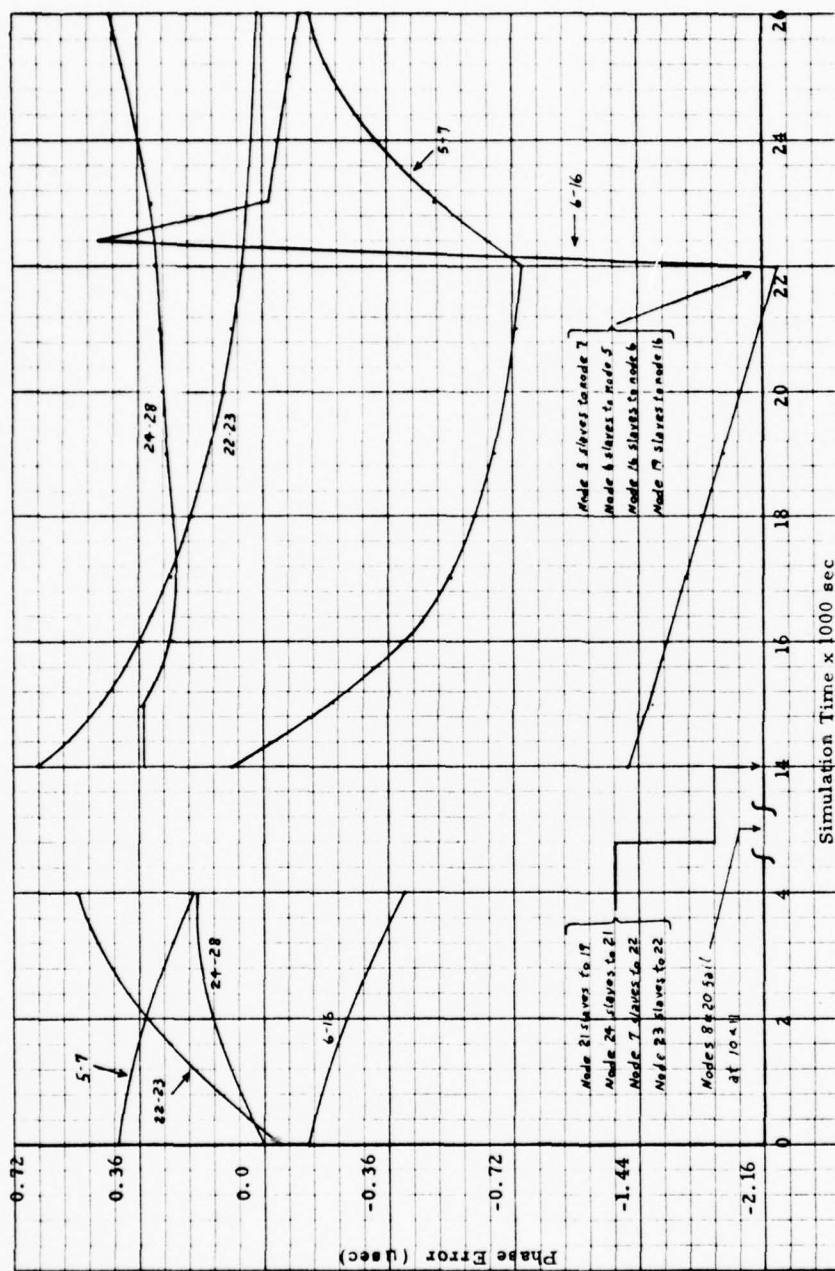


Figure 7.3.6.2.2-2. Master-Slave Configuration D, Phase Plots IT + ND + SE

This run shows an initial transient plus a major network reorganization. The initial transient is only shown out to 4000 seconds. The time scale then resumes at 14,000 seconds. The vertical scale of the frequency plot is also broken below -6.5 parts in 10^{10} of f_0 and picks up again at -130 parts. The initial transient shows that all nodes begin with initial frequency errors of less than 1.8 parts in 10^{10} and are close to zero by 4000 seconds. The phase errors shown except for 24-28 are with respect to nodes in different timing chains during the initial transient and do not appear to have settled out by 4000 seconds, but errors are all less than $0.5 \mu s$. At 10,000 seconds Node 8 fails. Node 20 fails at 11,000 seconds. The first part of reorganization then begins at 14,000 seconds when Node 21 slaves to 19, Node 24 slaves to 21, Node 7 slaves to 22 and Node 23 slaves to 22. This causes a step change in Node 23's frequency of $+2.93$ parts in 10^{10} . Nodes 24 and 7 experience smaller steps. The plot shows Node 16 with approximately $+2.3$ parts in 10^{10} of error at 14,000 seconds but the difference between its initial value and this value is only the smallest increment of the computer output. The second part of the reorganization occurred at 22,000 seconds when Node 5 slaves to 7, Node 6 to 5, Node 16 to 6 and 19 to 16. This left the remaining network completely linked in a timing sense with Node 22, the new network master. Of those nodes shown only Node 16 changed references at this time. Since Node 16 had a phase error with respect to the new reference signal via Link 6-16 of greater than $-2 \mu s$ when the switch occurred it immediately went into its acquisition mode. This caused its frequency error to jump from $+2.3$ parts in 10^{10} to -194 parts in 10^{10} . The errors at this node were then rapidly reduced during the period 22,000 to 26,000 seconds.

7.3.6.2.3 Configuration E

Figures 7.3.6.2.3-1 and 7.3.6.2.3-2 show composite initial transient - normal link disturbance - stress events plots for link to node phase errors 10-8, 14-15, 14-18 and 18-25 and nodal frequency errors for Nodes 8, 15, 18 and 25.

This run shows an initial transient, a link failure, two node failures and subsequent reorganization following these failures. The initial transient is shown out to 4000 seconds after which the time scale is broken. The peak frequency errors of the nodes shown during the initial transient were less than 3 parts in 10^{10} . Peak phase errors were all less than $0.6 \mu s$. All depicted nodes had reached approximately steady state conditions with close to zero frequency

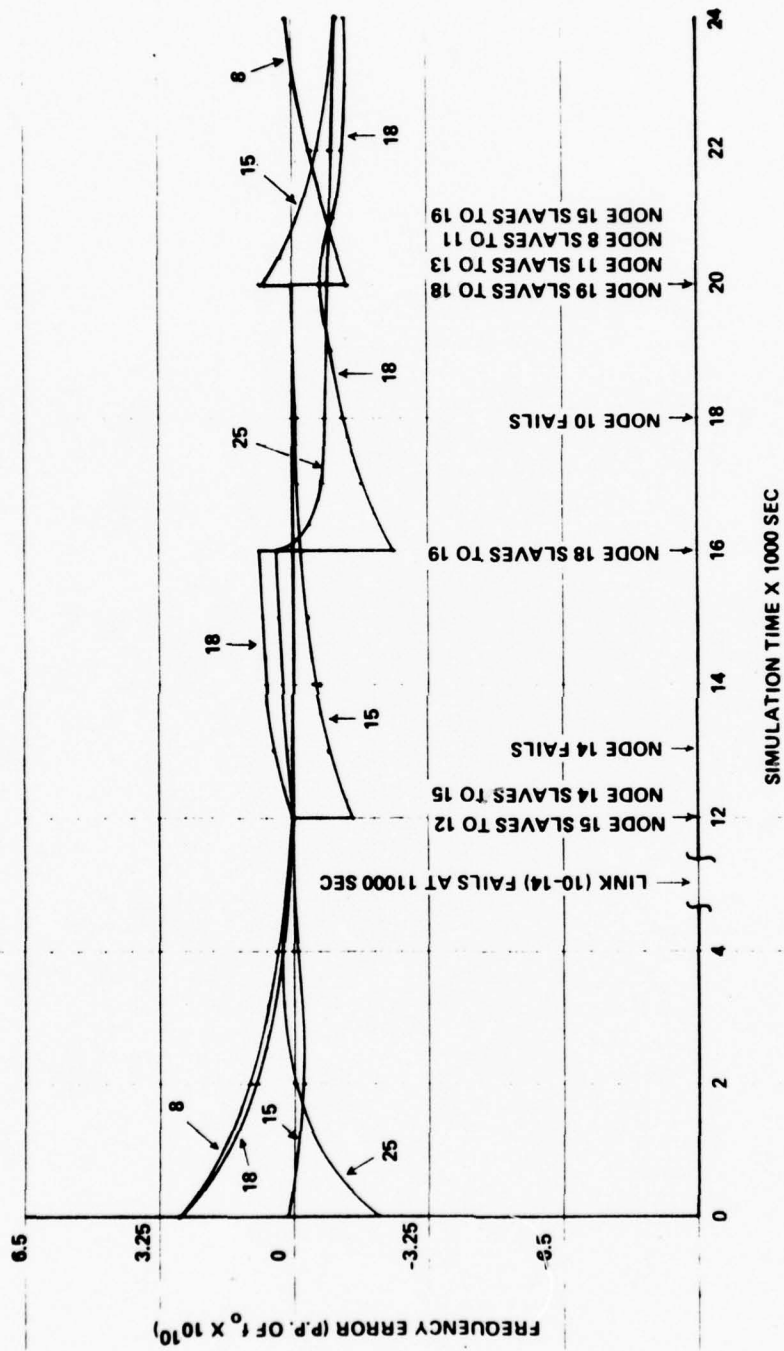


Figure 7.3.6.2.3-1. Master-Slave, Configuration E, Frequency Plots, IT + ND + SE

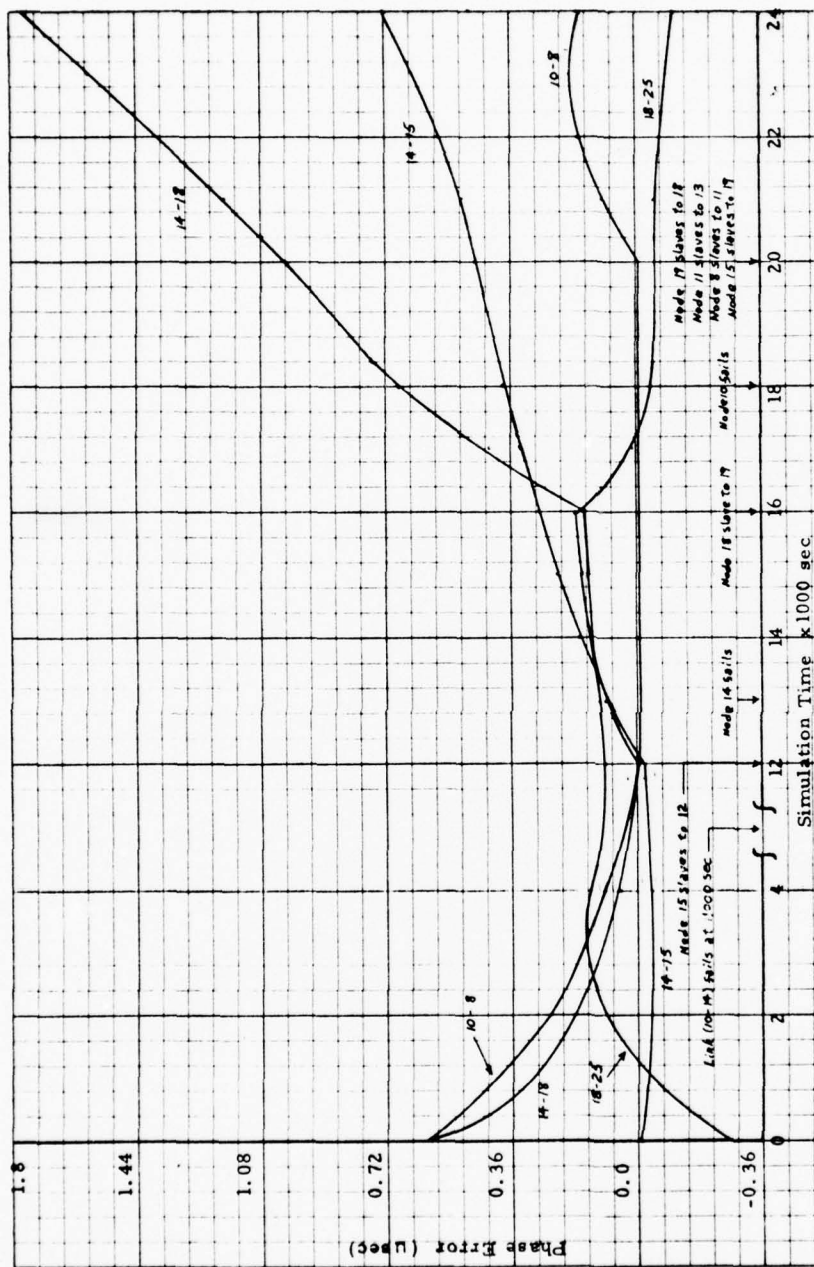


Figure 7.3.6.2.3-2. Master-Slave Configuration E, IT + ND + SE Phase Plots

and phase errors by 12,000 seconds. At 11,000 seconds Link 10-14 failed and Node 14 coasted without reference until 12,000 seconds at which time Node 15 changed reference from 14 to 12 and Node 14 began referencing Node 15. This reorganization caused a step change in Node 15's frequency of approximately $-1.4 \times 10^{-10} \times f_0$. Nodes 18 and 25 followed Node 15 via Node 14. At 13,000 seconds Node 14 failed and Node 18 coasted until 16,000 seconds at which time it began to reference Node 19. This caused a step change in Node 18's frequency of approximately $-3.25 \times 10^{-10} \times f_0$ due to the phase error between Node 18's clock and that at the receiving end of Link 19-18 of approximately $0.15 \mu s$. Node 25 began to follow this change. At 18,000 seconds Node 10 failed and Node 12 began coasting. At 20,000 seconds Node 19 began to reference Node 18 with 18 still referencing 19. Nodes 18 and 19 then referenced each other for the remainder of the run. Also at 20,000 seconds much of the remainder of the network changed references but the changes of most interest were that Node 15 referenced 19, 13 referenced 16, 11 referenced 13 and 8 referenced 11. This caused a step change in Node 15's frequency of approximately $+0.65 \times 10^{-10} \times f_0$ after which it then approached Node 19's frequency. Node 8's frequency changed by approximately $-1.3 \times 10^{-10} \times f_0$. Since Node 8 was then four nodes away from its ultimate reference and this entire chain was undergoing a transient it was still heading away from its ultimate reference's frequency at the end of the simulation. After a node fails, the simulator stops updating the nodal frequency, i.e., the nodal frequency remains at the last value before the failure. Thus, phase errors may increase rapidly as shown for 14-15 and 14-18 after 13,000 seconds or 10-8 after 18,000 seconds.

7.3.6.3 Time Reference Distribution

It should be noted that what is plotted as phase is the phase error between the local node and the received phase. The nominal delay of the link is taken mode π and then any delay variation and/or difference between the reference node's clock phase and the local clock phase is added to this module value to obtain the phase values that are plotted. This value is actually the error signal of the phase-locked loop in the master-slave scheme. On the other hand, the TRD scheme tends to adjust each local clock's phase so that it corresponds to the phase of the master clock without regard for link delays or variations thereto. Thus, there is no fixed relationship between the error signal which is fed into each of TRD node's phase-locked loops and

the values that are plotted as phase. Thus, the phase plots for the TRD scheme will not in general be zero in the steady state. One consequence of this is that, to the degree that the TRD scheme accomplishes its purpose, the total link perturbations should show up in the TRD phase plots.

7.3.6.3.1 Configuration A

Figures 7.3.6.3.1-1 and 7.3.6.3.1-2 show composite initial transient - normal link disturbance - stress events plots for link to node phase errors for Links 19-13, 16-17, 16-25, 18-19, and 25-29 and nodal frequency errors for Nodes 13, 17, 25, 19 and 29.

This run shows an initial transient and a step change in natural frequency of one clock in the network. Other events occurred but no perturbations were observed on the links or nodes which are shown. Due to an initial frequency error at Node 13, a phase error sufficient to trigger into the acquisition mode ($2 \mu\text{s}$) is acquired by 1300 seconds at which time Node 13 switched to its acquisition mode. This resulted in a step change in Node 13's frequency of $-111 \times 10^{-10} \times f_0$. These errors then quickly return to close to zero by 2200 seconds. Similarly, Node 17 had an initial frequency error of approximately $+12 \times 10^{-10} \times f_0$. Consequently, it built up enough phase error by 2450 seconds to switch to its acquisition mode. This caused a step change in Node 17's frequency of $-150 \times 10^{-10} \times f_0$. The reason for the difference between these two changes in the graph is that the step size of the computer output was too coarse to catch the actual peaks. At 31,100 seconds Node 25's clock made a step increase in frequency of $1 \times 10^{-10} \times f_0$. At 31,300 seconds the phase error between Node 25 and the ultimate reference reached a sufficient value ($2 \mu\text{s}$) to cause Node 25 to switch to its acquisition mode. This caused its frequency to change by approximately $175 \times 10^{-10} \times f_0$ to an error of $-85 \times 10^{-10} \times f_0$. These errors were then reduced to approximately zero by time 32,000 seconds. Node 29 which was slaved to 25 saw the sum of the error between itself and Node 25 and the error between Node 25 and the master node. This would be zero during the entire transient except that the information that it obtains about the error between Node 25 and Node 16 is one sample period older than that between itself and Node 25. Thus, it saw a small error signal and remained fairly close in phase and frequency to Node 16, the ultimate reference. Table 7.3.6.3.1 lists the times at which the various nodes made transitions from tracking to acquisition mode and vice versa. Nodes 21, 24 and 30 were not monitored.

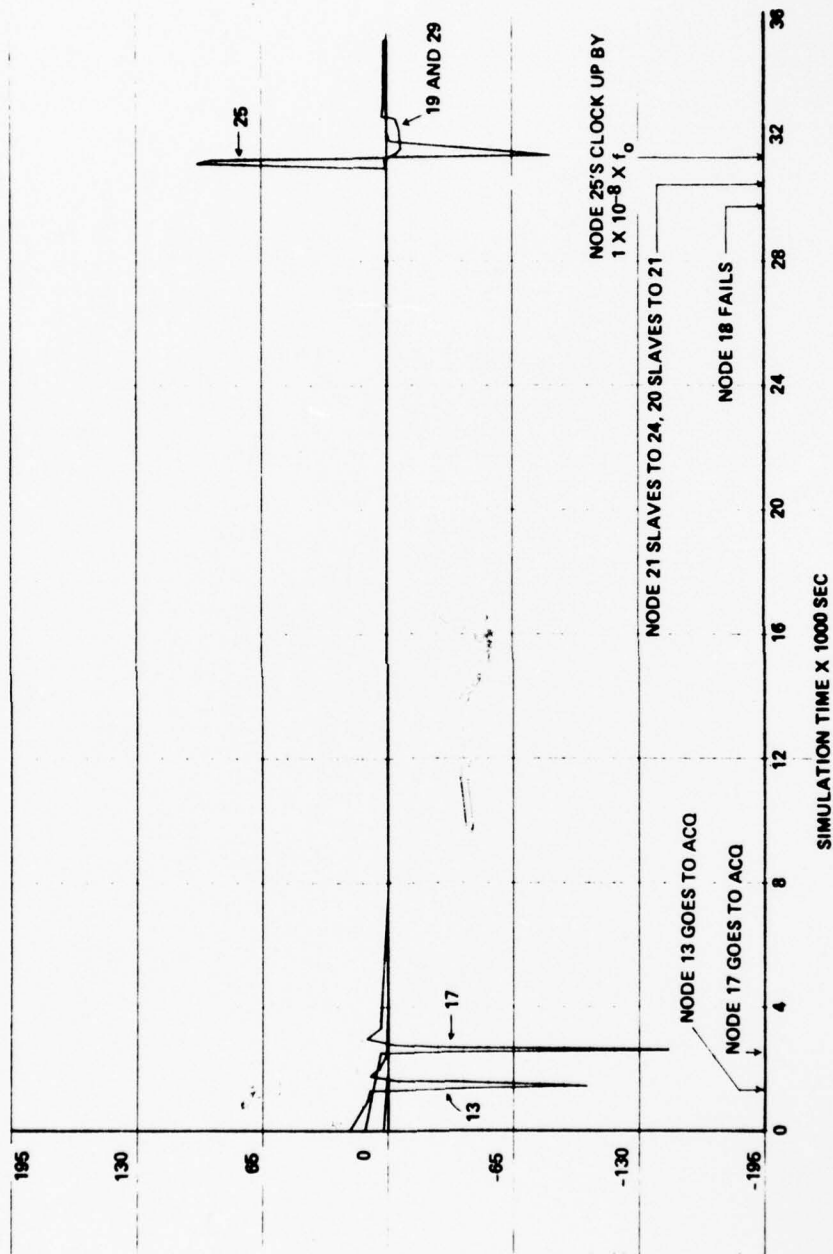


Figure 7.3.6.3.1-1. TRD Configuration A, Frequency Plots, IT + ND + SE

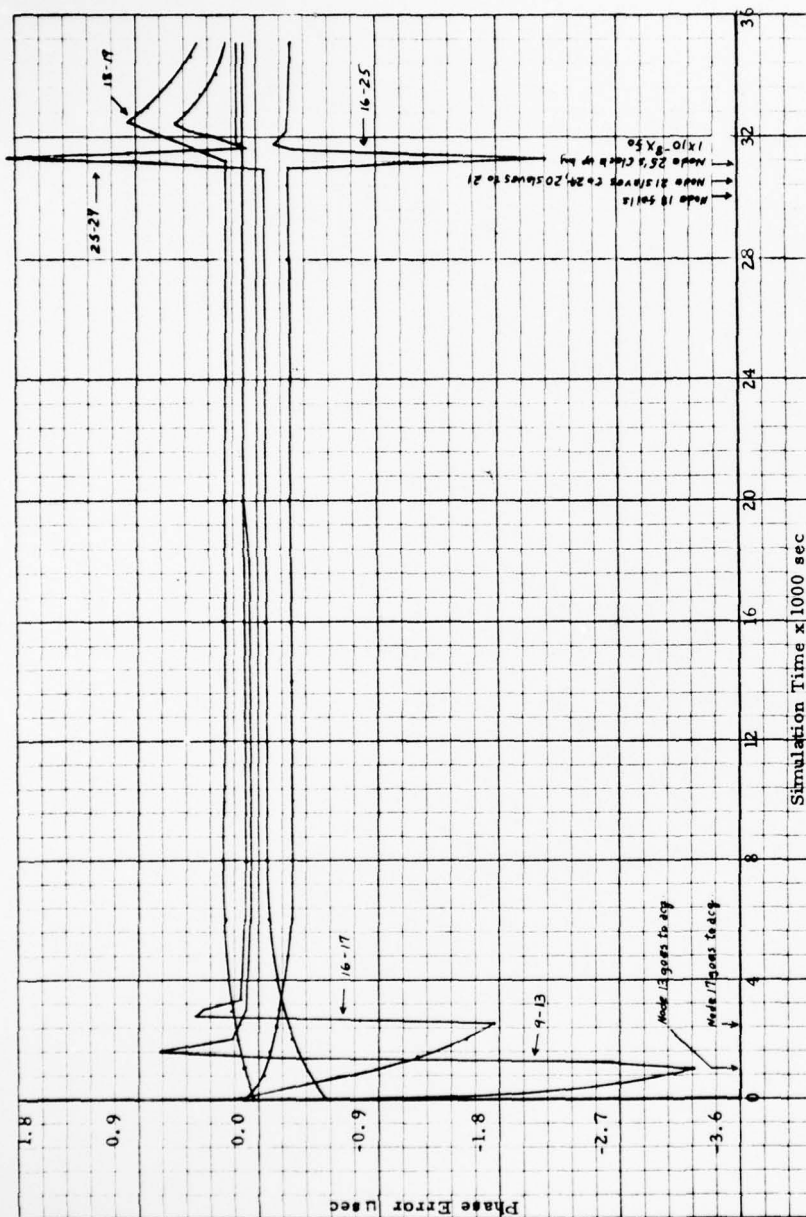


Figure 7.3.6.3.1-2. TRD Configuration A, Frequency Plots, IT + ND + SE

Table 7.3.6.3.1. Track/Acquisition Mode Changes

Run 1

<u>Node</u>	<u>Track to Acq.</u>	<u>Acq. to Track</u>
9	1155	2310
13	1305	2460
17	2445	3600
21	2625, 4095	3780, 5250
24	2640, 4110	3795, 5265
30	2640, 3795, 31500, 33000	3795, 4950, 32655, 34155
25	31305	32460

Run 2

<u>Node</u>	<u>Track to Acq.</u>	<u>Acq. to Track</u>
13	1380	2535
9	1440	2595
17	2550	3705
21	2730, 4200	3885, 5355
24	2730, 4200	3885, 5355
30	2730, 3900, 31500, 33000	3885, 5055, 32655, 34155
25	31305	32460

7.3.6.4 Simulation Run Results Summary

A tabular summary of the simulation run results is shown in Table 7.3.6.4.

A link dropout or node failure results in changing references in the TRD and master-slave techniques. It results in reaveraging phase errors from the remaining references in the mutual sync technique. As a result of these types of stresses the master-slave technique showed peak frequency errors up to 3.25 parts in 10^{10} . The mutual sync technique showed peak frequency changes of from 10 to 20 times that of master-slave while no variation in nodal frequency was experienced with the TRD technique due to these stresses.

The response of the TRD node to a VCO center frequency change was due to a time skew in the components that make up the total time reference signal with respect to the master at nodes further down the timing chain than where the stress occurred. This time skew in error components was a result of the method of implementation of the simulator but is not inherent to the TRD technique. This response does not die out in going further out the chain as with the master-slave technique because with TRD each succeeding node receives the same error due to the skewed samples.

The master-slave and TRD techniques experienced the same change in nodal frequency when switching from tracking to acquisition mode. However, this is strictly a function of the loop parameters and phase threshold at which the switch occurs.

Table 7.3.6.4. Summary of Generalized Simulation Results

<u>DISTURBANCE</u>	<u>PEAK FREQUENCY CHANGE ($\Delta f/f_o \times 10^{10}$)</u>			
	<u>NODES AWAY</u>	<u>MUTUAL SYNC</u>	<u>MASTER- SLAVE</u>	<u>TRD</u>
LINK DROPOUT OF NODE FAILURE	1	MAX. - 65 NOM. - 20-30	MAX. 3.25 NOM 2	0
	2	MAX - 30 NOM 3-10	MAX 2 NOM 1	0
CHANGE IN VCO CENTER FREQUENCY OF 1×10^{-8}	1	10-33	81	7
	2	0-10	10	7
SWITCH FROM TRACKING TO ACQUISITION MODE	0	-----	192 192 $\left[2(\delta_A \omega_{nA} - \delta_T \omega_{nT}) \Delta \phi \right]$	
SATELLITE LINK DISTURBANCE	1	MAX 7.5	0.6	0
	2	2.5 - 5.5		—

SECTION 8.0
EVALUATION OF TIMING TECHNIQUES

8.0 EVALUATION OF TIMING TECHNIQUES

In the paragraphs that comprise this section each of the four timing techniques, independent clocks, mutual synchronization, time reference distribution and master-slave are analyzed in order to determine the degree to which each technique provides the desirable characteristics discussed in Section 4.0.

8.1 Survivability

Survivability indicates the degree to which the timing subsystem continues to perform its function (to provide network timing) during periods of stress. Fallback modes of operation shall be provided so that the timing subsystem itself will not cause significant degradation in overall DCS network capability to provide dependable digital communications during these periods. Survivability is important because:

1. One of the primary goals of the DCS is to provide dependable digital communications for its users during periods of network stress.
2. The network timing subsystem must be operational to provide acceptable digital communication during such periods.

Network synchronization is necessary because the slip rate that two nodes will experience in communicating is directly proportional to the frequency offset between their nodal clocks. If this offset increases in a stressed environment then slip rate increases which leads to misaligned frames in multiplexers and switches and a need to resynchronize cryptos. Since timing subsystem performance is directly tied to slip rate, we will measure slip rate as a function of level of stress to indicate the survivability of each timing approach.

There are two parts to the problem of minimizing the slip rate in a digital network:

1. Keep the nodal clocks of all communicating node pairs synchronous as much as possible.
2. Minimize the frequency offset between the nodal clocks of asynchronous communicating nodes and minimize the amount of time they must communicate with asynchronous nodal clocks.

To put these comments in perspective we note that the independent clock technique uses asynchronous clocks at every node. The slip rate due to buffer overflows is strictly a function of the clock accuracy and the buffer size and will not change as a function of stress level. On the other hand, one could reduce the slip rate by slaving these clocks to a common master through some master-slave timing distribution hierarchy. This would make all nodal clocks synchronous and slips due to buffer overflows could be avoided entirely providing there were no link or node failures. If link or node failures occur, then some nodes may lose their reference to the master. Then some nodes with asynchronous nodal clocks may be communicating and could experience slips. We will call such nodes "asynchronous communicating nodes." Such nodes will remain asynchronous until they once again become locked to a common reference. It is very desirable that the timing approach minimize the period of time during which such nodes are asynchronous.

From these comments one can see that we take issue with the common misconception that the independent clock approach offers the ultimate in survivability. We will argue that a disciplined technique with a fixed timing distribution network has better survivability because nodes will not experience slips as long as they can obtain a reference, and when a reference is not available, they revert to a self-reference approach which has performance equivalent to an independent clock approach. However, the improvement in using this approach is not great because of the significant probability that a node will lose its reference. This is the reason that master-slave approaches have been criticized for having poor survivability. However, there is a better way for distributing timing. In fact, a dramatic improvement in survivability can be obtained by using an adaptive timing distribution network approach such as has been implemented in the Canadian Data route⁹² and has been proposed for use with TRD.²⁰⁵ This is due to the ability of each node connected to the network to find another reference after the loss of a reference.

We have performed some analyses to demonstrate the points discussed in the preceding paragraph. This will allow suitable comparisons to be made and will demonstrate significant characteristics of each approach.

The independent clock approach is the easiest to analyze. All communicating nodes are asynchronous. The time between slips (or buffer overflows) at a node can be calculated from

$$T_s = B/\delta \quad , \quad (8.1-1)$$

where δ is the frequency offset (in Hz) between the two nodal clocks and B is the buffer size (buffer fill may change by up to $\pm B$ bits before an overflow occurs). The performance achieved with this approach is simply a function of the ratio B/δ . There is a direct trade between buffer size and clock accuracy. One may reduce the clock accuracy by a factor of K if the buffer size is increased by a factor of K , and the value of T_s will be unchanged. Note also that the performance is independent of network stress level.

The performance of several approaches for implementing a disciplined timing distribution system will be evaluated. The parameter B/δ is considered to be one of the fundamental design parameters for each of these approaches. In this case the clock offset, δ , refers to the offset between any two nodal clocks that will occur if they lose their references. Normally, all nodes will have a common reference. Slips will not occur in this case. The only time that slips will occur is when one or both of the nodes loses its reference and has to run "asynchronously." A good disciplined approach will attempt to minimize the product of the amount of time any node must run asynchronously and the offset, δ , that will occur during this time.

The first approach to be considered is the use of a fixed timing distribution network. That is, even though each node may have several links over which it is communicating, it will only have one link from which it may derive a reference. If that reference is lost, the node must run asynchronously. This approach will have the poorest performance of the disciplined approaches in terms of minimizing the amount of time each node must run asynchronously. However, it performs better than the independent clock approach. The performance will be dependent on topology of the network. Because of this, completely general results cannot be obtained. However, by assuming a specific topology that can be analyzed, one can obtain results that indicate the important characteristics of this approach. The topology that will be used is the "starred polygon" with connectivity 4. This topology for an 8 node network is

shown in Figure 8.1. Node 1 is the master, and timing is distributed via the routes indicated by the arrows. Note that there are four independent timing chains that distribute timing (1-2-4; 1-3; 1-7-5; 1-8-6).

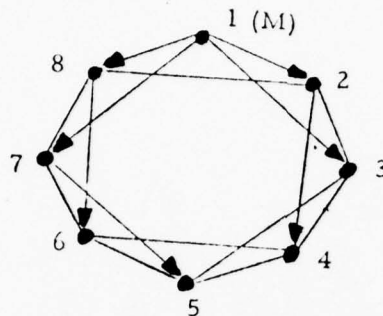


Figure 8.1. Starred Polygon With Connectivity of 4 and 8 Nodes

This topology was chosen mainly for convenience in analysis. This particular problem is very tedious to analyze for any general topology. However, results can be obtained for regularly structured topologies such as that shown in Figure 8.1. Thus, the results will serve mainly to demonstrate important characteristics of the approaches being analyzed rather than provide highly accurate comparisons which will be valid for general network topologies. Such results cannot be obtained.

The details of the analysis are presented in Appendix B. The analysis will consider only link failures for purposes of simplicity. Addition of node failures to the model would add significant complexity to the analysis effort without significantly improving the results. The average fraction of asynchronous communicating node pairs was calculated and is given by Equation (B.3). Asymptotically, for small p , $\eta \text{ Fac} \approx kp$, where p is the probability of link outage. Thus, as one might expect since single link outages can cause many nodes to lose their timing references this term dominates Fac . The worst case is for large $p \rightarrow 1$ for which Fac is almost 0.5. This is shown in Figure B.2. These results were related to the time between slips by observing that slips only occur on that fraction of the nodes that are asynchronous. Then

$$T_s = B/\delta \text{ Fac} \quad (8.1-2)$$

Since the worst-case $\text{Fac} \approx 0.5$ then $T_s \approx 2B/\delta$. Thus, this approach has an average time between slips of about twice that of an independent clock approach with the same value of B/S . However, at small values of p the time between slips improves dramatically as shown in Figure B.3.

Next, we analyzed a system with a primary reference and a fixed alternate reference. The same network topology was used, and the primary reference was the same as is shown in the figure. It was assumed that each node took its alternate reference from the node adjacent to it looking back toward the master. Again, F_{ac} was calculated and is given by (B.5). Asymptotically, for small p , we find that $F_{ac} \approx kp^2$. This is consistent with our approach of providing two available references per node. Then two link outages can cause a node to lose its reference to the master and become asynchronous with respect to the rest of the network. The worst-case occurs for $p \approx 0.5$ for which $F_{ac} \approx 0.11$ for a 20 node network. At this value of p , $T_s \approx 9B/S$ which is a considerable improvement but still does not offer dramatically higher survivability than the independent clock approach. These results are also shown in Figures B.2 and B.3.

The final approach considered was a disciplined system with the capability of adaptively reconfiguring the timing distribution network as link outages occur. This technique has been implemented in the Dataroute network⁹² and has been proposed for use with Time Reference Distribution.²⁰⁵ This approach has the properties that:

1. All communicating nodes are synchronous in the steady-state (after a sufficiently long period following the last failure).
2. The only time a nodal clock will act as a self-reference is while the timing distribution network is being reconfigured (which is a relatively short period of time).

This approach has a high degree of survivability. The system can be designed so that no slips occur in the steady-state. The only time slips can occur is during the transients associated with reconfiguring the network. Obviously, one of these transients occurs every time an outage occurs, and any single outage can cause the network to be reconfigured in such a manner that several nodes may have to act as a self-reference during this process. Performance in a stress environment is influenced by both the time required to reconfigure the timing distribution network and the length of time a node can act as a self-reference without experiencing slips (which is a function of the buffer size and frequency offset).

There is a trade-off here between time required for reconfiguration, buffer size, and the fractional frequency offset between the nodal clock and the network frequency. For example, a cesium clock could operate without reference for 24 hours while accumulating only about $1 \mu\text{s}$ of phase error relative to the network master. In actual practice, though it should be no problem to accomplish network reconfiguration in 10 minutes. In this case even the phase errors accumulated with quartz clocks will be rather small.

The only way that this approach can encounter a problem is if it must spend all of its time attempting to find a suitable reference without ever obtaining a reference for a period long enough to allow it to resynchronize. In order for this to happen the reference must fail soon after the node tries to lock to it. A rather crude, but conservative, analysis was carried out to relate T_s to link failure rate as a function of certain design parameters. The results are shown in Figure B.4. This approach is many orders of magnitude better than the independent clock approach with the same value of B/S even at very high failure rates. In fact, the larger the value of B/S , the greater the advantage of using this adaptive approach. For example, for $B/S = 24$ hours this approach is 7 orders of magnitude better than the independent clock approach even with $F_d = 10$ (i.e., 10 link failures per day per link). One would expect at most just a few failures per day per link even under severe stress because a high level of stress would imply greater difficulty in making repairs. Certainly, there would be many failures caused by physical damage which could take days or longer to repair. Thus, the nature of most failures is not such that a link may fail, be repaired in a few minutes, then fail again a short time later followed by a quick repair, etc. Certainly this type of failure mechanism which could lead to a higher value of F_d poses the only threat to a disciplined timing subsystem with adaptive reorganization. The reason for this is that links which behave in this way cause the network to have to reorganize too often. Such behavior could be caused by a link which was frequently jammed for short periods of time. Thus, an enemy could try to disrupt the synchronization subsystem by frequently jamming a number of links. However, this tactic can be effectively countered by not allowing any node to use a link as a reference which has failed more than a few times a day.

These results indicate that the performance of master-slave timing subsystem with adaptive reorganization is greatly superior than that of an independent clock timing subsystem at virtually all stress levels even using much smaller values of B/δ . One might add that precisely the same comments could be made about the time reference distribution approach because it also uses the adaptive reorganization technique. This is the key to achieving a high level of performance under stress. In fact, the TRD approach should perform slightly better than the master-slave approach because of its ability to remove the effects of path delay variations on nodal frequencies. This will allow it to operate at a slightly better offset, δ , from the network master.

The mutual synchronization approach also achieves a high degree of survivability. In fact, one might even think that it should perform better under stress than the adaptive reorganization approach since, if a node has at least one operational link it has a reference. Thus, in a pure mutual sync network nodes never communicate asynchronously. In actuality, though, the master-slave and TRD systems with adaptive reorganization can be designed so that even under severe stress, the probability that node pairs have to communicate asynchronously for long enough to result in slips (or buffer overflows) is extremely small. Thus, the mutual sync approach would offer no measurable advantage. In fact, it is likely that there will be more variation in nodal clock frequencies (or more error propagation) with the mutual sync approach under stress which is an undesirable characteristic.

One of the principal objectives of a network synchronization scheme is to maintain very stable nodal frequencies at each node in the network. Thus, it is highly desirable to prevent perturbations in the frequency of one nodal clock from propagating and influencing the frequency of nodal clocks in other parts of the network. By minimizing such perturbations of nodal clocks, one maximizes the stability of each nodal clock and minimizes the probability of a bit slip.

The degree of error propagation for several types of disturbances will be evaluated for each of the synchronous timing techniques, master-slave, mutual sync, and time reference distribution. Four types of disturbances will be evaluated. These are a link dropout, a step change in nominal VCO frequency, a step change in path delay, and sinusoidal path delay variations. The disturbances will be applied at one point in the network and the effect on other nodal frequencies will be measured as a function of distance (in number of nodes) from the disturbance. This will be evaluated entirely by simulation. The results of the simulations will be summarized in tabular form for each type of disturbance. In addition, plots of nodal frequencies as a function of time after a link dropout will be shown for the three timing techniques.

Two network configurations will be used in these evaluations. The network shown in Figure 8.2-1 will be used to evaluate master-slave and TRD. Node 1 is the master, and the

Master

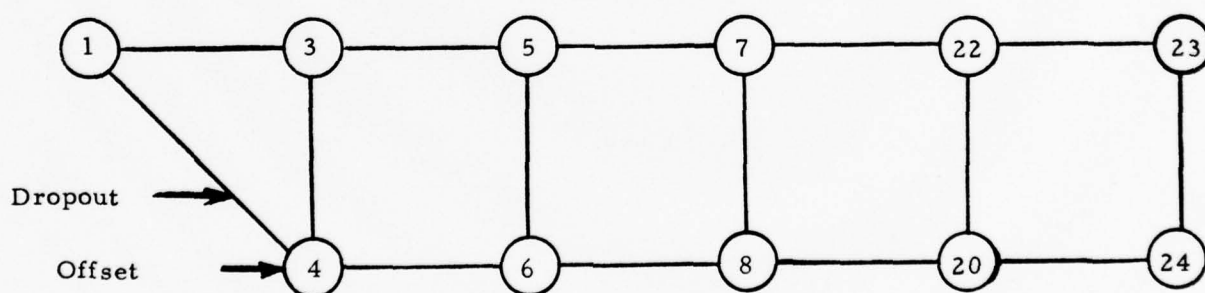


Figure 8.2-1. Master-Slave and TRD Error Propagation Experiment

timing distribution chains are 1-3-5-7-22-23 and 1-4-6-8-20-24. The disturbances will occur on the second of these two chains and will propagate down the chain. The first chain will remain undisturbed, and comparisons between the two can be made. One could also use this network to test mutual sync by placing a disturbance at the left end and determining the degree of

propagation. However, this configuration is probably not representative of how errors will typically propagate in a mutual sync network. For this reason, we have chosen to use the more fully connected network of Figure 8.2-2. Propagation of disturbances to distant nodes can occur over many parallel paths. In general, there will be multiple nodes at distance one, two, three, etc. The results presented will display the average effect on all nodes at distance one, two, three, etc.

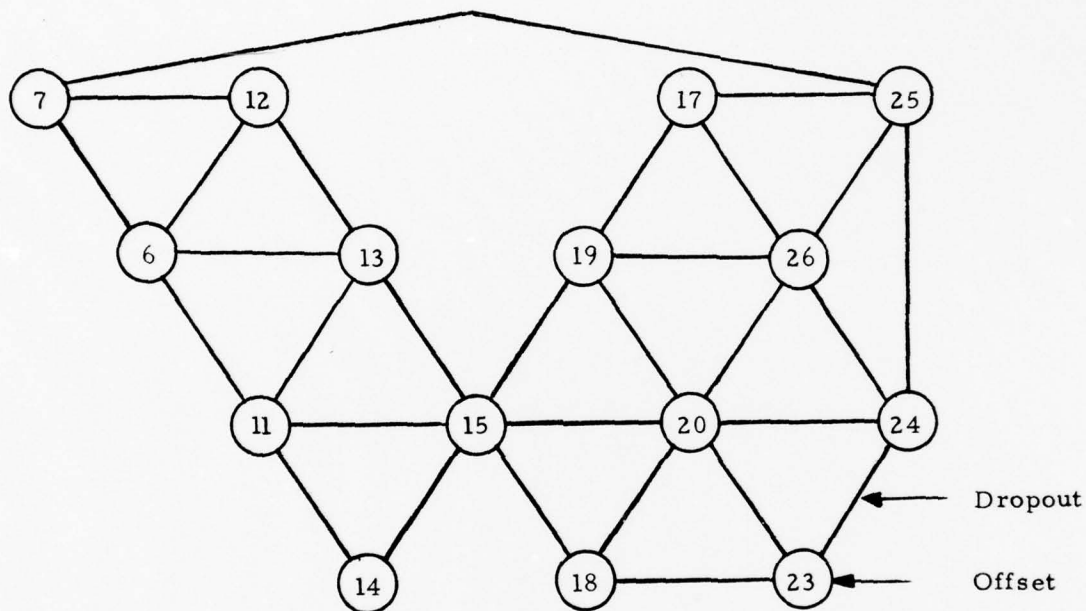


Figure 8.2-2. Mutual Sync Error Propagation Experiment

Two simulations were performed to compare perturbations due to path delay variations. In the first, a step change in path delay with a magnitude of $0.65 \mu\text{s}$ was introduced on one link (Links 1-4 in the master-slave and TRD simulations and Links 23-24 in the mutual sync simulation). The peak fractional change in nodal frequency as a function of distance from the disturbance for these simulations is shown in Table 8.2-1. The results indicate that mutual sync is relatively less affected by the step change than master-slave. The reason is that the link with delay variation is only one of several being averaged to obtain a reference at the nodes nearest the disturbance. However, there are two undesirable properties of mutual sync which are not reflected in Table 8.2-1. First, the disturbance causes a slight permanent change in system

Table 8.2-1. Error Propagation Due to a $0.65 \mu\text{s}$ Step Change in Path Delay

Distance (Nodes)	Peak $\Delta f/f_0$		TRD
	Master-Slave	Mutual Sync	
1	3×10^{-10}	10^{-10}	-
2	10^{-10}	3×10^{-11}	-
3	6×10^{-11}	2.5×10^{-11}	-
4	4×10^{-11}	2.5×10^{-11}	-

frequency. Second, the disturbance will propagate to all nodes in the network in a mutual sync system, but the disturbance will propagate only to nodes lower in the timing distribution chain in a master-slave system thereby affecting only a small fraction of all the nodes in the network. The simulation of TRD displayed no measurable effect on nodal frequencies due to the step change in path delay. This indicates the advantage of using a double-ended system to eliminate the effect of path delay variations.

Rapid path delay variations are effectively attenuated by all three techniques, and there is very little effect on nodal frequencies. However, very slow path delay variations will perturb the nodal frequencies. A typical case is that of variations with a period of 1 day. This case was simulated with the variation placed on all links in the network. The magnitude of the variation was $0.65 \mu\text{s}$ (peak-to-peak) on each link. The results of the simulations are shown in Table 8.2-2.

Table 8.2-2. Error Propagation Due to a Sinusoidal Path Delay Variation on All Links With a Magnitude of $0.65 \mu\text{s}$ Peak-to-Peak and a Period of 1 Day

Distance (Nodes)	Peak $\Delta f/f_0$		TRD
	Master-Slave	Mutual Sync	
1	2.5×10^{-11}	1.4×10^{-10}	-
2	5×10^{-11}	1.4×10^{-10}	-
3	7×10^{-11}	1.4×10^{-10}	-
4	9×10^{-11}	1.4×10^{-10}	-

Neither master-slave nor mutual sync successfully attenuates the effect of the path delay variations. The distance shown for master-slave refers to the distance from the master. The node that is distance one away receives the effect of only one link variation, the node at distance two receives the effect of two link variations, etc. Thus, the perturbation of nodal frequencies due to path delay variations grows as a function of distance from the master. Of course, this result is to be expected, and typically the requirements for stable nodal frequencies are less severe at the tails of the network. In contrast, we note that all nodes in a mutual sync system are perturbed to the same degree. The amount of the perturbation at all nodes in a mutual sync network is about twice that experienced at the third level of the master-slave network. Thus, one would expect that the perturbation in a master-slave network would not be worse than that in this mutual sync network until the sixth or seventh level of the network. The mutual sync network of Figure 8.2-2 could have been configured as a master-slave network with all timing chains of length three or shorter, and thus master-slave would perform considerably better than mutual sync on it. One would expect similar results for larger networks. The effect of path delay variations on a mutual sync network will grow as a function of network size since these perturbations propagate throughout the network.

We note that once again TRD is unaffected by path delay variations. The magnitude of the fractional frequency variations in master-slave and mutual sync networks due to path delay variations is several parts in 10^{10} . Because of this, one cannot take advantage of the inherent stability of atomic clocks at nodes other than a master node using these techniques. However, by using the double-ended technique of TRD, one can use more stable clocks and improve the stability of nodal frequencies by an order of magnitude to a few parts in 10^{11} .

The third disturbance simulated was a link outage. Link 23-24 was removed in the mutual sync network. For master-slave and TRD Link 1-4 was removed and Node 4 then slaved to Node 3. The results of the simulation are summarized in Table 8.2-3. The output from the simulation runs is shown in Figures 8.2-3, 8.2-4, and 8.2-5. Note that the scale for fractional frequency offset is different for mutual sync than for master-slave and TRD. Several observations can be made. First, mutual sync is much more severely affected by a link dropout than the other approaches. The reason is that the VCO at each node must be held to the network frequency by a nonzero steady-state phase error. If a node is averaging the phase error on n links to provide

Table 8.2-3. Error Propagation Due to a Link Outage

Distance (Nodes)	Peak $\Delta f/f_0$		TRD
	Master-Slave	Mutual Sync	
1	1.7×10^{-10}	4.5×10^{-9}	6.5×10^{-11}
2	6.5×10^{-11}	8×10^{-10}	6.5×10^{-11}
3	4.5×10^{-11}	4×10^{-10}	6.5×10^{-11}
4	4×10^{-11}	4×10^{-10}	6.5×10^{-11}

an input for the loop filter, then it must average the other $n-1$ links when one of the references is lost. At that instant, the average of the phase errors on the $n-1$ links can be considerably different from the average of the phase errors on the original n links. Thus, the loop can be hit with a large phase step. The magnitude of this effect can be quite variable, and one principal contributor is the offset between the system frequency and the nominal VCO center frequency at a node which loses a link (since bigger offsets result in bigger phase errors). In this simulation the fractional offsets at Nodes 23 and 24 (Curves 1 and 2 in Figure 8.2-3) were approximately 10^{-8} which is normal for good quartz crystal VCO's. As we discussed in Paragraph 3.2.4 one could possibly reduce the magnitude of this transient by not allowing such a large step change in phase error be applied to the loop filter but making it occur more slowly. Even if this were successful, one would still have permanent changes in the steady-state system frequency due to link dropouts. Such a change was not observed in this simulation because the scale chosen for the printout was not adequate, but in previous simulations the steady-state frequency has changed by an amount about an order of magnitude less than the peak frequency change.

We note that the perturbation on master-slave is about a factor of 20 less than that of mutual sync. The reason there is any perturbation at all is that the references arriving on Links 1-4 and 3-4 are not in phase with each other. Thus, the loop must recover from a phase step after the switchover to the alternate reference.

During the switchover to an alternate reference with TRD, the fact that the references arriving on Links 1-4 and 3-4 are not in phase will not cause a transient (because TRD is a double-ended system). However, if there are constant link asymmetries on the two links that are different, then the effect will be the same as if the loop were perturbed by a phase step. In this

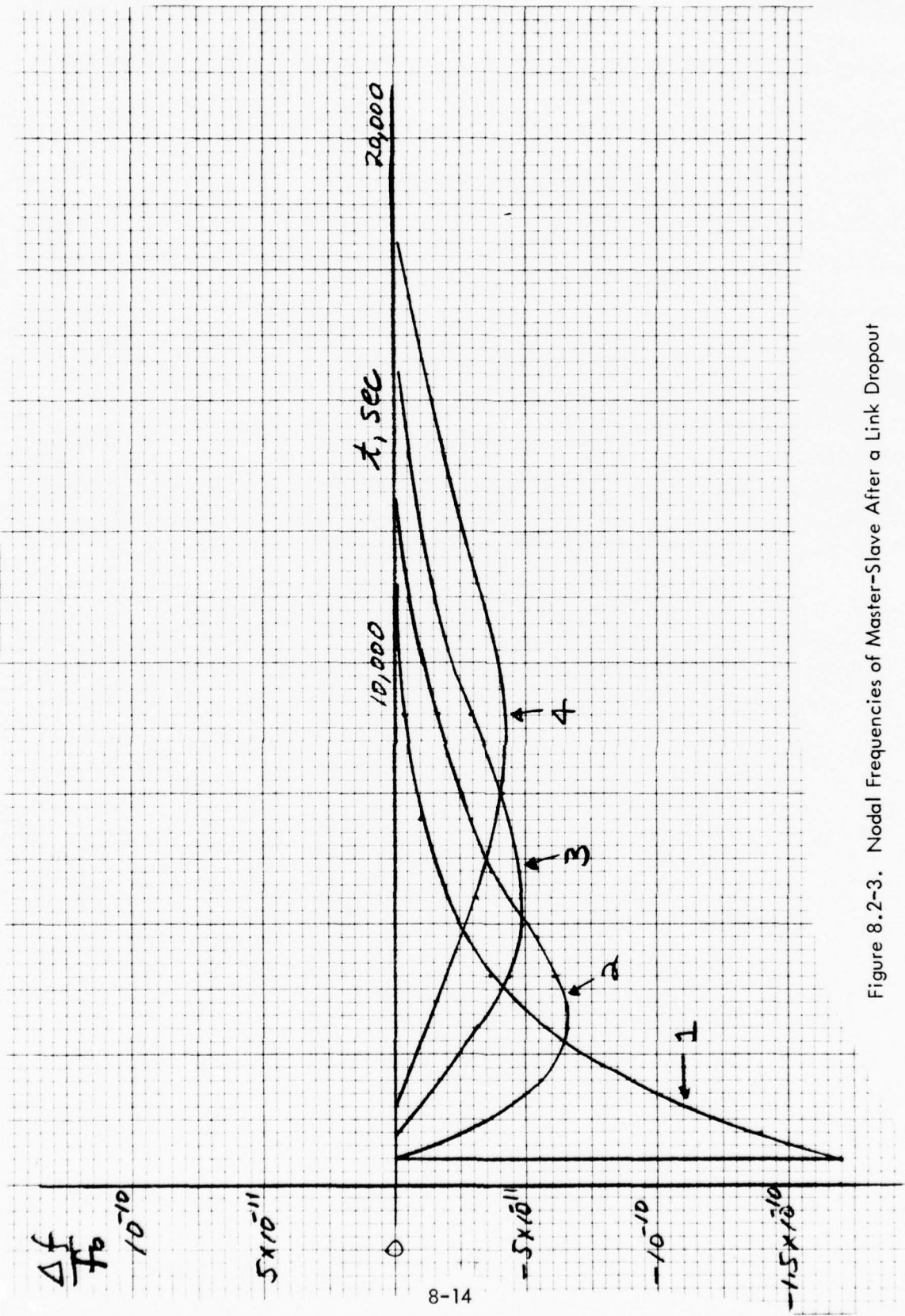
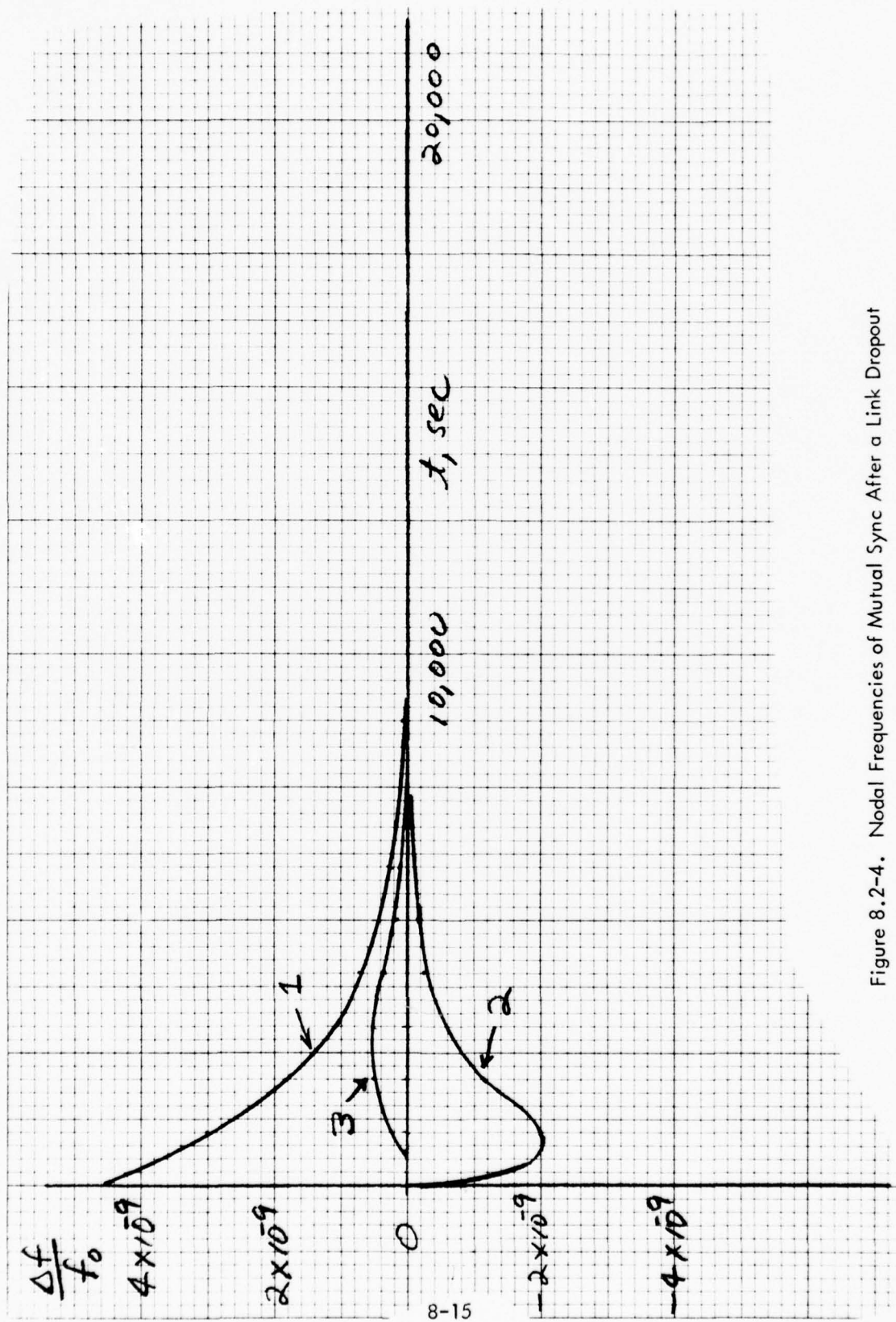


Figure 8.2-3. Nodal Frequencies of Master-Slave After a Link Dropout



8-15

Figure 8.2-4. Nodal Frequencies of Mutual Sync After a Link Dropout

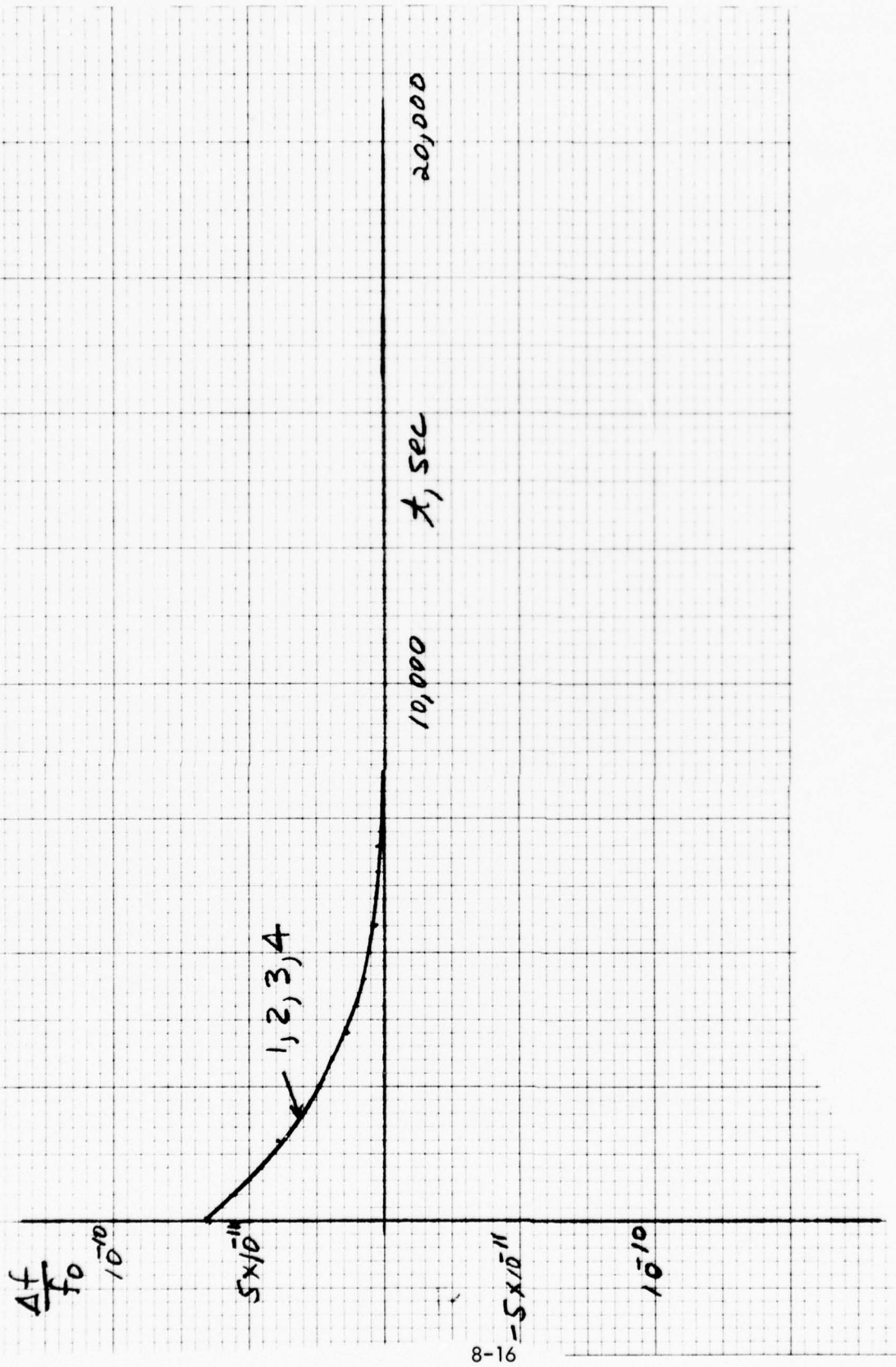


Figure 8.2-5. Nodal Frequencies of Time Reference Distribution After a Link Dropout

simulation, the link asymmetry was 300 ns on link 1-3 and 0 on link 1-4. Thus, the difference in link asymmetries is 300 ns. Then the loop responds to a phase step of half this amount or 150 ns. The magnitude of this asymmetry term is probably rather conservative. The peak frequency change on TRD is about half that of the master-slave approach and about a factor of 40 less than mutual sync. If the asymmetry term was different, the peak frequency change would scale accordingly. This simulation run assumed the quartz crystal VCO loop parameters. Another run using the cesium clock loop parameters improved the TRD results by another factor of 10.

The final simulation was a step in nominal VCO center frequency equal to a fractional frequency change of 10^{-8} . The frequency steps occurred at node 4 in the master-slave and TRD networks and at node 23 in the mutual sync network. Of course, this results in a severe frequency transient at the node at which the frequency step occurs. The three techniques were compared on the basis of how severely the adjacent nodes were affected. The results are shown in Table 8.2-4.

Table 8.2-4. Error Propagation Due to a Fractional Frequency Step of 10^{-8} in Nominal VCO Center Frequency

Distance (Nodes)	Master-Slave	Peak $\Delta f/f_0$	Mutual Sync	TRD
1	8×10^{-10}		1.4×10^{-9}	8×10^{-10}
2	6.5×10^{-11}		5×10^{-10}	8×10^{-10}
3	1.3×10^{-11}		5×10^{-10}	8×10^{-10}
4	1.3×10^{-11}		5×10^{-10}	8×10^{-10}

We note that master-slave is better than mutual sync by about a factor of two.

The TRD simulation used the wider band loop used with quartz crystal clocks. It had the same peak Δf as master-slave at distance one, but its comparison suffered at greater distances because the transient was not filtered out. All nodes further down the timing chain behave virtually the same as the node nearest the disturbance. Normally, a perturbation in a nodal clock frequency in the TRD technique should not affect the frequencies at clocks further down in the timing chain since all phase errors are referenced to the master. However, in order to do this the quantities used to compute the phase error, ΔT_{bm} , relative to the master

(i.e., ΔT_{am} , ΔT_a , and ΔT_b) must all be measured at the same time. In our simulation we did not do this. The quantities ΔT_a and ΔT_{am} were computed 1 minute earlier (in simulated real time) than the value of ΔT_b to which they were added. This introduced the measurement error which allowed the effects of the frequency step to propagate. Had these measurements been perfectly synchronized no effect would have been observed. Obviously, one could do a much better job of synchronizing these measurements than we did, and the benefit would be proportionately better performance, i.e., if they could have been synchronized to within 6 seconds, the error propagation would have been reduced by a factor of 10. Simulations of the cesium clock loop parameters at all nodes following the node with the frequency offset (node 4) indicate that the transient at other nodes is reduced by another order of magnitude due to the smaller value of ω_n . In addition, if the clock at node 4 had been a cesium clock with the cesium clock loop parameters, then a frequency step as large as was experienced (one part in 10^8) could have never happened. Any such frequency step would have been about one part in 10^{11} . In this case the transients would have been reduced by an additional order of magnitude. Actually, the comparisons between master-slave and TRD are so close on this disturbance that we would have to say they were even. However, the performance of the TRD technique can be considerably improved as discussed above.

In summary, we have tried to obtain an overall ranking of the three approaches on the basis of the four types of disturbances. Fortunately, the results were virtually the same on each evaluation. A summary of the rankings for each type of disturbance and the overall rankings are shown in Table 8.2-5.

Table 8.2-5. Ranking of Timing Techniques on the Basis of Error Propagation for Four Types of Disturbances

<u>Disturbance</u>	<u>Ranking</u>		
	Master-Slave	Mutual Sync	TRD
Path Delay Step	3	2	1
Sinusoidal Path Delay Variation	2	3	1
Link Dropout	2	3	1
Frequency Offset	1	3	1 (tie)
Overall Ranking	2	3	1

Mutual sync was third in the comparisons. Not only did a disturbance typically affect other nodes at a given distance to a greater degree than the other techniques, but it affected many nodes since disturbances in TRD and master-slave would affect only those nodes in the same timing chain. On the other hand, time reference distribution offers a clear advantage over the other two techniques in maintaining highly stable nodal frequencies under normal operating and stress conditions. The reason, of course, is due to the double-ended nature of the technique. The resulting stability of nodal frequencies is a few parts in 10^{11} which is very close to that of cesium standards. Thus, one can effectively utilize atomic standards in the network at those nodes where highly stable nodal frequencies are required with the TRD approach. The cheaper quartz crystal standards can be used at other nodes with slightly degraded performance, but even at these nodes the nodal frequencies will be more stable than if master-slave or mutual sync were used.

The compatibility of the DCS timing subsystem with other global timing sources is a desirable characteristic because it can conceivably result in an increase in the availability of the timing function for the DCS. Such an increase in availability results when the external timing source provides timing for a node after a failure that prevents the node from attaining timing internal to the DCS.

In order to compare the alternative timing techniques with respect to their compatibility to external timing subsystems, two points must be examined: First, do any of the timing techniques facilitate the hardware implementation necessary to provide this compatibility? Second, do any of the techniques result in a more effective transfer from primary to backup timing sources? By more effective, one means; do the buffers at the node switching to the backup timing source and for that matter, all buffers in the network, fill or empty more slowly for a timing subsystem based on one specific technique?

A third point concerning compatibility with other timing sources is whether or not it is a cost-effective method for providing additional redundancy for the timing function. Since this point impacts the overall significance of compatibility rather than the comparison of levels of compatibility between techniques, it has been addressed in Section 10.0 dealing with the ranking of desirable characteristics.

Timing subsystems for the DCS based on independent clocks, mutual synchronization, master-slave or time reference distribution can all be designed to utilize an external timing source. Timing sources such as LORAN C, OMEGA or GPS can be used as the backup source. In comparing the requisite hardware necessary to incorporate an external reference as a backup timing source, there is little difference between any of the techniques. This is true especially from a cost point of view where the dominant cost by far is the receiver necessary for the backup timing source. The functional implementation for the master-slave technique is merely to input the timing signal derived from the external receiver to the switch that selects the appropriate reference that disciplines the local clock. In the mutual synchronization technique, the functional implementation merely requires the addition of a switch to which both the external and internal timing signals are applied. The selection can then be made as to which timing signal

to utilize in disciplining the local oscillator. In the independent clock approach, a switch would be included to inject the timing signal derived from the external receiver to the appropriate distribution amplifiers that would under ordinary operating conditions accept a signal from the local clock. In the time reference distribution approach, the local oscillator that had been disciplined via a time transfer technique would now be disciplined via the external timing signal.

In summary, the hardware implementations appear only marginally different and therefore, all four techniques would rate equal in this respect.

The second point to be explored is the transient with respect to buffer fill that results when the backup timing source is used at one or a number of nodes. Buffers begin to fill or empty relative to their previous fill when the alternate timing source is introduced at a node because the frequency of the new source will not be precisely the same as the frequency of the original source. In comparing the different techniques, the major question to be raised is the size of the frequency step between primary and backup timing sources. The bigger the frequency step, the faster the buffers will fill or empty and the greater the probability of bit slip. As is mentioned in several places in this report, it appears likely that a time reference distribution approach, if implemented, would be ultimately referenced to a world-wide time standard such as UTC. Similarly, potential backup timing sources such as LORAN-C are also referenced to UTC. Thus, it can be anticipated that a switch to a backup timing source in a subsystem based on TRD will result in a smaller frequency step than any of the other techniques since both primary and backup systems could very well be referenced to the same ultimate source. The second point to be considered is the degree to which the frequency step at the single node affects the frequency at the other nodes of the network. This point has been examined in detail in the evaluation of other desirable characteristics (see error propagation). Again, it appears from our simulation results that TRD provides superior insulation for the remainder of the network than do the other disciplined clock approaches. Naturally, there is infinite isolation in the independent clock approach.

In summary, TRD must be given the highest ranking of the alternative techniques for compatibility based on the likelihood of a minimum frequency step when a backup timing

source is employed. The remaining alternatives ranked from highest to lowest are independent clocks, master-slave and mutual synchronization with these rankings based on the level of insulation of the frequency step in the remainder of the network.

8.4 Precise Time Availability

Of the four techniques being considered, only time reference distribution has the ability to provide precise time. That is, TRD has the ability of maintaining time-of-day synchronization between each of the network clocks and the internationally accepted time scale, Coordinated Universal Time (UTC). As is noted in other sections of this report, the availability of precise time is not a prerequisite for network synchronization; however, benefits do accrue if such a capability is provided.

Since timing subsystems are based on the independent clock technique, master-slave technique and mutual synchronization technique do not provide precise time, and a timing subsystem based on the time reference distribution technique does provide precise time, a comparison of the techniques for this particular characteristic is unnecessary. Rather, a brief explanation of why TRD does provide precise time and why the other techniques do not provide precise time appears appropriate.

Time reference distribution can provide precise time at each nodal clock because the timing signal that disciplines the nodal clock is precisely the timing signal that is generated at the node to which it is slaved. That is, the disciplining signal has not been corrupted by the path delay variations inherent in the link connecting the two nodes. By correcting the slaved clock so that the phase error between the disciplined and disciplining signals is driven to zero, and by taking as an ultimate reference a source of UTC, precise time is then made available at each node in the network.

Independent clocks by definition cannot supply precise time since the clocks are not disciplined. Even the most accurate clocks have finite frequency differences and such frequency differences necessarily result in an accumulation of phase difference, thus precluding the availability of precise time.

Mutual synchronization, similarly, by definition cannot provide precise time. Even if a node within the network was a source of UTC, this is not to say there is a rationale

for including UTC in a mutual system. The simple fact that each nodal frequency is determined by an average of the frequencies received at that node dictates that the system frequency will not be the same as the frequency provided by the UTC referenced node. Thus, precise time cannot be available at the nodes of the network.

Master-slave has the hierarchial structure necessary for the distribution of time and could also be ultimately referenced to a source of UTC. However, the master-slave system is appropriate for the distribution of time since it cannot completely remove the path delay variations on the link connecting master and slave nodes. Unlike the TRD technique, the clock at the slaved node in the master-slave technique is disciplined by the timing signal received at that node. Although appropriate filtering will remove much of the path delay variations, over a long period of time, phase error between clocks can accumulate.

8.5 Stability

The DCS timing subsystem must be a stable system in the sense of a feedback control system. If this were not the case, the nodal clocks would be subject to ever increasing fluctuations in frequency (to the limit of each VCO's control range) in response to perturbations. The result would be buffer overflows and continual bit slips. The stability considerations for each of the four timing techniques are discussed below.

Independent Clocks. Since every nodal clock is independent of every other nodal clock, there are no closed timing loops. Thus, this technique is unconditionally stable.

Master-slave. This technique is unconditionally stable when the timing reference to each nodal clock is distributed via a fixed master-slave tree network. However, there is one problem that can occur when an adaptive timing distribution network is used. The configuration of the timing distribution network is controlled by information transmitted between nodes. Errors in this data could cause the network to erroneously configure itself. A stability problem occurs if these errors cause a portion of the network to be configured as a mutual sync network. For example, if Node A slaves to Node B and Node B slaves to Node A, then these two nodes form a mutual sync network. Since the loop filters in the nodal synchronizer have not been designed for mutual sync operation (they will likely be type two loops) the synchronizers

at nodes A and B and will become unstable. Fortunately, there is a rather simple but important remedy for this situation, i.e., the use of error detection or error correction coding on this data to prevent the use of erroneous data. One can make the probability of accepting erroneous data as low as desired by adding the appropriate number of parity bits (by using error detection one can make the probability of accepting an erroneous message equal to 2^{-p} at low signal-to-noise ratios by adding p parity bits). Assuming the use of coding, then even on the rare occasions when erroneous data is accepted, the error will be detected rather quickly when the next update of that information is received. Since very narrowband loops are used, the VCO's will not be pulled very far during this period. Thus, there is no chance that a serious problem can occur.

Time Reference Distribution. The only problem that can occur with time reference distribution is the same problem that can occur with a master-slave system, i.e., the adaptive timing network configuration can be erroneously configured into a mutual sync network. Again, the remedy for this problem is the use of sufficient coding to prevent the acceptance of erroneous data. Thus, there is no chance that a serious problem can occur.

Mutual Synchronization. Constraints on system parameters to produce a stable mutual synchronization system have taken two forms. First, one must ensure that changes in nodal frequencies at some nodes must not proceed too far before they affect the frequencies at other nodes. This results in the bounds on gain/delay products (loop gain and link delay) that have been derived by many investigators for example networks. The bound will depend on network configuration, but typically the upper bound on gain/delay product is on the order of 1. Since very narrowband loops will be used, link delays of many seconds would be required before there would be a stability problem. Thus, in a real network, one does not have to be concerned about gain/delay products. The other constraint to ensure stability is on the loop filter. The loop filter must be chosen such that the closed loop transfer function has magnitude less than one at all $\omega > 0$. When this criteria is satisfied, all jitter frequencies are attenuated. This is rather important because of the closed loops in a mutual sync network. If any jitter frequency were amplified, then it could cause a perturbation in nodal frequency which would be continually amplified from node to node in the network resulting in an unstable network. With a type one loop using a simple low pass filter, the stability criterion is satisfied if one ensures that the

damping coefficient $\xi > \sqrt{2}/2$. Assume that for safety $\xi = 1$ is chosen. Then the only way instability could result is if the loop gains at several nodes increased, thereby making $\xi \leq \sqrt{2}/2$. For this example, the loop gain would have to double for this to happen. A change in the loop gain by a factor of two is certainly within the realm of possibility, either through human error in calibration or through device changes. Before implementing such a system, one should devise a technique for detecting when the gain gets out of the tolerance range to ensure that instability will not occur.

In summary, we find that the independent clock technique is unconditionally stable. In addition, the master-slave and time reference distribution techniques can have stability problems if certain errors occur in control data. However, this problem is easily fixed by the use of error control coding. Thus, we would rank these approaches equally with regard to stability. By contrast, the mutual sync technique normally has closed loops in the network, and to achieve stability the loop gain at every node must be held within tolerance. This task may not be easy to ensure, given the possibilities of human error in calibration and device changes. Thus, we rank mutual synchronization as less desirable than the other three on the basis of system stability.

8.6 Monitorability

The characteristic of monitorability is the level to which the timing subsystem can provide data used in assessing its own performance. It is apparent that monitorability is valuable at least to the extent that an option such as a redundant piece of equipment, an alternate link or another timing source is available and can be utilized as the result of decisions made on the basis of monitored information.

Monitorability is a significant characteristic because it can lead to greater availability through providing tolerance to failure. If potential failures can be identified prior to failures actually occurring, these situations can be remedied in an off-line basis or more rapidly by knowing the nature of the failure before it occurs. The result is, therefore, both an increase in MTBF and a reduction in MTTR and therefore a greater availability. The parameter that must be measured is the difference in availability due to monitoring.

This discussion will encompass a comparison of the four timing system techniques, a focus on the time reference distribution approach, discussions of several inferences that may be derived, a representative fault scenario, the relationship of monitorability to availability and some side benefits derived on the basis of monitorability.

8.6.1 Comparison of Techniques

The four techniques of independent clocks, master-slave, mutual synchronization and time reference distribution can be compared with regard to their relative monitorability. It can be seen that all four techniques have a fundamental identical monitorability capability in that they can see those actions that take place within a given node of interest and at the periphery of that node. Thus things as the characteristics of a node's clock, backup clock, frequency dissemination circuitry, phase-locked loop operation, modem operation and receipt of signals from adjacent nodes are readily available through any of the four timing approaches. A significant addition exists with time reference distribution (TRD).

Generally, with the exception of TRD each of the techniques is limited to data that exists within a node with the exception of some hybrids which might be defined wherein data is shared between nodes of the system as it is in TRD. Therefore, it can be stated that all other

techniques fundamentally have the same degree of monitorability capability. The differences in TRD will be discussed in the following paragraph which sets it significantly aside and above the other approaches in terms of monitorability capability.

8.6.2 Time Reference Distribution

The time reference distribution technique has all the capability of the other techniques in assessing its internal nodal operation. In addition, it has the ability to predict impacting failures, detection of external stresses, determination of out-of-specification trends and the ability to isolate faults.

The enhanced monitorability of TRD is based on the fact that data is shared throughout the network between all of the nodes in the TRD case. Adaptive action such as organization and reorganization provide hints of other failure or operational activity within the overall network. Some of the data that is available for monitorability purposes includes the time of the local clock, time differences between the local clock and adjacent clocks, measured but uncorrected time differences between each adjacent node and its ultimate master, measured time difference between the local clock and its ultimate reference via each adjacent node, propagation time between the local node and each adjacent node, rank of all nodes and demerits of all paths of the network.

There are a number of sources wherein the above data is derived and these include buffer status, time difference between transmit and receive multiplexer framing epochs, received frequency values, local frequency value, local time, received data from adjacent nodes, local node rank, connecting path demerits, manual inputs possibly inserted to diagnose the system, update counter contents, the rank and identification of each ultimate reference associated with either the node in question or its adjacent neighbors, accumulated path demerit, failed nodes and links and overall network status. These sources provide a picture of the overall network operation especially from a timing standpoint at any given node in a TRD scheme. The analysis job is to look for unexpected changes from time frame to time frame and assess their importance. In addition to the discrete values of above sources of data, sets of information are available by

gathering groups of information such as link time delays to all adjacent nodes or to all adjacent nodes associated with each nearest adjacent node.

Some of the information that can be important in assessing TRD operation and predicting network malfunctions which can lead to timing system malfunctions include the information in Table 8.6.2.

Another factor in addition to the above is that of the occurrence and magnitude of the clock corrections. The subscripts a and b are used to denote pairs wherein adjacent nodes may number from anything up to roughly 10 nodes, each having a set of values corresponding to items listed in Table 8.6.2. Examples of sets would be all of the buffer contents at the adjacent nodes referred to the given node in question or all of the buffer contents at a given node for the links connected to the adjacent nodes.

Therefore, in summary, it has been noted that such things as the status of all connecting buffer, links, and update counters can be made available at any given node in the TRD system. From this data numerous inferences can be made as to just what is happening within the network.

8.6.3 Inferences

A few representative inferences based on data that can be accumulated by a TRD node will be discussed in this paragraph.

In the event of a change of the ultimate reference, an inference could be made that 1) the original ultimate reference failed, 2) failure or change of a path or node connecting the original ultimate reference has occurred, 3) activation of a better path to a new ultimate reference has been determined, or 4) activation of a better ultimate reference has occurred.

Another inference would occur when a change of adjacent node from which timing is derived occurs and this might denote 1) all possibilities in the previous example, 2) failure or change in the path to the adjacent node originally used, 3) activation of a new best adjacent reference or restoral of a prior failed condition, or 4) periodic maintenance outage is occurring. A third inference can be derived if a change in path delay or measured time difference over any one or more connecting links should occur, then it might denote that 1) frequency or phase change

Table 8.6.2. Available Data

B_{ab}	buffer contents - connected to b
\dot{B}_{ab}	buffer fill/empty rate at a connected to b
K_{ab}	multiplexer frame time difference measured at a re b
F_n	frequency received from n
F_a	local clock frequency
T_a	local time
R_a	local node rank
D_{ba}	demerit of path between a and b
C_a	update counter contents at a
K_{ba}	multiplexer frame time difference measured at b re a
R_b	rank of node b
U_b	ultimate reference node for node b
R_{ub}	rank of ultimate reference node for node b
D_{u-b}	path demerit - node b to U_b
N_f	identity of failed node
L_f	identity of failed link
C_b	update counter contents at b
B_b	buffer contents at b
t_b	time at b
B_{ba}	buffer contents for the link at node b connected to a
\dot{B}_{ba}	rate of change of B_{ba}

of a clock or clocks along the path to the ultimate reference has occurred; 2) alternate routing has occurred due to a network switching assignment; 3) link equipment has failed, or changed, or 4) spoofing is being encountered.

Several other areas from which one might derive inferences are assessments of demerit values and changes thereto, update counter activity and contents, buffer activity and contents, a change occurring in "local time" value, rank changes and variations in frequency values. A synergism of available data could be used through applying techniques of predictive analysis to groups of data available.

8.6.4 Example Fault Scenario

A somewhat typical fault scenario will be briefly discussed to show simply how network failures can be detected at a given node if TRD is utilized. Reference is called to Figure 8.6.4 which shows two network configurations and timing source paths both before and after failures have occurred. The failures are denoted by the x's on the links between Nodes 9 and 13 and 12 and 14. When the failures are introduced in a TRD based timing system the network must reorganize itself per the reorganization rules to a configuration possibly like that shown in the second part of the figure which denotes the case after reorganization. At Node i data is available or can be made available as to all of the activity in the network through its adjacent Nodes 1, 2, 3 and 4 gathering data as discussed in earlier paragraphs on monitorability. It is possible to deduce just what has occurred and be prepared should a trend develop in failures.

8.6.5 Availability Impact

The characteristic of monitorability is only important when it can be used to enhance the availability of the system. This comment applies to the timing system as such and not to other benefits of having a very monitorable approach. It is possible to enhance availability through increasing the time between failures and reducing the time it takes to restore operation after a failure has occurred. It is possible to determine whether various frequencies in the network are drifting out of specification frequency-wise and switch to backup thus avoiding a failure where one would have occurred should such action not have been taken. If a failing time source is being used it is possible to switch to an alternate source ahead of time avoiding a failure.

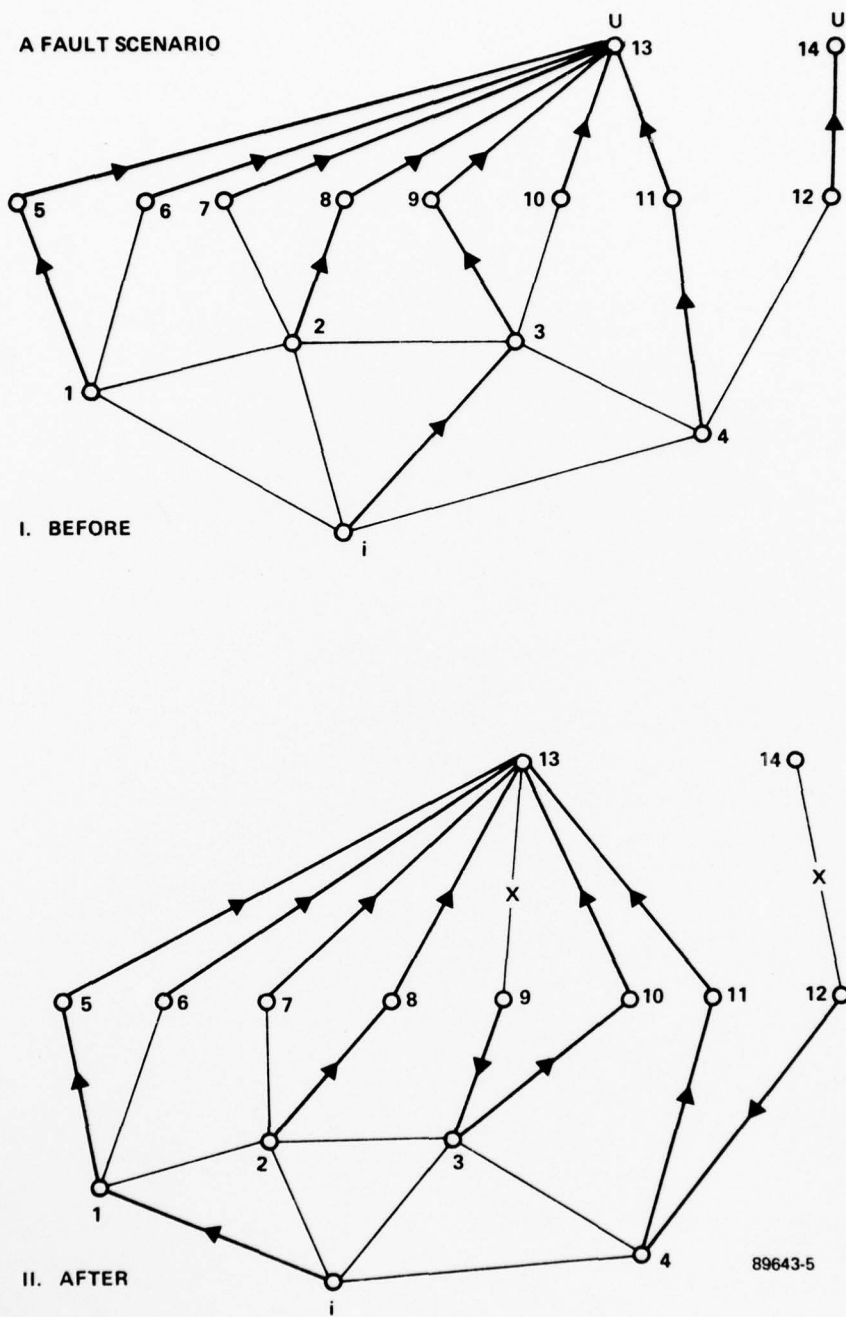


Figure 8.6.4

Also, switching in any available redundancy to heal a sensed failure or potential failure can enhance the overall availability. The detection of spoofing and developing strategies to avoid it can be beneficial from an availability standpoint. The restoral time required to reactivate a network that would have failed can be minimized through alerting maintenance personnel ahead of time to the nature of a potential failure and thus minimizing MTTR. Selective redundancy switching can also enhance availability.

The data discussed in reference to TRD is available on essentially a free basis for monitorability purposes. Much of the data mentioned is required just to implement TRD as a timing scheme.

8.6.6 Benefits

In addition to enhancing the availability of the timing subsystem, side benefits will evolve that can apply to the overall DCS network SYSCON. The synergism of the many data available can be used to predict other system failures and restoral thereof not directly associated with timing subsystem. Although this is not fundamentally important to the decision of a timing approach, it comes along pretty well free of charge and can be made use of by the DCS thus enhancing the desirability of the time reference distribution approach.

8.6.7 Conclusions

It is evident that a time reference distribution technique is far superior to the other approaches when the characteristic of monitorability is considered. Also, it is projected that the cost of obtaining data for monitorability is essentially negligible since the information already resides in the system when TRD is implemented. The cost that would ensue would be the storage over a period of time of historical quantities of the information such that inferences may be made from the data. Obviously there would be some slight cost in addition to basic TRD operation which in itself only requires a limited portion of the data available.

Jammer Strategy

A major attribute of a communications network is its connectivity. Thus, an antagonist would like to disconnect the network into some number of partitions. He may attempt to do this through physical destruction of parts of the network or by producing interfering signals (jamming). In case the network facilities are heavily protected, in a physical sense, the antagonist may concentrate much of his effort toward jamming selected portions of the network. He will select those portions which he believes will produce the most disturbance. Hopefully, from the standpoint of the network, the jammer will not be able to actually disconnect the network due to inability to locate his jamming emitters in the most strategic geographical positions. Thus, he may concentrate on jamming selected portions of the network in such a manner as to disrupt some vital network subsystem such as the timing subsystem of the TDM network. The different timing techniques may be affected by different amounts depending on the strategy used by the jammer. The independent clocks technique is less susceptible to disruption by a jammer than any of the other timing techniques. In fact, under extreme jamming conditions, the network utilizing other techniques will appear to tend to revert to an independent clocks configuration when viewed externally.

Types of Information

Each node of the timing subsystem obtains essentially two types of information from other nodes of the network. These include timing information and control information.

Timing Information - For master-slave and mutual sync timing information is contained in the bit transitions of each data stream. As the jamming intensity increases from zero to the point at which the link is lost, the timing jitter increases until no useful timing information can be extracted with available equipment from the contaminated data stream. It is not anticipated that techniques can be developed to significantly reduce the effects of jamming on timing information for all levels of jamming. However, monitoring of channel signal-to-noise ratio can give some indication of the timing information quality obtainable at a given period from each incoming link. This can aid in selecting the best timing reference at each node.

Control Information - Adaptive reorganization schemes as well as fault detection and isolation apparatus at each node may use control information obtained from remote nodes. Control information will most probably be transmitted between nodes via overhead channels (orderwire). These channels may be protected to some extent by error detection and/or forward error correction encoding. Thus, the problem of incorrect control information can almost be avoided at the expense of possibly no new updated control information during those periods of most intense active jamming. Aside from error detection and correction encoding of control information messages, the overhead channels are susceptible to the same types of jamming as the data channels.

Adaptive Reorganization

An intermittent jammer on selective links may cause the reorganization scheme to remain in a constant state of reorganization because there is a time lapse between a network fault and the actual recognition at the affected node of the faulty condition. There is then a further time delay in selecting a new reference and becoming frequency and phase locked to the new reference. This causes a transient in that portion of the timing tree below the first affected node. Concomitantly, nodes in other timing chains that are communicating with nodes in the disturbed chain will experience effects of the disturbance. Upon removal of the jamming from a selected link, the adaptive reorganization scheme may decide to again select this link for obtaining its reference and thereby cause another transient in part of the network. Thus, it is easily envisioned that a concerted attack by a small set of intermittent jammers might be able to induce the network to go into a perpetual state of reorganization. In order to reorganize properly, each node must have an adequate amount of correct control information. If this is not the case, then one of the following may happen:

1. The network timing subsystem may become partitioned
2. Portions of the network may become configured as mutual sync
3. Portions of the network may not sync to its best available reference

If none of the above happens, the subsystem will still tend to revert to an independent clocks system. This is true because during the reorganization process, the individual nodes must revert to self-reference.

Aside from encoding of the control information one possible counteraction against the intermittent jammer is for each node to maintain a running monitor of the links in question and refrain from referencing any of those whose recent history of outages conform to the intermittently jammed conditions described above. Both master-slave and TRD may be configured to utilize an adaptive reconfiguration scheme.

It is believed that coding of control information and careful monitoring of links at each node to detect the intermittent jamming strategy can be used to virtually eliminate the dangers to the timing subsystem via the adaptive reorganization scheme discussed above.

Master-Slave and TRD

The master-slave and TRD techniques are similar in that timing information is dissipated from a master or ultimate reference node to all other nodes in the network via a tree structure of links and nodes. The major conceptual difference is that the TRD technique attempts to remove the uncertainties associated with link delay variations by taking advantage of two-way timing information whereas the master-slave merely averages the one-way timing information. Thus, loss of links due to jamming affects both techniques in the same manner but the total effect can be different depending on how closely each can maintain the individual nodes instantaneous frequencies to each other. In either case, changing references following degradation or loss of a link due to jamming causes a phase and frequency transient in the affected nodal clock. This transient is coupled to all nodes in the chain of the tree below the affected node.

Mutual Sync

The mutual sync configuration will experience a transient when a link's contribution to the total phase error is removed if that link is being jammed and again if the link is reinserted. These disturbances will cause a change in network frequency. Thus, a concerted effort by intermittent jammers may set up a seesaw movement of system frequency. Such disturbances may be accentuated by the mutual sync network because of the longer time constants associated with the overall network when compared with that of individual nodes and the larger swings on buffer contents at individual nodes when compared with master-slave. The network's response to each disturbance (loss or reinsertion of links following jamming activation/deactivation) may vary considerably depending on where it occurs in the network. In general, the disturbance should be

more pronounced if it occurs at nodes that are highly connected to the remainder of the network, i.e., nodes near the connectivity center of the network. Disturbances occurring at fringe nodes should have a lesser affect on the overall network than those occurring near the center of the network. Nevertheless, it appears that such disturbances in the mutual sync technique propagate further and require a longer period to settle out than for other techniques.

TRD, master-slave and Mutual Sync can monitor the phase error between the local clock and each of its actual or potential reference sources. Comparisons can be made between these errors and abnormal conditions resulting from jammer strategy may be detectable from these comparisons. The cost of implementation of such a scheme is not believed to differ significantly among the three disciplined techniques since each technique must provide buffers between the local node and each communicating link. However, it is believed that this scheme would be most effective with the TRD technique and least effective with the mutual sync scheme with master-slave somewhere in between. The reason for this is due to the amount of deviation in nodal clock error phases that is expected to occur throughout the network. It is expected that the normal amount of deviation for TRD will be considerably less than for master-slave since TRD attempts to remove the affect of link disturbances as well as intermediate node perturbations. Furthermore, the amount of deviation in master-slave phase errors is less than that for mutual sync. The simulation results of Section 7.0 support these conjectures.

In conclusion, the timing techniques may be ranked from least susceptible to most susceptible to jamming (with or without strategy) as follows:

1. Independent Clocks
2. TRD
3. Master-Slave
4. Mutual Sync

8.8 Flexibility

Flexibility has been defined as the impact on orderly implementation growth and extension of the future synchronous switched digital DCS. It would appear that many other factors have a substantially greater effect on the flexibility of the DCS than does the choice of

timing subsystem. Furthermore, there is nothing inherently problematic from a flexibility point of view in any of the timing techniques. Each technique can be implemented on a piece meal basis. Each technique, once implemented, can be extended to provide timing to additional nodes in different geographical areas. Obviously a detailed analysis would be required once system specifics are better defined. However, from a broad overview based on the fundamental differences in the timing techniques, there is no reason from a flexibility point of view to favor any one technique over any other.

8.9 Interoperability

The characteristic to be evaluated is whether the application of any of the candidate timing techniques to the DCS will substantially facilitate the interface between the DCS and other communications systems. The specific problem of concern exists at the DCS node that transmits and receives data streams from both a node external to the DCS and other DCS nodes. It seems apparent that the clock at such a node should in no way be influenced by the received bit rate on the interface link. Thus, the amount of buffering required on such a link, which is a measure of interoperability from a timing point of view, is directly related to the difference in clock frequencies at the two nodes on either side of the interface link. The timing technique that holds promise for minimizing this frequency difference would be preferable. This question is not unlike one of the questions addressed in the compatibility of the CDS timing subsystem with other global timing systems. Again, one is concerned with the possibility of common timing for separate systems; and again, the answer is the same. Independent clocks by definition preclude any advantage that would accrue as a result of common disciplining. Mutual synchronization offers no relief because of limited connectivity between systems. Master-slave and time reference distribution have the potential of supporting timing commonality between systems as a result of their hierarchical structures. However, the practicality and probability of a common reference is much greater in a time reference distribution system where the ultimate reference would be UTC. Naturally, greater interoperability would not result if systems interfacing with the DCS chose not to reference their timing to UTC; however, based on the potential that exists, time reference distribution is determined to be the best technique from an interoperability point of view. There is little to separate the other techniques.

8.10 Availability

Availability is the quotient of mean-time-between-failures (MTBF) and the sum of MTBF and the mean time to repair or restore (MTTR). Availability is a significant characteristic for all major systems and its importance is apparent for the timing subsystem by nature of the mission of the DCS.

In order to provide an availability number for each timing subsystem alternative, MTBF and MTTR would have to be calculated for each. This calculation would follow a paper design of the alternatives and therefore the accuracy of the availability estimates would be a function of the level of detail undertaken in the paper design. However, it is significant to note that only the relative availability of the approaches is of significance in the elevation of timing approaches rather than the absolute availabilities. The evaluation of relative availability appears to be achievable with less detailed designs than the detail required to derive absolute availability. Additional availability can be built into any of the timing subsystem alternatives. Relative inherent availability with minimum redundancy for the alternatives is most desirable from a cost-effectiveness standpoint.

In this section the common and unique aspects of each of the four timing approaches will be investigated and discussed with respect to their impact on relative availability.

8.10.1 Comparison of Techniques

Time reference distribution, mutual synchronization, master-slave and independent clock timing approaches are discussed in the following paragraphs.

8.10.1.1 Common Factors

In assessing the various timing approaches, several constituent elements of each timing approach at a given node are considered common to all. These include buffers, clocks, frequency synthesizers and phase-locked loops. The buffers in some cases may have more or less bits in buffer capability, but generally their availability will be roughly equal. These several techniques call for different degrees of complexity in their clocks, and this could be considered a factor in their relative availability, but it is a rather tenuous one to quantify. A brief discussion will be included later in this section.

AD-A041 004

HARRIS CORP MELBOURNE FLA ELECTRONIC SYSTEMS DIV
STUDY OF ALTERNATIVE TECHNIQUES FOR COMMUNICATION NETWORK TIMIN--ETC(U)
MAR 77

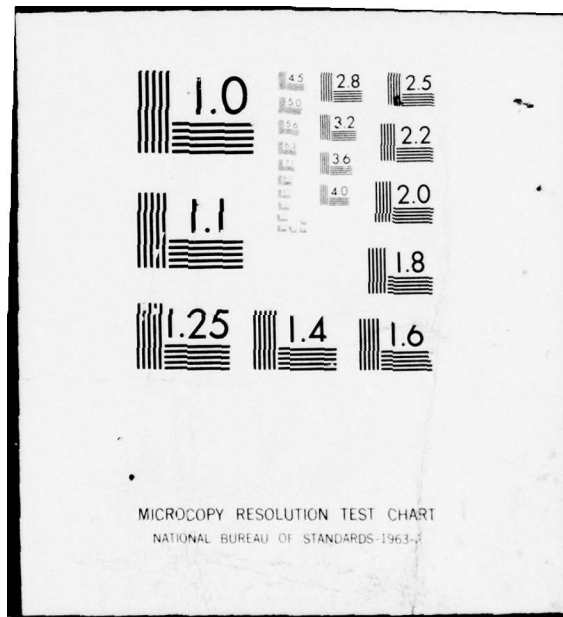
F/G 17/2
DCA100-76-R-0028
NL

UNCLASSIFIED

3 OF 4

AD
A041 004





8.10.1.2 Time Reference Distribution

The time reference distribution approach has several unique elements that apply to its relative availability compared with the other approaches. Also, some devices that are inherent in all timing approaches impact the TRD node uniquely and will be discussed here. First the link selection processor is that element which conducts the evaluation of the organization and reorganization process for a given TRD node. The time interval measurement unit is unique to TRD in that it is the means whereby received time epoch is referred to the station time. The clock error processor is also unique to TRD in that it provides a calculated value for clock compensation which is the result of shared information between the TRD node and one or more of its adjacent neighboring nodes.

The highest level multiplexer and demultiplexer uniquely impact TRD in that they are utilized to initiate the identification of the station epoch to the neighboring node and to interpret the received epoch for the purpose of calculating time difference between adjacent nodes and the TRD node. The modems on the receive side of each interconnecting link are important both for their reception of the carrier which provides the determination of frequency and the receipt of data which is utilized in the process of sharing information between the various nodes of a TRD oriented timing network.

8.10.1.3 Mutual Synchronization

In the case of a mutual sync node, the weighting and sum circuitry, control, and multiple phase detectors represent unique elements applicable to the unique or relative availability of this timing approach compared with the others. Also, the receive modems are important in that they must be capable of providing carrier output for the purpose of ascertaining the frequency characteristics of the received links. Differing from the TRD modem impact is that data is not really important in a pure mutual sync approach.

8.10.1.4 Master-Slave

The unique aspects of the master-slave timing node are its control and the single phase detector utilized in tracking the received timing signal. Also, the carrier detection of the modems represents an availability oriented need.

8.10.1.5 Independent Clocks

Based on the statement that the clocks have a unique and very difficult to determine impact on relative availability, the independent clock nodes would have no other impacting unique relative availability subsystems.

8.10.2 Subjective Evaluation

In order to ascertain qualitatively the relative availability of the various timing approaches, a scale of one to 10 is posed. This scale is defined as least to most complex wherein the complexity should impact both MTBF and MTTR and, thus, the inherent availability on a relative basis for each of the approaches. The complexity factors for the various approaches have been assigned as follows. Independent clocks are assigned a complexity factor of unity, master-slave a factor of five, mutual synchronization a factor of seven, and TRD a factor of 10. Thus it is seen that TRD being more complex of the selected approaches for evaluation most likely represents the lowest relative availability of the bunch. The spread of relative availabilities in the actual terms probably isn't extremely significant among the master-slave, mutual synchronization, and TRD approaches. However, the independent clock approach which is basically autonomous should allow the best relative availability. The type of clock used certainly must have some impact on the relative availability. Although the cesium beam standards have reported MTBF's of 25,000 hours, the other clocks, namely rubidium and crystal, represent quite reliable mechanisms. Therefore, the spread should not be extremely broad in the availabilities of each of these clocks. If anything, the various clocks impacts can be related on a qualitative basis with a scale of one to 10 reflecting least reliability to most reliable. An evaluation would show this to be unity for independent clocks, 10 for master-slave, five for mutual synchronization, and 10 for time reference distribution. The assumption above is that independent clocks will require the most stringent and complex clock, whereas master-slave and TRD require a fairly loose clock, and mutual sync in between. It is possible to use the best clocks in all systems, thus equalizing the relative impact of clocks, but unfortunately, impacting the cost-effectiveness of the system implementation in each case.

SECTION 9.0
RANKING OF THE DESIRABLE CHARACTERISTICS

9.0

RANKING OF THE DESIRABLE CHARACTERISTICS

Early in the study, two efforts resulted in 1) the definition, discussion, and adoption of the various timing schemes to be applied in combination or individually to provide the Network Timing and Synchronization function, and 2) the key system characteristics that would be used for the relative evaluation of the performance of the timing schemes in the context of certain scenarios and nodal configurations.

In this section, the relative importance of each of these aforementioned characteristics is addressed. These results, when combined with the results of Section 8.0 will then enable one to arrive at a figure of relative worth or utility of the timing subsystem being evaluated.

The Desirable Characteristics Are Reviewed Below

Survivability

The degree to which the timing subsystem continues to perform its function (to provide network timing) during periods of stress. The measure of survivability is slip rate which is directly proportional to the frequency offset between nodal clocks. If offset increases in a stressed environment, bit slips increase. Slip rate may be defined as the number of times per unit that buffers must be reset. This is a factor which is directly proportional to the rate of phase error between the nodal clocks. To evaluate this parameter we must measure the rate of accumulation of phase error between nodal clocks under a variety of possible scenarios.

Error Propagation

To prevent disturbances (such as stresses or path delay variations) in one part of the network from propagating and influencing the phase of nodal clocks in other parts of the network. The measure of error propagation is the offset in phase of each nodal clock from its steady-state value as a result of network stresses.

Compatibility With Other Global Timing Systems

The degree with which the DCS network frequency and/or precise time agrees with that provided by other global timing systems such as Loran C, Omega and GPS. Compatibility will be evaluated by measuring the additional capability provided; the greater availability and survivability of the timing subsystem and the greater availability of precise time.

Precise Time Availability

Precise time can be defined as the correct absolute time as kept by a standards laboratory such as the USNO. The characteristic to measure is the availability of and accuracy of precise time.

Stability

Stability is defined in terms of feedback control. Either perturbations die out with time and/or distance, in which case the transient interval is of importance, or the system degrades with increasing time, thus constituting a failure.

Monitorability

The level to which the timing subsystem can provide data used in accessing its own performance. The parameter that must be measured is the difference (increase) in system availability due to self-monitoring.

Susceptibility

Susceptibility is the degree to which the timing subsystem may be spoofed, jammed or disrupted by an electrical means as well as disrupted due to natural phenomena. Slip rate will again be the measurable quantity.

Flexibility

Flexibility is the degree to which the timing subsystem is compatible with the orderly implementation, growth and extension of the future synchronous switched digital DCS.

Interoperability

Interoperability is the degree to which the timing subsystem influences the traffic interface between DCS and other military and commercial communication systems. Interoperability will be quantified in terms of slip rate at the interfaces. It is directly proportional to the rate of accumulation of phase between the timing subsystems of the interfacing systems.

Availability

Availability is a defined quantity and equals MTBF divided by the sum of MTBF and MTTR.

This is no unique approach to use as a guide in a characteristics sensitivity study, i.e. (the sensitivity of system utility to the absence or presence of each of the characteristics) and the approach can range from a rigorous mathematical treatment to purely qualitative judgement. As will be pointed out, the approach planned for this phase of the effort lies between these two extremes hopefully taking advantage of mathematical rigor where rigor is possible and enlightened qualitative judgement where mathematical rigor is not possible or advisable.

Such a study would be relatively amenable to mathematical rigor if certain assumptions could be justified. Among these are:

1. The parameters employed in the sensitivity study must be measurable without ambiguity. Many of the parameters above can be measured as defined and evaluated on a quantitative basis; however, others require qualitative judgement for evaluation. The requirement for qualitative judgement does not invalidate the parameter or reduce its importance to the study. It merely points out the difficulty of measurement of some important parameters.
2. The parameters employed in the sensitivity study must be independent or correlatable in a rigorous manner. Monitorability can be considered an independent parameter; however, the measurement of monitorability is a change in availability resulting from the benefits of monitorability. Considerable judgement will be required to evaluate how monitorability extrapolates into availability. Again, monitorability and flexibility are two very important characteristics of the system. They do not lend themselves to a mathematically rigorous approach in a characteristics sensitivity study however. Survivability is also a very important criterion for the system, yet survivability results from a very complex combination of other characteristics. Thus, it cannot be claimed that the characteristics are - or should be in this particular case - independent. As for "correlatable" in a mathematical sense, considerable subjective judgement would be involved in this approach as well.

3. The parameters employed in the sensitivity study must constitute a complete set, a fact which is contrary to ease of mathematical assessment.
4. Success or failure of the system must be evaluated in terms of the mission of the system. The mission of the NTSS is intimately related to the mission of the DCS and will remain basically the same in all scenarios. All parameters chosen for evaluation of the various NTSS schemes have an effect on the accomplishment of the mission; however, the relative weight to apply to subsets of the overall mission, and thereby to specific characteristics of the NTSS, is a complex function of employment - peacetime/wartime, CONUS/OCONUS - and a host of other variables. The evaluation is further complicated by the fact that the mission statement for the DCS will not be static but will change and evolve with time.

From the above, we conclude that a rigorous mathematical trade-off analysis of the various NTSS schemes, based upon a rigorous mathematical characteristics sensitivity study is not an advisable route to pursue. Numerical results could be obtained which, on the surface, would imply mathematical rigor but which would in fact be based upon subjective inputs of questionable validity. Further, the implied mathematical rigor would detract rather than enhance the credibility and net worth of the effort. Thus, we propose to allocate weighing factors to the system characteristics listed above using judgement and an assessment of the desires of the ultimate user - the DOD and other government agencies.

The following series of quotations from statements made by government leaders in discussions of the DCS, WWMCCS, and the interplay between the two should bear heavily upon the judgement applied to this portion of the program. All of the following quotations are extracted from the March 1975 issue of Signal Magazine, a special issue on Command and Control.

Secretary of Defense, James R. Schlesinger "Our National Security strategy places emphasis on providing the President with greater flexibility and selectivity in the nuclear response options available to him in times of crisis. Implicit in this strategy is the need for a responsive, flexible and survivable WWMCCS that provides appropriate command and control not only for the strategic forces but also for the tactical forces as well."

Thomas C. Reed, Director, Telecommunications and Command and Control Systems, OSD. "Implicit to this objective is the recognition that C³ is integral to the full structure and deployment; that survivability of the functional command and control compatibility is fundamental to continuity of operations under stress conditions; and that the C³ elements must be sufficiently dynamic to adapt to the rapidly changing environment."

Lt. Gen. Lee M. Paschall, USAF, Commander Defense Communications Agency. "The connectivity provided by large scale, general purpose communication network such as the DCS, is essential to the operation of a worldwide command and control system. The DCS with its more than 42M channel miles of various types of circuits interconnecting more than 1,000 locations throughout the world provides the majority of all WWMCCS communications requirements" - General Paschall continues, "It ensures the flexibility, survivability, redundancy, and finally, the restorability the communications network supporting command and control requirements must have." - Also, General Paschall states: "The priorities under which the DCS is engineered, operated, and managed state with unmistakable clarity that communications which support command and control are examined and weighed on the basis of their survivability, reliability, security and cost - and in that order." - It is difficult to predict precisely at this time the communications requirements for interconnecting the WWMCCS and the various tactical command and control systems. However, it seems certain that the future DCS will be heavily oriented towards interoperability with U.S. tactical communications systems and with the communication systems of our major allies. - The DCS quite obviously cannot satisfy all the command and control requirements inherent in flexible response strategy and scene of action force control. However, it is the only system capable of interconnecting the National Command Authority with the communications serving the operating forces."

General Russell E. Dority, USAF, Commander in Chief of the Strategic Air Command. "Once a decision is made to protect or employ nuclear forces, the combat crews must receive the validated directives with a degree of accuracy and reliability that cannot be compromised or confused. There must be no opportunity for misrepresentation of valid directives - nor possibility of improper reaction to unauthorized orders from any source" - "The attributes discussed earlier characterize the resources of quality that must be realized in the system; reliability, survivability, flexibility, speed, and accuracy. Without reliability,

other system attributes have little meaning. Reliability is a prime concern of the SAC control system. Survivability is also a crucial objective for any military communication system, and its importance to SAC is self-evident. Flexibility implies a capability to accommodate and adapt to the full range of changing environments and unplanned requirements."

Maj. Gen. Herbert Summers Cunningham, USA, Chairman WWMCCS Council Support Group. "The basic qualities required of such a system (WWMCCS) were credibility, flexibility, responsiveness, survivability and security. These qualities must exist to the maximum extent possible within the restraints imposed by resources and technology."

Maj. Gen. Thomas M. Rienzi, USA - Director of Telecommunications and Command and Control, DCSO, U.S. Army. "Regardless of the size of the command and control system or the echelon it supports, such a system must be:

- Survivable - At least to the extent that the people it supports are survivable.
- Integrated - With other administrative and management systems outside the organization chain of command to permit collection, processing and transfer of information and decisions responsibility without unduly burdening the tactical commanders for the reports or reporting.
- Responsive - To provide rapid feedback to the original source of information to confirm accuracy of perception by the recipient.
- Flexible - To provide for the coordination and direction required to change missions or resources allocations."

In light of the above and with the goal of not complicating this process, it has been decided to divide the characteristics into a primary list and a secondary list. Those in the primary list will have greater weighing than those in the secondary list. The primary list consists of those characteristics that directly relate to the characteristics mentioned in the above quotations. Those characteristics that do not directly, but rather indirectly provide the key characteristics, have been placed in the secondary list.

Primary Characteristics

Survivability

Susceptibility

Flexibility

Interoperability

Availability

Secondary Characteristics

Error Propagation

Compatibility with Other Global Timing Sources

Precise Time Availability

Stability

Maintainability

SECTION 10.0
COST EVALUATION

10.0 COST EVALUATION

The analysis carried out in the costing area was not an absolute costing of each technique. Rather, what was attempted was to determine if any of the techniques was inherently more expensive irrespective of the implementation of the technique.

In comparing costs between the candidates there are some significant points to be considered at the outset. First, timing subsystem costs are dominated by clock costs.

An ROM cost for a cesium clock is \$25,000. An ROM cost for a good crystal clock is \$3500. The remaining hardware that comprises the timing subsystem, irrespective of technique and as shown in Figures 10.0-1, 10.0-2, 10.0-3, and 10.0-4, has an ROM cost of less than \$500.

Second, only the independent clocks technique must be configured with expensive cesium clocks at every node. The disciplined techniques can utilize a majority of less expensive crystal clocks with the placement of the cesium clocks determined by the network connectivity pattern.

Therefore, the conclusion has been reached that cost differentials between the disciplined techniques are not significant. Also, that the independent clocks approach is inherently more expensive.

10.1 Relative Costs

Relative costs can be explained most easily by reference to Figures 10.0-1 through 10.0-4. Figure 10.0-1 is a simplified functional block diagram of a node in a network utilizing an independent clock approach.

The row of components along the top shows the flow of data traffic in the node and is the same for all the techniques. Each demodulator at a node (the i^d demodulator is illustrated) provides an input to a demultiplexer. The demultiplexer provides a number of lower bit rate outputs, each of which is written into an elastic stores buffer at a rate determined from the bit sync in the demodulator. Data is read out of every buffer at the node at a rate determined by the nodal clock and all such data streams are therefore synchronous. The nodal switch and multiplexers are all timed by the same nodal clock.

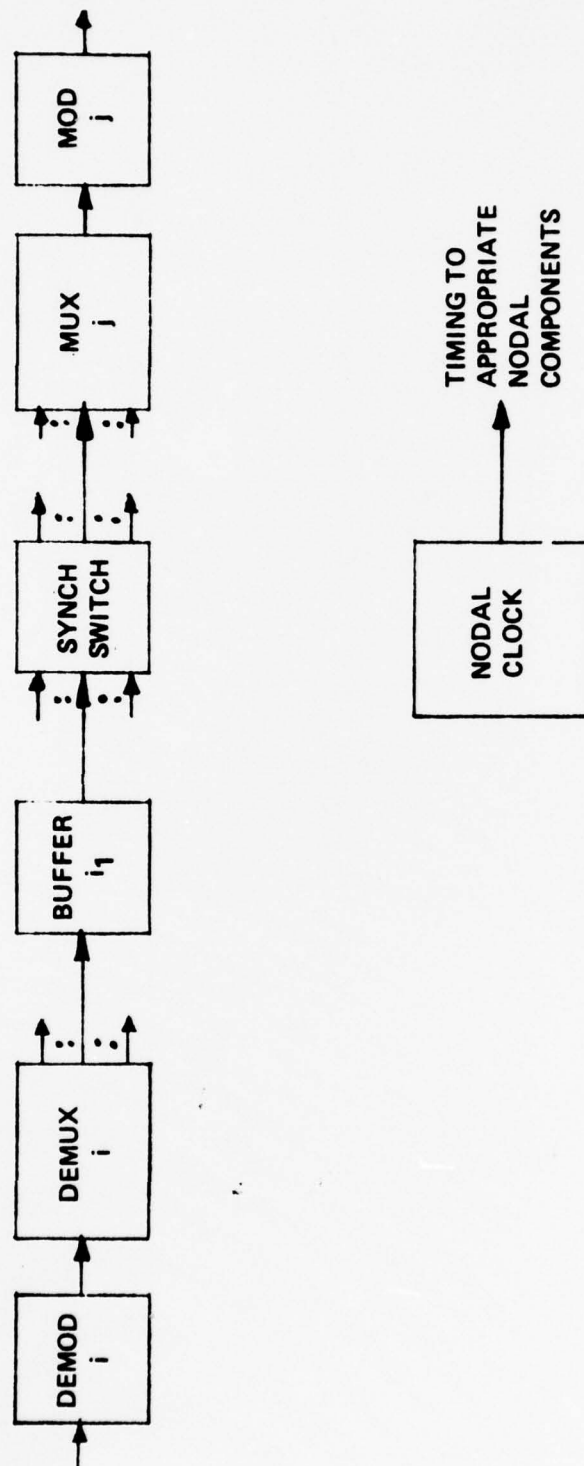


Figure 10.0-1. Independent Clocks Nodal Block Diagram

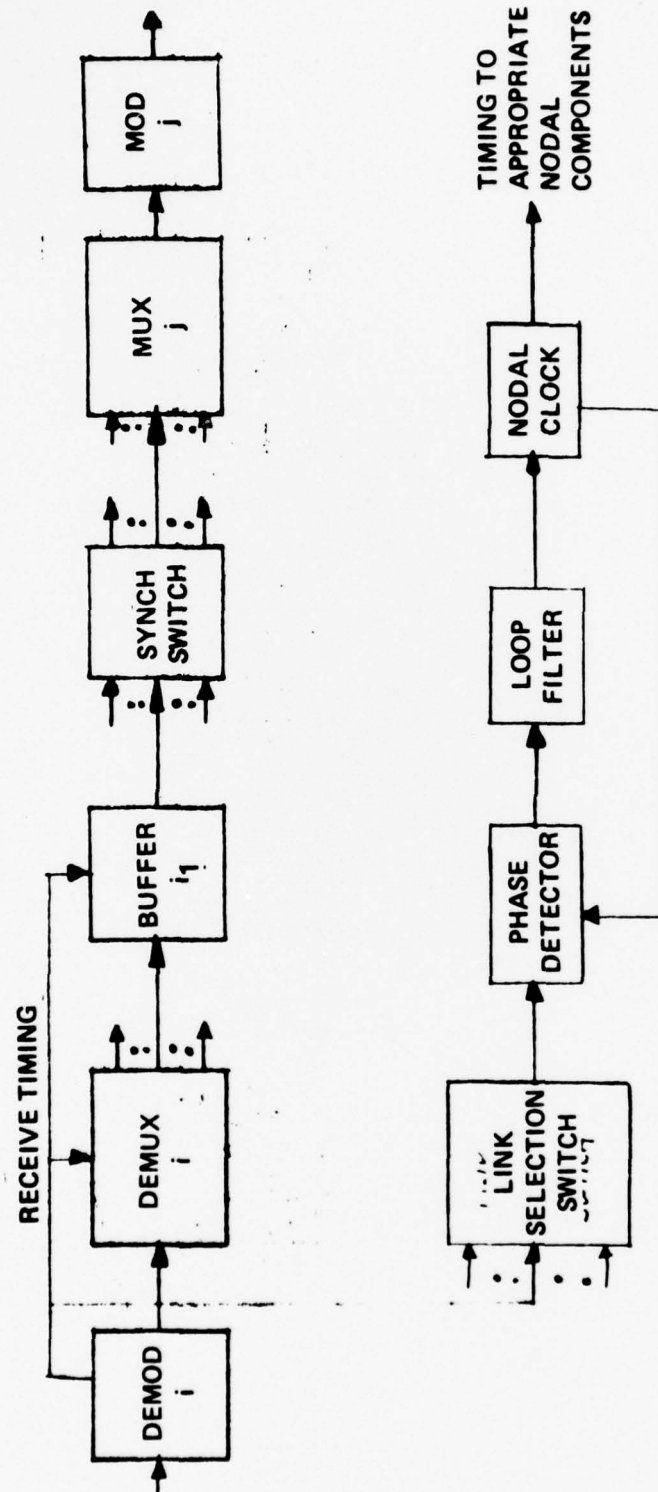


Figure 10.0-2. Master-Slave Functional Block Diagram

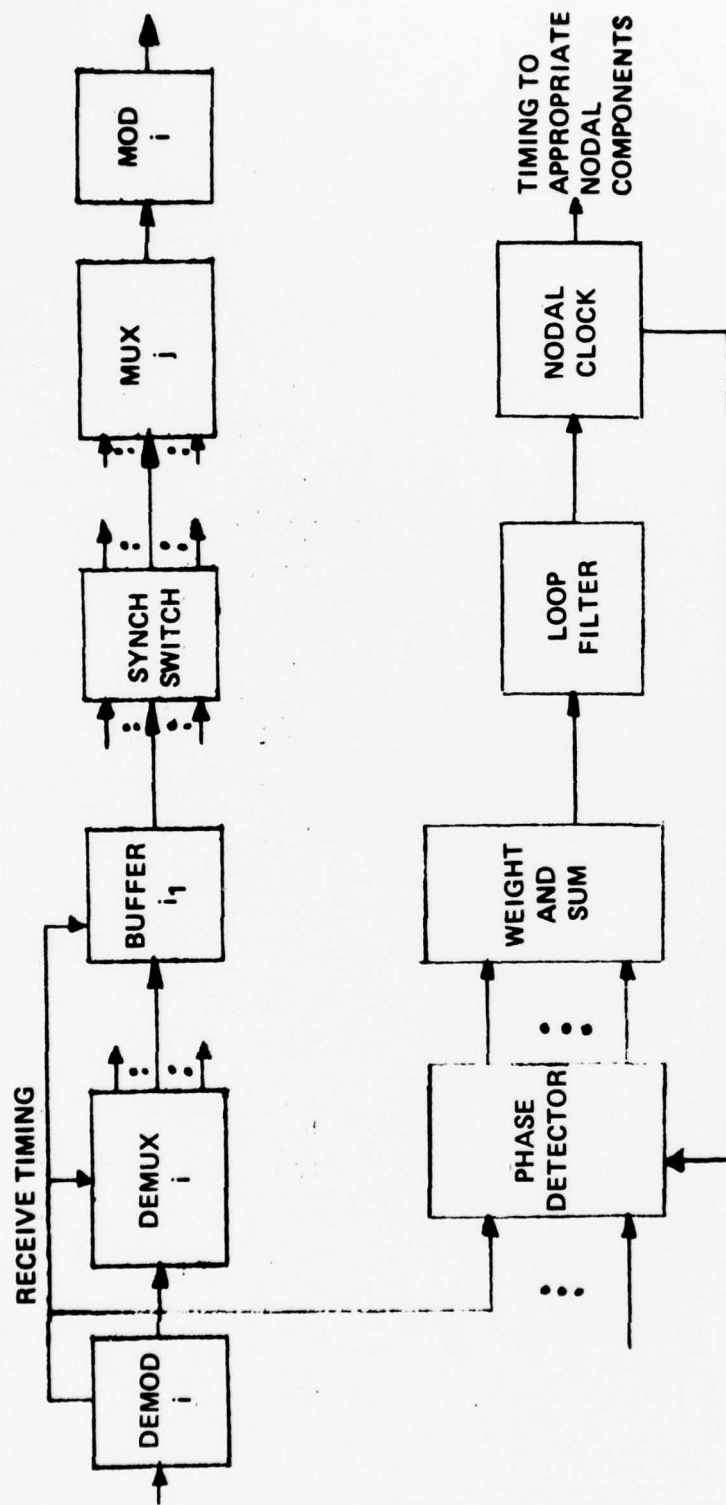


Figure 10.0-3. Mutual Synchronization Functional Block Diagram

In the independent clock approach, the free running clock provides this timing to the buffer outputs, the switch and the multiplexers. As stated earlier, this clock is undoubtedly a cesium standard and would, therefore, have an ROM acquisition cost of \$25,000.

Figure 10.0-2 is a simplified functional block diagram of a master-slave node. Again, the same components are shown along the top row. Timing as derived in each of the demodulator bit syncs is applied to a link selection switch which chooses the appropriate reference to apply to the phase-lock loop. The loop locks the nodal clock to the receive timing signal. As mentioned earlier, the nodal clock need not be a cesium standard since it is a disciplined clock. Assuming 10 percent of the clocks in the network are cesium clocks with a \$25,000 cost and the remaining clocks are crystal clocks with a \$3500 cost, the average nodal clock cost is \$5650. The switch, phase detector and loop filter that comprise the remainder of the nodal timing subsystem can be implemented for an ROM cost of \$300.

Figure 10.0-3 depicts a simplified functional block diagram of a mutual synchronization node. Again, receive timing is derived from each of the modem bit syncs. These clocks are then applied to the phase detector in the loop shown. Phase errors for each of the inputs are weighted and summed and then applied to the loop filter. In turn, the output of the filter provides the discipline to the local nodal clock.

The nodal clock need not be a cesium standard. If the 10 percent assumption is made as before, the average clock cost is \$5650.

The phase detector, weight and sum circuitry and loop filter could be implemented for an ROM cost of \$300.

Figure 10.0-4 depicts a simplified functional block diagram of a TRD node. The same components shown in the previous figures are along the top row. The components noted along the second row form the heart of the implementation difference between the TRD approach and the other disciplined techniques. The nodal clock shown below is present in all the techniques. The nodal frame generator shown at the lower right is also present independent of timing technique.

The demux provides inputs to each of the three components across the center of the figure. The link selection processor on the left receives node and link status information. It is the basis for the adaptive reorganization feature. It could be implemented with one microprocessor chip, one interface device chip, five 1024-word Read Only Memories, and a 1024-word Random Access Memory. An ROM cost would be under \$200.

The start/stop counter measures the time delay between the transmitted framing bit and the receive framing bit. This measurement is required in the time transfer calculation to be made by the clock error processor. A binary counter essentially provides this function. An ROM cost would be \$100.

The clock error processor on the right receives from the demultiplexer the delays measured at the adjacent nodes which is the remaining information necessary to make the time transfer calculation. Based on this calculation and the clock offsets at the adjacent nodes, also provided by the demux, a local correction is generated. It would appear that the clock error processing can be done by the same components that constitute the link selection processor.

As in the other disciplined approaches the average clock cost is estimated to be \$5650 and the entire nodal timing subsystem to be \$5950.

In summary, acquisition costs for each of the disciplined techniques appear equal. The independent clock approach has higher acquisition costs.

Nothing was found to indicate that maintenance costs would be significantly different from technique to technique.

Likewise, there is little to indicate that front-end development costs would be significantly different for any technique. The master-slave technique has been implemented by Bell and others. The TRD approach has been essentially implemented in the Canadian Data Route. The independent clock technique is being developed by Tri-Tac. The mutual sync technique, while not implemented to our knowledge, has certainly been exhaustively analyzed in the literature.

SECTION 11.0
ALTERNATIVE TIMING SUBSYSTEMS

11.0 ALTERNATIVE TIMING SUBSYSTEMS

11.1 Introduction

Each of four techniques have been extensively examined with respect to the feasibility of their application to the DCS timing subsystem. A significant conclusion that was anticipated earlier and confirmed during this work was that limiting the timing subsystem to the use of a single technique would be overly restrictive. Network configurations and the inherent characteristics of each technique guarantee that such a restriction will only provide a suboptimal solution. Discussed below are candidate timing subsystems that are both feasible and not limited by such a restriction. Preceding this, the key factors that impacted the selection of the candidate timing subsystems are discussed. It should be noted that the results of Section 8.0 were not used to eliminate candidate timing subsystems as such; rather the results of Sections 8.0, 9.0 and 10.0 will be used in the concluding section to select the best of the candidates.

11.2 Network Considerations

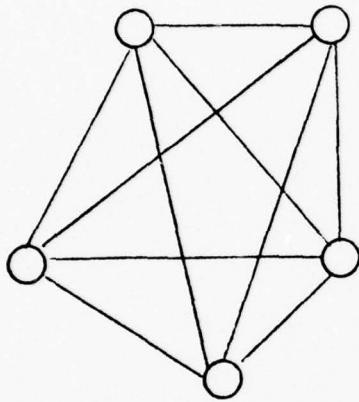
The network configuration influences what combinations of timing techniques form an appropriate timing subsystem. In turn, the requirements on timing components are surely dependent on timing technique. However, due to the relative small cost of the timing subsystem in relation to the overall cost of the DCS network, it is not feasible that timing considerations should dictate any overriding limitations on the present or future characteristics of the network itself. Thus, the timing subsystem must be made to fit the requirements of the network and not vice versa.

The network may be thought of as being composed of a hierarchy of nodes with different numbers of nodes at each level of the hierarchy and a certain amount of connectivity between the nodes at each level as well as some connectivity between levels.

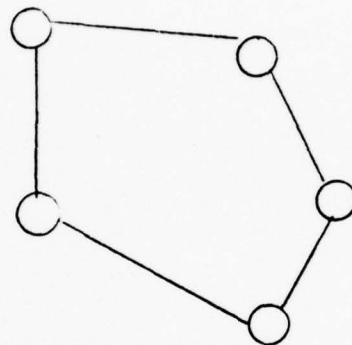
The key factor which determines the level to which a node belongs is the criticality or importance of the node. In general, this factor varies with:

- Amount of traffic handled
- Geographic location of node
- Number of other nodes directly connected to it

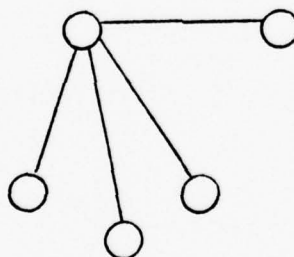
On the basis of these factors, a number of levels could be postulated for the DCS network, but it is believed that three levels is adequate for representing its essential characteristics. At each level there exists three basic connection types. These types are: 1) fully connected; 2) ring connection; and 3) star connection. The topologies of these basic connection types are shown in Figure 11.2-1. The actual network connectivity will very likely not fit any



Fully Connected



Ring Connection



Star Connection

Figure 11.2-1. Three Basic Network Connection Types

of the three basic types at any of its hierarchical levels. At the highest level, the actual network may be characterized as consisting of several highly connected clusters with a small amount of connectivity between clusters. An exaggerated form of this type of connectivity is shown in Figure 11.2-2. Even though the highest level of the actual DCS network may not be fully connected, it is sufficiently connected that any of the four generic timing subsystem configurations may be applied at this level.

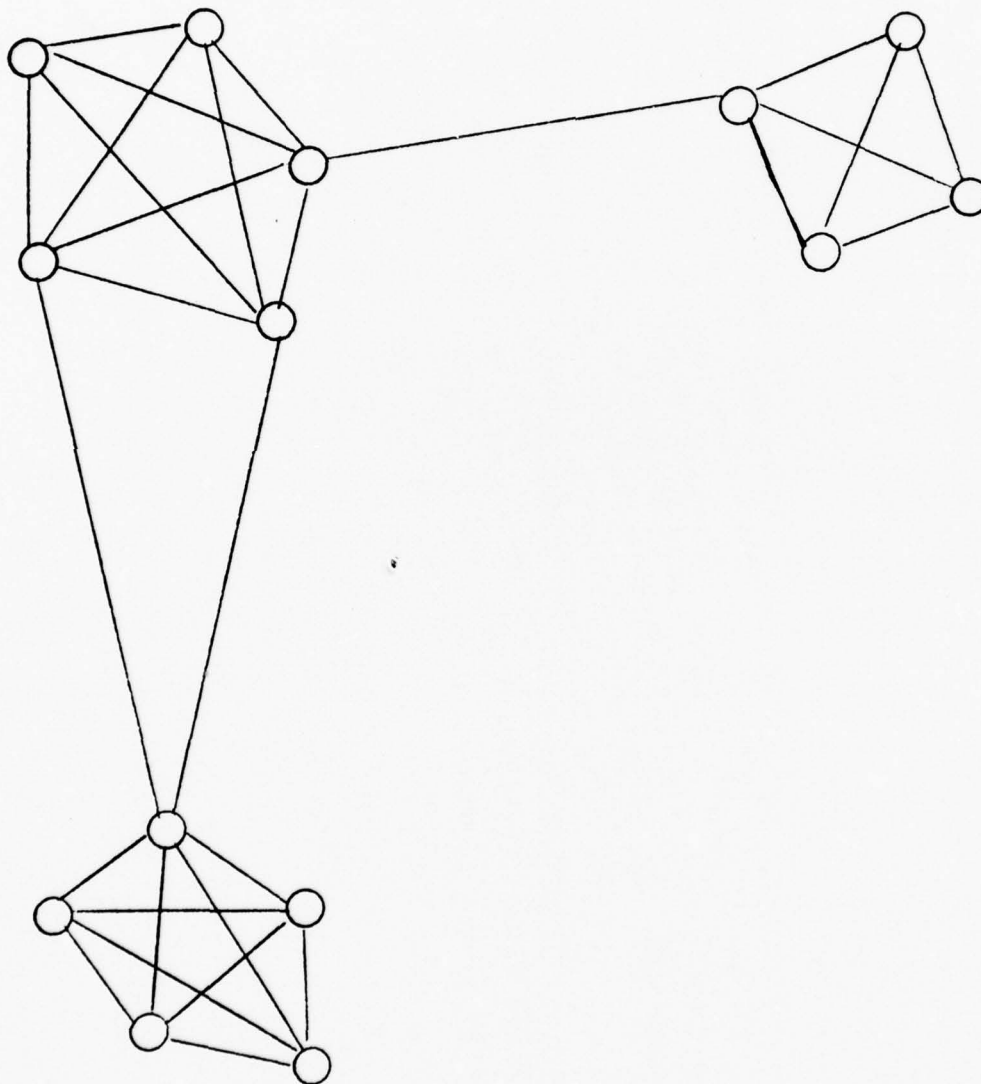


Figure 11.2-2. Clustering Network Connectivity

Intermediate level nodes tend to be clustered around the highest level nodes. In each cluster of intermediate level nodes, the total connectivity may vary considerably from one cluster to the next, but the connectivity between intermediate level clusters is small.

The lowest level nodes tend to be connected directly to only a single intermediate or highest level node with little connection between other nodes at the lowest level.

11.3 Major Network Synchronization Components

The major network synchronization components include the following:

- Stable clocks
- Data buffers at each node
- Phase lock loops
- Transmission media
- Fault detection and recovery protocol
- Maintenance aids

The various timing subsystem techniques place different requirements on these components, individually and collectively. Distinct possibilities exist for trading severity of requirements on one component for those on another in accordance with the timing subsystem that is chosen for the DCS. Requirements on these components may also vary in time as the DCS is utilized in new applications.

11.4 Timing Subsystems

From the preceding discussion, it is apparent that any one of the four generic timing subsystem techniques is applicable at the highest level of the DCS hierarchy. It also seems that due to connectivity of the network that the lowest level nodes should be slaved to their corresponding intermediate or highest level node. This results from the limited connectivity that characterizes the lowest level nodes. Thus, we are left with deciding which generic techniques at the intermediate level are most appropriate given that a particular technique has

been chosen for the highest level of the network. Some pairings of techniques at the highest and intermediate levels are illogical and consequently should not receive serious consideration. For example, *non-time reference distribution at the highest level nodes and time reference distribution at the intermediate level* is unsuitable because the greatest time and phase accuracies should be available at the major nodes and timing information dissemination should flow from the higher to the lower levels in accordance with the criterion for ranking the nodes of the network. Another factor which should be kept in mind is that there exists a natural tendency to slave lower level nodes to higher level nodes via highest quality links. Due to the topology at the intermediate level, this in general translates into slaving a cluster of intermediate nodes to the cluster's primary higher level node via a highest quality link. Fallback protocol for first alternate would then involve switching to alternate links and second alternates would involve slaving to alternate higher level nodes. Thus, we see that a natural tendency is against progression from tighter coupling to looser coupling when traversing from the higher level nodes to the lower level nodes. It then follows that given mutual sync or master-slave at the highest level, mutual sync or master-slave at the intermediate level is most appropriate.

With these tendencies in mind, the following timing subsystems seem good candidates for analysis and simulation:

1. Master-Slave Throughout

A further impetus for including this timing subsystem is that almost all commercial systems will utilize this form of timing subsystem.

2. Mutual sync at highest and intermediate levels with lowest level nodes slaved to their corresponding intermediate or highest level node.

3. Time reference distribution at highest level, master-slave at intermediate level, and each lowest level node slaved to corresponding intermediate or highest level node.

This timing subsystem will combine the attributes of time reference distribution with the simplicity of the master-slave technique applied to the majority of the nodes in the network.

4. Time reference distribution at highest level, mutual sync at intermediate level and each lowest level node slaved to corresponding intermediate or highest level node.

This timing subsystem should have greater potential for survival than (3) but will retain the attributes of the TRD configuration.

5. Time reference distribution at both the highest level nodes and the intermediate level nodes and each lowest level node slaved to one of the intermediate or highest level nodes.
6. Independent clock at highest level, master-slave at intermediate level, and lowest level nodes slaved to either an intermediate or a highest level node.

SECTION 12.0
CONCLUSIONS

The results of both the analysis and simulation efforts have led to the recommendation of time reference distribution as the technique to employ at the major nodes of the future switched digital Defense Communications System. The analysis effort indicated that as a technique, TRD ranked higher in more of the primary as well as more of the secondary desirable characteristics than any of the other techniques. The simulation indicated that TRD could maintain closer frequency coordination between nodal clocks in the face of both stress and normal operating conditions. The cost analysis indicated that the performance benefits resulted without an increase in the cost of the nodal timing subsystem equipment.

In examining the results of this study, the high evaluation of time reference distribution resulted from four key features of the technique. The most significant feature was the double endedness of the approach. This removed the effect on nodal clocks caused by variations in link phase delay. The second significant feature was the adaptive reorganization capability which assured the utilization of the best possible available reference after a failure. This feature resulted in smaller differences between the instantaneous frequencies of the nodal clocks after such failures. The third feature was the natural separation of error measurement and error correction. This feature which allows simultaneous correction of each clock with respect to the master clock rather than the disciplining clock, also results in minimizing the instantaneous frequency differences between nodal clocks. The fourth significant characteristic was the provision of precise time which opens the door for many potential benefits as well as aiding monitorability, and helping to ensure synchronous operation.

In summarizing the capabilities of the techniques it is worthwhile to reiterate a point made in Section 2.0 of this report: Any of the techniques, time reference distribution, master-slave, mutual synchronization or independent clocks can be made to work. The differences in performance capabilities between the techniques while clear, do not preclude the use of any of the techniques. Furthermore some of the four key features of time reference distribution discussed above can in certain instances be included in a few of the other techniques. To the degree that they are, the differences in capabilities between the techniques narrows. The approach taken in this study was to lump the four features strictly into the time reference distribution approach. The rationale was that each of these features depends upon an overhead link capability for its

operation. Once the overhead link is provided, one is essentially settling for an inferior subsystem if all four of the features are not included; and TRD is the only technique that can provide all the features.

Having chosen time reference distribution as the timing technique to be utilized at the major DCS nodes, it was clear that master-slave should be implemented at the lower level nodes. (See Section 11.0). At the lower level nodes in the network which are characterized by limited connectivity and lower bit rates the benefits of TRD that are highlighted at a highly connected node are not as significant. Also the overhead channel required for TRD would represent a larger percentage of the data traffic.

Although in Section 11.0 two such candidates were discussed, differing only in the technique to be used in the intermediate nodes, one is reluctant to choose between the two. This is because of the somewhat loose and arbitrary designation of three nodal levels. Suffice it to say that the results of this study should make one very comfortable with 1) the selection of time reference distribution at major nodes because of its overall utility and 2) the selection of master-slave at the lower level nodes where many of the TRD benefits are precluded by network configurations.

SECTION 13.0
TESTING PROGRAM

13.0 TESTING PROGRAM

The conclusions reached in this study were based on substantial analytical and computer simulation efforts. It is reasonable to expect that a well organized experimental test effort will provide additional data. Outlined below is such a testing program. It is suggested that media and transmission rates included in the test program should be troposcatter to 13 Mb/s, microwave LDS to 20 Mb/s, and satellite to 180 Mb/s.

13.1 Parameters To Be Tested

The following paragraphs describe the appropriate parameters to be tested.

Phase Jitter

Jitter or instability of the phase of the bit synchronizer timing waveform is an important parameter. The spectrum of this jitter should be determined under a representative set of conditions; different types of links, data rates, signal-to-noise ratios, jamming environments, etc. Jitter is an important parameter, affecting bit error rate and the probability of a bit slip in the bit sync. It also affects nodal synchronizer clock stability if that clock is derived from the bit sync timing waveform, such as in the master-slave and mutual sync techniques. This parameter impacts a number of characteristics by which timing techniques were evaluated, including bit count integrity, bit and frame sync performance, susceptibility to jamming, survivability, error propagation, and precise time availability. In most of these cases, the impact is on slip rate which, in turn, impacts quality of digital communication in a digital network. For the error propagation characteristic, knowledge of the phase jitter spectrum allows selecting a design such that error propagation is not troublesome. (For example: The proper loop bandwidth in a master-slave timing subsystem can be chosen.) For the precise time availability characteristic, phase jitter characteristics must be known to determine the accuracy of time transfer techniques such as are used in the time reference distribution approach.

Propagation Delays

Several measurements should be carried out in this area including total propagation and equipment delays between two nodes, the variation in this total delay as a function of

multipath or other effects, and difference in time delay between the paths in both directions between two nodes (reciprocal path delays). These parameters cause several effects. Variations in path delay result in additional phase jitter on the receive timing waveform (and the effects caused by phase jitter as discussed above) and cause a requirement for additional buffering at communication nodes to smooth out these variations. Differences in reciprocal path delays impose a limit on the accuracy with which time transfers can be accomplished and, therefore, a limit on the accuracy of the time reference distribution technique. These parameters impact a number of characteristics, including bit count integrity, bit and frame sync performance, survivability, error propagation, and precise time availability.

RSL, S/N, and C/N

The quantities received signal level (RSL), signal-to-noise ratio (S/N), and carrier-to-noise ratio (C/N) are indicative of channel conditions. These quantities should be measured and correlated with other quantities, such as bit error rate, fade rate/duration/depth, and bit count integrity for each type of link. Certain quantities, such as very small values of bit slip probabilities, should probably be measured only once on each link as a function of S/N. The quantities RSL, S/N, and C/N do not all provide equivalent information. One could have both a high RSL and a low S/N if, for example, one were in a jamming environment. These quantities are not only highly correlated with other parameters that should be measured, but they impact several key timing subsystem characteristics. These characteristics are bit count integrity, data rates, bit error rates/signal outages/fading, bit and frame sync performance, and susceptibility to jamming.

Bit Error Rates at Various Transmission Rates

Link measurements should be made to determine bit error rate for various transmission rates on each link as a function of RSL, S/N, and C/N. Thus, bit error rate can be determined for a variety of channel conditions such as fading, jamming, etc. Average bit error rate is one of the fundamental parameters that determines the quality of digital communication in a digital network. In addition to the average error rate, statistics of the error events should be determined. This parameter impacts several characteristics, including bit count integrity, susceptibility to error rate, bit and frame sync performance, and signal outages/fading.

Bit errors can affect the nodal synchronizer since they can corrupt control information sent from node to node. This can occur with any technique that requires control information, such as master-slave, time reference distribution, or pulse stuffing.

Bit Count Integrity

Bit count integrity is necessary for maintaining frame sync for multiplexer, switches and crypto sync. This parameter should be measured by determining the bit sync slip rates as a function of RSL, S/N, and C/N for a variety of links and data rates. Characteristics affected by this parameter are frame sync performance, communications security, survivability, and susceptibility to jamming.

Fade Rate/Duration/Depth

Fading characteristics of each type of link will be obtained as a function of frequency, data rate, and distance. These characteristics should be correlated with RSL, S/N and C/N. In fact, RSL, S/N, and C/N provide a means by which these fading characteristics may be measured. The fade rate indicates the rapidity with which a fade occurs, i.e., the signal level rate of decrease is measured in dB/sec. Knowledge of this quantity is important in implementing hardware for detecting the onset of fades and providing switchover to diverse paths not experiencing a fade. Fade duration is the length of an outage (in seconds), and fade depth is the amount by which the signal level has decreased (in dB) from its nominal value (with no fading). Since each fade is different, these parameters should be characterized statistically, i.e., a probability distribution of fade rates, fade durations, and fade depths will be obtained for each case. Characteristics impacted by the fading parameters are bit count integrity, bit and frame sync performance, error propagation, and susceptibility to error rate. Any network timing technique which attempts to derive the nodal clock from a fading signal will be affected to some degree by this phenomena. About the only approach not affected is independent clocks.

Buffer Fill

This is an example of a quantity that would be monitored in a network test. Buffer fill provides a measure of the absolute phase difference between the nodal clock and the receive timing waveform. Buffer overflows can be a significant source of bit slips. Thus,

the buffer size required to make the effect of these bit slips on system performance negligible is a significant design parameter for all timing techniques. This requirement will vary, depending on the type of link and data rate. This parameter will impact several characteristics, including bit count integrity, frame sync performance, susceptibility to jamming, and survivability.

The parameters described above should be measured in several different types of tests including point-to-point, tandem link, and network. The number of parameters measured in each type of test should get successively smaller. Parameters to be measured on point-to-point tests involve a variety of link types and all parameters discussed above, including phase jitter, propagation delay measurements, bit count integrity, bit error rates at various transmission rates, fade rate/duration/depth, and RSL, S/N, C/N. In proceeding to tandem link tests, no additional information is provided by making further measurements of fade rate/duration/depth or RSL, S/N, C/N. However, statistics of several parameters change in passing through several tandem links, and measurements of these effects must be made to accurately model them. The parameters measured in tandem link tests should be accumulated phase jitter, propagation delay measurements, bit error rate, and bit count integrity. Measurements should be made for simple IF repeaters and regenerative repeaters that retune the transmitted digital sequence. All tests done to this point involve gathering data that can be used to improve the accuracy and validity of the analytical work. Network tests involve an evaluation of a specific network synchronization approach. In performing this evaluation, buffers at each node to temporarily store the received data, and a nodal synchronizer of some type to retune the digital sequences at each node are required. Several network configurations representative of the future DCS can be used. Basic parameters to be monitored in this type of test are buffer fill at each node and bit slips due to both slips in bit syncs and buffer overflows (for various size buffers). These parameters should be monitored for various network configurations, fading environments, and stress scenarios. A major result of this series of tests should be a verification of the analytical and simulation results obtained thus far.

13.2 Summary and Test Example

A general listing of tests includes media from Table 13.2-1 and parameters from Table 13.2-2. Each test should likely be run as functions of frequency and data rates. Efforts should be made to require testing to be applied to equipment to be used in the timing system.

Table 13.2-1. Communications Media

Ground-to-satellite links

Microwave links

Troposcatter radio links

Wire line links

HF radio links

Table 13.2-2. Critical Operational Parameters

Phase jitter

Doppler effects

Propagation delays

Differential propagation delays

Reciprocal propagation delays

Received signal level

Signal-to-noise ratio

Carrier-to-noise ratio

Bit error rate

Bit count integrity

Bit synchronism

Fade rate

Fade duration

Fade depth

Buffer fills

Synchronism losses (frame and crypto)

Time to establish synchronism (initial and resync)

Test Example

This paragraph is an example test plan included to show how a typical test should be documented.

The test example is actually two separate tests that establishes a baseline for a third test which is of prime importance to the Time Reference Distribution scheme for network timing. Ultimately this test example should be worked into three separate subplans which will define the tests in more detail than presented here. Because of the similarity of the tests, all three are discussed here. These tests are: 1) measurement of propagation delay, 2) measurement of differential time delays and 3) measurement of the reciprocal time delays (differential delay between both directions of a full duplex link). This example considers these delays as associated with a troposcatter radio link.

- a. Test Objective - To determine the absolute time delay between two troposcatter radio terminals and the frequency dependent differential delays. This measurement includes both the propagation delay and equipment delay. Corollary tests should be defined to determine equipment delays and reciprocal time delays.

- b. Definition of Parameters to be Measured

Propagation Delay - The total time differential in nanoseconds required for the coding, modulation, transmission, propagation, reception, demodulation and decoding of a 13 Mb/s data stream.

Differential Delay - A differential delay expressed in nanoseconds/MHz. This delay difference is from the nominal 70 MHz carrier for which the propagation delay was determined.

- c. Measurement Technique - A link with the capability to handle 13 Mb/s data is assumed. At this data rate, the magnitude of the variations is expected to cover a significant number of bit periods (several hundred) and the rate of variation is expected to be slow relative to a bit period. A cesium standard (HP 5061A) clocks a PN generator providing a PN sequence of sufficient length

to prevent ambiguities over the expected delay variation. A 70 MHz sub-carrier is PSK modulated with this sequence and transmitted across the tropolink.

At the receive end, a conventional PSK demodulator and bit sync extract the transmitted PN sequence. This sequence is compared to an identical sequence generated in the same manner as the transmitted sequence. The PN generator is clocked by a second cesium standard. A simple range extractor circuit is used to determine the time delay between the sequences. A strip recorder is shown since it will probably be desirable to record variations in propagation delay over long periods with a strip recorder.

Note that if both cesium standards are at the worst limits of their accuracy, the resulting time delay error will be only 72 ns/hr.

Since delay variation as a function of frequency will be averaged over the bandwidth of the transmitted signal, two types of measurement are possible. By using a relatively high bit rate the average delay for the whole band of frequencies may be measured. By using a low bit rate (say 10 kb/s) spot checks of delay may be made at various points across the frequency band.

Figure 13.2-2 shows how a swept (or stepped) subcarrier may be added to provide a means for measuring and recording differential time delay. The test setup used for propagation delay (Figure 13.2-1) remains intact. In addition, the cesium standard clocks a frequency synthesizer HP 8660C which steps the center frequency across the band (step size and sweep rate are selectable).

At the receive end, an identical sweep rate and step size are generated with a 140 MHz center frequency. A mixer and bandpass filter are used to extract the difference frequency which is a constant 70 MHz. A digital delay adjustment and a counter are used to synchronize the sweeps manually. Once adjusted, drift will be insignificant due to the high stability of the cesium standard. A time marker from the cesium standard is provided to the recorder to provide a reference for frequency calibration.

- d. Test Stimuli - For the propagation delay test the cesium beam time standard driving the PN generator is the prime stimulus for the test. For the differential delay the test stimuli are the PN sequence and a stepped range of frequencies used to offset the 70 MHz subcarrier.
- e. Control Parameters - These parameters include the carrier frequency and transmitted power level. It is expected that the received signal level will be maintained sufficiently high to achieve a low BER during performance of the test. This test may be repeated for different carrier frequencies if believed beneficial to support the overall program objectives, i. e., network and link analysis.
- f. Test Setup - Figure 13.2-1 gives the test setup for the propagation delay and Figure 13.2-2 gives the setup for the differential delay test. All of the equipment required for these tests should be readily available.
- g. Data Gathering - Data gathering on these tests should consist of a plotting of time delay on a strip chart recorder. The recorder should have an event marker capability to mark time hacks. Identification of the test and any other desired information may be annotated directly on the recorder paper.
- h. Performance of Test - For the sake of brevity the test will be broken down into a few basic steps.

Step 1 - Gathering of Test Equipment. - This consists simply of getting all the needed test equipment to the appropriate test sites at the appropriate time. This includes the assembly of the special test circuits (range extractor, recorder interface).

Step 2 - Pretest Checkout. - A brief check should be performed to verify that each unit is capable of performing its test function. This includes verifying that each piece of equipment has a current calibration.

Step 3 - Connect Test Setup. - Hook the equipment together as required to perform the test. The function of the test setup should be verified to the maximum extent possible prior to start of test (radio transmission).

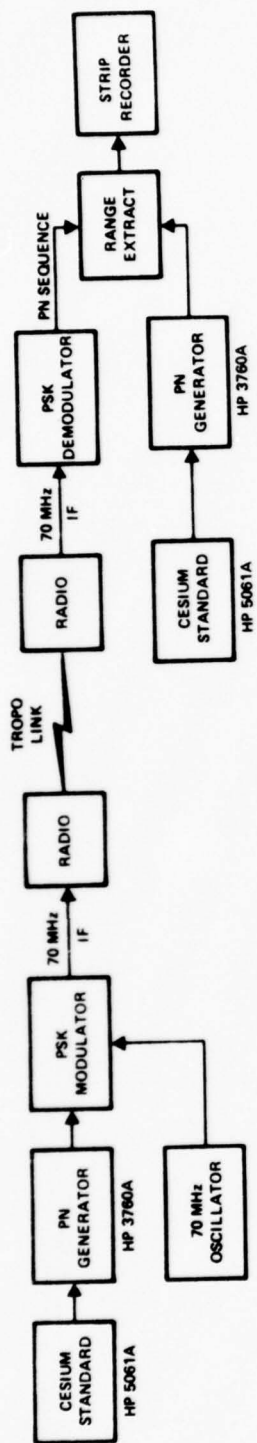


Figure 13.2-1. Propagation Delay Test Setup

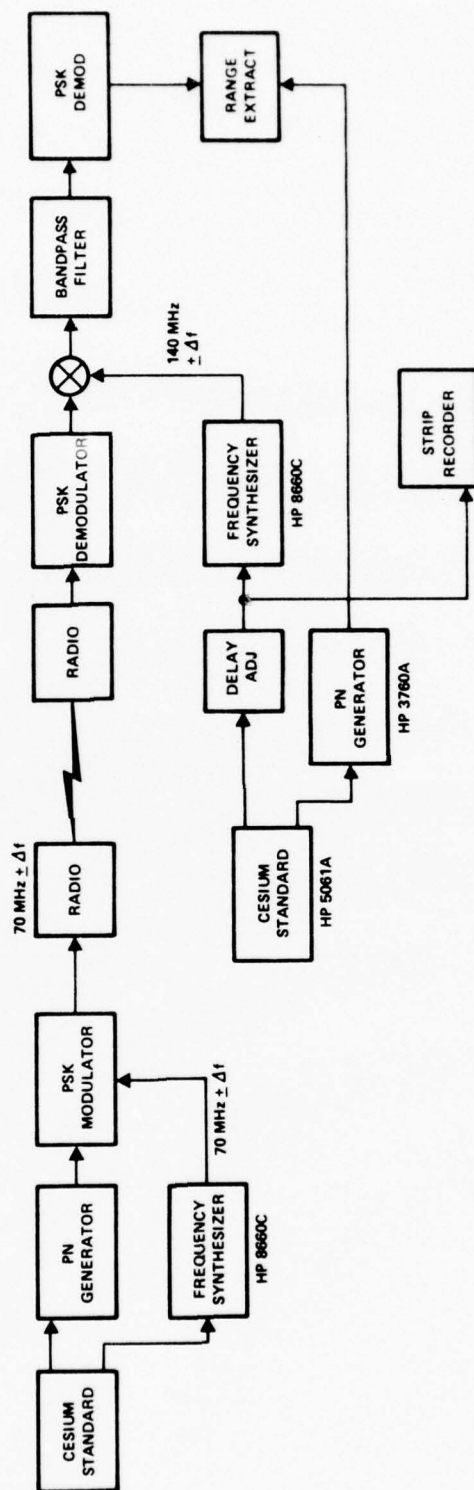


Figure 13.2-2. Differential Delay Test Setup

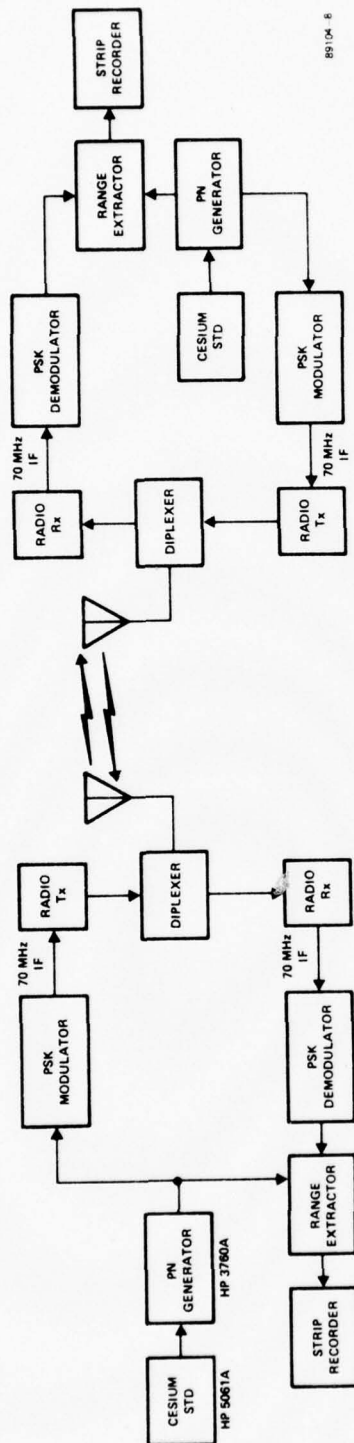
Step 4 - Synchronize the Cesium Time Standards. - With the standards side by side the two are to be synchronized to precisely the same time setting. The standards should then be taken to the test sites and connected into the test setups. This step may have to be repeated depending on the total time span of the testing effort in order to preserve the close agreement of the standards.

Step 5 - Performance of Test. - Using the appropriate carrier frequency(s) and levels the test is run for a TBD period. The strip chart recorder should be operated for the duration of the test to obtain a continuous time correlated record of the delays.

Figure 13.2-3 shows the test setup for measuring the reciprocal delay over the troposcatter radio link. A comparison to Figure 13.2-1 shows that this setup is basically a full duplex version of the propagation delay test. The prime concern here is to obtain a simultaneous measurement of the propagation delay in both directions so that the delay difference for the reciprocal paths may be computed.

Virtually all of the previously discussed parts of the subplan for propagation delay are applicable to the reciprocal delay test. The major difference, of course, is the full duplex radio link and the additional equipment needed for performing two simultaneous propagation delay measurements. The two radio transmitters must be operating with sufficient difference in their frequencies to obtain the necessary isolation of the local transmitter output at the receiver input via the duplexer. This difference in frequency will, of course, contribute a slightly different propagation path and corresponding delay. The remaining portion of the reciprocal delay differential is contributed by the difference in delays through the corresponding equipment in each path.

An alternative scheme for making a reciprocal time delay measurement exists which uses less equipment. For example, only one full duplex PSK modem would be required instead of two. This alternative technique would use a transponder approach and would require separate measurement of equipment and total propagation delays. It is expected that this approach would yield a lower accuracy measurement and should be used only if a sufficient amount of equipment is not available to support the primary test configuration.



89104 8

Figure 13.2-3. Reciprocal Delay Test Setup

SECTION 14.0
ADDITIONAL EFFORT

The recommended network synchronization subsystem employs time reference distribution at the highest levels in the network and master-slave at the other levels. An adaptive timing distribution network organization/reorganization technique will be used at all but the tail ends of the network. Extremely narrowband loops should be used throughout to maintain highly stable nodal clocks. The techniques being recommended are not entirely new. A considerable amount of work has been done on several aspects of these techniques. This section outlines additional work that should be done prior to any hardware development.

The application of time reference distribution on the digital DCS has been studied for several years. One of the more thoroughly studied aspects of this approach is the implementation of an adaptive timing distribution network organization/reorganization technique. The first technique for accomplishing this was proposed by Davies and Prim.²¹³ Modification of this technique have been proposed by Stover¹⁷⁰ and Clarkson College Investigations. In addition, the Canadian Dataroute network uses a similar technique.⁹² Since this problem has been so thoroughly investigated, additional work on the problem does not appear warranted at this time. Master-slave nodal synchronizers are well understood since several commercial digital networks are using this approach. Therefore, significant additional work is not required. Finally, trade-offs leading to selection of loop parameters for both TRD and master-slave were presented in Section 3.0, and no significant refinements of these parameters should be required.

However, there are several aspects of the implementation of the recommended timing subsystem which should be addressed prior to any hardware development. The implementation areas, some of which necessitate the exercising of the computer simulation tool developed during this effort, include:

- Transmission of periodic timing marks and measurement of timing error
- Technique for correction of atomic clocks
- Technique for measurement of fixed asymmetries and correction of timing error measurements
- Rate of clock error measurements and criteria for clock correction
- Time reference distribution, master-slave interface

The periodic timing marks transmitted between all pairs of TRD nodes are used to estimate the phase error between the local clock and the network master. The questions that need to be answered relating to the transmission of these marks and the measurement of timing error are the following.

1. How should these timing marks be transmitted within the expected multiplex structure of the digital DCS? Two possibilities are to let frame bits in either the T1 data stream or the highest available multiplex level be the timing marks. The advantage of using the T1 data stream framing bits would be that a single, common approach would be used at every node, while the advantage of using the framing bits from the highest available multiplex level is that better resolution can be obtained.
2. How should one measure the error between the received timing mark and the local clock phase? Several approaches of varying degrees of accuracy and complexity should be evaluated.
3. Each combination of approaches for transmission of the timing marks and measurement of the timing error should be compared on the basis of complexity at the desired level of performance. Each measurement approach will produce a measurement error per sample that is most likely greater than the measurement error that one can allow to enter the loop filter without degrading the stability of the nodal clock. The measurement error for each of the measurement techniques can be reduced to the desired value by averaging a large number of these measurements before allowing the sample average to enter the loop filter. The effect of the different requirements on sampling interval and averaging time for each technique should be considered in the comparisons.

The output of the loop filter supplies a voltage which is to be used in controlling the frequency of the local clock. This voltage can be used directly to control the frequency of quartz crystal VCO's. However, voltage-controlled frequency adjustment of available cesium and rubidium atomic frequency standards is not as easy. Several alternatives for providing this frequency control should be investigated.

1. There is a rubidium frequency standard available from Efratom which allows voltage control of the output frequency. In addition, one could make modifications to HP cesium standards to allow voltage control of its frequency. Thus, one option is the direct control of the frequency of the atomic standard.
2. Another possible solution is the use of an outboard phase shifter. The function of this unit would be to slightly shorten or lengthen the clock pulses coming from the frequency standard to produce a small change in frequency. The amount of this change should be directly controlled by the voltage from the loop filter. The advantage of this approach would be to avoid any modifications of frequency standards to allow voltage control of frequency. However, to achieve the very small changes in frequency that are desired may be difficult to do.

The performance of TRD may be improved by measurement of asymmetries in equipment delays and utilization of this information in correcting the estimated phase error between the local clock and its reference. It would be very beneficial to devote some time to determining typical values for these asymmetries, the best techniques for measuring them, and an approach for correcting the estimated phase error between the local clock and its reference. Fixed asymmetries will most likely be very small, and measurement of them will be needed infrequently. However, the removal of these asymmetries from the phase error estimate can result in better transient performance during acquisition of a new reference.

The rate at which clock error measurements should be made and the criteria for making a clock correction is a function of the types of clocks in the network, the network connectivity and the transmission bit rates. The computer simulation that has been developed will be a valuable tool in selecting an optimum approach as well as evaluating various options for processing error measurements.

The selected subsystem employs both the time reference distribution and master-slave techniques. Where one technique leaves off and the other begins is still a loosely defined point. Obviously this is heavily dependent on network connectivity patterns. Again the computer simulation tool should be used to great advantage to evaluate the performance at this interface and determine criteria for its placement.

It is believed that the areas discussed above should be included in future work on time reference distribution. Once this work is done, there are also several minor problem areas that should be considered:

- Refinement of design for the TRD phase-locked loop.
- Define interface between master-slave and TRD nodes and the method for measurement and report of buffer asymmetries of master-slave nodes to TRD nodes.
- Quantification of data transfer and processing requirements.

Investigation of each of these problem areas should allow the network synchronization to be very well-defined.

APPENDIX A
FREQUENCY ACQUISITION

APPENDIX A

FREQUENCY ACQUISITION

A1 Introduction

One important aspect of a network timing subsystem is its response to transient conditions. The purpose of the present exercise is to investigate the response of individual nodes to unit step transients under noiseless conditions. The major parameters to be observed are the size of buffers needed to avoid loss of data and the amount of time needed to overcome the transient. A comparison of the relative acquisition performances of a one cycle non linear sinusoidal phase detector versus an extended range linear phase detector such as might be obtained by using buffer fill will be made.

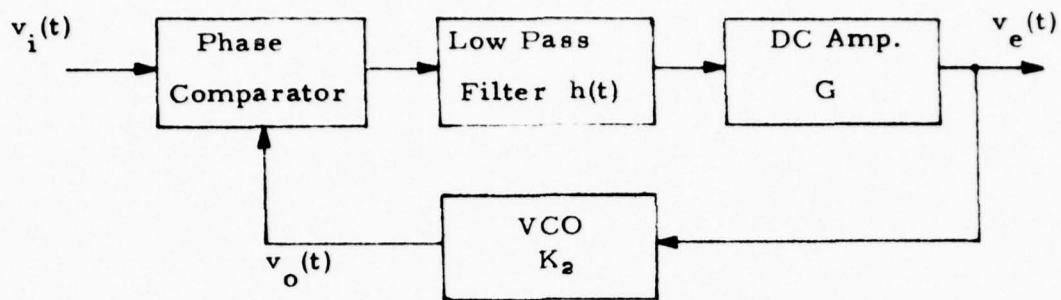
A2 Non Linear Noiseless Sinusoidal Model

A2.1 Block Diagram

A block diagram of a phase lock loop utilizing a non linear sinusoidal phase detector is shown in Fig A1. From this figure, it should be observed that the error voltage applied to the VCO is a sine function of the difference in phase between the reference signal and the VCO. For this reason the phase comparator is called a non linear sinusoidal phase detector. Due to this non linearity, exact analyses are not available and approximations must be utilized.

A2.2 The Relevant Equations

The following derivations of lock range and capture range are from Moschytz [54].



$$v_i(t) = E \sin (\omega_c t + \phi_i(t))$$

$$v_o(t) = A \cos (\omega_c t + \phi_o(t))$$

$$v_e(t) = K_1 h(t) * \sin [\phi_i(t) - \phi_o(t)] \quad , \quad K_1 = (G A E)/2 \quad \text{and}$$

* represents convolution.

Fig. A1 Block Diagram of a PLL Using a Sinusoidal Phase Detector.

Lock Range - The differential equation describing the dynamics of the loop of Fig A1 is

$$\frac{d\phi_i(t)}{dt} = \frac{d\phi(t)}{dt} + Kh(t) * \sin\phi(t) \quad (A1)$$

where $\phi(t) = \phi_i(t) - \phi_o(t)$, K is the open loop gain, $h(t)$ is the impulse response of the low pass filter and $*$ indicates convolution. For unity dc gain of the low pass filter and $\Delta\omega_i = d\phi_i/dt$ equation (A1) has steady state solution

$$\sin\phi = \Delta\omega_i/K \quad (A2)$$

Thus it is possible for the system to obtain a steady state condition with zero average frequency error between the reference signal and the local VCO provided

$$|\Delta\omega_i| \leq K_T \quad (A3)$$

A2.3 Capture Range - The capture range is that range of input frequencies to which the VCO can be synchronized to when initially in the unlocked state. If the loop filter were perfect, i.e., passed the low frequency difference components without attenuation and rejected the high frequency components from the phase comparator, then the capture range would exactly equal the lock range. Since practical filters are not perfect, the capture range is reduced from that of the lock range. Determining the actual capture range involves the solution of a non linear differential equation. The only known method for doing this is by means of a graphical technique involving a so called "phase plane method." However, an estimate of the capture range can be obtained by determining for an input offset frequency $\Delta\omega_i$ the amount of steady state error voltage at the VCO input

terminals under closed loop conditions and comparing this with the peak ac error voltage to the VCO input terminals when the input to the VCO is open circuited with input offset frequency also of value $\Delta \omega_i$. In either case, the output frequency $\Delta \omega_o$ must be equal to $\Delta \omega_i$. For the open loop condition the error voltage is

$$V_e(t) = K_1 H \Delta \omega_i \sin \Delta \omega_i t \quad (A4)$$

The peak of this voltage is

$$\hat{V}_e(t) = K_1 H \Delta \omega_i \quad (A5)$$

The closed loop steady state error voltage is

$$V_{ec} = K_1 \sin \phi_c \quad (A6)$$

From (A2) this becomes

$$V_{ec} = K_1 (\Delta \omega_i / K_T) \quad (A7)$$

Then, at the capture frequency (A5) and (A7) can be combined to give

$$K_1 H \Delta \omega_{ic} = K_1 (\Delta \omega_{ic} / K_T)$$

or

$$\Delta \omega_{ic} \cong K_T H \Delta \omega_{ic} \quad (A8)$$

As it turns out, the estimate of (A8) is often not particularly accurate for very narrow band filters because the associated bandwidth does not need to be as large as (A8) indicates in order to acquire a frequency offset of $\Delta \omega_{ic}$.

A2.3.1 Capture Range for Specific Filters

For the low pass filter of Fig A2-a the attenuation as a function of radian frequency is given by

$$H_{\omega} = 1/(1 + \omega^2 \tau_1^2)^{\frac{1}{2}}. \quad (A9)$$

Substituting (A9) into (A8) we obtain

$$\Delta \omega_{ic} \cong \sqrt{K_T \omega_{co}} \left\{ \left[1 + \left(\frac{\omega_{co}}{2 K_T} \right)^2 \right]^{\frac{1}{2}} - \left(\frac{\omega_{co}}{2 K_T} \right) \right\}^{\frac{1}{2}}. \quad (A10)$$

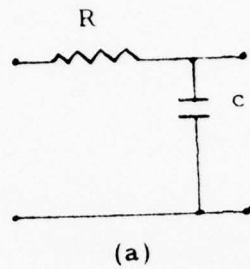
Where ω_{co} is the 3 dB cutoff frequency of the low pass filter and equals $\frac{1}{\tau_1}$. The term inside the braces is of the form $\sqrt{a^2 + 1} - a$. But $0 \leq \sqrt{a^2 + 1} - a \leq 1$ for all real positive a . Thus

$$\Delta \omega_{ic} \leq \sqrt{K_T \omega_{co}}. \quad (A11)$$

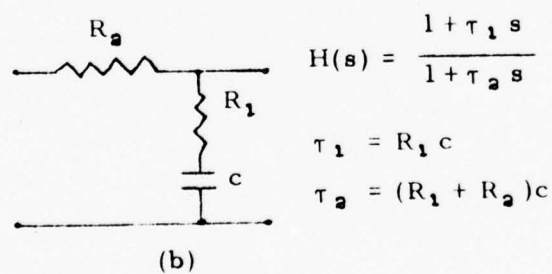
For the low pass filter of Fig A2-b the attenuation as a function of radian frequency is given by

$$H_{\omega} = \left[\frac{1 + \omega^2 \tau_1^2}{1 + \omega^2 \tau_2^2} \right]^{\frac{1}{2}}. \quad (A12)$$

Substituting $\Delta \omega_{ic}$ for ω in (A12) and substituting the resulting factor into (A8), solving for $\Delta \omega_{ic}$ and then substituting $2 \xi \omega_n = (1 + K_T \tau_1^2)/\tau_2$ and $\omega_n^2 = K_T/\tau_2$ in the solution we obtain



(a) Low Pass Filter



$$H(s) = \frac{1 + \tau_1 s}{1 + \tau_2 s}$$

$$\tau_1 = R_1 c$$

$$\tau_2 = (R_1 + R_2) c$$

(b) Lag Network Low Pass Filter

Fig. A2

$$\Delta \omega_{ic} \cong \omega_n \left\{ \left| 2 \xi \left(\frac{\omega_n}{K_T} - \xi \right)^2 + 1 \right|^{\frac{1}{2}} - 2 \xi \left(\frac{\omega_n}{K_T} - \xi \right) \right\}^{\frac{1}{2}}. \quad (A13)$$

For $\frac{\omega_n}{K_T} \ll \xi$ the term inside the braces may be approximated by

$$\sqrt{2 \xi^2 + \sqrt{(2 \xi^2)^2 + 1}}$$

By choosing the time constants τ_1 and τ_2 of Fig A2-b in a suitable manner, this circuit can be made to approximate that of the integral plus proportional filter, $K_p + K_I/s$. This is true provided $\tau_1 \gg \frac{1}{K_T}$ where K_T is the open loop DC gain.

For the integral plus proportional filter, the frequency response function is

$$H_\omega = \left[\frac{1 + \omega^2 \tau_1^2}{\omega^2} \right]^{\frac{1}{2}}$$

Substituting this factor into(A8) we find that the capture range is given approximately by

$$\Delta \omega_{ic} \cong \omega_n \sqrt{2 \xi^2 + \sqrt{(2 \xi^2)^2 + 1}} \quad (A14)$$

A2.4 Closed Loop Noise Bandwidth

Two sided closed loop noise bandwidth is defined by

$$W_L = \frac{1}{2\pi j} \int_{-j\infty}^{j\infty} |F(s)|^2 ds \quad (A15)$$

One sided noise bandwidth = $B_L = \frac{1}{2} W_L$.

For the basic phase lock loop, the closed loop phase transfer ratio is given by

$$F(s) = \frac{K_T H(s)}{s + K_T H(s)} \quad (A16)$$

where $H(s)$ is the low pass filter transfer function and K_T is the open loop DC gain. The integral in (A15) may be evaluated by the method of complex residues or by partial fraction expansion if $F(s)$ is a rational function. A short table of integral forms in the rational case is given in [56], p. 135. Evaluation of (A15) for four types of filters gives the following results:

$$H(s) = 1 \rightarrow W_L = K_T/2$$

$$H(s) = \frac{1}{1 + \tau_1 s} \rightarrow W_L = \frac{K_T}{2} = \frac{\omega_n}{4\xi}$$

$$H(s) = \frac{1 + \tau_1 s}{1 + \tau_2 s} \rightarrow W_L = \frac{K_T(\tau_2 + \tau_1^2 K_T)}{2\tau_2(K_T\tau_1 + 1)} \cong \omega_n \left(\frac{4\xi^2 + 1}{4\xi} \right) \text{ for } \tau_1 \gg \frac{1}{K_T}$$

$$H(s) = \frac{1 + \tau_1 s}{s} \rightarrow W_L = \frac{1}{2\tau_1} + \frac{K_T\tau_1}{2} = \omega_n \left(\frac{4\xi^2 + 1}{4\xi} \right)$$

A2.5 Time to Acquire Synchronization - For a second order loop with an integral plus proportional loop filter of the form

$$H(s) = \left(\frac{\tau_1 s + 1}{s} \right) \quad (A17)$$

$$T_{\Delta f} \cong \frac{\pi^2}{4\xi} \left(\frac{1 + 4\xi^2}{4\xi} \right)^3 \frac{(\Delta f)^2}{B_L^3} = \frac{2\pi^2}{\xi} \frac{(\Delta f)^2}{\omega_n^3} \quad (A18)$$

where Δf is the initial offset frequency in Hertz

$$B_L = \frac{1}{4\tau_1} (1 + 4\xi^2) = \frac{\omega_n (4\xi^2 + 1)}{8\xi} = \text{one sided loop noise bandwidth}$$

ξ is the loop damping ratio,

$$\tau_1 = \frac{2\xi}{\omega_n} \text{ is the time constant of the loop filter, and}$$

ω_n is the undamped natural frequency of the second order loop.

Derivations of equation (A18) can be found in Richman [55] Lindsey [56] chapters 3, 4, and 10. Stiffler [57] chapter 5 derives (A18) but states that there are no theoretical limits on the capture range. It should be observed from (A18) that the time needed to acquire frequency synchronization grows as the square of the initial frequency offset Δf . This fact will be used to obtain an expression for the frequency of the error signal as a function of time during the pull in process. Such an equation allows calculation of the buffer size required to hold all the bits slipped following a step transient in input frequency to the PLL. After frequency synchronization has been obtained, some additional time T_ϕ is required to obtain phase lock. T_ϕ can normally be approximated by

$$T_\phi \cong 4/B_L. \quad (A19)$$

Since T_ϕ is small in comparison to that needed for frequency synchronization when Δf is very large and no further cycles are slipped, this term will normally be neglected.

Example of time to acquire synchronization using (A18)

$$\text{Let } \xi = \frac{1}{\sqrt{2}}, \text{ and } \Delta f = 10^{-8} f_o = .01544 \text{ Hz}$$

$$\text{From (A14) the capture range is } \Delta\omega_{ic} \cong 1.55 \omega_n. \Rightarrow \omega_n = \frac{.01544}{1.55} \times 2\pi.$$

Therefore let us assume that $\omega_n = .0628$ rad/sec. Then

$$B_L = \frac{\omega_n (4\xi^2 + 1)}{8\xi} = \frac{.0628(3)}{5.656} = .033 \text{ Hz}$$

and

$$T_{\Delta f} = \frac{\pi^2}{4\xi} \left(\frac{1 + 4\xi^2}{4\xi} \right)^3 \frac{(\Delta f)^2}{B_L^3} = 4.16 \times \frac{2.384 \times 10^{-4}}{3.696 \times 10^{-5}}$$

$$= 26.83 \text{ sec.}$$

Actually, in order to filter out link disturbances, a value of ω_n on the order of 5.6×10^{-5} rad/sec would be required. Thus, reacquisition of synchronization following the above step change in reference frequency would first require a change in bandwidth of at least $.0628 / 5.6 \times 10^{-5} = 1121$ times that of the normal tracking bandwidth. Step changes in reference oscillator frequency of the size considered in this example can be expected in a timing subsystem when switching from one reference oscillator to another or as a result of abnormal link disturbances.

A2.6 Frequency Acquisition Techniques

From the above example, it should be apparent that due to the size of transients and the required loop time constants for filtering out normal link disturbances, some scheme is required for obtaining initial synchronization and for handling abnormal transients. Three major approaches have been suggested for accomplishing this objective. They are as follows:

1. Provide two filter bandwidths, a narrow one for tracking and a much wider bandwidth for initial acquisition.
2. Use a sweeping or search technique during acquisition to force the local VCO to approximately the correct value prior to final acquisition.

3. Use an extended range linear phase detector such as might be provided by buffer fill in order to develop a large error signal that is proportional to the number of bits slipped between the local VCO and the input reference.

It may actually turn out that some combination of the above approaches is the best solution for a particular timing subsystem. The remainder of this section will investigate the first two approaches while the next section will consider the third option.

A2.6.1 The Sweep Technique for Acquiring Synchronization

This technique consists of applying a sweep voltage directly to the VCO input and removing it as soon as frequency synchronization is detected.

It may be shown that if the sweep rate is greater than the total DC gain of the loop (K_T), the system cannot lock onto the reference signal, but if the rate is less than $K_T/2$, then lock can be obtained. At lower signal to noise ratios, the sweep rate must be smaller than for the ideal rate, but for many practical problems can be almost $K_T/2$. For the sake of this discussion, let us assume that a sweep rate of $K_T/4\pi$ is suitable. Then frequency acquisition time is given by

$$T'_{\Delta f} = \frac{4\pi \Delta f}{K_T} = \frac{\pi \Delta f}{\left(\frac{4\xi}{1+4\xi^2}\right)^2 B_L^2} \text{ sec.} \quad (\text{A20})$$

with $\xi = \frac{1}{\sqrt{2}}$, $\Delta f = .01544 \text{ Hz}$ and $B_L = 2.0833 \times 10^{-4} \text{ Hz}$ corresponding to a time constant τ_1 of 1 hour

$$T'_{\Delta f} = 1.2573 \times 10^6 \text{ sec} = 14.55 \text{ days.}$$

Thus, it appears that the sweep technique alone is unsuitable for acquiring

synchronization with bandwidths corresponding to time constants on the order of an hour if the frequency offset is on the order of $10^{-8} \times f_o$. Comparison of equation (A20) with (A18) indicates that the sweep technique can become effective if

$$\Delta f > \frac{4}{\pi} \frac{4 \xi^2}{1 + 4 \xi^2} B_L.$$

A2.6.2 Two Bandwidth Approach

The amount that the loop bandwidth can be increased is generally limited by noise considerations. However, due to the extremely narrow tracking bandwidths being considered and the high signal to noise ratios that can be expected for a communication network timing subsystem, this may not be a real problem. Nevertheless, the acquisition bandwidth must be great enough that the maximum input frequency deviation from that of the local VCO is within the PLL's capture range if this method is to be successful. From (A10), (A13), or (A14), depending on the loop filter chosen, we may choose values for closed loop parameters ω_n and ξ which will insure that the PLL will acquire synchronization for a given reference frequency offset. Fig A3 shows $T_{\Delta f}$, ω_n and bits slipped during frequency acquisition versus ξ when the loop parameters are adjusted for a capture value of $\Delta f = 5 \times 10^{-8} \times f_o = .0772$ Hz for the integral plus proportional filter. From this figure, it may be observed that the bandwidth required by capture equations (A8) and (A14) is probably larger than actually required for acquisition since under this condition no bits will be slipped for $\xi < 1.5$.

An implementation problem for an automatic two-bandwidth approach is to devise a mechanism which determines when to switch from tracking loop parameters to acquisition parameters and vice-versa. Basically, this reduces to determining the state of the VCO error voltage, i.e., whether it is at steady state dc corresponding to a locked state or has an ac component corresponding to an acquisition state. This will be pursued further for the extended range linear detector.

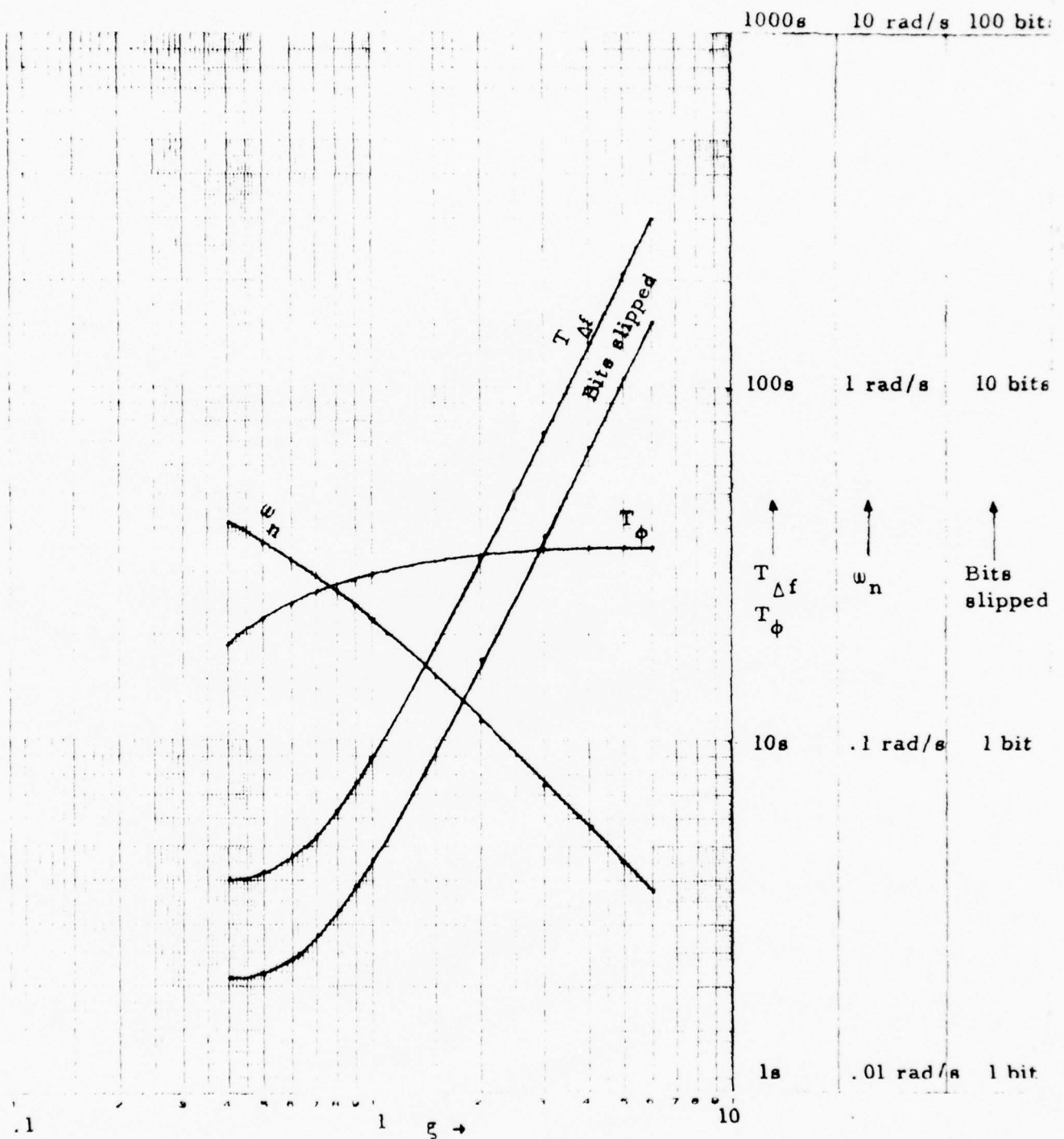


Fig. A3 $T_{\Delta f}$, T_{ϕ} , ω_n and bits slipped versus g with loop bandwidth adjusted to capture value for $\Delta f = 5 \times 10^{-8} \times f_0$ with integral plus proportional filter.

From Fig. A3 it is observed that for $\xi = 4$, $\omega_n \cong .057$ rad/s if the loop is to capture from an input frequency offset of .0772 Hz. In order to adequately filter out daily variations in link propagation delays in a long chain of timing nodes, a value for ω_n on the order of 5.6×10^{-5} rad/s and $\xi = 4$ is required. Thus, in order to be within the capture range with an offset of $5 \times 10^{-8} \times f_o$, ω_n must be increased by a factor of approximately 10^3 if the same damping ratio is maintained.

A2.7 Number of Bits for Non-Linear Model Pull in Strategies

A2.7.1 Natural Pull in

If we assume that the frequency difference remained at the initial difference during the entire transient, i.e., number of bits = NB = $\Delta f \cdot T_{\Delta f}$. Then our estimate would be too large because the local VCO frequency begins to be pulled toward the input reference signal as soon as the transient begins. The rate at which the frequency changes accelerates during the pull in period as is evidenced by the fact that $T_{\Delta f}$ is proportional to $(\Delta f)^2$. Conversely, if we assume that NB = $1/2 \Delta f \cdot T_{\Delta f}$ then our estimate would be too small. For example, if it takes $T_{\Delta f}$ seconds to achieve frequency synchronization when the initial frequency offset is Δf and pull in time is proportional to $(\Delta f)^2$ then the time required to pull in from $1/2 \Delta f$ is $1/4 T_{\Delta f}$. Thus the time required to go from Δf to $1/2 \Delta f$ is $3/4 T_{\Delta f}$. We may then write

$$T_{\Delta f} - t = \Omega (\Delta f(t))^2 \quad (A21)$$

where Ω is a constant of proportionality. Then

$$\Delta f(t) = \sqrt{\frac{T_{\Delta f} - t}{\Omega}} \quad (A22)$$

$$NB = \int_0^{T_{\Delta f}} \Delta f(t) dt = \int_0^{T_{\Delta f}} \sqrt{\frac{T_{\Delta f} - t}{\Omega}} dt$$

making a change of variable $y = T_{\Delta f} - t$, $-dy = dt$

$$NB = \int_0^{T_{\Delta f}} \frac{y^{1/2}}{\sqrt{\Omega}} dy = \frac{\frac{2}{3} y^{3/2}}{\sqrt{\Omega}} \bigg|_0^{T_{\Delta f}} = \frac{2}{3} \frac{T_{\Delta f}^{3/2}}{\sqrt{\Omega}}$$

$$= \frac{2}{3} T_{\Delta f} \cdot \Delta f \quad (A23)$$

A2.7.2 Sweep Assisted

If a sweep voltage is applied that results in a frequency change rate that is as high as the PLL can lock to as the phase detector output signal frequency passes through zero, then we may assume that the average frequency of the error signal over the acquisition period is $\frac{1}{2} \Delta f$. In this case

$$NB = \frac{1}{2} \Delta f \cdot T_{\Delta f} \quad (A24)$$

A3 Linear Model With Extended Range Phase Detector

A3.1 Development of the Model and Its Solution

A linear model for the PLL may be obtained by using an extended range phase detector such as buffer fill or an up-down counter provided the buffer or counter is chosen large enough to hold the largest transient. This will be assumed for the following analysis. Under this assumption, the objective

is to determine the time required to obtain synchronization and the amount of buffering required when a step difference in frequency Δf is applied at the input.

A3.1.1 Phase Error Equation

Using the second order loop shown in Fig A4 with a proportional plus integral filter we may obtain

$$\begin{aligned}\frac{B_f(s)}{F_i(s)} &= \frac{1}{s + K_B K_V H(s)} = \frac{1}{s + K_T \frac{1 + \tau_1 s}{s}} \\ &= \frac{s}{s^2 + K_T \tau_1 s + K_T}\end{aligned}\tag{A25}$$

where $K_T = K_B K_V$ and τ_1 is the time constant of the filter.

Thus,

$$B_f(s) = \frac{s F_i(s)}{s^2 + 2 \zeta \omega_n s + \omega_n^2}\tag{A26}$$

where $\omega_n = \sqrt{K_T}$ and $\zeta = (\tau_1 \sqrt{K_T})/2$

Now letting $F_i(s)$ correspond to a step function of magnitude Δf starting at time $t=0$ we obtain

$$B_f(s) = \frac{\Delta f}{s^2 + 2 \zeta \omega_n s + \omega_n^2}\tag{A27}$$

The poles of this function are

$$s = -\zeta \omega_n \pm \omega_n \sqrt{\zeta^2 - 1}$$

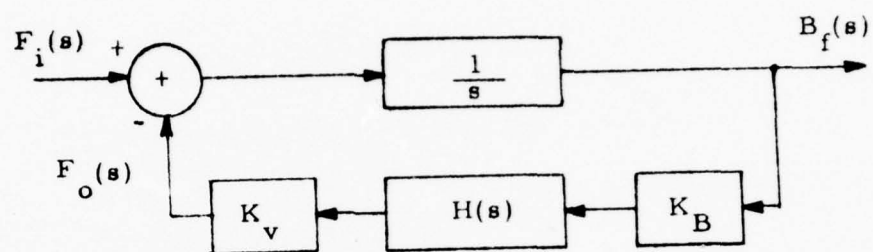


Fig. A4 PLL With Extended Range Linear Phase Detector

The following is noted

- (1) $\xi > 1$, both poles are negative and real.
- (2) $\xi = 1$, the poles are equal, negative, and real ($s = -\omega_n$).
- (3) $0 < \xi < 1$, the poles are complex conjugates with negative real parts ($s = -\xi \omega_n \pm j \omega_n \sqrt{1 - \xi^2}$).
- (4) $\xi = 0$, the poles are imaginary and complex conjugates
- (5) $\xi < 0$, the poles are in the right half of the s plane.

Cases (4) and (5) are oscillatory or unstable and will not be considered further.

For case (1) the solution is

$$b_f(t) = \frac{\Delta f}{b-a} (e^{-at} - e^{-bt}) \quad (\text{A28})$$

$$\text{Where } a = \omega_n (\xi + \sqrt{\xi^2 - 1}) , \quad b = \omega_n (\xi - \sqrt{\xi^2 - 1})$$

For case (2) the solution is

$$b_f(t) = \Delta f t e^{-\omega_n t} \quad (\text{A29})$$

For case (3) the solution is

$$b_f(t) = \frac{\Delta f}{\omega_d} e^{-\xi \omega_n t} \sin \omega_d t \quad (\text{A30})$$

$$\text{where } \omega_d = \omega_n \sqrt{1 - \xi^2}$$

A3.1.2 Output Frequency Equation

From Fig A4

$$\frac{F_o(s)}{F_i(s)} = \frac{K_B K_V H(s)}{s + K_B K_V H(s)} \quad (A31)$$

For the integral plus proportional filter

$$\frac{F_o(s)}{F_i(s)} = \frac{K_T(1 + \tau_1 s)}{s^2 + K_T \tau_1 s + K_T} = \frac{K_T(1 + \tau_1 s)}{s^2 + 2 \xi \omega_n s + \omega_n^2} \quad (A32)$$

where K_T , τ_1 , ξ , and ω_n are the same as in (A25) and (A26). Letting $F_i(s)$ be a step of magnitude Δf at time $t=0$ we obtain

$$\begin{aligned} F_o(s) &= \frac{\Delta f K_T(1 + \tau_1 s)}{s(s^2 + 2 \xi \omega_n s + \omega_n^2)} \\ &= \frac{\Delta f \omega_n^2}{s(s^2 + 2 \xi \omega_n s + \omega_n^2)} + \frac{2 \Delta f \omega_n \xi}{s^2 + 2 \xi \omega_n s + \omega_n^2} \end{aligned} \quad (A33)$$

The corresponding time domain equations are as follows:

$$\xi > 1, \quad f_o(t) = \Delta f \left\{ 1 - \frac{1}{2\sqrt{\xi^2 - 1}} \left[(\xi + \sqrt{\xi^2 - 1}) e^{-(\xi + \sqrt{\xi^2 - 1}) \omega_n t} - (\xi - \sqrt{\xi^2 - 1}) e^{-(\xi - \sqrt{\xi^2 - 1}) \omega_n t} \right] \right\} \quad (A34)$$

$$\xi = 1, \quad f_o(t) = \Delta f \left[1 - e^{-\omega_n t} + \omega_n t e^{-\omega_n t} \right] \quad (A35)$$

$$0 < \xi < 1, \quad f_o(t) = \Delta f \left\{ 1 + \frac{1}{\sqrt{1 - \xi^2}} e^{-\xi \omega_n t} \left[2 \xi \sin \omega_d t - \sin(\omega_d t + \phi) \right] \right\}$$

$$\text{where } \omega_d = \omega_n \sqrt{1 - \xi^2} \quad \text{and} \quad \phi = \cos^{-1} \xi \quad (A36)$$

A3.2 Time of Peak Phase Error

In order to determine the time t_m corresponding to the maximum value of $b_f(t)$ we take the derivative of $b_f(t)$ and set equal to zero and solve for t_m . Thus we obtain:

$$\xi > 1, \quad t_m = \frac{1}{a-b} \ln\left(\frac{a}{b}\right) \quad (\text{A37})$$

where $a = \omega_n (\xi + \sqrt{\xi^2 - 1})$ and $b = \omega_n (\xi - \sqrt{\xi^2 - 1})$

$$\xi = 1, \quad t_m = \frac{1}{\omega_n} \quad (\text{A38})$$

$$0 < \xi < 1, \quad t_m = \frac{1}{\omega_d} \cos^{-1}(\xi) \quad (\text{A39})$$

where $\omega_d = \omega_n \sqrt{1 - \xi^2}$

A.3.3 Peak Phase Error

Substituting (A37), (A38) and (A39) into (A28), (A29) and (A30) respectively, we obtain peak phase errors:

$$\xi > 1 \quad b_f(t_m) = \frac{\Delta f}{b-a} \left[\left(\frac{a}{b}\right)^{\frac{a}{b-a}} - \left(\frac{a}{b}\right)^{\frac{b}{b-a}} \right] \quad (\text{A40})$$

where $a = \omega_n (\xi + \sqrt{\xi^2 - 1})$ and $b = \omega_n (\xi - \sqrt{\xi^2 - 1})$

$$\xi = 1 \quad b_f(t_m) = \frac{\Delta f}{e \omega_n} \quad (\text{A41})$$

$$0 < \xi < 1 \quad b_f(t_m) = \frac{\Delta f}{\omega_n} e^{-(\xi \cos^{-1} \xi) / \sqrt{1 - \xi^2}} \quad (\text{A42})$$

A3.4 Settling Time

The time to settle following a step change in input reference frequency may be conveniently defined as the time at which the transient has died to within some fractional part p of its peak value. In practical situations p is often chosen as .01. The desired relations are as follows:

$$\xi > 1, \quad e^{-at_s} - e^{-bt_s} \leq p \left[\left(\frac{a}{b} \right)^{\frac{a}{b-a}} - \left(\frac{a}{b} \right)^{\frac{b}{b-a}} \right] \quad (A43)$$

where $a = \omega_n(\xi + \sqrt{\xi^2 - 1})$ and $b = \omega_n(\xi - \sqrt{\xi^2 - 1})$

$$\xi = 1, \quad \omega_n t_s e^{-\omega_n t_s} \leq \frac{p}{e}, \quad t_s > \frac{1}{\omega_n} \quad (A44)$$

$$0 < \xi < 1, \quad e^{-\xi \omega_n t_s} \sin \omega_d t_s \leq p \sqrt{1 - \xi^2} e^{-(\xi \cos^{-1} \xi) / \sqrt{1 - \xi^2}} \quad (A45)$$

For $\xi \geq 1$, the equations are not readily solved by algebraic methods. However, simple plots of the left hand sides provide answers for particular cases. For $\xi > 1.8$ the ratio of the two poles is > 10 . Hence, in this case the left side of (A43) can be approximated by the dominant pole term, e. g. the term involving the smaller of a and b . For $0 < \xi < 1$, the sinusoidal factor on the left side of (A45) can be ignored (approximated by its peak value), thereby approximating the response by the exponentially damped envelope.

A3.5 Time Of Peak Output Frequency

Differentiating equations (A34) - (A36) and setting equal to zero and solving for t we find that the time of peak frequency, t_{pf} , is given as follows:

$$\xi > 1, \quad t_{pf} = \frac{1}{\omega_n \sqrt{\xi^2 - 1}} \operatorname{Ln} \left(\frac{\xi + \sqrt{\xi^2 - 1}}{\xi - \sqrt{\xi^2 - 1}} \right) \quad (\text{A46})$$

$$\xi = 1, \quad t_{pf} = \frac{2}{\omega_n} \quad (\text{A47})$$

$$0 < \xi < 1, \quad t_{pf} = \frac{1}{\omega_n \sqrt{1 - \xi^2}} \tan^{-1} \left(\frac{2 \xi \sqrt{1 - \xi^2}}{2 \xi^2 - 1} \right) \quad (\text{A48})$$

A3.6 Peak Output Frequency

Substituting (A46) - (A48) into (A34) - (A36) respectively, we find that peak output frequency (f_{op}) is as follows:

$$\xi > 1, \quad f_{op} = \Delta f \left\{ 1 + \frac{\omega_n}{b-a} \left[a \left(\frac{a}{b} \right)^{\frac{2a\omega_n}{b-a}} - b \left(\frac{a}{b} \right)^{\frac{2b\omega_n}{b-a}} \right] \right\} \quad (\text{A49})$$

where $a = \omega_n (\xi + \sqrt{\xi^2 - 1})$ and $b = \omega_n (\xi - \sqrt{\xi^2 - 1})$

$$\xi = 1, \quad f_{op} = \Delta f (1 + e^{-2}) \cong 1.135335 \Delta f \quad (\text{A50})$$

$$0 < \xi < 1, \quad f_{op} = \Delta f \left\{ 1 + \frac{1}{\sqrt{1 - \xi^2}} e^{-\frac{\xi \beta}{\sqrt{1 - \xi^2}}} \left[\xi \sin \beta - \sqrt{1 - \xi^2} \cos \beta \right] \right\} \quad (\text{A51})$$

where $\beta = \tan^{-1} \frac{2 \xi \sqrt{1 - \xi^2}}{2 \xi^2 - 1}$

A3.7 Example of Settling Time (Linear Model)

Let $\xi = 4$, $\omega_n = 5.6 \times 10^{-5}$, $\Delta f = 5 \times 10^{-8} \times f_o = .0772 \text{ Hz}$, and $p = .01$.

From (A37) $t_m = \frac{1}{a-b} \operatorname{Ln} \left(\frac{a}{b} \right)$

$$a = 5.6 \times 10^{-5} (4 + \sqrt{15}) = 4.4088 \times 10^{-4}$$

$$b = 5.6 \times 10^{-5} (4 - \sqrt{15}) = 7.1129 \times 10^{-6}$$

$$b-a = -4.3377 \times 10^{-4}, \quad a/b = 61.98$$

$$\text{then } t_m = 9514 \text{ sec}$$

From (A40) peak phase error is

$$b_f(f_m) = 163.6 \text{ bits}$$

Using (A43) and approximating the left hand side by the dominant pole,
 $t_s \geq 659279 \text{ seconds.}$

From this example, it is evident that the system will not acquire synchronization very quickly with the tracking loop parameters designed to filter out daily path delay variations. Thus, an investigation of a two bandwidth scheme for the linear model will be made next.

A3.8 Two Bandwidth Linear Model

A3.8.1 Motivation

In order to reduce buffer size using the linear model, two bandwidths may be provided, one for normal tracking and one for fast acquisition. In the normal tracking mode each node should track the long term average of the incoming frequency, but filter out normal link perturbations and clock jitters. It is also desirable to provide the capability of flywheeling through short link outages without slipping bits. The purpose of the fast acquisition mode is to quickly acquire synchronization following large abrupt changes in input frequency such as during initial system startup or following failures in which a new reference must be obtained. Once the phase lock loop parameters have been chosen to accomplish the above system dynamics, the task then becomes one of determining criteria for switching from the tracking mode to the fast acquisition mode and vice-versa.

A3.8.2 A Simple Mode Switching Technique

A simple technique for accomplishing the mode switching task is to switch from normal tracking to fast acquisition as soon as phase error exceeds some threshold amount ϕ_{th} which is above that which can be expected for normal link perturbations and clock jitter and drifts, and to switch from fast acquisition mode to normal tracking mode after having been in fast acquisition mode for an interval of time T_{fa} sufficient to reduce frequency offset to within a specified tolerance. T_{fa} is determined by the acquisition mode loop time constants and by the amplitude of the initial frequency and phase error. The following analysis is made to determine suitable values of ϕ_{th} and T_{fa} .

Study line of sight and cable link perturbations and clock drifts indicate that the combined equivalent normal maximum frequency offsets under normal tracking conditions should be less than $5 \times 10^{-10} \times f$. Scaling from example A3.7, this corresponds to a peak buffer fill of $1.09 \mu s$. For large short term variations such as with tropo, maximum propagation time variation may be as much as 3.3 ns/mile over a 1 minute interval. For such a short time the loop will not respond, so a phase error will result. A 300-mile link would then give a total time variation of $0.99 \mu s$, which would result in $0.99 \times 1.544 = 1.53 \text{ bits}$. A 400-mile link would result in $1.32 \mu s$. Expected maximum tropo link distances are 300 miles. Normal satellite variation should result in an approximately $8.42 \mu s$ daily variation clock, but it will be assumed that techniques are available for removing all but about 1 percent of this variation. Thus, timing network nodes connected to satellite links can expect to see a daily variation of approximately $\pm 8.42 \mu s$ variation 1.544 Mb/s rate when referenced to the input frequency. If it is assumed that this accumulation of phase error occurs at a constant rate over a 12-hour period, then the equivalent frequency offset is $1.95 \text{ parts in } 10^{10}$.

This implies an instability of $s = 3.009 \times 10^{-4} / 1.544 \times 10^6 = 1.9488 \times 10^{-10}$.

Thus, the peak phase error would be less than .673 bits. If the accumulation is over a 4 hour period rather than 12, then the equivalent instability is 5.85×10^{-10} which results in a peak phase error of 1.98 bits.

A3.8.3 Buffer Fill In Fast Response Mode With Non-Zero Initial Phase Error

When switching from the normal tracking mode to the fast acquisition mode, after a phase error b_0 has been built up following a step change in frequency Δf , the response is not the same as it would be with zero phase error. In this case

$$B_f(s) = \frac{s(F_1(s) - b_0)}{s^2 + 2\zeta\omega_n s + \omega_n^2} = \frac{\Delta f - s b_0}{s^2 + 2\zeta\omega_n s + \omega_n^2} \quad (A52)$$

and

$$b_f(t) = \frac{\Delta f}{\omega_d} e^{-\zeta\omega_n t} \sin \omega_d t - \frac{b_0}{(a-b)} (a e^{-at} - b e^{-bt}) \quad (A53)$$

where $\omega_d = \omega_n \sqrt{1-\zeta^2}$

$$a = (\zeta + \sqrt{\zeta^2 - 1})\omega_n$$

and $b = (\zeta - \sqrt{\zeta^2 - 1})\omega_n$

For $\zeta = 1/\sqrt{2}$ this becomes

$$b_f(t) = \frac{\Delta f}{\omega_d} e^{-\zeta\omega_n t} \sin \omega_d t + b_0 \left[e^{-\zeta\omega_n t} (\sin \omega_n \zeta t - \cos \omega_n \zeta t) \right] \quad (A54)$$

From this equation it should be observed that the initial buffer offset is exponentially damped with time constant $1/\xi \omega_n$ which is the same as that for the initial frequency offset.

A3.8.4 Frequency In Fast Response Mode With Non-Zero Initial Phase Error

In the case of non zero initial phase error upon switching to the fast acquisition mode, we have

$$F_o(s) = (F_i(s) - b_o) \times \frac{2\xi\omega_n s + \omega_n^2}{s^2 + 2\xi\omega_n s + \omega_n^2} \quad (A55)$$

Letting $f_i(t)$ be a step of amplitude Δf beginning at $t = 0$

$$F_o(s) = \left(\frac{\Delta f}{s} - b_o \right) \times \frac{2\xi\omega_n s + \omega_n^2}{s^2 + 2\xi\omega_n s + \omega_n^2} \quad (A56)$$

For $\xi < 1$ and $\beta = \sqrt{1 - \xi^2}$

$$\begin{aligned} f(t) = & \frac{2\xi\omega_n \Delta f}{\omega_d} e^{-\xi\omega_n t} \sin \omega_d t + \Delta f \omega_n^2 \left[\frac{1}{\omega_n^2} - \frac{1}{\omega_n \omega_d} e^{-\xi\omega_n t} \sin(\omega_d t + \phi) \right] \\ & - 2\xi\omega_n b_o e^{-\xi\omega_n t} \left[\cos \beta\omega_n t - \frac{\xi}{\beta} \sin \beta\omega_n t \right] \\ & - \frac{\omega_n^2 b_o}{\omega_d} e^{-\xi\omega_n t} \sin \omega_d t \end{aligned} \quad (A57)$$

where $\omega_d = \sqrt{1 - \xi^2} \omega_n$,

In case $\xi = 1/\sqrt{2}$ this reduces to

$$f(t) = \Delta f \left\{ 1 + e^{-\xi \omega_n t} \left[\sin \xi \omega_n t - \cos \xi \omega_n t \right] \right\} \\ - 2 \xi \omega_n b_o e^{-\xi \omega_n t} \cos \xi \omega_n t \quad (A58)$$

From (A58) if Δf is equal to $10^{-8} \times f_o = .01544$, $\xi = .707$, and $\omega_n = .014$, then the transient due to the initial frequency offset has an initial amplitude of 10^{-8} while that due to the initial phase offset has initial amplitude of $.02 b_o$.

A3.8.5 Strategy for Changing Loop Parameters

Each node will normally be in its tracking mode, but if phase error exceeds ϕ_{th} then the node shall automatically switch to its fast acquisition mode and remain so for a period of time T_{fa} sufficient to reduce the frequency error to less than or equal to 1% of the initial frequency offset. After this elapsed period of time, T_{fa} the node will automatically switch back to its normal tracking mode.

As already observed, the phase error in the normal tracking mode due to normal link perturbations or oscillator drifts should be no greater than $1.3 \mu s$. Thus, a threshold of $\phi_{th} = 2 \mu s$ is adequate for switching from normal tracking to fast acquisition mode. In this case, the initial amplitude of the transient due to the initial phase offset in equation (A58) may be obtained from (A58) as follows:

$$2 \xi \omega_n b_o e^{-\xi \omega_n T_{fa}} \leq .01 \times \Delta f$$

$$\text{or } T_{fa} \geq \frac{\text{Ln}(2 \xi \omega_n \cdot b_o / .01 \times \Delta f)}{\xi \omega_n} \quad (\text{A59})$$

with $\xi = .707$, $\omega_n = .014$ and $\phi_{th} = b_o = 3$

$$T_{fa} \geq \frac{\text{Ln}(384.72)}{.0099} = 601.26 \text{ sec.} \quad (\text{A60})$$

A3.9 Comparison Between Linear and Non Linear Models

In order to get a comparison between the acquisition time of the linear model and that of the non linear sinusoidal model, we must choose the same parameters as are shown in Fig. A3, i.e., we must choose loop parameters to coincide with those required at the capture point of the non linear model. Although, as discussed in A3.8.5, the linear model would actually start its acquisition process with a non zero initial phase error, a better comparison between the two can be obtained if it is assumed that the initial phase error is zero. In this comparison, the settling time for the linear model will be taken to be that value of time for which the phase error has settled to less than .01 times the peak error. The results for the linear model are shown in Fig A5. From this figure we note that the fastest settling time occurs at $\xi = .707$ but that there is little difference in this parameter for ξ between .4 and 1. Also, the peak phase error never exceeds about 60° . This corresponds to no cycles slipped in the non linear one cycle phase detector case. On the other hand, from Fig A3 the non linear model slips cycles for $\xi > 1.5$ with about 15 cycles being slipped at the $\xi = 6$ point. The ratio of the settling time of the linear model to the frequency acquisition time for the non linear model varies from approximately

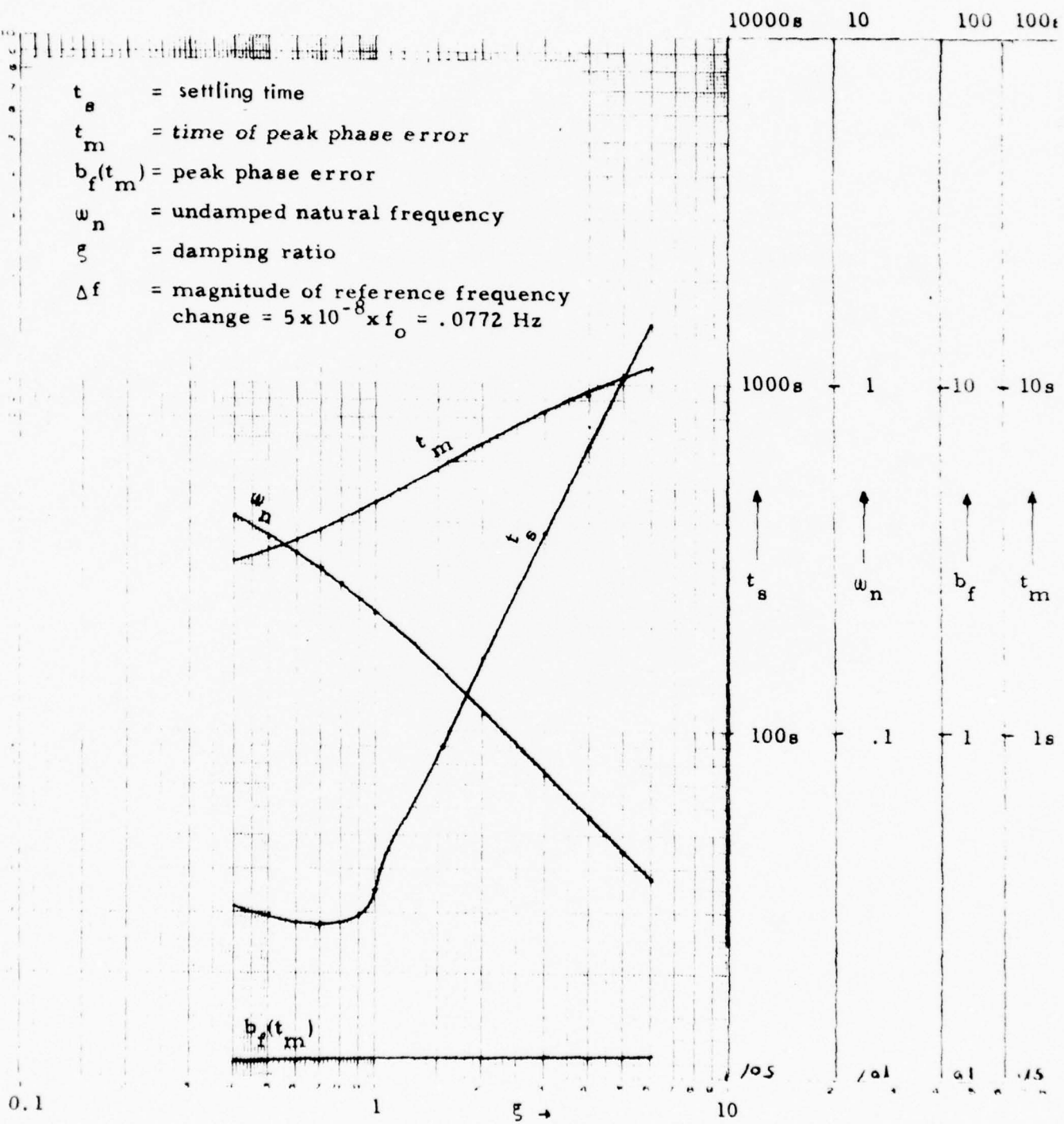


Fig. A5 Response of Δf of second order PLL using integral plus proportional filter with extended range linear phase detector.
A-30

8 at $\xi = .4$ to 5 at $\xi = 6$. However, settling time includes part of the corresponding phase acquisition process of the non linear model. If phase acquisition time of $T_\phi = 4/B_L$ is added to $T_{\Delta f}$ the ratio $t_s / (T_{\Delta f} + T_\phi)$ becomes about 1.4 at $\xi = .4$ and 5 at $\xi = 6$. It has been suggested that the point in time, t_m , at which the peak phase error occurs in the linear model is more closely analogous to frequency acquisition time, $T_{\Delta f}$, of the non linear model than is settling time, t_s . The reason for this is that the point of peak phase error is the time at which the frequency of the VCO is first equal to the reference frequency following the step change in reference. This is easily shown by substituting equations (A37), (A38), and (A39) into (A34), (A35), and (A36) respectively. The values of t_m are shown plotted in Fig. A5. A normalized plot of output frequency versus $\omega_n t$ is shown in Fig. A6. From the curves plotted in this figure we see that the above argument is approximately correct for large ξ but less correct for small ξ . The output frequency curves rise rather rapidly toward the new reference frequency line, cross the line, and then settle at a much slower rate to the new frequency. For $\xi \geq 1$ the output frequency curve crosses the reference line, peaks above the line and then settles asymptotically to the reference. For $0 < \xi < 1$, the peak occurs between the first and second crossing but crosses repeatedly thereafter with exponential damping. From these curves we conclude that a better measure of frequency acquisition time for the linear model is that time, t_a , required to bring the output frequency to within some small fraction λ of the reference change Δf . If λ is large for all ξ under consideration, then the rise time constants determine t_a . If λ is small for all ξ under consideration, then the fall time constants determine t_a . However, if λ is small for some values of ξ under consideration but large for others, then a mixture of rise and fall time constants determine t_a over the range of ξ 's. For example, if $\lambda = .01$ then for the (ω_n, ξ) pairs required at the capture point of the non linear one cycle phase detector with $\Delta f = 5 \times 10^{-8} \times f_0 = .0772$ Hz, the following results are obtained:

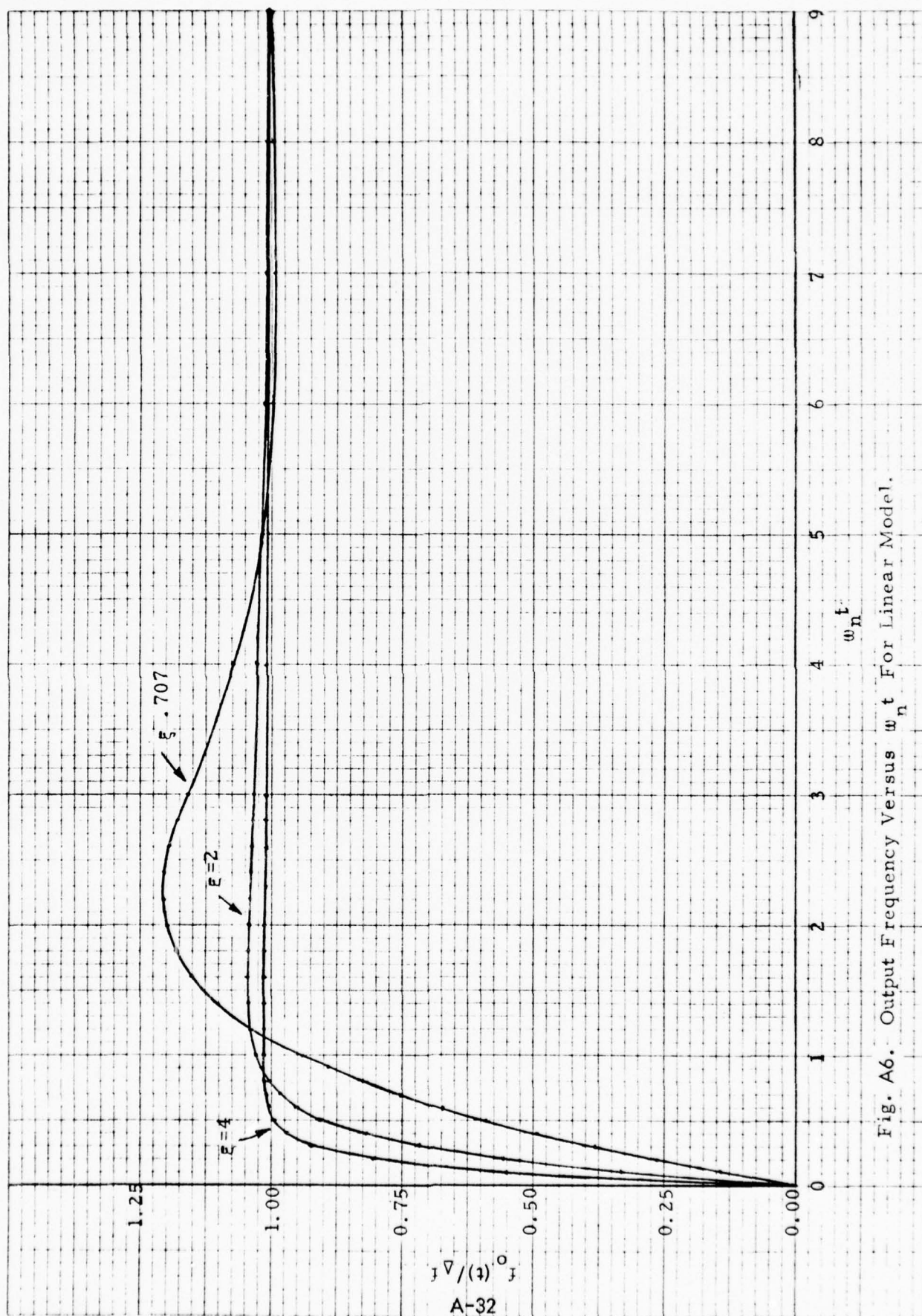


Fig. A6. Output Frequency Versus $w_n t$ For Linear Model.

<u>ξ</u>	<u>ω_n</u>	<u>$\omega_n t_a$</u>	<u>t_a</u> (seconds)
.4	.415	11	26.51
.707	.286	5.5	19.23
1	.220	6.25	28.41
2	.113	7.5	66.37
3	.075	6.5	86.67
5	.045	.45	10.0

These results show that for $\xi = 5$ the peak overshoot and hence, the entire fall time is within the λ tolerance chosen. However, this does not indicate any fault in the choice of λ . Figure A7 shows a plot of output frequency with an initial phase offset. Figure A8 and Figure A9 show output phase with initial frequency offset and phase error respectively for the linear model.

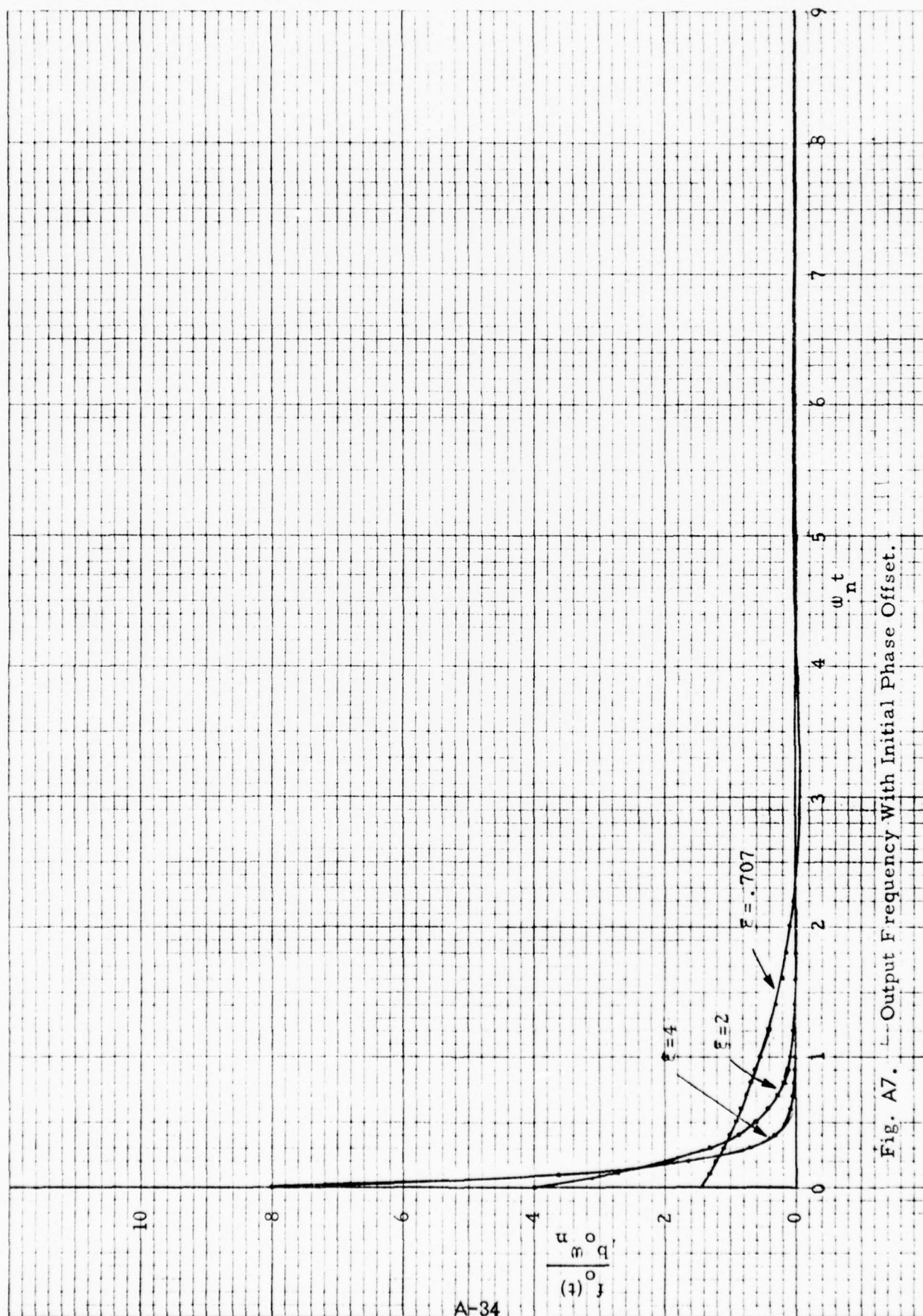


Fig. A7. Output Frequency With Initial Phase Offset.



Fig. A8. Output Phase With Initial Frequency Offset

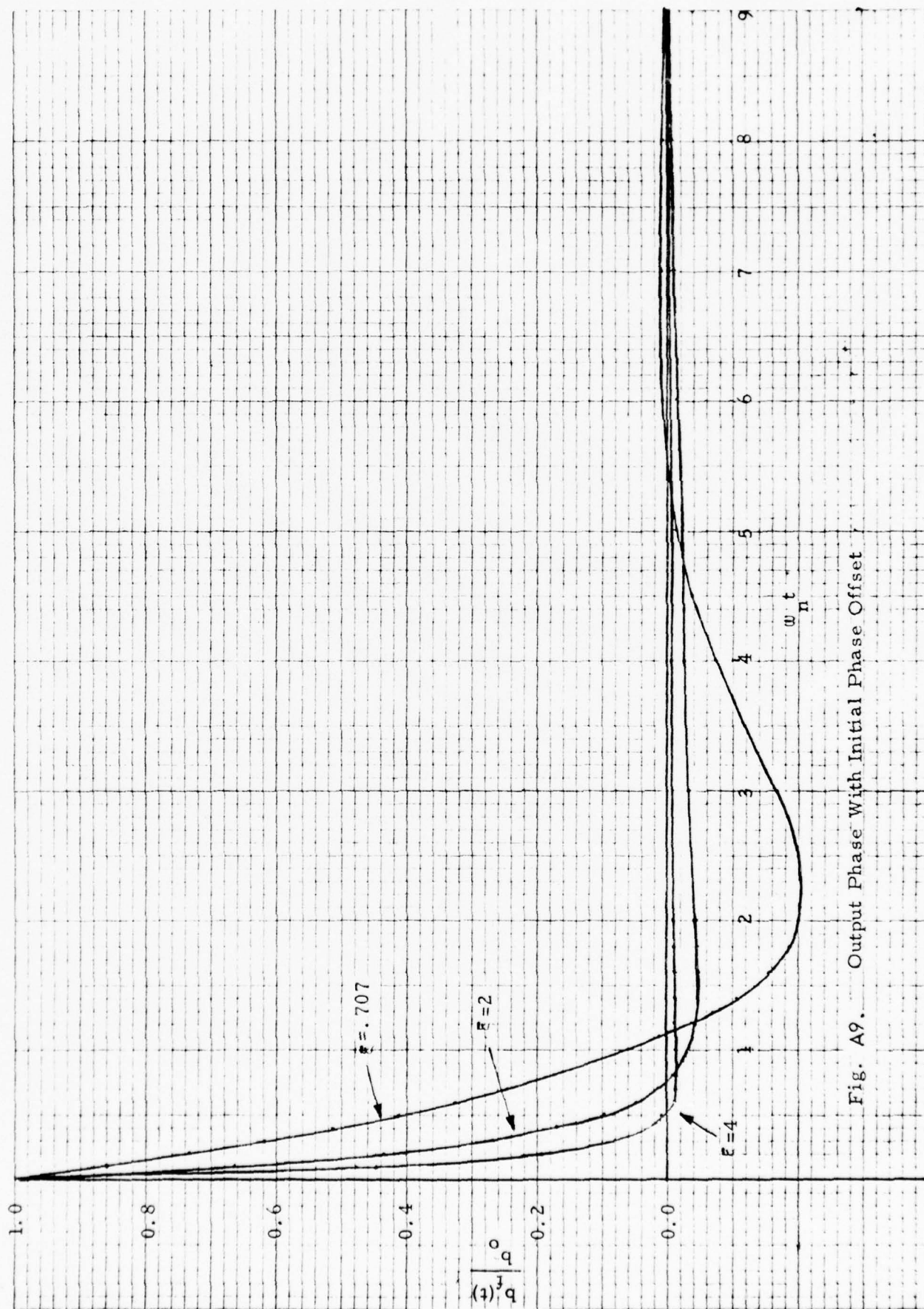


Fig. A9. Output Phase With Initial Phase Offset

APPENDIX B
SURVIVABILITY ANALYSIS

APPENDIX B

SURVIVABILITY ANALYSIS

The details of a survivability analysis discussed in Paragraph 8.1 are presented in this section. The purposes of the analysis were twofold. First, the advantages obtained by using a disciplined timing technique over the independent clock approach is shown. Of course, the independent clock approach has an average time between slips of

$$T_s = B/\delta \quad . \quad (B.1)$$

Secondly, the performance improvement of using an adaptive timing distribution network over the fixed approach is demonstrated.

The performance of several approaches for implementing a disciplined timing distribution system will be evaluated. The parameter B/δ is considered to be one of the fundamental design parameters for each of these approaches. In this case B is the buffer size, and the clock offset, δ , refers to the offset between any two nodal clocks that will occur if they lose their references. Normally, all nodes will be phase-locked to a common reference. Slips will not occur in this case. The only time that slips will occur is when one or both of the nodes loses its reference and has to run "asynchronously." A good disciplined approach will attempt to minimize the product of the amount of time any node must run asynchronously and the offset, δ , that will occur during this time.

The first approach to be considered is the use of a fixed timing distribution network. That is, even though each node may have several links over which it is communicating, it will only have one link from which it may derive a reference. If that reference is lost, the node must run asynchronously. This approach will have the poorest performance in terms of minimizing the amount of time each node must run asynchronously. The performance will be dependent on topology of the network. Because of this, completely general results cannot be obtained. However, by assuming a specific topology that can be analyzed, one can obtain results that indicated the important characteristics of this approach. The topology that will be used is the "starred polygon" with connectivity 4. This topology for an 8 node network is shown in Figure B.1. Node 1 is the master, and timing is distributed via the routes

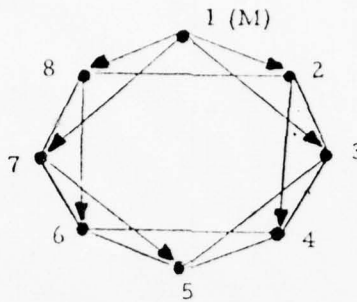


Figure B.1. Starred Polygon With Connectivity of 4 and 8 Nodes

indicated by the arrows. Note that there are four independent timing chains that distribute timing (1-2-4; 1-3; 1-7-5; 1-8-6).

For convenience in analysis, we will assume that the number of nodes is a multiple of 4, i.e., $m = 4k$. We will first calculate the average fraction of communicating node pairs that are communicating asynchronously. Note from the manner in which timing is distributed that each timing chain contains only odd-numbered nodes or even-numbered nodes (other than the master). Thus, Node i is always synchronous with Node $i-2$ or Node $i+2$ if those links are operational since they are in the same timing chain. However, Node i can communicate asynchronously with Node $i-1$ if the link from i to $i-1$ is operational and there is an outage in the timing chains from Node 1 to Node i or from Node 1 to Node $i-1$ (assume $i \leq 2k+1$). There are a total of $i-1$ links on these two chains. Then the probability that Nodes i and $i-1$ are communicating asynchronously as a function of the probability of link outage, p_e , is

$$\text{Pr}(i \text{ to } i-1 \text{ asynchronous}) = (1-p_e) \left[1 - (1-p_e)^{i-1} \right]. \quad (\text{B.2})$$

There are $2m$ links and of these, an average of $2m (1-p_e)$ is operational.

Since the network is symmetrical, the average fraction of communicating nodes pairs that are asynchronous may be calculated by summing twice the contributions over half the network ($i=3, 2k+1$) and adding in the contributions from the links connecting the two halves (Link 2 to $4k$ and Link $2k$ to $2k+2$). This fraction

$$\Delta = \frac{1}{8kp} \left[p(1-p)^{2k} - p^3 + 2p^2 + p \right]$$

is then given by

$$\begin{aligned}
 F_{ac} &= \frac{(1-p)}{2m(1-p)} \left[\sum_{i=3}^{2k+1} 2 \left[1 - (1-p)^{i-1} \right] \right. \\
 &\quad \left. + \left[1 - (1-p)^2 \right] + \left[1 - (1-p)^{2k} \right] \right] \\
 &= \frac{1}{8kp} \left[2(1-p)^{2k+1} - p(1-p)^{2k} - p^3 \right. \\
 &\quad \left. + (4k+3)p - 2 \right] . \tag{B.3}
 \end{aligned}$$

The example just analyzed had only one reference per node with no alternate references available. We can improve the performance significantly by using alternate references. The simplest case is to have one fixed alternate reference per node. Thus, if the link supplying the primary reference fails, then the timing subsystem will use the alternate reference. If both of these references fail, then the nodal clock must run asynchronously. Note that this timing distribution network cannot adaptively reorganize to achieve the optimum configuration. The "starred polygon topology" will again be used in the analysis.

The network topology shown in Figure B.1 is assumed. The primary reference for each node is shown in this figure, i.e., for right half of the network Node i obtains its primary reference from Node $i-2$. We will assume that Node i obtains its alternate reference from Node $i-1$ in the right half of the network and from Node $i+1$ in the left half of the network.

Again since the network is symmetrical we will treat just the right half. When Nodes i and $i-2$ are communicating it is always synchronously since this link is the first choice of Node i with which to derive a reference. Node i communicates asynchronously with Node $i-1$ only when Node i is deriving its reference from Node $i-2$, (i.e., both Links i to $i-1$ and i to $i-2$ are operational) and Nodes $i-1$ and $i-2$ are asynchronous. Proceeding back toward the master we find that Nodes $i-1$ and $i-2$ are asynchronous if both Links $i-1$ to $i-3$ and $i-1$ to $i-2$ are down or if Link $i-1$ to $i-3$ is operational and Nodes $i-2$ and $i-3$ are asynchronous,

etc. Then for large m (ignoring end effects) the probability that Nodes i and $i-1$ are communicating asynchronously is

$$\begin{aligned}
 P_i &= \text{Pr} (i \text{ to } i-1 \text{ asynchronous}) \\
 &= (1-p^2) \left[p^2 + (1-p) \left[p^2 + (1-p) \left[p^2 + \dots \right. \right. \right. \\
 &= p^2 (1-p)^2 \sum_{k=0}^{i-3} (1-p)^k \\
 &= p(1-p)^2 \left[1 - (1-p)^{i-2} \right]
 \end{aligned} \tag{B.4}$$

Then as before the fraction of nodes communicating asynchronously is obtained by summing over all links and is given by

$$\begin{aligned}
 F_{ac} &= \frac{2}{2m(1-p)} \sum_{i=3}^{2k+1} P_i \\
 &= \frac{(1-p)}{4k} \left[(2k-1)p - (1-p)^3 + (1-p)^{2k+2} \right] .
 \end{aligned} \tag{B.5}$$

If Equation (B.5) is expanded in powers of p we find that the leading term is $\left[(2k^2 + 3k - 2)/4k \right] p^2$. This is consistent with the approach of having two available references per node. Then two link outages can cause a node to lose its reference to the master and become asynchronous with respect to the rest of the network. This term gives the asymptotic behavior of F_{ac} for small p . In addition, for small p and large k , $F_{ac} \approx p^2/2$.

The fraction of communicating node pairs that are asynchronous is plotted in Figure B.2 as a function of p , the link outage probability for networks with 20 and 80 nodes ($m = 20$ and 80). As one would expect, the performance degrades as the number of nodes in the network increases because the connectivity of the network is fixed (equal to 4) and thus the length of the timing chains will grow giving a higher probability that any chain will be disrupted due to link failures. This effect is more pronounced in the case where no alternate reference is available. However, the worst-case values of F_{ac} are not too different for $m = 20$ and $m = 80$.

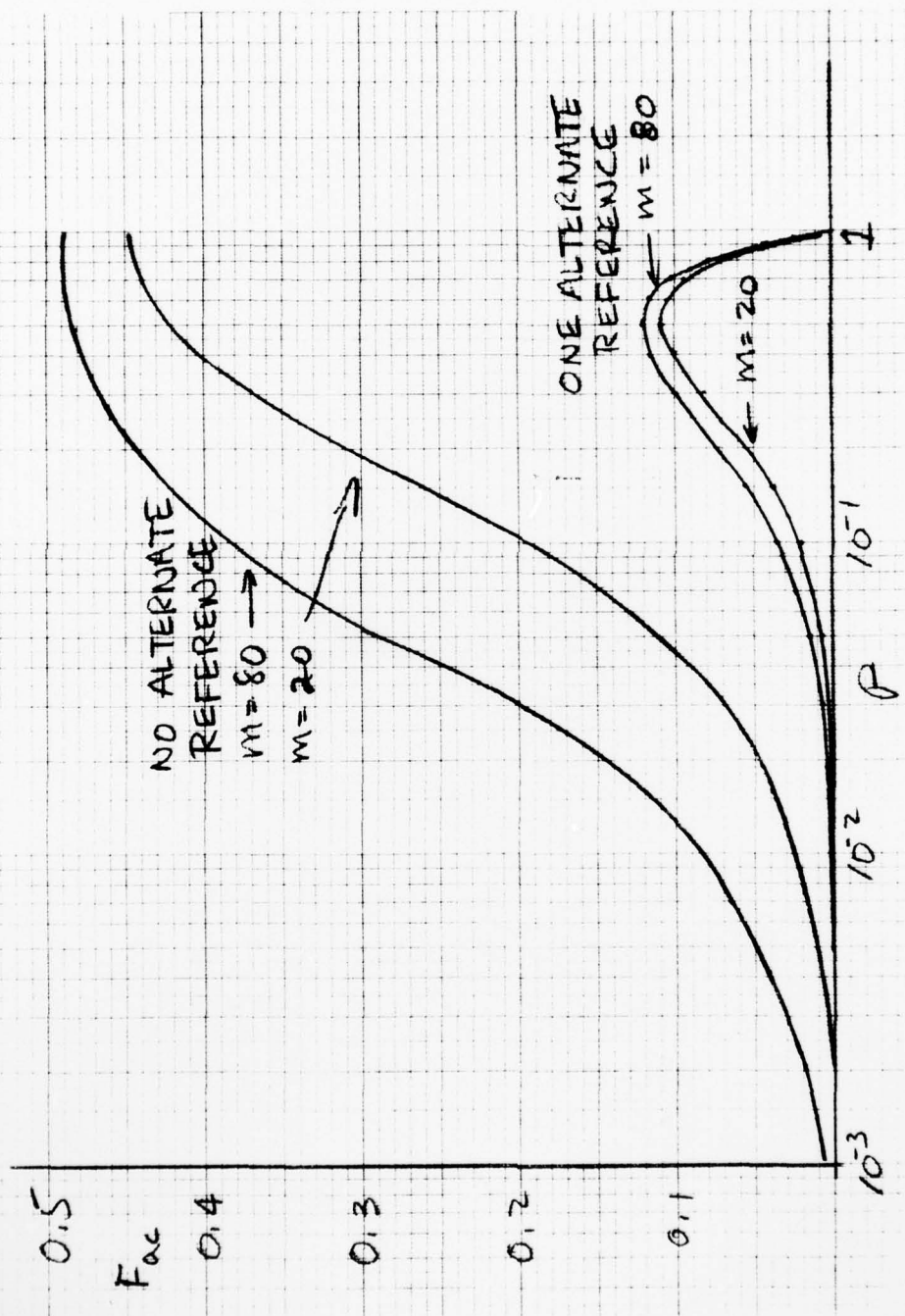


Figure B-2. Fraction of Communications Nodes that are Asynchronous as a Function of Probability of Link Outage

These results can be related to slip rate by observing that the only time a node experiences a slip is when it is communicating asynchronously with another node. In this case the time between slips is B/δ . Then the average time between slips at each node in the network may be estimated as

$$T_s = B/\delta F_{ac} \quad (B.6)$$

This quantity is plotted in Figure B.3 for $m = 20$. Note that the performance is better than the independent clock technique for the same value of B/δ at all values of p . We also note that if one alternate reference is used, the value of B/δ can be reduced to one-fifth that of the independent clock technique and still maintain better performance over all values of p .

Although these results indicate that some performance improvements may be obtained by using one or more fixed references in a master-slave manner, these improvements are not that great when the link outage probability is high because the timing distribution network is disrupted so frequently. This is the reason that master-slave systems have been frequently criticized because of poor survivability. However, one can make an additional improvement in a master-slave system by giving it the capability of adaptively reconfiguring the timing distribution network as link outages occur. This approach has the properties that:

1. All communicating nodes are synchronous in the steady state (after a sufficiently long period following the last failure).
2. The only time a nodal clock will act as a self-reference is while the timing distribution network is being reconfigured (which is a relatively short period of time).

This approach has a very high degree of survivability. The system can be designed so that no slips occur in the steady state. The only time slips can occur is during the transients associated with reconfiguring the network. Obviously, one of these transients occurs every time an outage occurs. In the following analysis the average time between slips will be calculated as a function of the rate at which link outages are occurring.

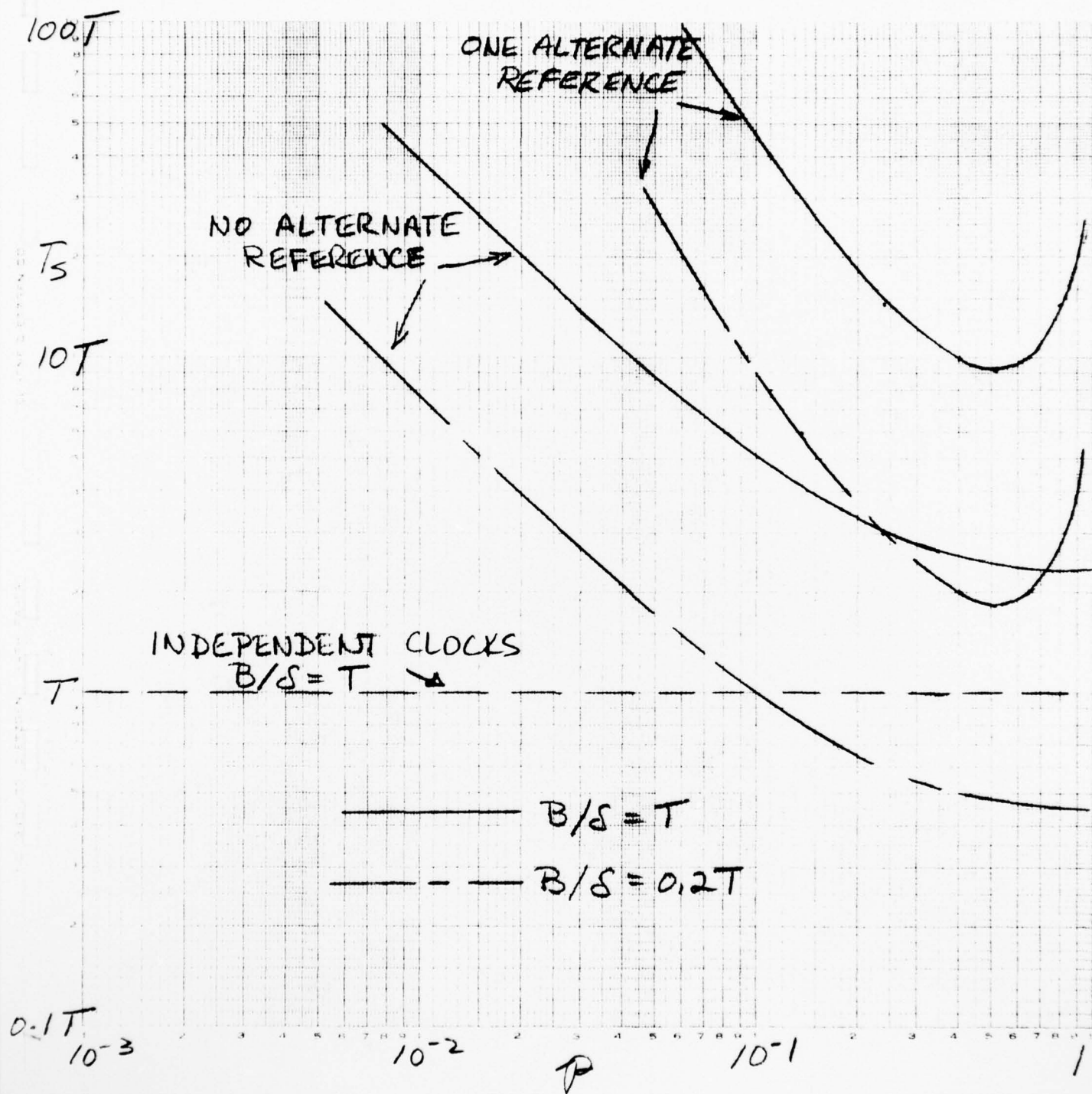


Figure B-3. Average Time Between Slips as a Function of the Probability of Link Outage for $m = 20$

Let τ represent the time required to reconfigure the timing network (a function of topology) and τ^* represent the time required to bring the nodal clocks back into lock after the timing network is reestablished. The average length of time a link is operational before a failure is denoted by $1/\lambda$ (second), and the average link outage time is denoted by $1/\mu$ (second). Then the probability of a link outage is

$$p = \frac{2}{\lambda + \mu} \quad (B.7)$$

Each node needs a reference, a significant fraction of the total time while the network is under stress if slips are to be avoided. If the nodal clock can act as a self-reference for at most T seconds ($T = B/\delta$) without a slip (or buffer overflow), then within T seconds of a failure, the nodal clock needs to acquire a reference for long enough (τ^* seconds) to allow resynchronization. Thus, after a failure a total of $x = \tau + \tau^*$ seconds with no failures is required to allow all nodes affected by the failure to select a new reference and resynchronize. The x failure-free seconds must occur within T seconds of the failure or slips will occur. It would be desirable to analytically determine the average time between slips as a function of T , x , λ , and μ , but this is a very unwieldy analytical problem. However, we can make some rough estimates that will illustrate the important trade-offs.

To simplify the analysis the link up times will be considered to be exponentially distributed, i.e.,

$$p(t) = \lambda e^{-\lambda t} \quad (B.8)$$

Then the probability that any specific link fails during the interval $(0, x)$ is

$$\begin{aligned} \text{Pr (link failure)} &= p_f \\ &= \int_0^x \lambda e^{-\lambda t} dt \\ &= 1 - e^{-\lambda x} \end{aligned} \quad (B.9)$$

The probability that there are no link failures in k operational link in $(0, x)$ is

$$\Pr(\text{no failures in } k \text{ links}) = (1-p_f)^k e^{-k \lambda x} . \quad (\text{B.10})$$

Finally, the probability that there are one or more failures in k links is

$$\Pr(\text{one or more failures}) = 1 - e^{-k \lambda x} . \quad (\text{B.11})$$

We will now proceed through a relatively crude analysis to demonstrate that with an adaptive timing distribution network approach very high failure rates must be experienced before there is any chance of slips. A specific network topology is not used. We will only make assumptions about the length of the timing chains. It will be assumed in this analysis that the timing chain between any node and its master has k links. Then Equation (B.11) gives the probability that a failure occurs in the timing chain during the interval $(0, x)$ when the node is attempting resynchronization. To obtain a conservative estimate of the probability of not achieving resynchronization, we divide the interval $(0, T)$ into T/x intervals each of length x . $\lfloor Lx \rfloor$ represents the integer part of (x) . Each of these $\lfloor T/x \rfloor$ intervals provides an opportunity to resynchronize in. Then the probability that resynchronization cannot be achieved is equal to the probability that there are link failures in each of these $\lfloor T/x \rfloor$ intervals, i.e.,

$$\begin{aligned} R_p(\text{no resync}) &= \left(1 - e^{-k \lambda x} \right)^{\lfloor T/x \rfloor} \\ &= P_{\text{nrs}} . \end{aligned} \quad (\text{B.12})$$

If resynchronization is not achieved within T seconds, a slip is assumed to occur. Then the nodal clock has another T seconds within which to resynchronize or a second slip will occur, etc. The average number of slips that occur before resynchronization is achieved is

$$\begin{aligned} N_s &= P_{\text{nrs}} + 2 P_{\text{nrs}}^2 + 3 P_{\text{nrs}}^3 + \dots \\ &= \frac{P_{\text{nrs}}}{(1-P_{\text{nrs}})^2} . \end{aligned} \quad (\text{B.13})$$

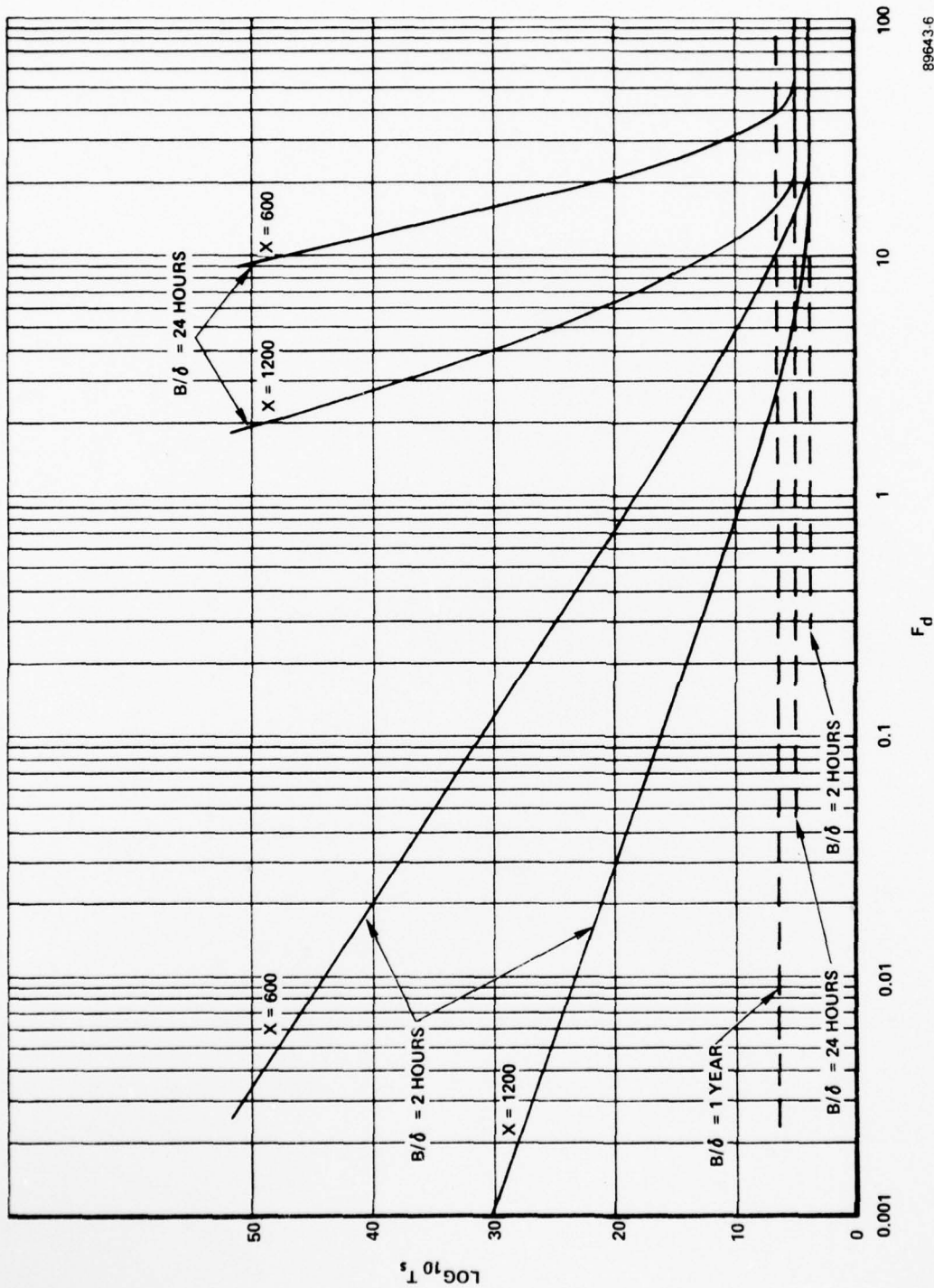
The average time between failures in a timing distribution chain with k links is

$$T_f = \frac{1}{k \lambda N_s} \quad , \quad (B.14)$$

where N_s is given by Equation (B.13).

The average time between slips as a function of the number of failures per day ($F_d = 86,400 \lambda$) per link is shown in Figure B.4 for several values of the parameters. The number of links between any node and its reference is set a $k=10$. Performance is improved by decreasing x , the failure-free interval required for resynchronization, and by increasing B/δ , the maximum interval over which a node may act as a self-reference without slips. The values used for the parameters x and B/δ in this figure are in the range that would probably be implemented. Note that the average time between slips is extremely long even for very high failure rates. One would probably expect at most just a few failures per day per link even under severe stress because a high level of stress would imply greater difficulty in making repairs. Certainly, there could be many failures caused by physical damage which could take days or longer to repair. Thus, the nature of most failures is not such that a link may fail, be repaired in a few minutes, then fail again a short time later followed by a quick repair, etc. Certainly this type of failure mechanism which could lead to a higher value of F_d poses the only threat to a master-slave timing subsystem with adaptive reorganization. The reason for this is that links which behave in this way cause the network to have to reorganize too often. Such behavior could be caused by a link which was frequently jammed for short periods of time. Thus, an enemy could try to disrupt the synchronization subsystem by frequently jamming a number of links. However, this tactic can be effectively countered by not allowing any node to use a link as a reference which has failed more than a few times a day.

These results indicate that the performance of master-slave timing subsystem with adaptive reorganization is greatly superior than that of an independent clock timing subsystem at virtually all stress levels even using much smaller values of B/δ . One might add that precisely the same comments could be made about the time reference distribution approach because it also uses the adaptive reorganization technique. This is the key to achieving a high level of performance under stress.



89643-6

Figure B-4. Average Time Between Slips as a Function of Number of Failures Per Day Per Link with $k = 10$

The mutual synchronization approach also achieves a high degree of survivability. In fact, one might even think that it should perform better under stress than the adaptive reorganization approach since, if a node has at least one operational link it has a reference. Thus, in a pure mutual sync network nodes never communicate asynchronously. In actuality, though, the master-slave system with adaptive reorganization can be designed so that even under severe stress, the probability that node pairs have to communicate asynchronously for long enough to result in slips (or buffer overflows) is extremely small. Thus, the mutual sync approach would offer no measurable advantage. In fact, it is likely that there will be more variation in nodal clock frequencies (or more error propagation) with the mutual sync approach under stress which is an undesirable characteristic.

APPENDIX C
IMPACT OF FUTURE TECHNOLOGY

APPENDIX C

IMPACT OF FUTURE TECHNOLOGY

An activity that was addressed during the course of this study was an assessment of future technology and its impact on the selection of the most appropriate timing subsystem. It was concluded that several areas of advancing technology would affect capabilities of timing subsystems but that no one timing technique would be more substantially affected than any other timing technique. It was therefore concluded that the impact of future technology would not influence the evaluations of either timing techniques or timing subsystems.

The particular areas investigated are discussed in the paragraphs below:

Clocks

In the area of stable clocks the specific point being investigated was the possibility of a price breakthrough that would essentially make the independent clocks approach more cost competitive with the disciplined approaches.

Clock possibilities range between quartz crystal at one extreme through rubidium gas cells, cesium beam devices to hydrogen masers. These clocks at this time provide daily stabilities ranging between 1 part in 10^{10} through 1 part in 10^{14} . The potential improvement in these devices is at least one order of magnitude better daily accuracy, but this is yet to come. There are several new concepts that could be available within the next 10 years. These include the techniques known as the dual crystal, the cesium gas cell, the passive hydrogen standard, a utility atomic standard and a superconducting cavity oscillator. These techniques have predicted daily stabilities that range between 1 part in 10^{11} to 1 part in 10^{16} . The general evolution in cost of all devices is toward cheaper implementations, but the cesium and hydrogen approaches are still predicted to be rather expensive. A change of, say, \$100,000 to \$50,000 for hydrogen devices is a dramatic reduction, but still leaves a lot to be desired from a single-item cost standpoint. The short-term stabilities of most of these devices are roughly around the same general order of 1 part in 10^{11} through 1 part 10^{13} even considering predictions to the future. No dramatic breakthrough is expected in this area.

AD-A041 004

HARRIS CORP MELBOURNE FLA ELECTRONIC SYSTEMS DIV
STUDY OF ALTERNATIVE TECHNIQUES FOR COMMUNICATION NETWORK TIMIN--ETC(U)
MAR 77

F/G 17/2
DCA100-76-R-0028
NL

UNCLASSIFIED

4 OF 4

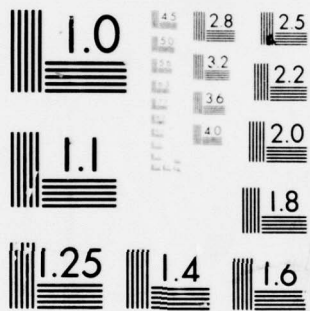
AD
A041 004



END

DATE
FILMED

7-77



MICROCOPY RESOLUTION TEST CHART
NATIONAL BUREAU OF STANDARDS-1963-A

Integrated Circuitry

Current technology in large-scale integrated circuitry is available in both standard off-the-shelf and custom computer-aided designed varieties in a number of technologies. In the high-speed area, these include the ECL,¹ IIL,² and CCD³ techniques. Lower speed technologies that are currently available are metalgate CMOS, PMOS and SOS CMOS. The trends are to provide possibly larger chips with greater density of individual elements and possibly an evolving multilevel interconnection capability that is producible. Effort will continue throughout industry to reduce the cost such that competition will drive the per gate cost down on logic-oriented LSI devices. Computer-aided design, which is used in many organizations throughout industry, serves to optimize the total process of design, fabrication, test, and implementation. Hybrid multilayer thin-film substrates are currently used for extremely small, reliable and cost-effective equipments. Evolution in this area would be towards a higher density of large-scale integrated circuits implemented on hybrids with a continuation of individual chip packaging techniques which foster increased yield and reliability of the end product.

The advances in this area while most pertinent to the Time Reference Distribution approach did not appear to significantly impact either the approach or its evaluation.

Microprocessors

There is a current proliferation of microprocessors available as off-the-shelf devices which already have basic programs developed. These are available in several technologies including Schottky-TTL, PMOS, NMOS and very shortly, SOS CMOS. The microprocessor will become a circuit element used throughout systems as one might use a transistor or resistor as time goes on. The evolution in technology will probably see the same size chips being used but the number of components per chip increasing dramatically. The IIL technology has the possibility of 10,000-50,000 components per chip depending upon fabrication advances. That is, is it not possible to economically build chips like this today but that limitation could go away with time? There would be some increase in speed but there is plenty of speed capability in the current repertoire of technology available for microprocessors. IIL should allow operation of 100 MHz or more. As far as microprocessor architecture development goes, more CPU functions will likely

¹Emitter Coupled Logic

²Integrated Injection Logic

³Charge Coupled Devices

be placed on an individual chip and functions such as multiply/divide will be integrated into the fundamental CPU chip. Many applications now tolerate a slow-speed microprocessor as long as a high-speed multiply/divide function is separately associated with said microprocessor. The fundamental problem of pin limitation will persist. A breakthrough of some sort is solely required in this area in that it is just not possible to physically make many more connections to an individual chip. Associated with the basic microprocessor are memories such as PROM, EAROM, RAM, and ROM devices where LSI application could derive a megabit storage capability. In the area of Charge-Coupled Devices (CCD), it has been estimated that in the not too distant future, as many as two million bits per chip of storage can be available. Some guesses are much higher. Bubble memories, although not heavily in use at this time, could afford an area of breakthroughs to occur.

The microprocessor also provides the opportunity to design complex self-healing or checking subsystems that could be integrated into a highly reliable timing subsystem or, indeed, any subsystem. Other possibilities are precise clock correction through extremely detailed and complex predictive techniques which could be implemented through complex hardware in a cheap and efficient manner using the microprocessor as the fundamental element.

While microprocessor technology has a direct impact on the implementation of the Time Reference Distribution approach current capabilities and costs already guarantee cost-effective implementation of timing subsystem functions. Future advances while interesting and applicable will be of extremely marginal importance.

Optical Circuitry

The optical circuits area is rampant with new developments and innovations. Fiber optic techniques are now being considered for application to long-haul communication systems, secure protected communication links, ground-to-balloon communication links, instrumentation for equipments in an EMP environment or other hardened requirement, TEMPEST design approaches for RED/BLACK applications and internal wiring interconnections which allow fail-safe cryptographic design and EMC acceptable designs. The advent of an optical switch or computer could dramatically change the timing needs associated with a nodal switch. The multiplex scheme in an optical environment could require dramatically different timing accuracies and organization. Optical storage media are currently available in terms of film and holographic devices.

The probability of transmitting significantly higher bit rates puts further emphasis on the need for accuracy in the timing subsystem. This point has been considered throughout the study.

APPENDIX D
REFERENCES AND BIBLIOGRAPHY

APPENDIX D

REFERENCES AND BIBLIOGRAPHY

1. "Final Report of Committee on Interoperability of DoD Communications," Sept. 1973.
2. NSIA, "DCA Briefing," 25 Sept. 1974, Washington, D.C.
3. MIL STD-188-() Series of Documents
4. DECEC, TR 3-74, Mar. 1974, "Digital Transmission System Design."
5. DCA Circular 370-() Series on AUTOVON and AUTODIN.
6. DCA Circular 330-175-1 Series of Standards.
7. "Introduction of TDM into the DCS," DCA, 1 Jan. 1969.
8. "Application of PCM, TDM, and Digital Transmission in the DCS," DCA/DCEO, 7 Jan. 1972.
9. DCAC 310-1 30-2, "Communications Requirements."
10. Proceedings of the fourth, fifth, and sixth annual NASA and DoD Precise Time and Time Interval (PTTI) Planning Meetings, Nov. 1972, Dec. 1973, and Dec. 1974.
11. "Base Communications Mission Analysis, Executive Summary and Highlights," Vols. 1A and 1B, AFSC/ESD, Apr. 1973.
12. DNA Defense Nuclear Agency EMP Handbook series.
13. Radiation Effects in Quartz Crystals, Part 1-A on Contract DASA 01-71-C-0092, DNA 3518T-1, Dec. 1974.
14. Army Specification SCCC-73017, May 1973, "System Specification for FKV Project, Phase I."
15. Army, Statement of Work, ELCP0144-00013, Mar. 1973, "Megabit Digital Tropo Subsystem."
16. Army, APPI, EL-75-001, Dec. 1974, "Digital Radio and Multiplex Assembly."

17. Army Specification (Draft), CCC-74047, Apr. 1975, "Specification for Multiplexer/Demultiplexer, TD-1192 () (P)/F."
18. Army Specification (Draft), CC-74048, Apr. 1975, "Specification for Multiplexer/Demultiplexer, TD-1193 ()/F."
19. Army Specification (Draft), CCC-74049, Apr. 1975, "Specification for Radio Set, AN/FRC-163 ()."
20. RADC, Statement of Work, "Broadband Digital Modem," PRC-4-2029, Dec. 1973.
21. RADC, Statement of Work, PR C-5-2422, Dec. 1974, "Wideband Digital Radio Terminal."
22. Specification - TRI-TAC No. TT-B1-1101-0001A, June 1974, "Performance Specification, Central Office, Communications, Automatic AN/TCC-39() (V)."
23. Specification - TRI-TAC No. TT-B1-2202-0013, June 1974, "Family of Digital Group Multiplex, Pulse Restorers, Cable Driver Modems, Cable Order Wire Units."
24. "Planning of Digital Systems," AT&T Contribution to CCITT Special Study Group D, Vol. III - Question I/D, p. 13.
25. Allen, D. W., et al., "Precision and Accuracy of Remote Synchronization via Portable Clocks, Loran-C and Network Television Broadcasts," Proc. 25th Annual Symposium on Frequency Control, pp. 195-208, Apr. 1971.
26. Alpert, A., and Murphy, D., "Establishing, Synchronizing and Maintaining a Standard Clock for the USAF Calibration Program," Frequency, May 1968.
27. Andrews, D. H., "Reception of Low Frequency Time Signals," Frequency, Sept. 1968.
28. Baart, J. G., Harting, S., and Verma, P. K., "Network Synchronization and Alarm Remoting in the Dataroute," IEEE Trans. on Communications, Vol. COM-22, pp. 1873-1877, Nov. 1974.
29. Babler, G. M., "Selectively Faded Nondiversity and Space Diversity Narrowband Microwave Radio Channels," BSTJ, Feb. 1973.
30. Babler, G. M., "A Study of Frequency Selective Fading for a Microwave Line-of-Sight Narrowband Radio Channel," BSTJ, Mar. 1972.

31. Bachmann, A. E., "Development of Communications in Switzerland," IEEE TRANSCOM, Vol. 22, No. 9, Sept. 1974.
32. Barber, R. E., "Short-Term Frequency Stability of Precision Oscillators and Frequency Generators," BSTJ, Vol. 50, No. 3, Mar. 1971.
33. Barducci, I., et al., "Quantization Noise in a PCM System and Its Influence on the Quality of Transmission," CCITT Study Group XII - Contribution No. 67, 27 Aug. 1963.
34. Barnett, W. T., "Microwave Line-of-Sight Propagation with and without Frequency Diversity," BSTJ, May 1970.
35. Barnett, W. T., "Multipath Propagation at 4, 6, and 11 GHz," BSTJ, Feb. 1972.
36. Batterson, C. C., et al., "Pulse Code Modulation, Initial Application at W. V.," W. V. Technical Review, Summer 1968.
37. Bayne, C. J., Karafin, B. J., and Robinson, D. B., "Systematic Jitter in a Chain of Digital Regenerators," BSTJ, p. 2679, Nov. 1963.
38. Beesley, J. H., "Practical Multistage Space-Time Switching Networks," IEEE TRANSCOM, Aug. 1973.
39. Belle, P. A., et al, "Tropo-Scatter Multichannel Digital Systems Study," RADC TR-67-218, May 1967.
40. Bittel, R. H., Elsner, W. B., Helm, H., Mukundan, R., and Perreault, D. A., "Clock Synchronization Through Discrete Control Correction," IEEE Trans. on Communications, Vol. COM-22, pp. 836-839, June 1974.
41. Bondurant, E. H., "An Evolution of Synchronization Methods for the DATRAN System," IEEE ICC '71 Record, pp. 23.23-23.28.
42. Bosworth, R. H., et al., "Design of a Simulator for Investigating Organic Synchronization Systems," BSTJ, Vol. 47, No. 2, p. 209, Feb. 1968.
43. Bosworth, R. H., Kammerer, F. W., Rowlinson, D. E., and Scattaglia, J. V., "Design of a Simulator for Investigating Organic Synchronization Systems," BSTJ, Vol. 47, pp. 209-226, Feb. 1968.

44. Boxall, F. S., "A Digital Carrier-Concentrator System with Elastic Traffic Buffer," IEEE TRANSCOM, Vol. 22, No. 10, Oct. 1974.
45. Brilliant, M. B., "The Determination of Frequency in Systems of Mutually Synchronized Oscillators," BSTJ, Vol. 45, p. 1737, Dec. 1966.
46. Brilliant, M. B., "Dynamic Response of Systems of Mutually Synchronized Oscillators," BSTJ, Vol. 46, pp. 319-356, Feb. 1967.
47. Bruce, R. A., "A 1.5 to 6 Megabit Digital Multiplex Employing Pulse Stuffing," ICC 1969, pp. 34-1 to 34-7.
48. Bruun, R., "Dataroute, Pioneer in Data Communications," Infosystems, Nov. 1973.
49. Buchner, M. M., Jr., "An Asymmetric Encoding Scheme for Word Stuffing," BSTJ, Mar. 1970.
50. Buckley, J. E., "AT&T's Digital Transmission Service," Computer Design, June 1974.
51. Buckley, J. E., "Trans-Canada Dataroute," Computer Design, Oct. 1973.
52. Bullington, K., "Phase and Amplitude Variations in Multipath Fading of Microwave Signals," BSTJ, Vol. 50, No. 6, July-Aug. 1971, pp. 2039-2053.
53. Butmann, S., "Synchronization of PCM Channels by Method Word Stuffing," IEEE Trans. on Communications, Vol. 16, No. 2, p. 252, Apr. 1968.
54. Candy, J. C., and Karnaugh, M., "Organic Synchronization: Design of the Controls and Some Simulation Results," BSTJ, Vol. 47, pp. 227-259, Feb. 1968.
55. Chang, R. W., "Analysis of a Dual Mode Digital Synchronization System Employing Digital Rate-locked Loops," BSTJ, Vol. 51, No. 8, pp. 1881-1911, Oct. 1972.
56. Chen, W. Y., "Estimated Outage in Long-Haul Radio Relay System with Protection Switching," BSTJ, Feb. 1972.
57. Chow, P. E. K., "Jitter Due to Pulse Stuffing Synchronization," IEEE Trans. on Communications, pp. 854-859, July 1973.

58. , Chow, L. R., et al., "A Linear Bit Synchronizer With Learning," IEEE TRANSCOM, Mar. 1973.
59. Chu, D. C., "Time Interval Averaging; Theory, Problems and Solution," H. P. Journal.
60. Cohen, L., "IDDS - System Concepts Improve Performance and Reliability (WUI)," Telecommunications, May 1974.
61. Cox, J. E., "Western Union Digital Services," Proc. of the IEEE, "Vol. 60, pp. 1350-1357, Nov. 1972.
62. Davies, A. C., "Discrete-Time Synchronization of Digital Data Networks," IEEE Trans. on Circuits and Systems, Vol. CAS-22, pp. 610-618, July 1975.
63. Davies, A. C., "Discrete-Time Synchronization of Communication Network Having Variable Delays," IEEE Trans. on Communications, Vol. COM-23, pp. 782-785, July 1975.
64. Davies, A. C., "The Effects of Clock Drift Upon the Synchronization of Digital Communications Networks," IEEE Trans. on Communications, Vol. COM-22, pp. 1842-1844, Nov. 1974.
65. Day, R. A., "Use of Loran-C Navigational System as a Frequency Reference," Signal, pp. 26-30, Nov. 1973.
66. Day, R. A., "The Effect of Changes in Absolute Path Delay in Digital Transmission Systems," publication unknown.
67. Dell, F. R. E., "Features of a Proposed Synchronous Data Network," IEEE Trans. on Communications, Vol. 20, No. 3, p. 499, June 1972.
68. DeWitt, R. G., "Network Synchronization Plan for the Western Union All Digital Network," Telecommunications, pp. 25-28, July 1973.
69. DeWitt, R. G., "Nationwide Digital Transmission Network for Data," Telecommunications, Sept. 1971.

70. Dimitriev, V. P., "Self-Synchronization of Digital Communication," Telecommunications and Radio Engineering (Translation from Russian), Part 2, Vol. 23, No. 4, p. 135, Apr. 1968.
71. Dingeldey, R., "Present State and Trends of Public Communications in the Federal Republic of Germany," IEEE TRANSCOM, Vol. 22, No. 9, Sept. 1974.
72. Dorros, I., et al., "An Experimental 224 Mb/s Digital Repeater Line," BSTJ, Sept. 1966.
73. Duttweiler, D. L., "Waiting Time Jitter," BSTJ, Vol. 51, pp. 165-207, Jan. 1972.
74. Edström, N. H., et al., "The Satellite System as an Integrated Switching Center," IEEE TRANSCOM, Apr. 1973.
75. Ellingson, C. E., and Kulpinski, R. J., "Dissemination of System Time," IEEE Trans. on Communications, Vol. 21, No. 5, pp. 605-624, May 1973.
76. Farinholt, E. V., "Domestic Digital Transmission Services," Signal, pp. 28-34, Apr. 1975.
77. Fey, A. L., et al., "An Ultra-Precise Time Synchronization System Designed by Computer Simulation," Frequency, Jan. 1968.
78. Fick, H., et al., "Multiplexing and Switching of Data in Synchronous Networks and the Realization in the EDS System," IEEE TRANSCOM, Aug. 1973.
79. Flanagan, T. M., and Wrobel, T. F., "Radiation - Stable Quartz Oscillators," Final Report on Contract DASA01-71-C-0151, DNA 2960F, Nov. 1972.
80. Fleig, W., "Stuffing TDM for Independent TI Bit Streams," Telecommunications, Vol. 6, No. 7, p. 23, July 1972.
81. Folts, H. C., "Time and Frequency for Digital Communications," Proc. of the Fourth Precise Time and Time Interval Planning Conference (NASA and Department of Defense), pp. 194-202, Nov. 1972.
82. Frank, H., "Survivability Analysis of Command and Control Communications Networks - Parts I and II," IEEE TRANSCOM, May 1974.

83. Fritz, P., "CITEDIS Production PCM Public Telephone Switching System," IEEE TRANSCOM, Vol. 22, No. 9, Sept. 1974.
84. Fultz, K. E., and Penick, D. B., "The T-1 Carrier System," BSTJ, Sept. 1965.
85. Gallant, R., "Troposcatter Multipath Analyzer," NTIS, Document No. AD-712-415, Aug. 1970.
86. Garodnick, J., et al., "Response of an All Digital Phase-Locked Loop," IEEE TRANSCOM, June 1974.
87. Gerke, P. R., et al., "The Time Division Multiplex Switching of Digital Speech Channels," IEEE TRANSCOM, Vol. 22, No. 9, Sept. 1974.
88. Gersho, A., and Karafin, B. J., "Mutual Synchronization of Geographically Separated Oscillators," BSTJ, Vol. 45, pp. 1689-1704, Dec. 1966.
89. Gigli, A., et al., "Present Status and Expected Development of the Italian Telecommunications Network," IEEE TRANSCOM, Vol. 22, No. 9, Sept. 1974.
90. Gitlin, R. D., and Hayes, J. F., "Timing Recovery and Scramblers in Data Transmission," BSTJ, Mar. 1975.
91. Glastone, S., "The Effects of Nuclear Weapons, U.S. Atomic Energy Commission," Apr. 1962, as discussed in a paper by R. A. Pohl titled, "Approaches to System Hardening," July 21, 1971, presented to the IEEE Annual Conference on Nuclear and Space Radiation Effects.
92. Glave, F. E., and Dunn, L. B., "Dataroute Transmission: System Growth and Extensions," ICC 1974, pp. 2E1-2E5.
93. Graf, C. R., "The Unclear-Channel, Standard-Frequency Stations," Telecommunications, Feb. 1972.
94. Gray, D. A., "Transit-Time Variations in Line-of-Sight Tropospheric Propagation Paths," BSTJ, July-Aug. 1970.
95. Grier, E. P., et al., "An Advanced Wideband Digital Communication System," Signal, Feb. 1975.

96. Gurn, J. F., "Digital Transmission on the L-4 Coaxial System," Telecommunications, Dec. 1970.
97. Haberle, H., "Frame Synchronizing PCM Systems," Electrical Communication, Vol. 44, No. 4, p. 280, 1969.
98. Hayes, J. F., "Performance Models of an Experimental Computer Communications Network," BSTJ, Feb. 1974.
99. Hedderly, D. L., et al., "Computer Simulation of a Digital Satellite Communications Link," IEEE TRANSCOM, Apr. 1973.
100. Hellwig, H., "Frequency Standards and Clocks," NBS Technical Note 616, Mar. 1974.
101. Ho, E. Y., "Optimum Equalization and the Effect of Timing and Carrier Phase on Synchronous Data Systems," BSTJ, Vol. 50, No. 5, pp. 1671-1689, May-June 1971.
102. Horton, D. J., and Bowie, P. G., "An Overview of Dataroute: System and Performance," ICC 1974, pp. 2A1-2A5.
103. Hoth, D. F., "Digital Communications," Bell Lab Rec., Vol. 45, pp. 38-43, Feb. 1967.
104. Huff, R. J., "Multifunction TDMA Techniques," OSURF Report No. 3364-1.
105. Hurst, G. T., and Gupta, S. C., "Quantizing and Sampling Considerations in Digital Phase-Locked Loops," IEEE TRANSCOM, Jan. 1974.

106. INTELSAT RFP-IS-564, "4-Phase CPSK Modems," 1973.
107. Ishii, R., "Dynamic Response and Stability of Mutually Synchronized Systems," IEEE TRANSCOM, Apr. 1975.
108. James, R. T. and Muench, P. E., "AT&T Facilities and Services," Proc. of the IEEE, Vol. 60, pp. 1342-1349, Nov. 1972.
109. Jespersen, J. L., et al., "Characterization and Concepts of Time-Frequency Dissemination," Proc. of IEEE, Vol. 60, No. 5, pp. 502-521, May 1972.
110. Job, F., et al., "New Telecommunications System Under Development in France," IEEE TRANSCOM, Vol. 22, No. 9, Sept. 1974.
111. Johannes, V. I. and McCullough, R. H., "Multiplexing of Asynchronous Digital Signals Using Pulse Stuffing with Added Bit Signalling," IEEE Trans. on Communications Technology, pp. 562-568, Oct. 1966.
112. Johnson, M., "Digital Transmission in the Near Term DCS," URSI/IEEE Symposium Proceedings, 1973.
113. Karnaugh, M., "A Model for the Organic Synchronization of Communications Systems," BSTJ, Vol. 45, pp. 1705-1736, Dec. 1966.
114. King, J. C. and Sanders, H. H., "Transient Change in Q and Frequency of AT Cut Quartz Resonators Following Exposure to Pulsed X-Rays," IEEE Trans. Nucl. Sci., Dec. 1973.
115. Krishnan, K. R., et al., "Synchronization of A Digital Communication Network by Discrete-Control-Correction," IEEE ISACS '74 Proceedings, pp. 411-415, Apr. 1974.
116. Krishnan, K. R., et al., "Discrete Control Correction for Synchronization of Digital Communication Networks with Different Correction Parameters at Different Nodes," IEEE ICC '74 Conf. Record, pp. 6C-1 - 6C-4, June 1974.
117. Lay, M. D. and Davis, D. T., "A Simple Airborne System for Calibration of Remote Precision Clocks," Frequency Technology, Dec. 1969.

118. Lin, S. H., "Statistical Behavior of a Fading Signal," BSTJ, Vol. 50, No. 10, Dec. 1971, pp. 3211-3270.
119. Louthaller, W. E., "Systems Considerations for European Communications Satellites," IEEE TRANSCOM, Apr. 1973.
120. Lubowe, A. G., "Path Length Variation in a Synchronous Satellite Communication Link," BSTJ, Dec. 1968.
121. Marino, P. J., et al., "A Time Division Data Switch," IEEE Transactions, Nov. 1974.
122. Markowitz, W., et al., "Clock Synchronization Via Relay II Satellite," IEEE Trans. Instr. and Meas., Dec. 1966.
123. Martin Marietta Corp. Technical Data Sheet, "Asynchronous Time-Division Multiplexer Set, AN/GSC-24 (✓).
124. Matsuura, Y., Kuzuka, S. and Yuki, K., "Jitter Characteristics of Pulse Stuffing Synchronization," IEEE ICC '68 Conference Record, pp. 259-264, 1968.
125. Mayo, J. S. "An Approach to Digital System Networks," IEEE Trans. on Communication Technology, Vol. COM-15, pp. 307-310, Apr. 1967.
126. Mayo, J. S., "Experimental 224 Mb/s PCM Terminals," BSTJ, Vol. 44, pp. 1813-1841, Nov. 1965.
127. Mayo, J. S., "Synchronization of PCM Networks," IEEE NEREM Record, Vol. 7, p. 166, 1965.
128. Mazo, J. E., "Theory for Some Asynchronous Time-Division Switches," BSTJ, Vol. 50, No. 5, pp. 1671-1689, May-June 1971.
129. McEvoy, J. B. and Sturdevant, N. J., "DICEF, RADC's Digital Communications Experimental Facility," Signal, July 1974.
129. McRae, D. D. and Smith, E. F., "Bit Synchronizer Requisition and Timing Error Performance (A) Trades," Harris ESD TR No. 46, Jan. 1972.
130. Mensch, J. R., "Future DCS Objectives in Communication Network Timing and Synchronization," Proc. of Fifth Precise Time and Time Interval Planning Meeting, Dec. 1973.

131. Miller, M. R., Parks, P. C., and Yamato, J., "Comments on Synchronization of a PCM Integrated Telephone Network," IEEE Trans. on Communication Technology, Vol. COM-18, pp. 269-270, June 1970.
132. Miller, M. R., "Some Feasibility Studies of Synchronized Oscillator Systems for PCM Telephone Networks," Proc. IEE, Vol. 116, pp. 1135-1143, 1969.
133. Moreland, J. P., "Performance of a System of Mutually Synchronized Clocks," BSTJ, Vol. 50, No. 7, pp. 2249-2464, Sept. 1971.
134. Mukundan, R., et al., "Clock Synchronization Through Discrete Control Correction," EUROCON '74 Conf. Digest, Amsterdam, The Netherlands, Apr. 1974.
135. Mumford, H. and Smith, P. W., "Synchronization of a PCM Network Using Digital Techniques," Proc. IEE, Vol. 113, pp. 1420-1428, Sept. 1966.
136. Pan, J. W., "Synchronizing and Multiplexing in a Digital Communications Network," Proc. of IEEE, Vol. 60, No. 5, pp. 594-601, May 1972.
137. Perreault, D. A., Mukundan, R., and Krishnan, K. R., "A Hybrid Simulator for Discrete Control Correction," EASCON '74, pp. 559-561.
138. Perreault, D. A., et al., "A Computer Simulator for Discrete Control Correction," Fifth Annual Pittsburgh Conference on Modeling and Simulation Proceedings, Pittsburgh, Pa., Apr. 1974.
139. Personick, S. D., "Optical Fibers," IEEE Spectrum.
140. Phillips Corp. Data Brief, "DELTAMUX for Digital Speech and Data Transmission in Military Telecommunications Networks."
141. Pierce, J. R., "Synchronizing Digital Networks," BSTJ, pp. 615-636, Mar. 1969.
142. Pinet, A. E., "Telecommunications Integrated Network," IEEE Trans. on Communications p. 916, Aug. 1973.
143. Poe, W. R., et al., "New Group Channel Modem," Signal, Dec. 1973, pp. 11-13.

144. Popov, V. M., "Dichotomy and Stability by Frequency-Domain Methods," Proc. of IEEE, May 1974.
145. Potts, C. E. and Wieder, B., "Precise Time and Frequency Dissemination via the Loran C System," Proc. of IEEE, Vol. 60, No. 5, pp. 530-539, May 1972.
146. Prabhu, V. K. and Enloe, L. H., "Inter-Channel Interference Considerations in Angle-Modulated Systems," BSTJ, Vol. 48, No. 7, Sept. 1969, pp. 2333-2358.
147. Pritsker, A. A. B., "The GASP IV Simulation Language," John Wiley & Sons.
148. Pritsker, A. A. B., and P. J. Kiviat, "Simulation With GASP II," Prentice-Hall.
149. Ramasastry, J., et al., "Clock Synchronization Experiments Performed via the ATS-1 and ATS-3 Satellites," IEEE Trans. on Inst. and Meas., Vol. 22, No. 1, pp. 9-12, Mar. 1973.
150. Ratheon Co. Technical Brief, "RDS-80 Digital Radio."
151. Ricci, F. J., "Hybrid Computer Simulation Model of a Circuit Switched Network and the Implementation of Adaptive Controls," Proc. of EASCON 1974.
152. Rich, M. A., "Designing Phase-Locked Oscillators for Synchronization," IEEE TRANSCOM, July 1974.
153. Roza, E., "Analysis of Phase-Locked Timing Extraction Circuits for Pulse Code Transmission," IEEE TRANSCOM, Sept. 1974.
154. Ruthoff, C. L., "Multiple-Path Fading on Line-of-Site Microwave Radio Systems as a Function of Path Length and Frequency," BSTJ, Vol. 50, No. 7, Sept. 1971.
155. Ruthoff, C. L. and Tillotson, L. C., "Interference in a Dense Radio Network," BSTJ, Vol. 48, No. 6, July-Aug. 1969, pp. 1727-1743.
156. Saltzberg, B. R. and Zydney, H. M., "Digital Data System: Network Synchronization," BSTJ, Vol. 54, pp. 879-892, May-Jun. 1975.
157. Sandberg, I. W., "On Conditions Under Which It Is Possible to Synchronize Digital Transmission Systems," BSTJ, Vol. 48, No. 6, pp. 1999-2022, July-Aug. 1969.

158. Sandberg, I. W., "Some Properties of a Nonlinear Model of a System for Synchronizing Digital Transmission Networks," BSTJ, Vol. 48, pp. 2975-2997, Nov. 1969.
159. Scholl Meier, G. and Schatz, N., "The Design of Nonlinear Phase-Tracking Loops By Simulation," IEEE TRANSCOM, Feb. 1975.
160. Shapiro, L. D., "Loran-C Sky-Wave Delay Measurements," IEEE Trans. on Inst. and Meas., Vol. 15, No. 4, pp. 117-189, Dec. 1966.
161. Shapiro, L. D., "Time Synchronization From Loran C," IEEE Spectrum, Vol. 5, pp. 46-5, Aug. 1968.
162. Shoaf, J. H., "Specification and Measurement of Frequency Stability," NBSIR 74-396, Nov. 1974.
163. Sinha, A. S. C., "Some Stability Results of a Delay-Differential System for Digital Networks," Proc. 16th Midwest Symposium on Circuit Theory, Waterloo, Canada, Part 17.9.1-17.9.7, Apr. 1973.
164. Sinha, A. S. C., "Further Stability Results of a Delay-Differential Systems for Digital Networks," Int. Jour. of Sys. Sci., Vol. 5, No. 4, pp. 317-321, Apr. 1974.
- 164(A). Smith, E. F. and McRae, D. D., "Bit Slippage Rates in Bit Synchronizers," Harris ESD TR-No. 49, May 1974.
- 164(B). Smith, E. F. and Davis, R. C., "Group Synchronization Performance Analysis," Harris ESD TR-No. 43, February 1971.
165. Smith, J. W., "A Unified View of Synchronous Data Transmission System Design," BSTJ, Vol. 47, No. 3, pp. 273-300, Mar. 1968.
166. Smith, W. L., "Frequency and Time in Communications," Proc. of IEEE, Vol. 60, No. 5, p. 589, May 1972.
167. Smith, W. H., et al., "PCM Microwave Links," Telecommunications, Apr. 1973.
168. Sorden, J. L., "A New Generation in Frequency and Time Measurements," H. P. Journal, Jun. 1974.

169. Stover, H. A., "Coordinated Universal Time (UTC) as a Timing Basis for Digital Communication Networks," EASCON Record, 1974.
170. Stover, H. A., "A Time Reference Distribution Concept for a Time Division Communication Network," Proc. of Fifth Precise Time and Time Interval Planning Meeting, pp. 505-523, Dec. 1973.
171. Subramanian, M., et al., "Phase Dispersion Characteristics During Fades in a Microwave Line-of-Sight Radio Channel," BSTJ, Dec. 1973.
172. Sullivan, W. A., "High Capacity Microwave System for Digital Data Transmission," Publication Unknown.
173. Sunde, E. D., "Digital Tropo Scatter Transmission and Modulation Theory," BSTJ, Jan, 1974.
174. Swanson, E. R. and Kugel, C. P., "VLF Timing: Conventional and Modern Techniques Including Omega," Proc. of IEEE, Vol. 60, No. 5, pp. 540-551, May 1972.
175. Takhar, G. S. and Gupta, S. C., "Analysis of Synchronous Digital-Modulation Schemes for Satellite Communications," IEEE TRANSCOM, June 1975.
176. Travis, L. F. and Yaeger, R. E., "Wideband Data on T-1 Carrier," BSTJ, Oct. 1965.
177. Un, C. K., "Transient Mean and Variance of Phase Error of the First Order Phase-Locked Loop," IEEE TRANSCOM, Jan. 1974.
178. Vigants, A., "The Number of Fades in Space-Diversity Reception," BSTJ, Vol. 49, No. 7, Sept. 1970, pp. 1513-1530.
179. Vigants, A., "Number and Duration of Fades at 6 and 4 GHz," BSTJ, Vol. 50, No. 3, Mar. 1971, pp. 815-841.
180. Walker, A. C., "PCM Multiplex For Microwave," Telecommunications, Apr. 1973.
181. Weinberg, A., "Discrete Time Analysis of Nonuniform Sampling First- and Second-Order Digital Phase Lock Loops," IEEE TRANSCOM, Feb. 1974.

182. Willard, D. G., "A Time Division Multiple Access System For Digital Communications," Computer Design, Dec. 1974.
183. Willard, M. W., "Analysis of a System of Mutually Synchronized Oscillators," IEEE Trans. on Communications, Vol. 18, No. 5, pp. 467-483, Oct. 1970.
184. Willard, M. W. and Horkan, L. J., "Maintaining Bit Integrity in Time Division Transmission," IEEE NAECON '71 Proc., Dayton, Ohio, pp. 240-247, May 1971.
185. Willard, M. W. and Dean, H. R., "Dynamic Behavior of a System of Mutually Synchronized Oscillators," IEEE Trans. on Communications, Vol. 19, No. 4, pp. 375-395, Aug. 1971.
186. Winkler, G. M. R., "Path Delay, Its Variations and Some Implications for the Field Use of Precise Frequency Standards," Proc. of IEEE, Vol. 60, No. 5, pp. 522-529, May 1972.
187. Witt, F. J., "An Experimental 224 Mb/s Digital Multiplexer-Demultiplexer Using Pulse Stuffing Synchronization," BSTJ, Vol. 44, pp. 1843-1885, Nov. 1965.
188. Worley, A. R., "The DATRAN System," Proc. of IEEE, Vol. 60, No. 11, p. 1357, Nov. 1972.
189. Yamato, J., Nakajima, S. and Saito, K., "Dynamic Behavior of a Synchronization Control System for an Integrated Telephone Network," IEEE Trans. on Communications, Vol. 2, No. 6, pp. 839-845, Jun. 1974.
190. Yamato, J., Ono, M. and Usada, S., "Synchronization of a PCM Integrated Telephone Network," IEEE Trans. on Communications, Vol. 16, No. 1, p. 1, Feb. 1968.
191. Yamato, J., "Stability of a Synchronization Control System for an Integrated Telephone Network," IEEE Trans. on Communications, pp. 1848-1853, Nov. 1974.
192. Zima, V., et al., "An Electronic System for the Phase Synchronization of Radio Transmitters," IEEE TRANSCOM, Sept. 1974.

193. "What We Can Learn From European Data Communications," Infosystems, Mar. 1974.
194. "Intelsat Upgrades Satellite Channels to Match Planned Terrestrial Data Networks," Comm. Design, Dec. 1972.
195. "Submarine Cable Systems," BSTJ, Vol. 49, No. 5, Jun. 1970.
196. "Bell Plans Synchronous Digital Network," Comm. Design, Aug. 1972.
197. "Data Under Voice System," Comm. Design, Aug. 1972.
198. "AT&T Network Improvements," Telecommunications, May 1974.
199. "Western Union Employs TDM Network to Carry Data Traffic Nationwide," Comm. Designers Digest, Aug. 1971.
200. "Specialized Common Carriers," Telecommunications, Sept. 1974.
201. "TDM Hierarchy Handles Nationwide Transmission of Variable Rate Data (DATRAN)," Comm. Designers Digest, Dec. 1971.
202. "Digital Data System," BSTJ, entire Vol. 54, No. 5, May-June 1975.
203. Crawford, A. B., Hogg, D. C., and Kummer, W. H., "Studies in Tropospheric Propagation Beyond the Horizon," BSTJ, pp. 1067-1177, September 1959.
204. Harting, S. and Verma, P. K., "Universal Time Frame: A New Network Feature for Delay Minimization," IEEE Trans. Comm., pp. 1339-1342, Nov. 1975.
205. DCEC Report TR 43-75 "Communications Network Timing"
206. Pierce, J. R., "Synchronizing Digital Networks" BSTJ, pp. 615-636, March 1969.
207. Gray, D. A., "Transit-Time Variations in Line-of-Sight Tropospheric Propagation Paths," BSTF, pp. 1059-1068, July-August 1970.
208. Crawford, A. B., et al., "Studies in Tropospheric Propagation Beyond the Horizon," BSTJ, pp. 1067-1176, Sept. 1959.
209. Lubowe, A. G., "Path Length Variation in a Synchronous Satellite Communication Link," BSTJ, pp. 2139-2144, Dec. 1968.

210. Wagner, C. A., "The Drift of a 24-Hour Equatorial Satellite Due to an Earth Gravity Field Through 4th Order," NASA Technical Note in D-2103, Feb. 1964, also in Publications of the Goddard Space Flight Center Vol. II Space Technology, 1964.
211. Kamen, I. and Dondoulakis, G., Scatter Propagation Theory and Practice, H. W. Sams and Co., Inc., Indianapolis, Indiana, 1956.
212. "DSCS-II Transponder Simulation and Operational Evaluation Study: Final Report," 11 Feb. 1972, TRW Report 18152-6004-R0-00 for U.S. Army Satellite Communications Agency Contract No. DAAG05-71-C-0733.
213. Darwin, G. P. and Prim, R. C., U.S. Patent No. 2,986,723 "Synchronization of a System of Interconnected Units."